

**The role of connexins in
tissue injury and repair**

Beverley Jane Lauren Glass

*A thesis submitted for the fulfilment of the degree of
Doctor of Philosophy*

Department of Cell and Developmental Biology

University College London

2014

Declaration of Authorship

I, Beverley Jane Lauren Glass, confirm that the work presented in this thesis is my own. Where information has been derived from other sources, I confirm that this has been indicated below:

1. Work carried out in Chapter 6 'The role of Cx43 in a model of pressure ulcers' was carried out in collaborative work with Abbie Omolu.

Signed _____

Date _____

Abstract

Skin integrity is essential for sustaining life and it is important to understand the processes involved in its maintenance and repair. There are several key stages involved in wound healing that rely on the complex communication through gap junctions and their connexins to ensure the resolution of the wound. Gap junctions are expressed in all cells linked with tissue repair and provide a regulated pathway linking the cytoplasm of neighbouring cells and allowing signals to pass freely between the two. In the skin there are three key connexins (Connexins 26, 30 and 43) that undergo dynamic changes and regulate the stages of wound closure. To date, extensive research has shown that inhibiting Cx43 expression can achieve significant improvements in wound repair. Synthetic connexin mimetic peptide Gap27 which possess a conserved homology to the second extracellular loop of Cx43 is now being considered as a candidate to improve the rate of wound repair. At low concentrations Gap27 has been shown to block hemichannels but can target gap junctional intercellular communication at higher concentrations and for longer incubation periods. By using Gap27 as a tool, this thesis explores the importance of connexins, hemichannels and gap junctions in tissue injury and repair. I have dissected out the relative contributions of connexins and their involvement with hemichannels and gap junctions in wound repair while investigating if and how Gap27 reduces other connexins. Further work using *in vitro* wound healing models has shown how Gap27 can enhance the rate of wound healing in early stages. In the second half of this thesis I continue to use Gap27 to investigate the connexin based communication involved in the spread of cell death and damage during ischemia reperfusion injury *in vitro* and *in vivo*. The potential therapeutic implications of the wound healing properties of Gap27 are exciting, novel and promising.

Acknowledgements

I would like to thank my supervisor Professor David Becker for the opportunity to complete a PhD in one of the top global educational establishments. His encouragement, practical guidance and many supportive discussions have been invaluable. Thanks are also due to Dr. Anthony Phillips for his advice, support and assistance throughout my research project. I would also like to express my gratitude towards CoDa Therapeutics and Impact, UCL for funding this research.

I am indebted to Dr. Christopher Thrasivoulou and the Data Analysis team; Daniel Ciantar, Tim Robson and Jane Pendjiky, who have been more than generous with their time from trivial matters in the confocal microscopy rooms to complex software macro creations. My sincere gratitude to my graduate tutor Professor David Whitmore; I am particularly grateful for his belief that I could complete this PhD. Thanks are also due to my second supervisor Professor Timothy Arnett whose pep talks and encouragement fuelled me through my research project. Thanks also to Dr. Peter Cormie, Dr. Antonio Serrano and Dr. Ariadna Mendoza for their guidance.

I certainly could not have completed this thesis without my laboratory colleagues. In particular I must thank Nikki Davis, Jessica Sutcliffe and Daniel Gilmartin who have been there for the entire duration of my PhD. They are all fantastic people that have supplied endless support (both academically and personally) and have been a complete joy to work with. In addition, Katie Heath and Xioming Hou have helped, supported and encouraged me throughout the later stages of my research project.

To my parents, Jaine and Stuart, who have been constant sources of encouragement to me throughout my PhD, a very special thank you for the months of emotional support you have both given me. I would also like to thank my family

and friends for their constant support and understanding throughout my research project.

Finally, this research project would never have been possible without the endless love, understanding and sacrifices made by my husband Simon. He has been my rock through these last few years and I certainly would not have completed my PhD and thesis without his perpetual support.

Contents

Declaration of Authorship.....	2
Abstract.....	3
Acknowledgements.....	4
Figures.....	9
Tables.....	12
1. Introduction.....	14
1.1 The skin.....	14
1.1.1 The epidermis.....	15
1.1.2 The dermis	16
1.2 Wound healing.....	18
1.2.1 Immediate response	20
1.2.2 Inflammatory response	21
1.2.3 Re-epithelialisation	22
1.2.4 Proliferation, migration and contraction.....	23
1.2.5 Resolution	24
1.3 Communication in the skin: gap junctions and connexins	25
1.3.1 History of gap junction research	26
1.3.2 Connexins, connexons and gap junctions.....	28
1.3.3 Innexins and pannexins	34
1.3.4 Function of gap junctions	36
1.3.5 Connexins in the intact skin	42
1.4 Connexin dynamics in normal wound healing	44

1.4.1	Connexin response in the epidermis during wound healing	46
1.4.2	Connexin response in the dermis during wound healing	47
1.5	Connexin dynamics in abnormal wound healing	51
1.5.1	Introduction to chronic wounds	51
1.5.2	Connexin dynamics in chronic wounds	55
1.5.3	Transient knockdown of Cx43 in wound healing	58
1.6	Connexin mimetic peptides in wound healing	59
1.6.1	History of connexin mimetic peptides.....	60
1.6.2	The benefits of connexin mimetic peptides in wound healing.....	62
1.7	General aim of this thesis	64
2.	Materials and methods	66
2.1	Reagents, antibodies and mimetic peptides.....	66
2.2	<i>In vitro</i>	69
2.2.1	Cell culture	69
2.2.2	Mimetic peptide incubation	70
2.2.3	Oxygen glucose deprivation re-oxygenation	71
2.2.4	Immunostaining cells	72
2.2.5	Western blots	73
2.2.6	Detailed assays using cell cultures	75
2.3	<i>In vivo</i>	82
2.3.1	Animals	82
2.3.2	General surgical procedures.....	82
2.3.3	Tissue processing and cryosectioning	86

2.3.4	Histology assay - Haematoxylin and Eosin stain.....	88
2.3.5	Immunostaining tissue.....	89
2.3.6	Detailed analysis.....	89
2.3.7	Confocal microscopy.....	92
2.3.8	Statistics.....	93
3.	Gap27 mechanisms <i>in vitro</i>	94
3.1	Introduction.....	94
3.2	Results.....	98
3.3	Discussion.....	119
4.	Gap27 in wound healing.....	134
4.1	Introduction.....	134
4.2	Results.....	140
4.3	Discussion.....	161
5.	Connexin based communication in ischemia reperfusion.....	172
5.1	Introduction.....	172
5.2	Results.....	175
5.3	Discussion.....	191
6.	The role of Cx43 in a model of pressure ulcers.....	204
6.1	Introduction.....	204
6.2	Results.....	208
6.3	Discussion.....	224
7.	General discussion.....	230
	Bibliography.....	239

Appendix I..... 260
Appendix II..... 264
Appendix III..... 267

Figures

Figure 1.1 The skin.....	15
Figure 1.2 The stages of normal wound healing	19
Figure 1.3 The phases of normal wound healing.....	20
Figure 1.4 Gap junctions.....	25
Figure 1.5 Gap junctions viewed under an electron microscope	28
Figure 1.6 Subclasses of gap junctions.....	31
Figure 1.7 Clinical and histological features of EVK.....	41
Figure 1.8 Connexin profiles in mature rodent and human skin.....	43
Figure 1.9 Dynamics of connexins during wound healing.....	45
Figure 1.10 Chronic ulcers.....	55
Figure 2.1 Connexin 43 with Gap27 and antibodies.....	68
Figure 2.2 Diagrams of surgical procedures.....	83
Figure 2.3 Ischemia reperfusion injury model.....	86
Figure 2.4 Tissue processing.....	87
Figure 2.5 Regions of interest in blood vessel leakiness analysis	90
Figure 2.6 Regions of interest in connexin profiling.....	92
Figure 3.1 Proposed mechanisms of action of connexin mimetic peptides.....	96
Figure 3.2 High concentrations of Gap27 significantly reduced gap junction communication in fibroblast cells	99
Figure 3.3 High concentrations of Gap27 significantly increased the rate of fibroblast cell migration	101
Figure 3.4 Effect of Gap27 on Cx43 expression in fibroblast cells; immunofluorescence analysis.....	104
Figure 3.5 Effect of Gap27 on Cx43 expression in fibroblast cells; Western blot analysis	105

Figure 3.6 Effect of Gap27 on connexin hemichannel expression in fibroblast cells; immunofluorescence analysis	107
Figure 3.7 High concentrations of Gap27 significantly increased the rate of keratinocyte cell migration	110
Figure 3.8 Effect of Gap27 on Cx43 expression in keratinocyte cells; immunofluorescence analysis	112
Figure 3.9 Effect of Gap27 on Cx43 expression in keratinocyte cells; Western blot analysis	114
Figure 3.10 Effect of Gap27 on Cx26 expression in keratinocyte cells; immunofluorescence analysis	116
Figure 3.11 Effect of Gap27 on Cx30 expression in keratinocyte cells; immunofluorescence analysis	118
Figure 3.12 Conformation of gap junction connexons	129
Figure 3.13 Sequence alignments	132
Figure 4.1 Gap27 significantly reduced blood vessel leakiness at the wound site, four hours after wounding	142
Figure 4.2 Gap27 significantly reduced Cx43 expression in blood vessels, four hours after wounding	145
Figure 4.3 Gap27 significantly reduced Cx43 expression at the wound edge, four hours after wounding	147
Figure 4.4 Gap27 significantly reduced connexin hemichannel expression at the wound edge, four hours after wounding	149
Figure 4.5 Regions of interest in polymorphonuclear leukocyte count.....	150
Figure 4.6 Gap27 significantly reduced the number of leukocytes in the dermis, twenty four hours after wounding	151
Figure 4.7 A low concentration of Gap27 significantly increased the extent of re-epithelialisation, twenty four hours after wounding	153

Figure 4.8 Gap27 did not significantly reduce Cx43 expression at the wound edge, twenty four hours after wounding	156
Figure 4.9 Gap27 did not significantly reduce Cx26 expression at the wound edge, twenty four hours after wounding	158
Figure 4.10 Gap27 did not significantly reduce Cx30 expression at the wound edge, twenty four hours after wounding	160
Figure 5.1 OGDR model of ischemia reperfusion reduced O ₂ in culture media	175
Figure 5.2 Cell viability significantly reduced in wild-type and PSupp 3T3 fibroblast cells during OGDR stress	177
Figure 5.3 Cx43 and connexin hemichannel expression in wild-type fibroblast cells significantly increased during OGDR stress	179
Figure 5.4 Cx43, p-Cx43 and connexin hemichannel expression in PSupp transduced cells significantly increased during OGDR stress.....	181
Figure 5.5 PI uptake after OGDR stress was reduced by Gap27 incubation	183
Figure 5.6 Hemichannels open during OGDR stress before wave of PI uptake in neighbouring cells occurs	185
Figure 5.7 Blocking purinergic signalling did not prevent the reduction in cell viability during OGDR stress	187
Figure 5.8 Communication between wild-type fibroblast cells significantly increased during OGDR stress	189
Figure 5.9 Reducing Cx43 during OGDR reduced cell death	190
Figure 6.1 The skin ischemia reperfusion model caused tissue damage at the pressure site	209
Figure 6.2 Cx43 expression in the skin ischemia reperfusion model four hours after pressure relief	212
Figure 6.3 Connexin hemichannel expression in the skin ischemia reperfusion model four hours after pressure relief	214

Figure 6.4 Cx43 expression in the skin ischemia reperfusion model twenty four hours after pressure relief	216
Figure 6.5 Connexin hemichannel expression in the skin ischemia reperfusion model twenty four hours after pressure relief	217
Figure 6.6 Blood vessel leakiness significantly increased at the pressure site four hours after pressure relief	219
Figure 6.7 Blood vessel leakiness further increased at and beyond the pressure site twenty four hours after pressure relief	220
Figure 6.8 The number of leukocytes significantly increased at the pressure site, four hours after pressure relief	222
Figure 6.9 The number of leukocytes significantly increased at the pressure site, twenty-four hours after pressure relief	223
Figure 7.1 Increased rate of internalisation theory	235

Tables

Table 2-1 Primary antibodies used in this investigation.....	60
Table 2-2 Secondary antibodies used in this investigation.....	61
Table 2-3 Sequences of connexin mimetic peptides.....	61
Table 2-4 Sequence of antisense oligodeoxynucleotide.....	62

1. Introduction

1.1 The skin

The integumentary system is the largest organ in the body and functions as a defensive barrier between the body and the external world. The skin is the body's first line of defence against an often hostile environment. This complex and highly specialised tissue is constantly abraded, attacked by microorganisms, irradiated by ultraviolet (UV) rays from the sun and exposed to environmental chemicals. At the same time, the skin carries out essential roles in support, nourishment, waterproofing and protection. Its long term integrity is essential for life and therefore a thorough understanding of the processes involved in its maintenance and repair is extremely important.

The skin (figure 1.1) can roughly be divided into two main layers; the thin external keratinocyte epidermal layer (consisting of sheets of plate-like cells) and the internal fibroblast dermal layer (rich in fibrous and elastic tissue, blood vessels, nerve fibres and accessory structures such as hair follicles and sweat glands). The deepest layer of the dermis anchors the skin to the underlying tissue. The thickness of human skin varies depending on its location in the body. Thick skin can be found on the palms of hands and soles of feet (approximately 4 mm thick) in areas where it is adapted to activities such as gripping. As these areas are subject to more 'wear and tear' thicker skin does not have hair follicles. Most of the rest of human skin is thin and is full of appendages such as hair follicles and sweat glands. The thinnest skin, found on the eyelids is approximately 0.5 mm thick (Waller and Maibach, 2005).

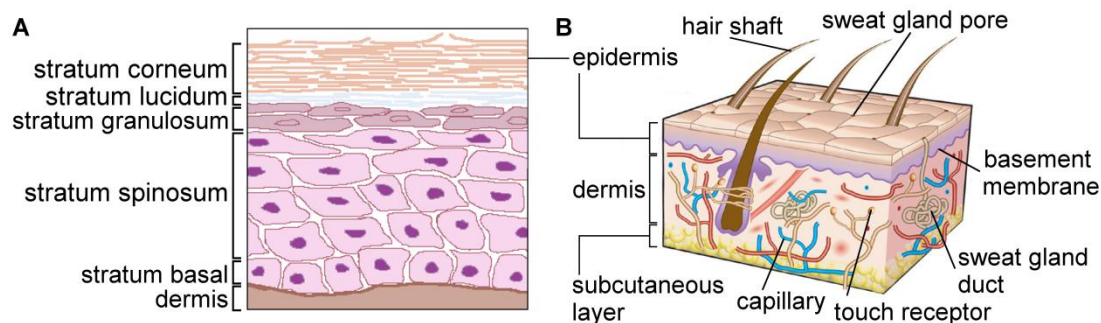


Figure 1.1 The skin

(A) Diagram illustrating the structure of the epidermis in human skin. The epidermis is the body's first barrier against the external environment, preventing pathogens from entering and regulating water loss. The epidermis is divided into five distinct layers. (B) Diagram illustrating the structure of the dermis in human skin. The dermis lies beneath the epidermis via the basement membrane and consists primarily of connective tissue to provide support and structure to the skin. The dermis contains many accessory structures including hair follicles, sebaceous glands and sweat glands. The deepest layer of the skin anchors to the underlying tissue. Diagram adapted from *Nature* 445; 874-880 (MacNeil, 2007).

1.1.1 The epidermis

The epidermis is formed of squamous epithelium and arranged in continuous layers of proliferating basal and differentiated suprabasal keratinocyte cells. It comprises (from interior to exterior) the stratum basal, the stratum spinosum, the stratum granulosum, the stratum lucidum and the stratum corneum. Being avascular, the epidermis relies on the diffusion of oxygen and nutrients from the blood vessels within the dermis in order to function. Cells in the stratum basal lamina have the highest metabolic demand (where the diffusion distance is short) and as a result superficial, differentiated cells far away from the source of nutrients are inert or dead, eventually shedding from the skin surface. Cells in the basal layer are the stem cells of keratinocytes that undergo a specified differentiation process through the layers of the epidermis, resulting in the production of flattened anucleate cells at

the stratum corneum (Fuchs, 2008). This final outer layer serves as the principle barrier and is formed as a continuous layer of protein enriched cells. Capable of withstanding mechanical stress (Madison, 2003), the stratum corneum is surrounded by extracellular non-polar lipids forming a hydrophobic matrix.

1.1.2 The dermis

The dermis lies between the epidermis and the subcutaneous layers and comprises two distinct levels; the superficial papillary layer (made up of capillaries, lymphatic tissue and sensory neurons that supply and sustain the epidermis) and the reticular layer (an interwoven meshwork of dense connective tissue). Both levels differ in composition and organisation of their matrices. The papillary dermis contains thin, poorly organised collagen fibre bundles whereas in comparison the reticular dermis is characterized by thick, well organised fibre bundles (Cormack 1987). The connective tissue protein elastin provides skin resilience, allowing it to resume its shape after stretching or contracting. In contrast to the highly orientated collagen fibres, elastin fibres occur naturally in a contracted state (Sephel and Davidson, 1986). Together these two levels of tissue provide support and elasticity to the skin.

The fundamental cell of the dermal connective tissue is the fibroblast. Representing heterogeneous populations of cells dependent on their location within the dermis (papillary or reticular), the main function of the fibroblast is to provide structural integrity to the skin. The first *in vitro* evidence regarding the origin of the fibroblasts was discovered within bone marrow by Friedenstein and colleagues (Friedenstein et al., 1970, Luria et al., 1971). After plating bone marrow cells in just medium and foetal bovine serum, they discovered colonies of fibroblasts growing. These cells adhered to culture dishes and were elongated and polygonal cytoplasm that are typical characteristics of fibroblast cells. More recent studies using green fluorescent protein as a marker of donor cells has further supported that bone marrow is a

source of both fibroblasts and myofibroblasts (Mori et al., 2005). Bone marrow is known to contain two types of stem cells; haematopoietic stem cells (HSCs) and mesenchymal stem cells (MSCs), both of which could be the source of origin of fibroblast cells. Using tissue reconstitution Ogawa and colleagues have found that fibroblasts and myofibroblasts in many organs are derived from HSCs (Ogawa et al., 2006) whereas Pittenger and colleagues have demonstrated that that human MSCs isolated from bone marrow can differentiate in a controlled manner into mesenchymal tissue that includes bone, cartilage, muscle and skin fibroblasts (Pittenger et al., 1999). Mesenchymal tissue is known as undifferentiated loose connective tissue that is derived from the mesoderm lineage.

In addition to structural properties for uninjured skin, fibroblast cells engage in paracrine and autocrine interactions during tissue injury (Gilchrest et al., 1983, Moulin, 1995). Fibroblasts are known to produce and releases chemokines that initiate the recruitment of bone marrow cells during tissue trauma (Smith et al., 1997) and also produce and release interleukin 8 (IL-8) when stimulated with primary cytokines such as IL-1 α and IL-1 β to assist in neutrophil recruitment to the site of the wound (Schröder, 1995).

However, fibroblasts are largely responsible for the synthesis and remodelling of extracellular matrix laid down in the dermis during wound repair. Elastin and collagen fibre precursors are produced and secreted by human skin fibroblasts, playing a key role in the repair process when the dermal layer has been torn, cut or punctured (Giro et al., 1985). The classical view in dermal wound healing indicates that fibroblasts are locally recruited from the dermis to aid in the formation of the granulation tissue to fill the gap and then aid in the contraction of the wound. During the resolution of wound healing, fibroblasts differentiate into myofibroblasts, a cytoplasmic stress fibre that express alpha smooth muscle actin (α -SMA). This key

differentiation process, which will be explored in more detail below, represents a significant phase during wound healing and repair and it is the high contractile force generated by myofibroblasts that plays a considerable role in physiological tissue remodelling (Hinz, 2007). The long term preservation of skin is fundamental for sustaining life and therefore, as highlighted above, a detailed understanding of the processes involved in its maintenance and repair is imperative.

1.2 Wound healing

The skin can regenerate effectively, even after considerable damage has occurred, through an overlapping sequence of events during the wound healing process (refer to figure 1.2). In brief; through a combination of platelet aggregation, vasoconstriction and a release of pro-inflammatory signals, wound repair begins within moments of the initial injury. A robust inflammatory response occurs soon after; signalling the arrival of the immune response cells whose main role is to defend the host from invasion by microbes while clearing debris from the wound. The granulation layer is formed once fibroblast cells and collagen tissue have migrated over the matrix of the fibrin plug and keratinocyte cells have re-epithelialised. The granulation tissue, along with the dense population of macrophages, help contract the wound and reduce its size by bringing the wound margins closer together. Collagen tissue continues to be synthesised (exceeding the rate of collagen degradation) as the wound remodels and a scar is formed. The final process of wound healing is the resolution of the scar, where collagen levels return to normal. This can take between 6-12 months to complete fully, depending on the size and depth of the initial wound (see figure 1.3). The wound healing process is explored in further detail below.

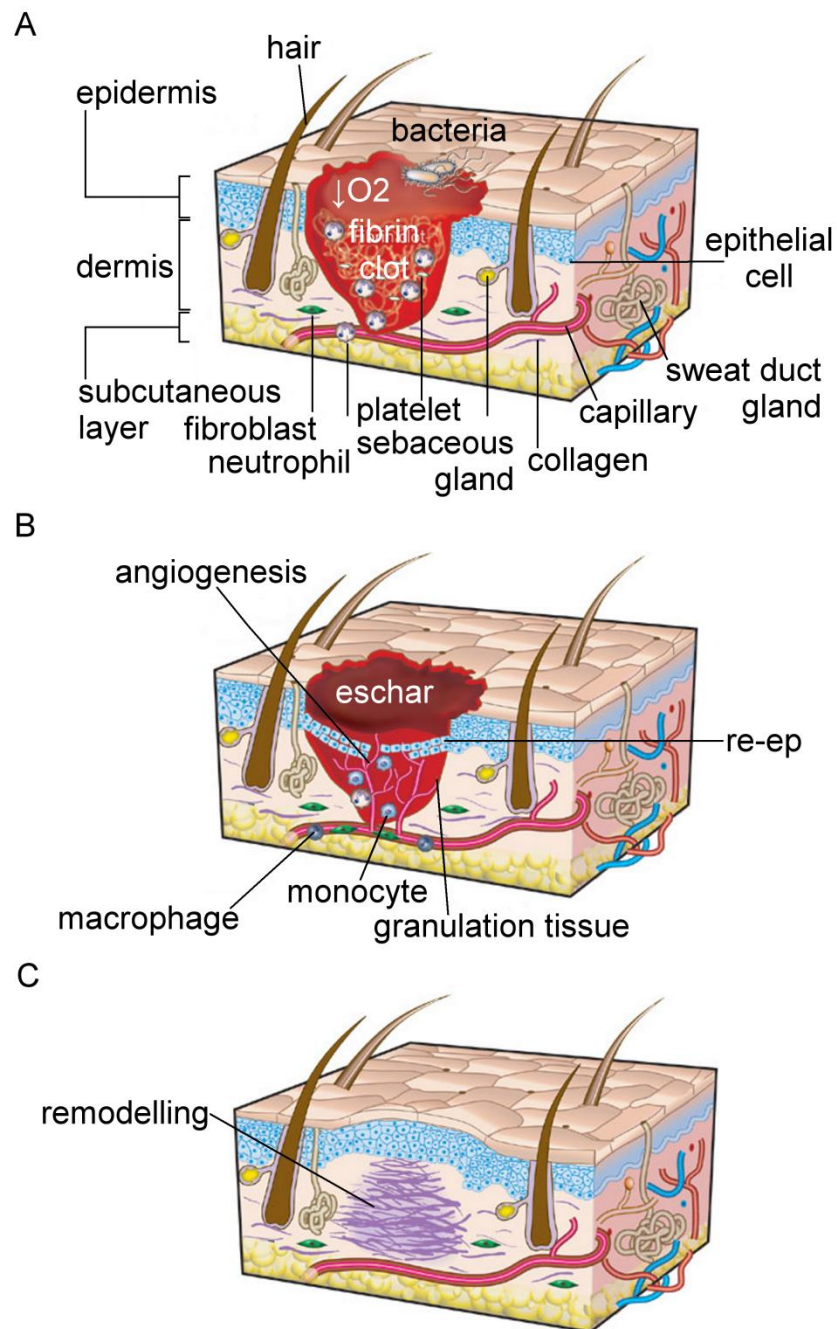


Figure 1.2 The stages of normal wound healing

There are three classic stages of wound repair; the immediate inflammatory response (A), new tissue formation (B) and remodelling (C). The diagram shows how the repair of skin requires the co-ordination of several sequential, yet overlapping, stages during wound healing. The processes involved in closing the wound begin immediately after the body's protective barrier has become damaged and ends through the resolution of the scar. Diagram adapted from Nature 453; 314-321 (Gurtner et al., 2008).

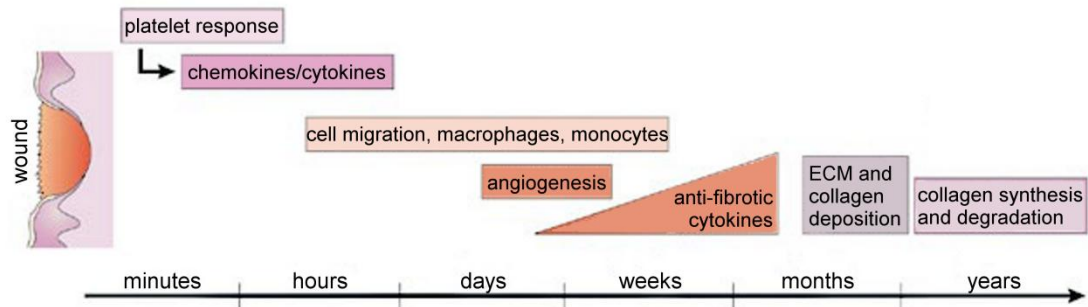


Figure 1.3 The phases of normal wound healing

Normal wound healing is governed by a series of overlapping sequences of events. Phases of wound healing begin with the initial platelet response, which occurs within minutes after trauma, and end in the final remodelling of the scar tissue, that can happen up to a year later. Diagram adapted from *Nature Reviews Cancer* 6; 702-713 (Bentzen, 2006).

1.2.1 Immediate response

The immediate response of wound repair launches as a consequence of both mechanical and chemical signals that are released en masse from the wound site. Damaged or stressed cells respond by activating and releasing various stress signals that can include signalling via the p38 mitogen activated protein kinases (MAPK), p44/42 MAPK and stress activated protein kinase / Jun N-terminal kinase SAPK/JNK pathways (Kobayashi et al., 2003, Yano et al., 2004). Phosphorylation of this cascade of signalling molecules starts a complex series of concurrent events that aim to restore normality in the damaged tissue. Endogenous molecules, such as damage associated molecular pattern molecules (DAMPs), are also released to further activate other cells in the damaged tissue area.

Damage extending through the epidermis into the dermis generally results in bleeding and therefore one of the earliest responses to injury is the stemming of blood loss from the damaged vessels through the formation of a clot. Normally isolated underlying collagen within the dermis is exposed to circulating platelets from

damaged blood vessels which bind together in the initial stages of clot formation. This binding is strengthened by von Willebrand factor (vWF). The coagulation cascade follows and is governed by the extrinsic pathway enabling a mass release of thrombin that converts fibronectin into fibrogen, the building block of a haemostatic plug. The blood clot serves as a temporary shield, protecting the exposed wound while providing a provisional matrix which cells can migrate to and through, and to which growth factors can bind. These growth factors include platelet derived growth factor, basic fibroblast growth factor (bFGF) and transforming growth factor beta (TGF- β). TGF- β is a protein that controls proliferation and differentiation and its signalling pathways are multi-potent in all stages of wound healing. Its roles are explored in detail below.

1.2.2 Inflammatory response

Within minutes of wounding, the inflammatory response begins with the rapid activation of resident immune cells (such as Langerhans and mast cells) in the wounded tissue and surrounding area (Springer, 1994). These cells release a torrent of cytokines and other inflammatory mediators (such as IL-1 and 6) that stimulate circulating leukocytes to actively leak from the blood vessels into the wound site in a process called extravasation. This process can be divided into four key stages; rolling, activation attachment and migration. In the first few moments of wound healing it is thought that vasodilatation occurs at the site of inflammation and this slows down and disturbs the blood flow, ultimately allowing neutrophil leukocytes to bump and roll along the endothelium. Surface receptors are activated on both neutrophils and the endothelium layer which catch rolling leukocytes in preparation to migrate through the vasculature wall. These leukocytes then migrate between endothelial cells in the blood vessel wall and are subsequently recruited to the site of wound damage (Hübner et al., 1996). TGF- β is also released at the site

of tissue damage and recruits neutrophils and monocytes in a positive feedback loop (Faler et al., 2006). These inflammatory cells are the body's first active defensive mechanism against infectious disease and foreign material. Neutrophils are activated and recruited into the wound and have primary roles in killing invading microorganisms using bursts of reactive oxygen species (Dovi et al., 2004). Monocytes drawn from the circulation later than neutrophils mature into macrophages (Martinez et al., 2006), a phagocytic cell whose role is to clear up matrix and cell debris. Unless the wound is particularly infected, the level of leukocytes falls after a few days and spent neutrophils are also phagocytised by macrophages (Haslett, 1992). Both neutrophils and macrophages serve as major producers of cytokines, chemokines and growth factors, amplifying earlier wound signals released by activated platelets and directing further cell and tissue migration (Theilgaard-Mönch et al., 2004).

1.2.3 Re-epithelialisation

Keratinocyte cells achieve re-epithelialisation through crawling and migrating along the edges of the wound while cutting a path through the fibrin clot. This process is regulated by the growth factors released by the inflammatory cells at the wound site and surrounding wounded tissue. Lower keratinocytes are anchored to the lamina by hemidesmosomes through integrin cell adhesions and in order for the cells to grasp hold of and crawl over the provisional wound matrix these attachments have to be dissolved and additional integrin proteins have to be formed (Cavani et al., 1993, Haapasalmi et al., 1996). These alterations to cell-cell and cell-matrix adhesions allow the advancing and migrating keratinocyte cells to progress from the basal membrane through the fibrin clot. Once beyond the free edge of the basal lamina, keratinocyte cells release interstitial collagenase matrix metalloproteinase 1 (MMP-1) enabling them to penetrate through the clot and along the interface

between the scab and the healthy dermis (Okada et al., 1997). A few hours after wounding and the onset of re-epithelialisation, the migrating keratinocyte cells experience a 'proliferative burst' which, although not crucial to the re-epithelialisation stage, can provide an extra reservoir of cells to aid in the wound healing process (Garlick and Taichman, 1994). New keratinocyte cells can also re-epithelise from hair follicle remnants if the wounding leaves a stump. Acting like a normal cut wound edge the cells will migrate into wound margins (Martin, 1997).

1.2.4 Proliferation, migration and contraction

Wound closure, through contraction, begins with the collective migration and proliferation of epidermal cells coupled with the recruitment of fibroblasts from the dermis. Fibroblasts are drawn in from several sources that can include the differentiation of circulating fibrocytes, bone marrow progenitor cells (Abe et al., 2001) and migrating fibroblasts from nearby healthy dermis (Hinz, 2007). A new stroma is formed which replaces the temporary fibrin clot once re-epithelialisation has finished. TGF- β acts as a chemo attractant to help pull fibroblasts into the wound site and stimulating them to proliferate (Faler et al., 2006).

In order for the migrating fibroblasts to crawl into the provisional matrix of the wound clot to lay down their own collagen-rich template, they must first down-regulate their own collagen receptors and up-regulate their own integrins that bind fibrin and fibronectin. Once in close proximity to the wound, TGF- β then drives differentiation of fibroblasts into α -SMA expressing myofibroblasts (Hinz et al., 2001a). The contractile bundles of actin within wound myofibroblasts enable tissue contraction and help draw the wound close. Actin also contributes to the synthesis, bundling and alignment of new collagen fibres with the capacity of generating strong contractile forces (Hinz et al., 2001b).

Angiogenesis is a critical component to successful wound repair that involves the generation of new blood vessels to supply the re-growing tissue with much needed nutrients and oxygen. The new microvascular network is apparent throughout the wound a few days after tissue damage. Known as granulation tissue due to its granular appearance, the growth of this wound connective tissue is promoted by FGF-2, vascular endothelial growth factor (VEGF) and TGF- β (Berse et al., 1992, Faler et al., 2006)

1.2.5 Resolution

Migrating and proliferating keratinocyte and fibroblast cells eventually meet their opposite counterparts as the wound completely closes. After several weeks the blood clot will have been shed (often leaving a depressed mark that indicates the site of injury) while dermal fibroblasts will continue to proliferate, gradually elevating the overlying epidermis and reducing the extent of the indentation. Normal architecture and complete resolution of the skin is rarely achieved in full. Dense collagen within the extracellular matrix will continue remodelling through a delicate balance of synthesis and degradation while the microvasculature within the scar tissue will refine and mature (Adams and Alitalo, 2007). Skin appendages, such as hair follicles and sebaceous glands which were damaged during the initial wounding, are not regenerated and are also replaced by fibrous tissue. The formation of non-flexible fibrous scar tissue completes the repair process but ultimately fails to restore the tissue to its complete original condition.

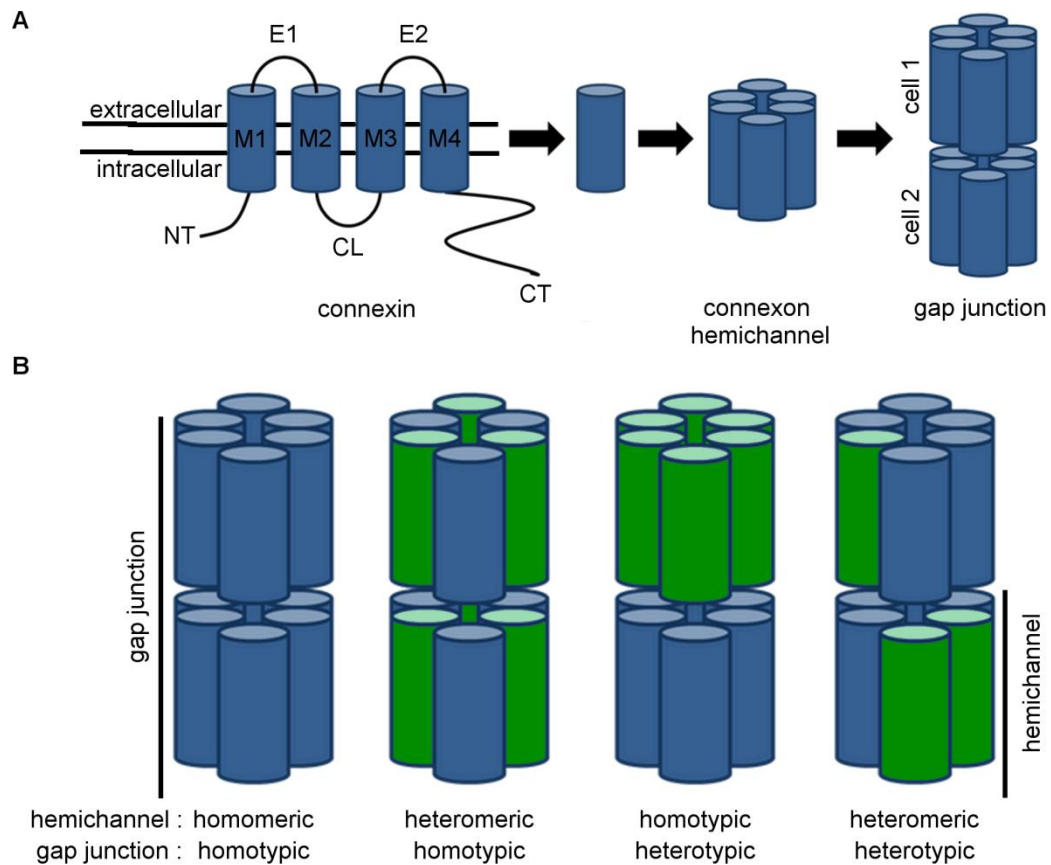


Figure 1.4 Gap junctions

(A) Four transmembrane loops (M1-4), two extracellular loops (E1-2), one cytoplasmic loop (CL), an amino terminus (NT) and a carboxyl terminus (CT) form one connexin. Six connexin subunits form a connexon (or hemichannel) and partner connexons in the plasma membrane of neighbouring cells dock to generate a gap junction. (B) Hemichannels can be arranged by homomeric or heteromeric connexins and gap junctions can be arranged by homotypic or heterotypic hemichannels. Diagram adapted from *Molecular Membrane Biology* 19; 121-136 (Evans and Martin, 2002a).

1.3 Communication in the skin: gap junctions and connexins

The highly complex sequence of events in skin wound healing relies heavily on the communication of signals released during the numerous, overlapping stages. Cell-to-cell communication is crucial in order for tissues to co-ordinate their processes

and mounting evidence now supports the theory that gap junctions play a pivotal role in the communication of these signals. Gap junctions are specialised connections that provide a regulated pathway linking the cytoplasm of adjacent cells and allow molecular signals to pass freely between the two. Each gap junction is made of two connexons from opposing cells, which in turn are composed of six protein subunits called connexins (figure 1.4A). Twenty connexin genes have been identified in rodents and 21 in humans, with at least ten detectable within the skin. Several genetic disorders of the skin have been continually attributed to mutations and defects in connexin genes. Through this substantial research, it has become apparent that connexins play an integral role in the various stages of wound healing.

1.3.1 History of gap junction research

The emergence of gap junction research began in the 1950s when it became apparent that neighbouring cells could communicate with each other via electrical pathways. Loewenstein was among the first to detect low-resistance ionic pathways between salivary gland of mosquitoes (Loewenstein et al., 1967). Watanabe and Weidmann also noted fast interaction of electrical activity, through resistant junctions between myocardial cells (Watanabe, 1958, Weidmann, 1969). However research in this topic during this time was dismissed as being controversial as it challenged the established idea that cells were individual entities, surrounded by electrically insulating membrane, that only communicated via the release of extracellular signals (Evans and Martin, 2002a).

In the early 1960s research emerged describing how non-excitabile cells could 'metabolically communicate' between their neighbours, through what are now known to be gap junctions. Enzyme deficient cells would normally perish in culture but when grown together with wild type cells, forming gap junctions with each other, the mixed cultures survived and grew at the wild type rates (Sybalska and Szybalski,

1962, Subak-Sharpe et al., 1969). This original research generated much enthusiasm and speculation into what type of cell-cell communication was occurring. This mechanism for sharing genetic ability paved the way for an exciting decade of gap junction discovery, further supporting the argument of gap junction communication existence between cells (Pitts, 1998).

Revel was the first to describe the hexagonal structure of junctions found between cells in the heart and the liver of mice (Revel and Karnovsky, 1967). Using electron microscopy, they eliminated their findings as being tight junctions (forming the closest contact between adjacent cells, mediating cell-cell adhesion and regulating transportation through the extra-cellular matrix) due to a 20 Å wide space found between these structures. Brightman further described the junctions in the vertebrate brain also noting that these structures were bisected by a median gap that was continuous with the rest of the interspace (Brightman and Reese, 1969). Through penetration of horse radish peroxidase into this gap, he further confirmed its polygon structure. It was from similar studies that the name 'gap junction' became common usage due to this unknown divide between neighbouring cells (figure 1.5).

Continued development of electron microscopy research also led to the further discovery of gap junction structures in the smooth muscle cells of sheep ureter, guinea pig and mouse heart (Uehara and Burnstock, 1970) and mouse liver (Goodenough and Revel, 1970). Gap junctions have now been identified in most tissues and only erythrocytes, platelets and sperm do not use this type of cell-to-cell communication (Evans and Martin, 2002a). However, it wouldn't be until 1986 that the biochemical structure of gap junctions would be identified (Paul, 1986).

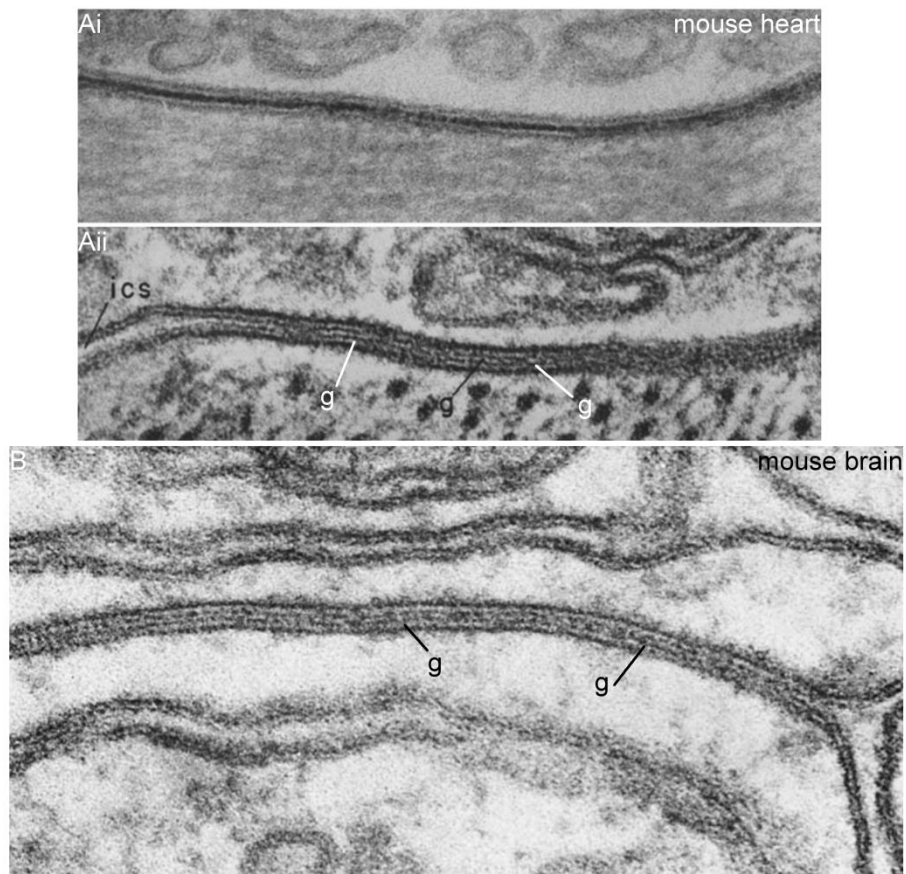


Figure 1.5 Gap junctions viewed under an electron microscope

High magnification of a longitudinal section from a block of mouse heart treated with lanthanum (Ai) or uranium (Aii) solutions. The normal intercellular space (ics) is reduced to a gap of about 20 Å wide (g) in the junctional area. Adjacent mouse astrocytic processes (B) connected by gap junctions (g). The gap is constant throughout the junctional area and is therefore unlikely to represent tight junctions. Diagrams from *Journal of Cell Biology* 33; C7-C12 (Revel and Karnovsky, 1967) and *Journal of Cell Biology* 40; 648-677 (Brightman and Reese, 1969).

1.3.2 Connexins, connexons and gap junctions

Gap junctional intercellular communication is facilitated by clusters of gated intercellular channels called gap junctions. Spanning the plasma membrane of two neighbouring cells gap junctions connect their cytoplasm and typically allow a rapid exchange of molecules up to 1000 Daltons (Da) in size. Gap junction subunits are

called connexins and at least 20 have been identified in vertebrates. All connexins share a common structure and have a highly conserved amino acid identity (Goodenough et al., 1996).

Each connexin protein is arranged as four hydrophobic transmembrane barrels (M1-M4), two extracellular (E1-E2) and three intercellular domains that include an amino-terminus (NT), a cytoplasmic loop (CL) and a carboxyl-terminus (CT). The E1 and E2 domains are the segments of the connexin protein that are involved in intercellular interactions. Each domain has three conserved cysteine residues joined by at least one disulfide bond between the loops.

By using specific anti-peptide antibodies to determine the topography of connexin 32 (Cx32) Rahman and Evans were the first to describe how cysteine residues were linked by disulphide bonds, both within and between loops (Rahman and Evans, 1991). Dahl, Werner and colleagues further suggested that the six cysteine residues found in the extracellular domain of gap junctions were crucial for gap junction formation (Dahl et al., 1992). Using mutational analysis in *Xenopus* oocytes they described that change of any of the conserved cysteine residues into serine residues resulted in an absolute loss of gap junction function. However further investigation using competing peptides against cysteine has shown no enhancement to the ability to delay gap junction formation (Warner et al., 1995) resulting in the theory that cysteine residues function is to maintain the extracellular loop topography within gap junctions instead of having a direct involvement in the docking process.

Like most plasma membrane proteins, connexins are synthesised by ribosomes and are delivered via vesicular trafficking from the endoplasmic reticulum (ER) via the Golgi apparatus. Connexins oligomerize after exiting the ER, most likely within the trans-Golgi network, to form hexameric connexons called hemichannels (Falk et al.,

1997, Diez et al., 1999, Musil and Goodenough, 1993). The hexameric structure of hemichannels was further suggested through calculating its molecular weight (Goodenough et al., 1996), as at the time the connexin molecular weight was thought to be between 26-27 kDa and the molecular weight of a hemichannel was between 140 and 170 kDa.

Kumar and Gilula were the first to propose that the gap junction family could be divided into two major subclasses, α and β (Kumar and Gilula, 1992). This decision was based on the evolutionary considerations, primary sequences and overall predicted topologic organization of the gap junction family. These included the observation that the connexin family is fairly conserved among vertebrates and that the major connexin classes appear to have evolved by gene duplications (Bennett et al., 1994, Cruciani and Mikalsen, 2006). Since then three more connexin subfamilies have been identified (figure 1.6). However, there was no attempt to imply that the class subdivision was based on functional properties of these gap junctions. During oligomerization connexins will arrange into homomeric (hemichannels assembled from the same connexin subtype) or heteromeric (hemichannels assembled from different connexin subtypes) hemichannels. Gap junctions can then be arranged into homotypic (gap junctions assembled from hemichannels formed of the same connexins) or heterotypic (gap junctions assembled from hemichannels formed of different connexins) channels, see figure 1.4B for more detail. Generally, heteromeric assembly only occurs between connexins of the same class (Evans and Martin, 2002a), such as between Cxs 26 and 32. The hemichannel is then transported to the plasma membrane and incorporated into the periphery of a pre-existing gap junction plaque.

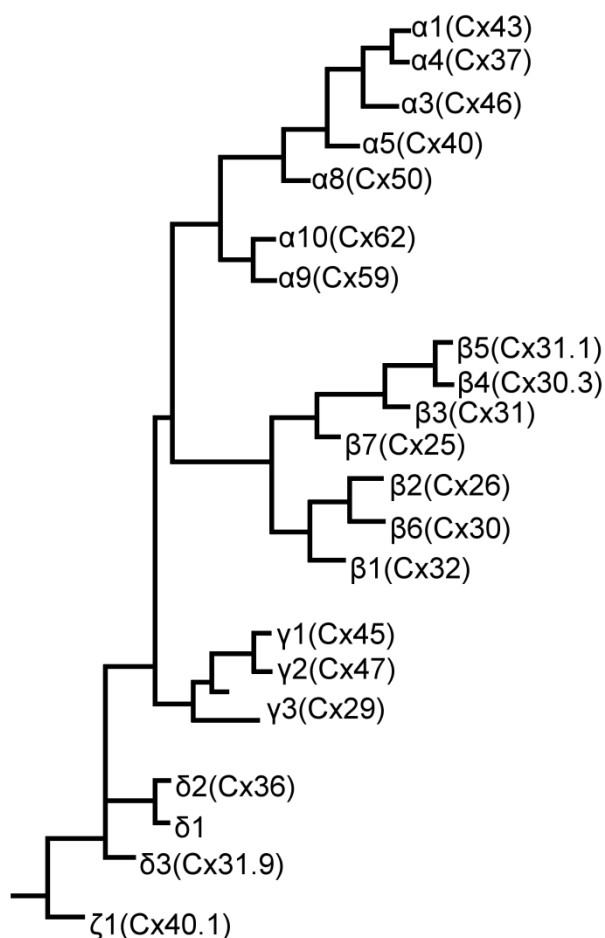


Figure 1.6 Subclasses of gap junctions

Diagram shows phylogenetic tree for several gap junctions. The branches indicate the relationships between and within the classes of α , β , γ , δ and ζ . Diagram adapted from *Evolutionary analyses of gap junction protein families in Biochimica et Biophysica Acta Biomembranes 1828; 4-14 (Abascal and Zardoya, 2013)*.

For many decades it was thought that hemichannels remained in a permanent closed state, until docked with their partner from a neighbouring cell, to avoid influencing cell death. However, in the last few years, research has shown how hemichannels can open in cultured cells and provide a signalling pathway between the cytoplasm of the cell and the extracellular environment (Evans et al., 2006). The first evidence that hemichannels could be in an open state was described in *Xenopus* oocytes (Paul et al., 1991). Cx46 hemichannels were opening, allowing

large permeability to cations and creating an osmotic imbalance that ultimately killed the cell. Hemichannels can open under several different external influences such as changes in pH (Trexler et al., 1999, Francis et al., 1999) but primarily open under stress. For example, low calcium (DeVries and Schwartz, 1992), metabolic (Contreras et al., 2002, John et al., 1999), mechanical (Stout et al., 2002) and ischemic (Shintani-Ishida et al., 2007) stresses can influence the opening of hemichannels.

It is still unclear as to whether surface hemichannels have different permeability properties to gap junctions formed of the same connexin (Saez et al., 2003). Hemichannels are known to be permeable to small fluorescent dyes such as Lucifer yellow and propidium iodide (Contreras et al., 2002, Kondo et al., 2000) so will be permeable to small molecules of the similar size and smaller. These include (NAD⁺) nicotinamide adenine dinucleotide (Bruzzone et al., 2001), (ATP) adenosine-5'-triphosphate (Stout et al., 2002), glutamate (Ye et al., 2003) and glutathione (Rana and Dringen, 2007). Through the release of small metabolites and secondary messengers, it is likely that open hemichannels have key roles in certain physiological and pathological conditions.

ATP released from Cx43 hemichannels can mediate the propagation of calcium signals in astrocytes and non-excitable cells (Stout et al., 2002) but can also cause cell death by acting on purinergic P2X receptors. This will trigger cellular permeation pathways to large molecules and ultimately cause cell death through osmotic imbalance (Poornima et al., 2012). In ischemic stress conditions Cx43 hemichannels speed up the mechanisms involved in cell death. This topic will be explored in more detail below and in chapter five.

In gap junction formation, the extracellular portions of connexons from opposing cells interact and dock to complete a fully formed channel. Successful connexon

docking occurs when non-covalent bonds seal the two opposing hemichannels and small molecules, passing through the channel, do not leak out into the extracellular space (Laird, 1996). Stability of a gap junction is correlated with the size of the gap junction plaque, which can grow to over 1 μm in diameter (Musil and Goodenough, 1991). Gap junction plaque size can vary depending on their location, for example in the inner ear gap junction plaques are numerous, often covering over 25% of the plasma membrane supporting cells, comprising more than 100,000 gap junctions (Forge et al., 2003a). Gap junction assembly relies heavily on correct connexin trafficking and there are a number of genetically inherited channel disorders which are linked directly to problems in connexin trafficking and gap junction assembly.

One of the most surprising early discoveries in gap junction research was that gap junction half life could be as short as five hours *in vivo* (Fallon and Goodenough, 1981). This research was later re-visited and confirmed *in vitro* showing even shorter half lives of 1.5-3.5 hours in Cxs 32 and 43 (Traub et al., 1987). This evidence and more suggests how gap junctions are not 'long-lived' structures but in fact undergo a continual process of formation and degradation (Laird, 1996). One of the first theories proposed on how gap junctions were internalised was based on annular gap junctions. These double-membrane intracellular structures were identified using electron microscopes and thought to be entire gap junctions that had originated from the cell surface (Larsen and Tung, 1978). Immunogold labelling confirmed that these structures were rich in connexin protein (Naus et al., 1993). Jordan and colleagues built on this research by using cells fluorescently tagged with Cx43-GFP, confirming that one of the two partner cells internalised the gap junction formed from both cells (Jordan et al., 2001). The degradation of internalised connexins occurs through lysosomal and proteosomal pathways in an ubiquitin-dependent fashion (Laing et al., 1997).

1.3.3 Innexins and pannexins

Innexins are a group of proteins that create gap junctions in invertebrates. To date 24 innexins have been identified in *C-elegans* but only eight in *Drosophila* (Phelan et al., 1998, Yen and Saier, 2007). Innexins exhibit gap junction like properties such as the ability to form intercellular channels in *Xenopus* oocytes and induce electrical coupling between oocyte pairs (Landesman et al., 1999). Like their connexin cousins, innexins have a common structure and are arranged as four transmembrane spanning segments, a cytoplasmic amino terminus and a carboxyl tail. Six innexin subunits create an innexon, a functional pore that links the cytoplasm of the cell with the extracellular environment (Bao et al., 2007). Stebbings and colleagues have shown through mRNA analysis that innexins can form hetero-oligomerization structures (Stebbing et al., 2000). Two innexons from opposing cells dock to form a continuous pore, in a gap junction formation, permeable to ions and small molecules.

Within the last 15 years, research within the gap junction field has become a little more complicated with the discovery of the pannexin. Being classed as a family within vertebrate and invertebrate proteins, pannexins can also create hydrophilic channels across a cell's plasma membrane (Panchin, 2005). Pannexins have a moderate sequence homology with invertebrate innexins but are evolutionary distinct from connexins. However, pannexins are structurally similar to both connexins and innexins, possessing four transmembrane segments and cytoplasmic amino-terminal and carboxyl-terminal domains. To date, three pannexins have been identified; Pannexins 1, 2 and 3 (Baranova et al., 2004).

Six pannexin subunits create a pannexon, connecting a cell's cytoplasm with the extracellular space, although there is contradicting evidence as to whether pannexons have the ability to form gap junction channels between neighbouring

cells. With only a few exceptions known to date, there is little evidence to suggest that pannexons do form gap junctions *in vivo* (Dahl and Harris, 2009). Functional conductance between paired *Xenopus* oocytes *in vitro* (Bruzzone et al., 2003) and dye transfer between unspecified channels in pannexin transfected cells (Vanden Abeele et al., 2006, Lai et al., 2007) have been the only evidence of pannexin based functional gap junction formation. There has been no evidence of successful dye or electrical coupling in cell cultures expressing Pannexin 1 (Huang et al., 2007), neither has there been convincing evidence of punctate staining, found typical in immuno-analysis of gap junction plaques (Locovei et al., 2006). Hence the only indications that pannexin subunits can form gap junctions are in those cases where there is an over expression of the protein. Perhaps pannexons are not designed for binding to a partner in a neighbouring cell (Boassa et al., 2007, Dahl and Locovei, 2006). *Xenopus* oocytes wouldn't naturally pair *in vivo*, but within a forced expression environment there may be a weak tendency that would be enough to exert a functional role that would never occur in nature.

On the other hand there is mounting evidence that suggests pannexins can form functional non-junctional plasma membrane channels (Dahl and Locovei, 2006). Along with their distant relative, the connexin hemichannel, the pannexon pore is highly permeable to ATP (Locovei et al., 2006, Ransford et al., 2009). This function is so strong in pannexons that ATP release in this manner has been shown to carry current (Dahl and Harris, 2009). The functional properties of pannexons overlap significantly with those of connexin hemichannels and to date there are no drugs to discriminate between the two. For this reason, care must be applied when interpreting data of specific conditions that may involve both protein classes.

For the purpose of this investigation, this thesis will restrict its focus to the connexin family of proteins.

1.3.4 Function of gap junctions

1.3.4.1 Gap junction communication

Gap junctions allow the direct passage of secondary messengers, small metabolites and electrical signals between the cytoplasm of connected, neighbouring cells. In excitable cells, such as neurons and cardiomyocytes, gap junctions allow electrical coupling, allowing the generation of synchronized and rapid responses. In addition to the secondary messengers and metabolites that transfer through hemichannels as described above (including NAD^+ , ATP, glutamate and glutathione) other secondary messengers and metabolites that can transfer between non excitable cells via gap junctions include calcium (Ca^{2+}) ions (Sáez et al., 1989a), (IP3) inositol triphosphate (Sáez et al., 1989a), (cAMP) cyclic adenosine monophosphate (Sáez et al., 1989b) and (ADP) adenosine diphosphate (Goldberg et al., 1998).

While gap junctions all serve a common role in allowing these signals to pass freely between neighbouring cells, there is a diversity of function that can be attributed to the different connexins expressed in a gap junction, as a result of hetero-oligomerization (White, 2003, Goldberg et al., 2004). For example cGMP and cAMP will pass equally well through homomeric channels of Cx32 but cGMP passes 'more effectively' through heteromeric channels of Cxs 32 and 26 (Bevans et al., 1998). This suggests preferential selectivity of Cx26 towards cAMP. Channels composed of Cxs 43 and 32 will allow the passage of glucose, glutamate, ADP and adenosine but generally homomeric channels of Cx43 will transfer these molecules better than channels of Cx32 and transfer ATP over 100-fold better than channels formed solely of Cx32 (Goldberg et al., 2004). Gap junctions have also been known to demonstrate charge selectivity as homomeric channels of Cx26 will favour cation transfer while homomeric channels of Cx32 prefer the passage of anion currents (Veenstra, 1996).

Functional assays of gap junction communication mainly fall into two categories; the first measures the transfer of molecules between neighbouring cells. This can be assayed through metabolic cooperation as described above or through monitoring the transfer of fluorescent dyes between communicating cells. Cells are injected with dyes with a typical weight of 500 Da (i.e. Lucifer yellow, MW = 443 Da) that will comfortably transfer through gap junctions. To establish whether the cells are functionally coupled by gap junctions, a time dependent diffusion of the molecules to neighbouring cells is monitored. A control would include the co-injection of a larger fluorescent dye such as rhodamine-dextran (MW = 10,000 kDa) which is too large to transfer between neighbouring cells via gap junctions. The second category of assays is designed to measure the electrical currents carried by ions and has been greatly improved through advancements in patch-clamp method technology (Goodenough et al., 1996).

Gap junctions exist in nearly every mammalian cell (Saez et al., 2003) and have roles in several physiological functions, including excitable cell contraction, cell growth and differentiation, cell death under pathological conditions and wound closure. Connexin defects within any of these systems can often cause severe disease and death. Current literature reports at least eight human diseases that are caused by germline mutations in the connexin family (Laird, 2006).

1.3.4.2 Gap junction mutations

The first connexin mutation was discovered in the Charcot Marie-Tooth X syndrome, a peripheral neuropathy disease that causes severe limb weakness (Bergoffen et al., 1993). Using Southern and Northern blot analysis, Bergoffen and colleagues were the first to describe base change mutations in the gene coding for protein Cx32 (GJB1). Since this first report, over 400 mutations in the gene GJB1 have been described that cause Charcot Marie-Tooth X syndrome. Many of these mutations

prevent normal Cx32 transfer to the membrane, whereas others can cause complete abolishment of Cx32 expression by affecting the promoter of the GJB1 gene or the translation of Cx32 mRNA (Scherer and Kleopa, 2012). These mutations ultimately lead to the disruption of Cx32 gap junction function in Schwann cells in peripheral nerves, leading to the failure of ion and small molecule transfer across the compact myelin. This results in myelin disruption, axonal degradation and progressive atrophy of distal muscles.

Cardiac tissue relies heavily on gap junction facilitated action potential propagation, to ensure symmetrical rhythmicity of the heart. Having three key Cxs 40, 43 and 45, (Kanter et al., 1992) it is not surprising that mutations in these key cardiac proteins can cause fatal ventricular arrhythmias present in cardiac diseases of the heart. For example, mutations on the carboxyl tail of Cx43 can abolish left-right symmetry seen in the severe heart disease viscera-atrial heterotaxia (Dasgupta et al., 2001). Knock-out mouse models of Cxs 40 (Simon et al., 1998, Bevilacqua et al., 2000), 43 (Reaume et al., 1995) and 45 (Nishii et al., 2001) confirm that gap junctions play a crucial role in cardiac conduction.

Freeze fracture studies have shown that gap junctions reside in large numbers within the inner ear epithelium in reptiles, birds and mammals (Forge et al., 2003a) and screening using reverse transcriptase polymerase chain reaction (RT-PCR), Western blots and immunohistochemistry has revealed four connexin subtypes in the mammalian inner ear (Cxs 26, 30, 31.1 and 43). The most abundant of these connexins, Cxs 26 and 30, co-localise to form heterotypic connexons in non-sensory epithelial cells (Forge et al., 2003b). One supposed function of gap junctions composed of Cxs 26 and 30 within the inner ear is to maintain the endocholear potential by recycling endolymphatic K^+ ions from the sensory hair back to the endolymph (Kikuchi et al., 2000). Recessive mutations in the gene coding for Cx26,

GJB2, have been continually associated with non-syndromic hereditary deafness (Iossa et al., 2011).

It is estimated that mutations in gene GJB2 are responsible for half of all non-syndromic hereditary deafness. Two of the most common genetic mutations responsible for deafness include mutations in 35delG (30delG) and 16delT. The first introduces a premature stop codon within the amino terminus at amino acid position 13, while the second introduces a premature stop codon within the first extracellular loop at amino acid position 56 (Martin et al., 1999). The properties of Cx26 mutations have been examined in transfected HeLa cells (Marziano et al., 2003) and *Xenopus* oocytes (White et al., 1998) revealing impaired intracellular trafficking and electrical deficiency which results in non-syndromic hereditary deafness.

Mutations that disrupt Cx26 are primarily confined to the inner ear (non-syndromic) but can occur with other clinical features (syndromic). One such clinical feature is hyper-thickening and increased roughness and browning of the epidermis that can be found in Keratitis-Ichthyosis Deafness (KID) and Hystrix-Like Ichthyosis Deafness (HID) syndromes (van Steensel, 2004, Richard, 2005). Both are clinically characterized by skin lesions (known as erythrokeratoderma), vascularising keratitis and mild to profound hearing loss. Another such disease is Vohwinkel's Syndrome that is characterised by disturbed epidermal differentiation, (manifested by hyperkeratosis on the soles of feet, palms of hands and knuckles) and pseudoainhum with spontaneous digital amputation. Like in KID and HID syndromes patients also suffer with moderate to profound hearing loss (van Steensel, 2004, Waller and Maibach, 2005, Richard, 2005).

One well characterised, yet rare, disease that has been attributed to mutation of the gene coding for Cx31 is Erythrokeratoderma variabilis (EVK) (Gottfried et al., 2002, Di et al., 2002, Common et al., 2005). Sufferers of EVK experience transient

erythema coupled with generalised hyperkeratosis (figure 1.7). The erythema patches are usually of variable intensity (hence the name of the disease) and can arise on normal skin as well as on hyperkeratotic plaques. These red patches of skin can last anything between a few hours and a few days. However, the hyperkeratosis is persistent and EVK patients will suffer from yellow-brown thickening of their skin, which can sometimes scale and peel (Brown and Kierland, 1966, Vandersteen and Muller, 1971). Being autosomal dominant, EVK can affect entire families and has enabled extensive genetic research to have been carried out (Richard et al., 1997). The genetic mutation associated with EVK is on the gene GJB3, which encodes for Cx31 (Richard et al., 1998). In total six out of eight GJB3 mutations have been identified in the 20 families investigated. The mutations involve either disruption to the amino terminus or to the transmembrane domains and interfere with the assembly and functional properties of Cx31. Mutations of GJB3 have also been found in progressive high-tone hearing loss. This mutation interferes with the E2 domain, preventing Cx31 connexons from docking to neighbouring partners (Richard, 2000).

Currently 28 mutations of Cx43 (GJA1) have been identified but it is only one frameshift mutation within the c-terminus that results in the loss of many phosphorylation and protein-binding sites. The autosomal dominant mutations results in the pleiotropic development disorder oculodentodigital dysplasia (ODDD). The disease is clinically characterized by patients exhibiting soft tissue fusion of the digits, craniofacial abnormalities, small eyes with lens and cornea defects, loss of teeth enamel, brittle nails, hair abnormalities and skin disease. However, since Cx43 is the most ubiquitous connexin in the human body, it is remarkable how patients' symptoms are not more severe. Sufferers appear to live long lives in relatively good health (Laird 2006, 2014).



Figure 1.7 Clinical and histological features of EVK

(A-C) Clinical features of *Erythrokeratoderma variabilis* (EVK). Sufferers experience hyperkeratotic plaques on their lower extremities (A-B) and palmoplantar keratoderma with peeling on soles of their feet (C). Histological section of EVK shows hyperkeratosis (D). Diagrams from *Experimental Dermatology* 9; 77-96 (Richard, 2000) and *Acta Dermato Venereologica* 90; 274-278 (Zhang et al., 2010b).

Connexins are expressed in all cells linked with tissue repair, with strong evidence indicating they mediate changes in migration, proliferation, inflammation and contraction (explored in further detail below). It is clear that defects in the connexins involved in these processes can give rise to sensorineural hearing loss and associated hyper-proliferative skin disorders. This shows that there is a complex relationship between the changes of the genotype and the phenotypic appearance of connexins and there is mounting evidence for a crucial role in connexin based communication in the skin

1.3.5 Connexins in the intact skin

In 1988, Salomon and colleagues were the first to describe how cells in normal and differentiated skin could communicate with each other through gap junctions (Salomon et al., 1988). By microinjecting keratinocyte and fibroblast cells with the gap junction permeant dye Lucifer yellow, they demonstrated that the fibroblast cell was the most communicative within the skin. However, cell-to-cell communication was not observed between the epidermal and dermal sub-units. Gap junction intercellular communication is governed by at least ten different connexin subtypes within the skin and although the spatial and differential expression pattern is similar (but not identical) between rodents and humans, experimental discoveries may not be comparable between the species. These include Cxs 26, 30, 30.3, 31, 31.1, 32, 37, 40, 43 and 45. Only Cxs 26, 30, 31.1 and 43 will be described in greater detail below (figure 1.8).

Using antibodies against different connexin epitopes, Western and Northern blots, and mRNA expression analysis, there is now an extensive map of connexins within the rodent and human skin (Guo et al., 1992, Butterweck et al., 1994, Kandyba et al., 2008). Cxs 26, 30, 31.1 and 43 are highly expressed in the differentiating strata spinosum and granulosum of the foetal rodent skin but only Cx43 can be found in

the stratum basal. Rodent hair follicles and sebaceous glands express Cxs 26 and 43 whereas sweat glands express just Cx26. Dermal fibroblast cells predominantly express Cx43. During the maturation of rodent skin, Cx26 down-regulates in the upper epidermal layers, whereas Cx31.1 up-regulates. However, no difference in gap junctional communication is observed (Kamibayashi et al., 1993, Goliger and Paul, 1994).

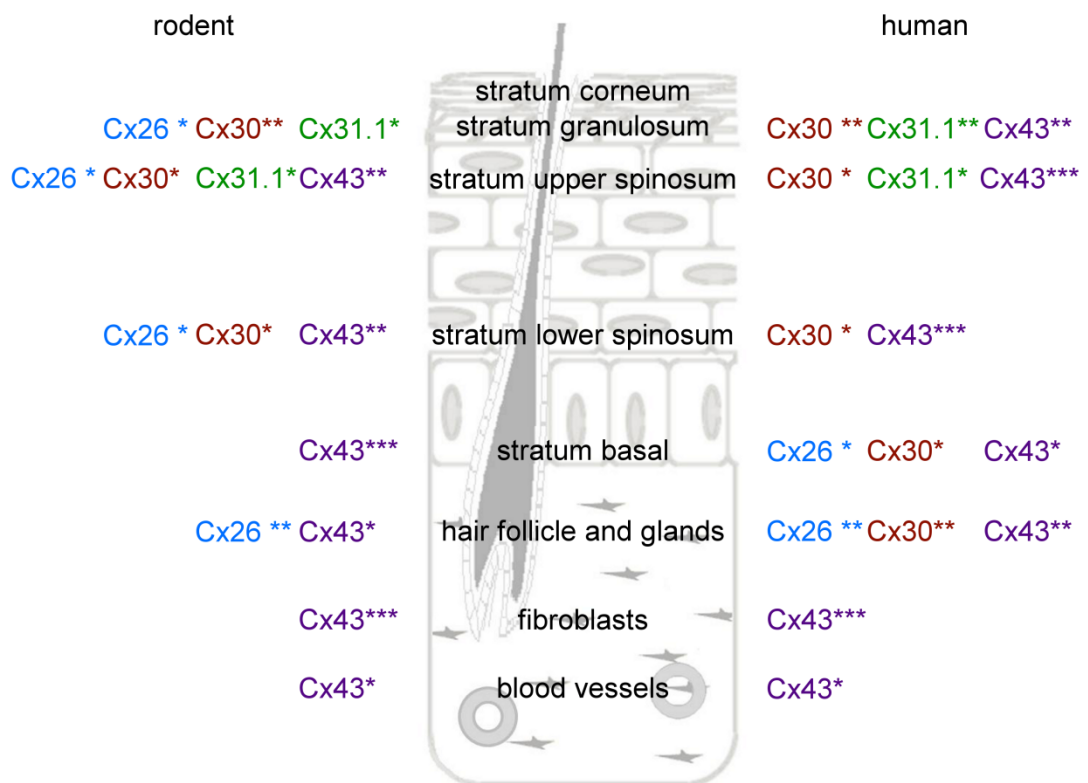


Figure 1.8 Connexin profiles in mature rodent and human skin

Original diagram shows the skin labelled with key areas of interest. Connexin expression within the skin is divided into four key connexins (Cxs 26, 30, 31.1 and 43) which are further divided between rodents and human expression. Intensity of expression is indicated by *, increasing * indicates increasing expression of relevant connexin. Refer to text for references.

Cx43 is the most widely expressed and ubiquitous connexin found in human skin (and indeed in the rest of the body). In the epidermis Cx43 is expressed throughout

the strata spinosum and granulosum and in a punctate and partly linear pattern, along the periphery of keratinocytes, in the stratum basal. Cx43 is also found in the sebaceous glands and abundantly in both the lower regions of the hair follicles and the dermal fibroblasts (Guo et al., 1992, Salomon et al., 1994, Tada and Hashimoto, 1997). Cx30 can be found in all layers of the epidermis (Brandner et al., 2004). Cx26 is barely detectable in the epidermis, except in the stratum basal (Locke et al., 2000), although staining can be 'patchy' and mainly in the skin of palms and soles. However, it is found in copious amounts within sweat glands and the base of hair follicles.

1.4 Connexin dynamics in normal wound healing

There are several stages during wound healing that rely heavily on the communication of signals to successfully complete wound closure. Gap junctions provide specialised connections between neighbouring cells that allow molecular signals to pass freely between the two. At least ten gap junction protein subunits have been found within the skin and at least four (Cxs 26, 30, 31.1 and 43) play integral roles during the wound healing process. Goliger and Paul were the first to describe connexin location and intensity in developing and mature rat skin (Goliger and Paul, 1994) and subsequently, among others, went on to describe the dynamics of these key connexins during the wound healing response (Goliger and Paul, 1995, Saitoh et al., 1997, Coutinho et al., 2003). Generally using Western blots and immunofluorescence, these researchers have described, in detail, the dynamics of the four key connexins during wound healing, linking their changes in expression and intensity with particular stages of the wound healing process (figure 1.9).

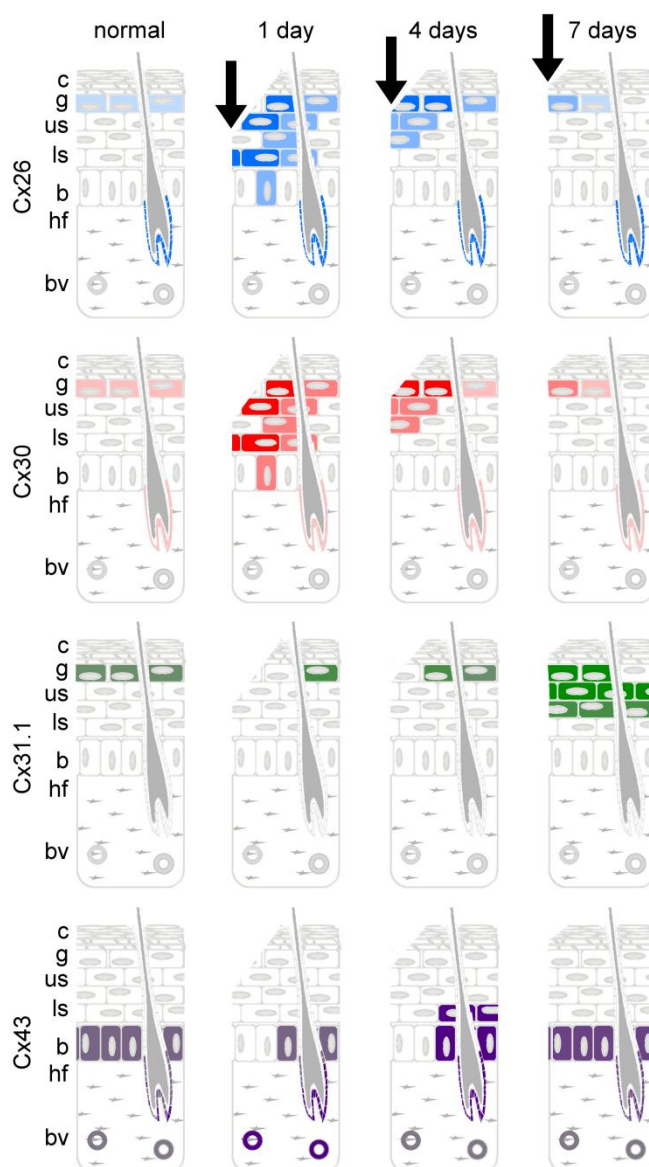


Figure 1.9 Dynamics of connexins during wound healing

Summary diagram that shows connexin dynamics in rodent skin during wound healing. Distribution of Cx26 (blue), Cx30 (red), Cx31.1 (green) and Cx43 (purple) are shown in normal, wounded and healing skin. Shading is used to indicate the level of expression, with darker shaded indicated higher levels of expression. Connexin expression within the hair follicles is also shown. Connexin expression is shown one, four and seven days after wounding. C = stratum corneum, g = stratum granulosum, us = stratum upper spinosum, ls = stratum lower spinosum, b = stratum basal, hf = hair follicle, bv = blood vessel. Diagram adapted from *Cell Biology International* 27; 525-541(Coutinho et al., 2003).

1.4.1 Connexin response in the epidermis during wound healing

In 1978, Gabbiani and colleagues were the first to observe a significant increase in the number of gap junctions present at the epidermal cell surface in wounded rat skin (Gabbiani et al., 1978). Using the same electron microscopy technology, Andersen and partners also noticed a large number of gap junctions in wounded guinea pig palate epithelium, when compared to non-wounded tissue (Andersen, 1980). They linked this increase in gap junction number with the process of epidermal differentiation. During the initial wound healing response, epidermal keratinocytes undergo dynamic processes as a result of the stress signals released during wounding. These include the disassembly of desmosomes, the redistribution of integrin receptors and the formation of actin bundles in the early stages of wound healing and hyper-proliferation during the later stages.

Cx26 is normally found in the stratum granulosum and stratum spinosum in relatively low levels in non-wounded rodent tissue. Within hours of wounding these levels of Cx26 decrease further at the wound edge, however Cx26 remains at a detectable level in the strata granulosum and upper spinosum near, but not at, the site of the wound. Approximately 24 hours after wounding Cx26 is greatly up-regulated in the middle and upper stratum spinosum and strata granulosum at the wound edge, but not in the stratum basal. This elevated expression is maintained throughout the migration of epidermal keratinocyte cells into the wound, linking heavily with the process of re-epithelialisation and the hyper-proliferation of the epidermis. Cx26 expression returns to pre-wounding levels between 7 and 12 days after wounding in rodent skin. It has been noted how Cx30 expression follows a very similar dynamic to Cx26 expression during rodent wound healing (Coutinho et al., 2003).

Expression of Cx31.1 can typically be found in very low levels, within the stratum spinosum and stratum granulosum in non-wounded epidermis in rodent skin. Following wounding in rodents, the expression of this connexin drops at the wound edge in a similar pattern to Cxs 26 and 30. However, unlike the significant up-regulation of Cxs 26 and 30 in migrating epidermal keratinocyte cells a day after wounding, Cx31.1 remains very low in proliferating and regenerating areas. Cx31.1 remains almost undetectable until six to seven days after wounding, where its expression significantly rises in intensity in the strata granulosum and spinosum (Coutinho et al., 2003). Nagata and colleagues note that in guinea pig epidermis, cells undergo apoptosis at a similar time, suggesting a role of Cx31.1 in terminal differentiation of keratinocyte cells (Nagata et al., 1999). Cx31.1 returns to pre-wound levels approximately 12 days after initial wounding.

Cx43 is moderately expressed in the strata basal and spinosum in non-wounded rodent tissue. Similar to the above connexins, Cx43 expression drops at the wound edge within the first hours after wounding in rodents. Cx43 expression remains absent in all proliferative and regeneration areas within the epidermis, similar to Cx31.1, until four days after wounding. Cx43 expression then significantly up-regulates in the proliferating epidermis and remains elevated until six to seven days after wounding, when expression returns to pre-wounding levels (Coutinho et al., 2003). It has also been noted in rodents that Cx43 expression is dynamic in dermal fibroblast cells and blood vessels during the wound healing process (Mori et al., 2006).

1.4.2 Connexin response in the dermis during wound healing

During the early inflammatory response, within hours of initial wounding, circulating leukocytes, prompted by a cascade of inflammatory signals, invade the wound site. This process of extravasation requires blood vessels to become more permeable to

the inflammatory molecules and ultimately causes dermal tissue to swell. Cx43 significantly up-regulates in wound edge blood vessel epithelium as inflammatory signals attract Cx43 expressing neutrophils (Coutinho et al., 2003). This up-regulation seen in blood vessels is maintained throughout the inflammatory response within the dermis and expression doesn't reduce until two days after wounding, returning to normal levels by day 12. The leukocyte-leukocyte and leukocyte-endothelial cell communication, facilitated by hemichannels and gap junctions composed of Cx43, is crucial for the transmigration of inflammatory cells from the vasculature to the wound site.

Gap junctions, hemichannels and connexins have been identified in leukocytes and vasculature endothelial cells and there is mounting evidence of functional communication in homotypic and heterotypic populations of these cell types (Oviedo-Orta and Howard Evans, 2004). Cxs 37, 40 and 43 have been identified in the vascular endothelium in both *in vitro* and *in vivo* settings (Polacek et al., 1993, Polacek et al., 1997, van Kempen and Jongsma, 1999). Intracellular communication between aggregated lymphocytes was first established in the early 1970s as shown by ion flow and intracellular communication through low resistance junctions (Hülser and Peters, 1971, Hülser and Peters, 1972). Levy and colleagues also reported that in a linear orientation, macrophages communicated via cytoplasmic bridges and possessed electrical coupling properties (Levy et al., 1976). Several years later, hamster leukocytes were seen to express Cx43 when treated by inflammatory stimuli (Jara et al., 1995). Human PMNs were also reported to express Cx43 when stimulated by inflammatory molecules and form functional gap junctions (Branes et al., 2002). Similar results were observed in human monocytes and macrophages when activated with lipopolysaccharides (LPS). Not only did these cells create functional gap junctions formed of Cx43 but their gap junction communication was inhibited by 18 α -Glycyrrhetic acid, a known gap junction communication inhibitor

(Eugenín et al., 2003). Time dependent and bi-directional cross talk between populations of PMNs and human umbilical vein endothelial cells (HUVECs) have also been observed (Zahler et al., 2003). Oviedo-Orta, Evans and colleagues were the first to observe Cx43 expression in non-activated lymphocytes (Oviedo-Orta et al., 2000). Using mRNA analysis they reported Cx43 expression in peripheral blood lymphocytes, tonsil lymphocytes and tonsil derived T and B lymphocytes. Activation using *in vitro* inflammatory stimuli resulted in T and B lymphocytes expressing more Cx43. Functional analysis studies using dye transfer confirmed gap junction communication between both homologous and heterologous co-cultures of T and B lymphocytes. Incubation with gap junction communication blockers decreased dye transfer and therefore confirmed gap junction based communication between these cells. These results suggest that gap junctions and their connexins have a heavy involvement in the complex sequence of events of the early inflammatory response.

Two key factors play important roles in the movement of cells during extravasation. The first is adhesion of leukocytes to endothelial cells before migration. The second is the role chemokines play in controlling where leukocytes travel to once they have left the bloodstream. In the research discussed here it is clear that PMNs, macrophages, monocytes, lymphocytes and endothelial cells of vascular walls express connexins and form functional gap junctions to enable cross talk between homologous and heterologous populations of these cells (Polacek et al., 1993, Jara et al., 1995, Polacek et al., 1997, van Kempen and Jongasma, 1999, Branes et al., 2002, Coutinho et al., 2003, Zahler et al., 2003, Saredine et al., 2009).

In an elegant study, conducted by Oviedo-Orta, Evans and colleagues, trans-endothelial migration was investigated using an *in vitro* model of heterotypic populations of endothelial cells and lymphocytes in a chamber system (Oviedo-Orta et al., 2002). HUVECs were grown on tissue culture inserts as a monolayer and

loaded with the dye Calcein-AM. Once confluent, the HUVEC tissue inserts were placed in a new plate containing a monocyte culture supernatant and an upper chamber was filled with a suspension of a mixed lymphocyte population. Attracted by the chemokines released by the monocyte culture, lymphocytes transmigrated through the monolayer of HUVECS to the lower chamber. Fluorescence-activated cell sorting (FACS) analysis was then carried out on the transmigrated cells and it was reported that lymphocytes had communicated with the endothelial monolayer and had accepted dye transfer. In a similar study using PMNs and HUVECS, conducted by Zahlar and colleagues, it was also reported that there was a bi-directional cross talk between populations of PMNs and HUVECS while PMNs transmigrated through a layer of HUVECs in a chamber system (Zahler et al., 2003).

Once neutrophils have left the bloodstream, they are governed by chemo-kinetic migration to determine where they next move to. Upon wounding, tissue macrophages release a torrent of cytokines such as IL-1, IL-6 and TNF α that have roles in vasodilatation, increasing vascular permeability and crucially recruiting monocytes and neutrophils to the wound site. Work carried out Oviedo-Orta, Evans and colleagues has shown that human T and B lymphocytes express Cx43 and incubation with gap junction communication blockers significantly reduced the synthesis of key chemokines IL-2, IL-10 and IFN γ , and immunoglobulin's IgA, IgG and IgM (Oviedo-Orta et al., 2001). It was thought that the reduction in immunoglobulins was linked to the reduction in IL-2 synthesis as lymphocytes stimulated with IL-2 will release these antibodies.

Gabbiani first described gap junctions between myofibroblasts (Gabbiani et al., 1978) and Salomon further described extensive coupling existed between dermal fibroblasts (Salomon et al., 1988). Using rodent models it has also been shown that

dermal wound edge fibroblasts naturally down-regulate Cx43 as they become migratory and lay down granulation tissue (Mori et al., 2006).

Brandner and colleagues compared murine wound healing connexin profiles with those of human and demonstrated that in acute wound healing there was an initial down regulation of Cxs 26, 30 and 43 (Brandner et al., 2004) confirming the work of Coutinho (Coutinho et al., 2003). Subsequently, one to two days after wounding, Cx26 and 30 were found in the regenerating epidermis whereas Cx43 remained low, following a similar pattern to the murine model (Coutinho et al., 2003). The lack of Cx43 at the wound margin in the early stages of healing seems to play an important role irrespective of species. It is clear that without the regulation of these connexin proteins, the natural system of wound healing stages would not progress and consequently it has come to light in recent years of research that connexins within the skin could play a vital role when wounds do not heal in a normal and timely manner (Becker et al., 2012).

1.5 Connexin dynamics in abnormal wound healing

1.5.1 Introduction to chronic wounds

Chronic wounds are those that do not heal in an orderly set of phases, nor in a predictable amount of time, the way in which most acute wounds do. Chronic wounds are clinically described as wounds that do not heal within 1-2 months or that have not shown a 20-40% reduction in wound area after one month of wounding (Flanagan, 2003). Non-healing wounds are characterized by prolonged inflammation, re-epithelialisation failure and defective re-modeling of a wound. A large percentage of chronic wounds fall into three main etiological categories; diabetic foot ulcers, venous leg ulcers and pressure ulcers (figure 1.10). A smaller fourth group covers ulceration caused by arterial deficiency or radiation damage

(Mustoe, 2004). As chronic wounds take a long time to heal, do not heal completely or constantly re-occur, independence and quality of life of the sufferer is compromised.

The three main types of chronic wounds are causing a major threat to the public health services and global economy, significantly contributing to the growing escalation in health care costs. The average age of a patient that develops a chronic wound is over 60 (Mustoe, 2004) and with the aging population in both Europe and the United States is expected to increase by 13-15% in the coming years (Sen et al., 2009), the global care costs for chronic wounds has been predicted to rise to \$13-15bn annually (Siddiqui and Bernstein, 2010). In the UK alone, treatment and after-care of chronic wounds costs the government £2-3.1bn per year, amounting to 3% of National Health Service (NHS) expenditure (Harding and Queen, 2010). This burden will only increase as the nation continues to make poor lifestyle choices, such as a lack of physical activity and poor diet, which will result in a rise in obesity and diabetes – some of the key precursors to the development of a chronic wound.

1.5.1.1 Diabetic foot ulcers

Diabetes mellitus is a metabolic disease in which a person suffers from elevated glucose levels, either due to inadequate production of insulin or because tissue no longer responds to the insulin produced. Chronic diabetic foot ulcers (figure 1.10A) arise from complications of the disease (such as peripheral neuropathy) causing arterial damage and decreased sensation to the extremities of the body. Abnormal forces or accidental trauma to the toes and feet can lead to broken skin. Coupled with tissue ischemia, continued trauma and poor management of the wound, chronic diabetic foot ulcers form which are very slow and difficult to heal. Estimates suggest that more than 15% of diabetic sufferers will develop a diabetic foot ulcer, frequently debilitating and often requiring amputation (Jeffcoate and Harding, 2003). The

prevalence of diabetes is on the rise prompting warnings from global health experts who predict a diabetic epidemic if changes do not occur.

Early studies estimated that by the year 2000, diabetes would be diagnosed in 2.8% of the global population and forecasted that by 2030 over 4% of the world would be diabetic (Wild et al., 2004). However, worldwide prevalence of diabetes in 2010 was 6.4% (Frag and Gaballa, 2011), already greatly exceeding previous projections, and new forecasts now predict global incidence of diabetes to reach nearly 440 million people by 2030, nearly 8% of the predicted global population (Shaw et al., 2010, Bruno and Landi, 2011). As the estimates continually increase the only explanation is that prevalence of diabetes is also generally increasing. Although diabetic foot ulcers are the least common chronic wound, 12% of global health expenditure is already spent on diabetes and its complications (Zhang et al., 2010c). At least 24,000 people in the UK are diagnosed with a diabetic foot ulcer annually, costing the NHS millions of pounds each year (Harding et al., 2002).

1.5.1.2 Venous leg ulcers

Venous leg ulcers (figure 1.10B) are caused by low blood circulation, due to damaged leg veins. Compromised blood vessels and valves cause blood to flow backwards, ultimately causing high blood pressure in leg veins, which become leaky. Subsequently the fluid causes swelling and damage, leading to hardened and inflamed skin that develop into painful venous leg ulcers. Leg ulcerations are common, accounting for 85% of all lower extremity ulcers (McGuckin et al., 2002) with 70,000-190,000 individuals in the UK suffering with a venous leg ulcer at any one time (NHS, 2013). They are more prevalent in the elderly population and as with all chronic wounds, as the elderly population rises, so will their frequency.

Improvements in Western civilization health care, living standards and socio-economic status means that more and more people are now living to an old age (Wicke et al., 2009). Relative to the general population, both the number and proportion of the older population is increasing. For example, it has been estimated that in the 17 years between 2008 and 2025 the European population will grow by just 1%, however in the same time, population of the over 65s will grow by 13% (Sen et al., 2009). By 2050, it is predicted that the European population growth will be static or declining whereas the number of the over 65s will be reaching 50 million; approximately 59% of the total European population. Current global estimates suggest \$3bn is spent each year on treatment of venous leg ulcers with a further \$2bn attributed to work days lost. This staggering financial burden will only get bigger.

1.5.1.3 Pressure ulcers

Pressure ulcers (figure 1.10C) can be caused by either prolonged or repeated pressure to the skin and are often found on bony prominences. Currently, there are an estimated 7.4 million pressure ulcers in the world and over 400,000 people in the UK will develop a pressure ulcer this year. Vulnerable patients generally include those who suffer from impaired mobility or sensation, such as the elderly, wheelchair bound or bedridden, and pressure ulcers are often seen in hospitalised patients. Approximately 25% of people resident in long-term geriatric wards will have a pressure ulcer and the prevalence of pressure ulcers in hospitals has risen by 63% in the past 10 years (Sen et al., 2009). As pressure ulcers are a major source of infection, leading to septicaemia and often death, there have been 60,000 avoidable deaths in that same time period and as the global elderly population grows so will the global nursing home population. Pressure ulcers also come with their own economic burden, with estimates suggesting treatment of pressure ulcers could cost

the NHS £2bn per year (Bennett et al., 2004). Pressure ulcers and their possible treatments will be explored in more detail in chapters five and six.



Figure 1.10 Chronic ulcers

(A) Diabetic foot ulcer found in a typical position under the second metatarsal head on the sole of the patient's foot. (B) Venous leg ulcer in a typical location, above the ankle. (C) Pressure ulcer on the heel of a patient's foot. Note that all the wounds have irregular borders and have a yellow, fibrinous base. Diagrams from *The Lancet* 361; 1545-1551 (Jeffcoate and Harding, 2003), *Journal of American Academy of Dermatology* 44; 401-421 (Valencia et al., 2001) and *Wounds International* 1 (Murando and Dealey, 2013).

1.5.2 Connexin dynamics in chronic wounds

As connexins, hemichannels and gap junctions play such integral roles within intact skin and the wound healing process, it is no surprise that connexins have been flagged to have possible roles in the failure of wound closure found in chronic, non-healing wounds. Current research pins this responsibility on Cx43 as it is the most ubiquitous connexin in rodent and human skin.

1.5.2.1 Cx43 in diabetic foot ulcers

The onset of diabetes can cause significant changes in connexin expression in tissues of the human body, including the skin (Wright et al., 2012, Mendoza-Naranjo et al., 2012b). Abdullah and colleagues have reported that human diabetic dermal

fibroblasts demonstrated significantly greater gap junction communication when compared to normal dermal fibroblasts (Abdullah et al., 1999). Investigations into the connexin profiles of human diabetic foot ulcers, which supported the above discovery, found that there was no loss of Cx43 in fibroblasts at or near the wound margins of the chronic wounds investigated but it was upregulated (Mendoza-Naranjo et al., 2012b). The key absence of normal down-regulation of this protein, which occurs in normal wound healing, may be a crucial factor in a wound's failure to heal normally in a diabetic foot ulcer (Becker et al., 2012).

Experimentally it is challenging to re-create a model of chronic wounds *in vivo*, as chronic wounds do not naturally occur in animals. This is primarily due to the absence of truly aged animals, neuropathy or chronic debility (Mustoe, 2004). Nonetheless, Wang, Becker and partners improved upon an FDA approved animal model in which it is known that normal wound healing is impaired. Delayed wound healing occurs in rat models of diabetes induced by streptozotocin (STZ). Wang and colleagues were the first to map the profiles of Cxs 26 and 43 in intact non-wounded skin and skin undergoing wound healing in this model (Wang et al., 2007). They discovered that, in comparison to normal intact skin, diabetes reduced the expression of Cxs 43 and 26 in the intact epidermis and increased Cx43 in the intact dermis. Diabetes also dramatically altered connexin dynamics during wound healing. Similar to human diabetic foot ulcers, Cx43 was significantly up-regulated in the wound edge epidermis, resulting in a thickened bulb of non-migrating keratinocytes. Over a day later than normal wound healing, Cx43 finally down-regulated in the epidermis and triggered the migration of keratinocytes into the wound. Although the dynamics of Cx26 did not change in diabetic rat skin, its distributions at the wound edge were abnormal and more widespread.

Further analysis by the same group confirmed that fibroblasts at the wound edge of human chronic foot ulcers had a 10 fold elevated expression of Cx43 in comparison to non-wounded skin, and that STZ-induced diabetic rats had an excess of Cx43 in their dermal fibroblasts (Mendoza-Naranjo et al., 2012b). Using an *in vitro* model of diabetes, where fibroblast cells were cultured in elevated glucose levels, it was found that Cx43 expression was significantly more elevated than in normal fibroblasts. Gap junction communication had significantly increased in these 'diabetic' fibroblasts and migration rates in scratch wound assays had significantly decreased. The results support the theory that increased fibroblast Cx43 expression *in vitro*, in diabetic rat and in human diabetic foot ulcer skin, may be fundamental to the impaired healing found in diabetic foot ulcers.

1.5.2.2 Cx43 in venous leg ulcers and pressure ulcers

Research relating connexin dynamics to the failure of wound closure in human venous leg ulcers is sparse. However, Raffetto has described reduced motility in human dermal fibroblasts in patients with chronic venous insufficiency (a precursor to the development of venous leg ulcers) and Mendoza-Naranjo has noted that the same fibroblasts have significantly more Cx43 than their dermal counterparts in intact skin (Raffetto et al., 2001, Mendoza-Naranjo et al., 2012a).

To date, there have been no published investigations (human or rodent based) into the role of connexins in the pressure ulcer. However, there has been progressive development on the design of an *in vitro* pressure ulcer model. Primarily using metal plates and/or magnets, models of cyclic ischemia-reperfusion injury on the back of rodents has been refined to mimic chronic pressure ulcers (Peirce et al., 2000, Reid et al., 2004). The models successfully mimic pressure sores, by creating tissue necrosis, hyper-thickened wounds and an increase in the inflammatory response.

1.5.3 Transient knockdown of Cx43 in wound healing

It is clear (at least in diabetic foot and venous leg ulcers) that Cx43 plays a significant role in the failure of wound healing leading to a potential therapeutic target to be developed.

1.5.3.1 Transient knockdown of Cx43 in acute wound healing

Cx43 dynamics during acute wound healing is tightly regulated to ensure successful closure of the wound. After several years of development and research from the Becker group, a promising therapeutic that could enhance the rate of acute and chronic wound healing has emerged. A number of years ago a Cx43 specific antisense oligodeoxynucleotide (Cx43 asODN) was developed (Law et al., 2006); a 30mer unmodified backbone antisense that targets to Cx43 mRNA and induces a Cx43 protein knockdown. This ODN has been demonstrated to promote accelerated wound healing (Qiu et al., 2003, Mori et al., 2006, Wang et al., 2007). However, being unmodified, this ODN will rapidly break down in cells (half life of 20-30 minutes) and break down even faster in blood (half life of fewer minutes), so will only act effectively where it is topically applied (Wagner, 1994). Exonucleases within serum are also known to break down unmodified oligodeoxynucleotides (Shaw et al., 1991). To counteract this short half-life and rapid breakdown, the therapeutic has been formulated within a Pluronic™ F-127 gel. This gel has thermo-reversible properties, (can be liquid on ice and gels at body temperature) that acts as a slow release reservoir and enables a constant topical delivery of Cx43 asODN over several hours.

When immediately applied to a rodent skin wound, Cx43 asODN rapidly reduces Cx43 expression in wound edge keratinocytes, fibroblasts and blood vessels within two hours, nearly a whole day faster than in nature (Qiu et al., 2003, Mori et al.,

2006). Early application of Cx43 asODN to acute wounds dampens tissue swelling and the inflammatory response, promotes early keratinocyte and fibroblast cell migration and closes the wound gap earlier than wounds left un-treated. Wounds treated with Cx43 asODN appear less red and swollen and rapidly reduce in size, resulting in smaller and thinner scar tissue (Qiu et al., 2003). Targeting the early stages of wound closure using Cx43 asODN appears to 'jump-start' the subsequent phases of wound healing.

1.5.3.2 Transient knockdown of Cx43 in diabetic ulcers

As described in much detail above, in both human diabetic foot ulcers and STZ-diabetic rat lesions, Cx43 fails to down-regulate at the wound edge, as seen in normal acute wounds 24h after wounding. Application of Cx43 asODN to acute wounds significantly reduces Cx43 at the wound edge and promotes an early wound healing response. Therefore application of Cx43 asODN to STZ-induced diabetic rat wounds should promote a better wound healing rate. Wang and colleagues confirmed this was the case, showing that a single application of Cx43 asODN on the wound immediately after wounding was sufficient enough to prevent Cx43 up-regulation at the wound site (Wang et al., 2007). This single topical application was able to prevent the formation of a bulb of non-migratory keratinocyte cells, restoring the healing rate back to normal. As early research has suggested that human diabetic foot ulcers show a similar Cx43 profile to STZ-induced diabetic rat lesions, there is promise for Cx43 asODN as a therapeutic to promote healing in these debilitating wounds.

1.6 Connexin mimetic peptides in wound healing

Although it is now certain that Cx43 plays integral roles in both acute and chronic wound healing, it is still unclear whether these responses are attributed to the

connexin hemichannels or gap junctions. Long term hemichannel down-regulation can be achieved through topical application of Cx43 asODN; however the differences between gap junction communication and hemichannel signaling can be teased out by application of small connexin mimetic peptides. Acting on the extracellular loops of connexins, these peptides can rapidly block hemichannels and prevent gap junction formation. However, with longer or more concentrated incubation periods, connexin mimetic peptides have been reported to inhibit gap junctional communication.

1.6.1 History of connexin mimetic peptides

There are many compounds that can block gap junctional communication but their mechanisms of action frequently lead to unwanted and non-specific effects. For example, aliphatic alcohols, such as octanol (Cotrina et al., 1998b) and heptanol (Guan et al., 1997) and anesthetics, such as halothane (Boitano et al., 1992) act to disrupt gap junctional communication through the mechanism of 'squeezing'; dissolving into the cell membrane and leading to the contraction of gap junctions. However, this action is likely to modify other non-gap junction channels in the area and therefore cannot be defined as a specific gap junctional communication limiter. Other methods to disrupt gap junction communication can be achieved by using lipophilic aglycones, such as 18 α -Glycyrrhetic acid which does not act directly on the gap junction. Instead they act indirectly via the activation of G proteins, protein kinases and ATPases, leading to the phosphorylation of the connexin, which will ultimately disrupt the gap junction assembly and channel gating (Taylor et al., 1998, Chaytor et al., 1999).

The development of a specific and reversible inhibitors of gap junction communication began shortly after the deduction of the complete amino acid sequences of Cxs 32 and 43 (Evans et al., 2012). Through understanding the

involvement of gap junctions in mouse embryo development, Becker, Evans and colleagues were among the first to raise antibodies that would interfere with gap junctional communication (Becker et al., 1995). Antibodies for Cx43 were raised against the amino terminus, cytoplasmic loop and the carboxyl tail, whereas antibodies for Cx32 were raised against the cytoplasmic loop and the first extracellular loop. Predicted amino acid sequence homology confirmed that the antibody towards Cx32 first extracellular loop was recognized by both Cxs 32 and 43. This particular antibody would not stain intact gap junctions. Parallel work carried out by Evans, Boitano and colleagues developed further antibodies towards Cx32 that would disrupt calcium waves in primary airway epithelial cells, propagated by gap junctions (Boitano et al., 1998).

Although the development of specific antibodies towards connexins was a major step forward in the pursuit to find a specific inhibitor of gap junction communication, these antibodies were deemed too large. Although useful tools in blocking the docking of hemichannels during gap junction assembly, due to their size, they had limited access to the gap between docked hemichannels. Their size could also ultimately compromise their specificity.

One of the key experimental studies that marked the beginning of the development of connexin mimetic peptides was conducted by Warner and colleagues (Warner et al., 1995). They developed and screened the efficiency of 15 short extracellular loop sequences that shared homology to amino acids in the first and second extracellular loops of Cx32. By testing the synchronization of the beating of embryonic chick heart myocytes, this group showed that all of the short peptides designed delayed gap junction formation. This work was successfully complimented in *Xenopus* oocytes that had been transfected with the mRNA of Cx32 (Dahl et al., 1994).

The potential of short mimetic peptides to disrupt gap junction communication had been realized and it was noted that Warner paid particular attention to two motifs on the two extracellular loops; SHVR on the first and SRPTEK on the second. As Cx43 is the most ubiquitous gap junction protein, two synthetic short connexin mimetic peptides were designed to encompass these motifs. Gap26 corresponded to the first extracellular loop (amino acid sequence VCYDKSFPISHVR) and Gap27 to the second (amino acid sequence SRPTEKTIFII). The names corresponded to the 26th and 27th synthesized connexin mimetic peptides that were designed by Evans in the Medical Research Council for gap junction projects.

1.6.2 The benefits of connexin mimetic peptides in wound healing

In recent years it has been realized that connexin mimetic peptides show a huge potential in tackling connexin-based maladies and show promise in translational and therapeutic possibilities. These prospects include enhancing the rate of wound repair in acute and chronic wounds and reducing the spread of damage caused in tissue ischemia reperfusion.

Early work conducted by the Martin group has not only shown that both Gap26 and Gap27 reduce gap junction communication in human keratinocyte and fibroblast cells but also that it has great potential in the wound healing environment (Wright et al., 2009, Pollok et al., 2011). Using scratch wound assays (creating an *in vitro* 'wound' across a confluent layer of cells) it was shown in both keratinocytes and fibroblasts that connexin mimetic peptides could increase the rate of migration across these scrapes (Wright et al., 2009). Further encouraging *ex vivo* work using 3D organotypic porcine wound models demonstrated that Gap27 could accelerate wound closure through an increase in keratinocyte re-epithelialisation and enhanced proliferation rates (Pollok et al., 2011). This work will be built upon and explored in further detail in chapters three and four of this thesis.

Tissue ischemia is a major medical problem that plagues a number of organs and is caused by a restriction of blood supply to tissue, causing a severe shortage of oxygen, glucose and other nutrients needed for cell survival. Tissue ischemia is common in cardiac (heart attacks), cerebral (strokes) and skin (pressure ulcers) tissue, however, the real damage often occurs upon reperfusion. This is when the blood supply returns in a restoration of circulation and causes inflammation and oxidative damage to the tissue that has been denied oxygen flow for a period of time. Often this damage spreads beyond the initial ischemic area and this spread of damage and cell death has recently been attributed to increased gap junction and hemichannel communication (García-Dorado et al., 2004, Cotrina et al., 1998a, Thompson et al., 2006, Orellana et al., 2010).

There is already potential therapeutic promise that connexin mimetic peptides could provide cardiac and neuronal protection during ischemia reperfusion. O'Carroll, Green and colleagues pioneered in showing that during an *in vitro* spinal cord injury model, treatment with connexin mimetic peptides could significantly reduce the cell damage that occurs (O'Carroll et al., 2008). Building on this research, using a model of cerebral ischemia in foetal sheep, Davidson and colleagues demonstrated that connexin mimetic peptide treatment could not only increase the survival rate of cells during ischemia reperfusion but also reduce seizure activity (Davidson et al., 2012b). Cardiac protection has also been noted when rat models of myocardial infarction are treated with connexin mimetic peptides (Hawat et al., 2012). Treatment significantly reduced the infarct size by over 60%.

To date, there has been no published work indicating that connexin mimetic peptides could reduce the extensive progressive damage often seen in pressure ulcers. Continued cyclic periods of pressure and relief during pressure ulcer formation causes severe tissue ischemia reperfusion damage in the skin, similar to

the damage formed in cerebral and cardiac ischemia reperfusion. There are currently no effective treatments for this irreversible pressure ulcer damage caused by ischemia reperfusion injury and understanding how cell death occurs and spreads will help in the discovery of a treatment to reduce the impact of ischemia reperfusion damage. This topic will be greatly explored in chapters five and six of this thesis.

1.7 General aim of this thesis

The potential therapeutic implications of the wound healing properties of connexin mimetic peptides are exciting, novel and promising. It has recently become apparent that gap junctions and their connexins play an integral and crucial role in wound healing. The overall aims of this PhD thesis are to further explore the role and potential therapeutic implications of the connexin mimetic peptide Gap27 in both *in vitro* and *in vivo* models of wound healing and to use Gap27 to investigate the mechanism of cell death and damage during ischemia reperfusion injury. Hypotheses will be addressed in individual research chapters.

Aims and objectives

1) To characterize the effect of Gap27 on connexin expression in fibroblast and keratinocyte cells, while exploring the effects of the connexin mimetic peptide in cell communication and *in vitro* models of wound healing.

2) To investigate the ability of connexin mimetic peptides to enhance wound closure. An examination of the potential enhanced wound healing properties of Gap27 will be carried out using a well-documented *in vivo* wound healing model. Detailed analysis will be executed on the effect of Gap27 treatment during the early stages of wound healing. This will include an assessment on the inflammatory response and re-

epithelialisation, while special attention will be given to the connexin profiles in treated and non-treated tissue to establish the importance of connexins during wound healing.

3) To investigate the mechanism of spread of cell death and damage during ischemia reperfusion injury *in vitro* by probing this with mimetic peptides. Connexin mimetic peptides have a unique dose response; at low doses, Gap27 has been shown to block hemichannels but can target gap junctional intercellular communication at higher doses and for longer periods of incubation. Using this tool, I plan to dissect out the relative contributions of the connexin based communication involved in the spread of cell death and damage during ischemia reperfusion during pressure ulcer formation.

4) Finally, using an *in vivo* model of pressure ulcers developed by Thomas Mustoe the role of Cx43 based hemichannels and gap junctions will be examined during ischemia reperfusion in the skin.

2. Materials and methods

This chapter covers all materials, reagents and protocols in detail and which are referred back to in the results chapters.

2.1 Reagents, antibodies and mimetic peptides

All chemicals and reagents were purchased from Sigma-Aldrich (Gillingham, UK) unless otherwise stated. Tissue culture reagents were purchased from Gibco (Paisley, UK) unless otherwise stated. Details of antibodies, connexin mimetic peptides and anti sense oligodeoxynucleotide (asODN) used in experiments are as follows.

Table 2-1 Primary antibodies used in this investigation

Name	Protocol	Host	Reactivity	Dilution	Incubation	Manufacturer	Catalogue #
rb anti Cx43	Immuno	Rabbit	Cx43	1 in 4000	1 hour at RT	Sigma, UK	C6219
	WB			1 in 4000	Overnight at 4°C		
rb anti Cx26	Immuno	Rabbit	Cx26	1 in 200	Overnight at 4°C	Life Tech, UK	51-2800
rb anti Cx30	Immuno	Rabbit	Cx30	1 in 200	1 hour at RT	Life Tech, UK	71-2200
rb anti Cx HC*	Immuno	Rabbit	Cx HC	1 in 1000	Overnight at 4°C	Custom made	n/a
rt anti α tubulin	Immuno	Rat	alpha tubulin	1 in 2000	1 hour at RT	Abcam, UK	ab64332

The table details all primary antibodies used in either cell culture (immuno), in mouse tissue (immuno) or in Western blots (WB). The table includes information regarding the name of the antibody, at what dilution the antibody was used at and for what incubation period.

** Rabbit anti connexin hemichannel antibody (rb anti Cx HC) is a custom made affinity purified antibody against a highly conserved portion of the 1st ECL of Cx43. Sequence: ESAWGDEQSAFRcntqqpgc. This antibody will only bind to E1 and prevent gap junction formation and therefore will only stain for non-docked hemichannels.*

Table 2-2 Secondary antibodies used in this investigation

Name	Protocol	Host	Reactivity	Dilution	Incubation	Manufacturer	Catalogue #
gt anti rb AF 488	Immuno	Goat	Rabbit	1 in 500	1 hour at RT	Life Tech, UK	A-11008
gt anti rb AF 568	Immuno	Goat	Rabbit	1 in 500	1 hour at RT	Life Tech, UK	A-11009
gt anti rb HRP	WB	Goat	Rabbit	1 in 1000	1 hour at RT	Life Tech, UK	G-21234
gt anti rt HRP	WB	Goat	Rat	1 in 1000	1 hour at RT	Life Tech, UK	A-10549

The table details all secondary antibodies used in conjunction with the primary antibodies, used in either cell culture (immuno), in mouse tissue (immuno) or in Western blots (WB). The table includes information regarding the name of the antibody, at what dilution the antibody was used at and for what incubation period.

Table 2-3 Sequences of connexin mimetic peptides

Name	Sequence	Connexin	Residue #	MW	Purity	Custom made by	Reference
Gap27	SRPTEKTIFII	43	204-214	1304 g/mol	95%	Thermo Scientific, Germany	Chaytor et al., 1997
Scrambled	RFKPSLCTTDEV	none	none	1396 g/mol	95%	Peptide2.0, USA	Danesh-Meyer et al. 2011

The table details mimetic peptides used in this investigation. Connexin mimetic peptide Gap27 (sequence SRPTEKTIFII) was designed against a portion of the second extracellular loop of Cx43 that leads into the fourth transmembrane domain (figure 2.1). The highly conserved sequence SRPTEK is found on Cxs 43, 26 and 30. Scrambled peptide (sequence RFKPSLCTTDEV) was designed by Colin Green and includes a scrambled portion of the highly conserved sequence (RFKPSLCTTDEV).

2.2 *In vitro*

2.2.1 Cell culture

2.2.1.1 Fibroblast and keratinocyte cell culture

Immortal fibroblast cells derived from mouse (NIH 3T3) were cultured in Dulbecco's Modified Essential Medium (DMEM; 4.5 g/l D-glucose, L-glutamine, pyruvate, phenol red) supplemented with 10% donor bovine calf serum (DBS), 100 U/ml penicillin and 100 µg/ml streptomycin. This complete medium is abbreviated to fibroblast DMEM.

Immortal keratinocyte cells derived from human (HaCaT) were a kind donation from J.Sutcliffe and cultured in 43.5% DMEM (4.5 g/l D-glucose, L-glutamine, pyruvate, phenol red) and 43.5% DMEM F-12 (L-glutamine) supplemented with 10% heat-inactivated foetal bovine serum (FBS), 1% GlutaMAX®, 1% RM plus supplement (final concentration of 5 µg/ml transferrin, 0.4 µg/ml hydrocortisone, 5 µg/ml insulin, 10 ng/ml EGF, 2×10^{-11} liothyronine and 10^{-10} M cholera toxin), 50 U/ml penicillin and 50 µg/ml streptomycin (Aasen and Izpisúa Belmonte, 2010). This complete medium is abbreviated to keratinocyte DMEM.

Fibroblast and keratinocyte cells were cultured in separate humidified incubators with atmospheres of 5% CO₂ and 95% air, at 37°C. Cell growth and health was regularly monitored and cell medium was changed every 2-3 days in both cell types. If cells reached 80% confluence and were not needed for experiments, they were split down 1 in 3 to reduce overcrowding.

2.2.1.2 Retroviral constructs and transduction

Fibroblast cells were transduced with a Cx43 specific shRNA construct (sequence 5'-GGTGTGGCTGTCAGTGCTC-3'; a gift from W. H. Moolenaar) or a retroviral empty vector (pSuppressor; Imagenx Co. San Diego, USA). The GP2-293 packaging cell line (Clonetech) was transfected by calcium phosphate precipitation with 5 µg pMD.G envelope plasmid, 10 µg pBSII SK-carrier plasmid (Stratagene) and 15 µg retroviral plasmid containing either Cx43shRNA or the empty vector. The viral medium was collected and used to infect NIH 3T3 cells growing in fibroblast DMEM at 37°C in 5% CO₂. Viral medium was replaced every 12 hours for 48 hours. Resistance to 2 µg/ml puromycin (Cx43shRNA) or 500 µg/ml geneticin (empty vector) was used to select transduced cells.

The first three passages of transduced pSuppressor (PSupp) and transduced Cx43shRNA (shRNA) NIH 3T3 fibroblast cells were used in all experiments. All cells were cultured in fibroblast DMEM at 37°C in a humidified incubator with an atmosphere of 5% CO₂ and 95% N₂, at 37°C. All experiments were carried out when cultures reached 80% confluence.

2.2.2 Mimetic peptide incubation

During *in vitro* experiments the connexin mimetic peptide Gap27 and scrambled mimetic peptide (refer to table 2.3) were prepared in reduced serum medium Opti-Minimal Essential Medium (OptiMEM) supplemented with 1% DBS. This complete medium is abbreviated to OptiMEM. As a modification of DMEM, OptiMEM allowed cells to continue to grow and proliferate successfully in a heavily reduced serum environment. This enabled the fragile peptide to incubate optimally while preventing its breakdown by proteases that reside within the serum. Control cells were also cultured in OptiMEM during experiments for direct comparison.

In dose response experiments, mimetic peptide incubation was the same for fibroblasts and keratinocytes, in immunostaining and in Western blots. For two hour incubation periods, cultures were treated with a single dose of Gap27 (10, 30, 100 or 300 μM) scrambled peptide (100 μM) or left untreated (naive OptiMEM). For six hour incubation periods, cultures were treated with Gap27 (10, 30, 100 or 300 μM) scrambled peptide (100 μM) or left untreated (naive OptiMEM) and medium was replaced every two hours with fresh medium containing peptide. Details of mimetic peptide incubation times and concentration in assays is detailed in the relevant sections below and addressed in individual research chapters.

2.2.3 Oxygen glucose deprivation re-oxygenation

Fibroblast cells were subjected to hypoxic conditions before reperfusion in an oxygen-glucose deprivation-reoxygenation (OGDR) insult. Cell medium was replaced with glucose and serum free medium (0 g/l D-glucose, L-glutamine, phenol red) that had been effervesced with 5% CO_2 and 95% N_2 for one hour. This medium is abbreviated to OGDR DMEM. Hypoxia was induced by placing the cultures inside a sealed chamber with an atmosphere of 5% CO_2 and 95% N_2 for 1.5 hours. Cells were then exposed to reoxygenation through medium change (OptiMEM) at 37°C in 5% CO_2 and 95% air for progressive periods of time (0, 1.5, 4 and 24 hours).

2.2.3.1 Measuring oxygen levels in the media

Partial pressure of oxygen within OGDR DMEM was measured using the fibre optic oxygen (FOXY) probe (Ocean Optics, Florida, USA), to confirm hypoxic conditions. Oxygen levels of fibroblast DMEM were measured as a control. FOXY probe tips are covered with a layer of ruthenium compound trapped in a matrix of a hydrophobic gel. When excited by an LED, the ruthenium compound fluoresces and if the excited ruthenium comes into contact with an oxygen molecule, the excess energy will

quench the ruthenium fluorescent signal. This intensity or phase shift of fluorescence is measured by a spectrometer (Ocean Optics, Florida, USA) and is then related to the partial pressure of oxygen.

Before sample measurements were taken, the FOXY probe was calibrated using 0% oxygen and 21% oxygen standards. The zero oxygen standard was prepared by dissolving one gram of sodium hydrosulphite in 20 ml of 1X phosphate buffered saline (PBS) and warming to 37 °C in a waterbath before being read with the probe. Sodium hydrosulphite is a strong reducing agent that removed all oxygen from the solution. The atmospheric oxygen standard was prepared using 1X PBS and warming to 37 °C before being read. A standard curve was created using the program OOISensors (Ocean Optics, Florida, USA). OGDR and fibroblast DMEM were also read at 37 °C.

2.2.4 Immunostaining cells

Cells were grown to confluence in 8-well chamber slides (Millicell EZ slide, Millipore, Watford, UK) and subjected to treatment as described above (OGDR insult and/or mimetic peptide incubation). At required time points, cells were fixed in 4% paraformaldehyde (PFA) in 1XPBS for 5 min, incubated with a blocking solution (1M lysine, 1X PBS, 0.05% Triton X-100) for a further 30 min and immunolabeled with a primary antibody diluted in blocking solution (refer to table 2.1 for dilutions and incubation periods). Negative controls were incubated overnight in blocking solution containing no primary antibody for the same time. Following removal of the primary antibody solution, cells were washed in triplicate using 1X PBS before incubation for one hour at room temperature with the secondary antibody (refer to table 2.2 for dilutions) diluted in blocking solution. A counter stain of Hoechst 33258 and 33342 (1:50,000) diluted in dH₂O was applied as a nuclear indicator. After a further three 1X PBS washes, the culture chamber slides were mounted onto microscope

coverslips using Citiflour™ mounting medium and viewed under a confocal microscope (Upright SPE, Leica, Milton Keys, UK). All images were acquired using identical parameters and camera settings to allow for direct comparison of staining intensity. Images were uploaded to ImageJ™ (version 1.46r, Wayne Rasband, NIH, USA) to analyse connexin profiles. A threshold was set to ensure maximum connexin expression was measured while taking care to eliminate the background. Nuclei count was achieved by creating a binary image of the nuclei and counting solid nuclei structures. All parameters were kept constant for all measurements while connexin pixel area per cell was quantified.

2.2.5 Western blots

2.2.5.1 Protein collection, quantification and preparation

Cells were grown to confluence in 6-well plates and subjected to treatment as described above (OGDR insult and/or mimetic peptide incubation). Cultures were washed in 1X PBS and lysed with ice cold radio immunoprecipitation (RIPA) buffer (0.05 M Tris pH 8.0, 0.15 M NaCl, 1% Triton X-100, 0.5% sodium deoxycholate and 0.1% SDS) with complete protease and phosphatase inhibitor cocktail tablets; one tablet of each per 10 ml RIPA buffer (Roche, Hertfordshire, UK). Cells were scraped and total cell protein was collected on ice. Lysates were sonicated for 30 min and centrifuged at 4°C for 10 min before the purified supernatant was collected. Cell homogenates were stored at -20°C until required for blotting.

Protein content of the samples was determined using a BSA assay (Thermo Scientific, Northumberland, UK) in a 96-well format according to the manufacturer's instructions. Equal amounts of protein were denatured using reducing Laemmli 4X buffer (Bio-Rad, Hertfordshire, UK) at 100°C for 10 min. Samples were allowed to cool before gel loading.

2.2.5.2 Gel electrophoresis, transfer and blocking

Protein samples were run on a precast 10% SDS-PAGE resolving gel (Bio-Rad, Hertfordshire, UK) for one hour at 150V. Samples were then transferred onto nitrocellulose membrane for one hour at 100V. Protein transfer was confirmed using Ponceau Red solution (1% acetic acid, 0.5% Ponceau Red) in dH₂O and membranes were subsequently washed thoroughly with PBS-Tween (1X PBS, 1% Tween20) to remove Ponceau Red stain. Following successful protein transfer the membrane was blocked in 1% non-fat milk diluted in PBS-Tween, for one hour at room temperature, under gentle agitation.

2.2.5.3 Antibody incubation and detection

The membranes were incubated with a primary antibody (refer to table 2.1 for dilutions and incubation periods) diluted in blocking solution, under gentle agitation. The following day the antibody solution was removed and membranes were washed in triplicate using PBS-Tween. The membranes were subsequently incubated with a secondary antibody (refer to table 2.2 for dilutions) conjugated with horseradish peroxidase (HRP), diluted in blocking solution, for one hour at room temperature, under gentle agitation. The secondary antibody was then removed and the membranes were washed in triplicate using PBS-Tween.

To visualise the immunoreactivity, ECL (West Pico chemiluminescent substrate, Thermo Scientific, Northumberland, UK) was used according to the manufacturer's instructions. Detection and visualisation of the proteins on the membranes were achieved through exposure using a ChemiDoc™ (Bio-Rad, Hertfordshire, UK). Digital images were collected and then loaded onto ImageJ for protein band intensity analysis. The intensity of the protein of interest was measured relative to the intensity of the housekeeping protein. Alpha tubulin was used as a

housekeeping protein (refer to tables 2.1 and 2.2 for dilutions and incubation periods). All protein collection for Western blots was repeated in triplicate.

2.2.6 Detailed assays using cell cultures

2.2.6.1 Migration assays – scratch wound

Scratch wound assays were used to investigate mimetic peptide effects on cell migration rates. Cells were cultured and grown to confluence in 24-well plates that had been pre-treated with an attachment factor. This prevented the cells from ruffling upon scratching. An *in vitro* model of wounding was performed by drawing a 200 µl pipette tip across confluent cells in each well. Cultures were rinsed of any cell debris and incubated with a single dose of 10, 30, 100 or 300 µM Gap27, 100 µM scrambled peptide or left untreated (naive OptiMEM). Images of migrating cells were taken on an Olympus inverted microscope (Olympus 1X81) on an XYZ stage (Prior XYZ stage, Cambridge, UK), in a temperature and gas controlled chamber (5% CO₂ and 95% air at 37°C). An image of a defined area at the edge of each scratch wound was taken and subsequent images were taken every hour of the same location, for six hours. The rate of migration was quantified by measuring the movement of the leading edge over time.

2.2.6.2 Communication assays - fluorescent recovery after photobleaching

Fluorescent Recovery after Photobleaching (FRAP) was used to investigate the connectivity of neighbouring cells, through gap junction communication, by monitoring the diffusion of a fluorophore between the two. FRAP was used to assess connexin mimetic peptide effect on communication between fibroblast cells and to assess communication between fibroblast cells during OGDR insult. Both experiments were subject to the same FRAP procedure (described in more detail below).

Communication of fibroblasts continuously incubated with Gap27 for 2 hours

Fibroblast cells were cultured on glass bottom 35 mm² dishes and grown to confluence. Cultures were washed in 1X PBS before undergoing continuous incubation for two hours with Gap27 (30 or 300 μM) or scrambled peptide (300 μM) prepared in OptiMEM. A control of non-treatment (naive OptiMEM) was used. After two hours of incubation in mimetic peptide, calcein acetoxymethyl ester, (calcein-AM; 1 μl/1000 μl of medium) was added to the cells for a 20 min incubation period. The medium was then removed and cultures were washed in triplicate using 1X PBS. Cultures were then replaced with fresh medium containing connexin mimetic peptide (or naive OptiMEM) and propidium iodide (PI; 1 μl/1000 μl of medium) before FRAP was carried out.

Communication of fibroblasts subjected to OGDR and treated with continuous incubation of Gap27 for 4 hours

Fibroblast cells were cultured on glass bottom 35 mm² dishes and were grown to confluence. Cultures were washed in 1X PBS before being subjected to OGDR insult as described above. After 1.5 hours of oxygen-glucose deprivation, cells were subjected to reperfusion. Cells were either continuously incubated with Gap27 (100 or 300 μM) or left un-treated (naive OptiMEM). A control of no OGDR and no treatment was used. After four hours of incubation in mimetic peptide, calcein-AM was added to the cells for 20 min. The medium was then removed and cultures were washed in triplicate using 1X PBS. As described above, cultures were then replaced with fresh medium containing connexin mimetic peptide (or naive OptiMEM) and PI before FRAP was carried out.

FRAP images were taken on a confocal microscope, with a temperature and gas controlled chamber (5% CO₂ and 95% air at 37°C). Using a 63X water immersion

apochromatic objective lens (NA, 0.9), optical sections were scanned in xyt mode. A zoomed region of interest (ROI) covering a connected cell was bleached of its fluorophore with increased laser power before being allowed to recover at a rate of 1.635 seconds per frame. Communication was monitored through fluorescent recovery; by timing how long it took for cells to transfer fluorescent calcein to their neighbouring bleached cell through gap junctions. Fluorescent recovery was measured by loading the images of recovery frames onto ImageJ. The average image intensity of the ROI was measured in every frame over the same time period.

Calcein-AM is commonly used in cell communication assays as the acetomethoxy (AM) ester segment and allows the diffusion of calcein through the cellular membrane. Once inside the cell, intracellular esterases cleave the AM group, hydrolysing calcein into a hydrophilic charged derivative. Calcein then becomes trapped within the cytoplasm and becomes fluorescent. Now at a MW of 622.55 g/mol, calcein is free to move between communicating cells via their gap junctions. Dead and dying cells lack active esterases and therefore only live cells are labelled. PI is a charged dye which is membrane impermeant and is often used as a dead cell indicator, although live cells with open hemichannels can also label with this dye. The role of PI in these experiments was to ensure imaging did not kill cells and give false results.

2.2.6.3 Cell viability assay - MTT

An MTT reduction assay was used to assess cell viability index in fibroblast cells subjected to an OGDR insult. Cell viability in wild-type, PSupp or shRNA fibroblast cells was measured. In subsequent experiments wild-type fibroblasts were either treated with Suramin or Gap27 after reperfusion before their cell viability was measured. All experiments were subject to the same MTT assay described in more detail below.

Cell viability in wild-type, PSupp and shRNA fibroblast subjected to OGDR

Wild type, PSupp or shRNA fibroblast cells were cultured in 96-well plates at a density of 10,000 cells per well and allowed to grow to 60-70% confluence. Cells were subjected to OGDR insult and cell viability was measured at progressive time points after 1.5 hours after reoxygenation (0, 4 and 24 hours) using an MTT assay.

Cell viability in fibroblasts subjected to OGDR then treated with Suramin

Wild type fibroblast cells were cultured in 96-well plates at a density of 10,000 cells per well and allowed to grow to 60-70% confluence. Hypoxia was induced as described above and cells were exposed to reoxygenation 1.5 hours after oxygen glucose deprivation. Cultures were treated with a single dose of 100 μ M Suramin in fibroblast DMEM or left untreated (naive fibroblast DMEM). A control of no OGDR was used. Suramin is a general, non specific P2Y and P2X purinergic receptor antagonist. Cell viability was measured at progressive time points after reoxygenation (0, 4 and 24 hours) using an MTT assay.

Cell viability in fibroblasts subjected to OGDR then treated with Gap27

Wild type fibroblast cells were cultured in 96-well plates at a density of 10,000 cells per well and allowed to grow to 60-70% confluence. Hypoxia was induced as described above and cells were exposed to reoxygenation 1.5 hours after oxygen glucose deprivation. Cultures were treated with a single dose of 30 or 300 μ M Gap27 in OptiMEM or left untreated (naive OptiMEM). A control of no OGDR was used. Cell viability was measured at progressive time points after reoxygenation (0, 4 and 24 hours) using an MTT assay.

Cell viability index was measured using the MTT reduction assay and was performed according to the manufacturer's instructions (Millipore, Watford, UK). Ten ml of 1X PBS was added to 50 mg of MTT (3-(4, 5-dimethylthiazol-2-yl)-2, 5-diphenyl tetrazolium bromide) and 10 µl of MTT solution was added to the culture medium in each well. Mitochondrial and cytosolic dehydrogenases reduced the yellow tetrazolium salt (MTT) to a dark blue formazan dye capable of spectrophotometric detection. This process required active mitochondria from living cells and therefore dead cells do not cleave MTT. After four hours of incubation at 37°C, 100 µl of isopropanol with 0.04N hydrochloric acid (HCl) was added to each well. The isopropanol dissolved the formazan to give a homogenous blue solution suitable for absorbance. Absorbance was measured on a microplate spectrophotometer (Spectra Max 340; Molecular Devices, Berkshire, UK) at a test wavelength of 570 nm and a reference wavelength of 630 nm. Absorbance is directly proportional to the number of live cells and was normalized to the untreated control cultures which represented 100% viability, zero hours after reperfusion. Percentage of viability was measured by dividing the mean absorbance of the sample by the mean absorbance of control, multiplied by 100.

2.2.6.4 Hemichannel activity assay during OGDR

In order to monitor cells for hemichannel activity, PI uptake was observed and measured in low confluence fibroblast cells. As PI is membrane impermeant it is often used as a dead cell indicator, although live cells with open hemichannels will also label with this dye. Cells were cultured and grown to low confluence in 24-well plates to ensure cell to cell contact was not achieved and therefore any hemichannels at the plasma membrane remained undocked. Cultures were subjected to OGDR insult as described above and after 1.5 hours of oxygen-glucose deprivation, cells were subjected to reperfusion. Calcein-AM was added to the cells

for a 20 min incubation period. The medium was then removed and cultures were washed in triplicate using 1X PBS. Cultures were then treated with a single dose of 30, 100 or 300 μM Gap27 in OptiMEM or left untreated (naive OptiMEM). This was to ensue 'plugging' of open hemichannels and not continuous disruption of Cx43. A control of no OGDR was used. Images of a defined area of low confluence were taken on an Olympus inverted microscope (Olympus 1X81) on an XYZ stage (Prior XYZ stage, Cambridge, UK), in a temperature and gas controlled chamber (5% CO_2 and 95% air at 37°C). Further images of the same region of interest were taken every 30 min for five hours in each group. PI uptake was measured as a percentage of calcein-AM labelled cells in the first frame taken.

2.2.6.5 Bystander effect assay during OGDR

In order to monitor gap junction communication activity, PI uptake and transfer to neighbours in confluent fibroblast cells was observed. PI will enter cells through open hemichannels and is therefore small enough to pass to neighbouring cells via gap junction communication. Cells were grown to confluence to ensure gap junctions had the best possible chance of forming between neighbouring cells. Cultures were subjected to OGDR insult as described above and after 1.5 hours of oxygen-glucose deprivation, cells were subjected to reperfusion. Cells were either incubated with Gap27 (10, 30, 100, 300 or 1000 μM), 100 μM scrambled peptide or left un-treated (naive OptiMEM). A control of no OGDR and no treatment was used. After four hours of incubation in mimetic peptide, calcein-AM was added to the cells for a 20 min incubation period. The medium was then removed and cultures were washed in triplicate using 1X PBS. As described above, cultures were then replaced with fresh medium containing connexin mimetic peptide in OptiMEM (or naive OptiMEM) and PI. Images of a defined area of confluent cells were taken on an Olympus inverted microscope (Olympus 1X81) on an XYZ stage (Prior XYZ stage,

Chapter 2 Materials and methods

Cambridge, UK), in a temperature and gas controlled chamber (5% CO₂ and 95% air at 37°C). Further images of the same region of interest were taken every hour for 24 hours in each group. PI uptake was measured as a percentage of calcein-AM labelled cells in the first frame taken. Total PI uptake over 24 hours was measured.

The protocol was repeated using shRNA fibroblast cells and total PI uptake over 24 hours was measured.

The protocol was also repeated under Brilliant blue G (BBG) treatment. As described above, fibroblast cells were subjected to 1.5 hours of oxygen glucose deprivation followed by reperfusion. Cells were incubated with 2 or 20 µM BBG, 300 µM Gap27 or left untreated (naive OptiMEM). BBG is an antagonistic P2Y purinergic receptor blocker. After four hours of incubation in BBG or mimetic peptide, calcein-AM was added to the cells for a 20 min incubation period. The medium was then removed and cultures were washed in triplicate using 1X PBS. As described above, cultures were then replaced with fresh medium containing BBG, connexin mimetic peptide or naive OptiMEM, and PI. . Images of a defined area of confluent cells were taken on an Olympus inverted microscope (Olympus 1X81) on an XYZ stage (Prior XYZ stage, Cambridge, UK), in a temperature and gas controlled chamber (5% CO₂ and 95% air at 37°C). Further images of the same region of interest were taken every hour for 24 hours in each group. PI uptake was measured as a percentage of calcein-AM labelled cells in the first frame taken. Total PI uptake over 24 hours was measured.

2.3 *In vivo*

Three sets of animal experiments were carried out and all procedures conformed to UK Home Office regulations under project licence PDL70/6778.

2.3.1 Animals

Six week old male mice from the Institute of Cancer Research (ICR, UK) were used in all experiments. These animals were individually housed in an environmentally controlled room (temperature $21\pm 3^{\circ}\text{C}$, humidity $50\pm 20\%$, a light/dark cycle of 12 hours) and allowed free access to food and water. All mice were 30-35 g in weight.

2.3.2 General surgical procedures

All mice received anaesthesia and analgesic before surgical procedures were carried out. Individual mice were initially placed in a sealed chamber and anaesthesia was administered via isoflurane (3-4% isoflurane in 100% oxygen) at an air flow rate of two litres per minute. During this time a large patch of fur was shaved from the mouse dorsum (covering the area of interest to be wounded). The mouse was then injected subcutaneously, in the scruff of the neck, with 0.1 mg/kg analgesic buprenorphine (Vetergesic™). The anaesthetised mouse was then transferred to a heated mat and laid on its ventral side, while isoflurane was continually administered through a nose cone at the same concentrations and rates described above. The mouse pad or ear was pinched to gauge the response to anaesthesia and analgesic. Wounding was only carried out on unresponsive mice.

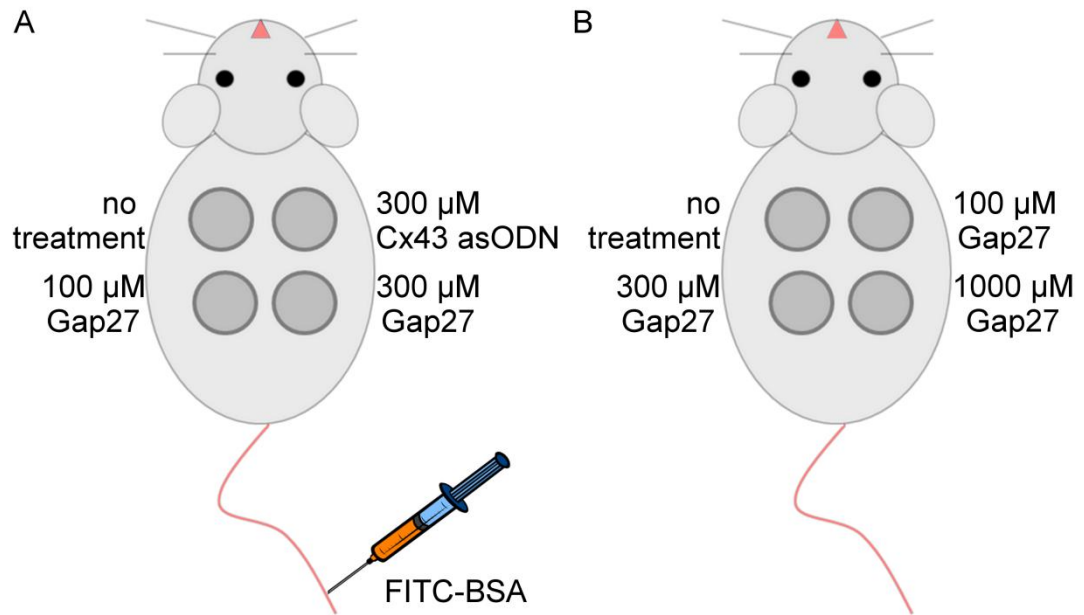


Figure 2.2 Diagrams of surgical procedures

(A) *Gap27* effect in vascular permeability. Mice were subjected to four 6mm wounds. Two wounds were treated with a single 25 μ l dose of either 100 or 300 μ M *Gap27*, one wound was treated with 300 μ M Cx43 asODN (positive control) and the final wound was left untreated (negative control). Four hours after wounding, a 200 μ l FITC-BSA was injected into the tail vein of each mouse. Mice were then euthanized 30 min after injection. (B) *Gap27* effect in wound healing. Mice were subjected to four 6mm wounds. Three wounds were treated with a single 25 μ l dose of 100, 300 or 1000 μ M *Gap27* and the final wound was left untreated (negative control). Mice were then euthanized 24 hours after wounding.

2.3.2.1 *Gap27* effect in vascular permeability during wound healing

A total of seven mice were wounded and treated with the investigational products; *Gap27* (100 and 300 μ M) and Cx43asODN (300 μ M). The drugs were dissolved in molecular grade water to make 1 mM stock before being formulated in 30% Pluronic™ gel. This delivery substance has thermo-reversible properties (can be liquid between 0 and 4°C and gels above 4°C) that enabled a constant and stable topical delivery of the drugs. Four circular 6mm full thickness punch wounds were

made on either side of the dorsal midline of each mouse. A single 25 μ l application of either 100 or 300 μ M Gap27 or 300 μ M Cx43 asODN were then applied to the wounds as detailed in figure 2.2A. Each mouse was kept anaesthetised for a further 30 min to allow the investigational products to absorb into the wound. The mice were then placed in a heated animal holding container, for recovery, before being returned to its home cage.

Three hours after wounding, each mouse was injected with 1.5% FITC-BSA via the tail vein. FITC-conjugated with Bovine Serum Albumen is used for vascular permeability measurements in inflammatory and oedema models. In order to see the delicate tail vein each mouse was warmed to 40°C in a heated chamber that caused vasodilatation. By using a clamp device to hold the mouse in place, 200 μ l of 1.5% FITC-BSA was injected directly into the base of the tail vein. Successful injections were indicated by observing the yellow dye travel up the tail vein towards the mouse torso. The FITC-BSA was given thirty minutes to travel around the mouse vasculature before the mouse was euthanized.

2.3.2.2 Gap27 effect in wound healing

A total of six mice were wounded and treated with three doses of Gap27 (100, 300 and 1000 μ M). The fourth wound was left untreated. Gap27 was formulated in 30% Pluronic™ gel. Four circular 6mm full thickness punch wounds were made on either side of the dorsal midline of each mouse. A single 25 μ l application of either 100, 300 or 1000 μ M Gap27 was then applied to the wounds as detailed in figure 2.2B. Each mouse was kept anaesthetised for a further 30 min to allow the investigational products to absorb into the wound. The mice were then placed in a heated animal holding container, for recovery, before being returned to its home cage. Twenty-four hours after wounding the mice were euthanized.

2.3.2.3 Ischemia reperfusion injury model

The following surgical procedure was adapted from a protocol developed by Thomas Mustoe (Reid et al., 2004). In this experiment a total of 20 mice were randomly divided into two equal groups. The first would undergo a single ischemic reperfusion cycle that would last 5.5 hours (1.5 hours ischemia; 4 hours reperfusion) whereas the second would undergo a single ischemic reperfusion cycle that would last 25.5 hours (1.5 hours ischemia; 24 hours reperfusion). Equal numbers within each timed group would receive 300 μ M of Cx43 asODN or would be left untreated; equalling to five mice within each group.

After the mouse dorsum had been shaved, it was cleaned with sterile water and disinfected with 70% ethanol (EtOH). A 1 cm transverse incision through the full thickness of the skin was made approximately 1 cm below the right shoulder. A 12 mm neodymium gold plated magnet was tunnelled under the skin and held in place. The incision was closed using a suture. An external gold plated neodymium magnet of the same size and strength was placed on the skin over the internal magnet for 1.5 hours (figure 2.3). After which the external magnet was removed and the pressure sites were either subcutaneously injected with 300 μ M Cx43 asODN formulated in 30% Pluronic™ gel or left untreated. The left side of the midline of the dorsum was considered as control skin within the mouse.

Thirty minutes before the mice were euthanized, 200 μ l of 1.5% FITC-BSA was injected into the tail vein of each mouse, as described above, to assess vascular permeability of the pressure site. The FITC-BSA was given thirty minutes to travel around the mouse vasculature before the mouse was euthanized.

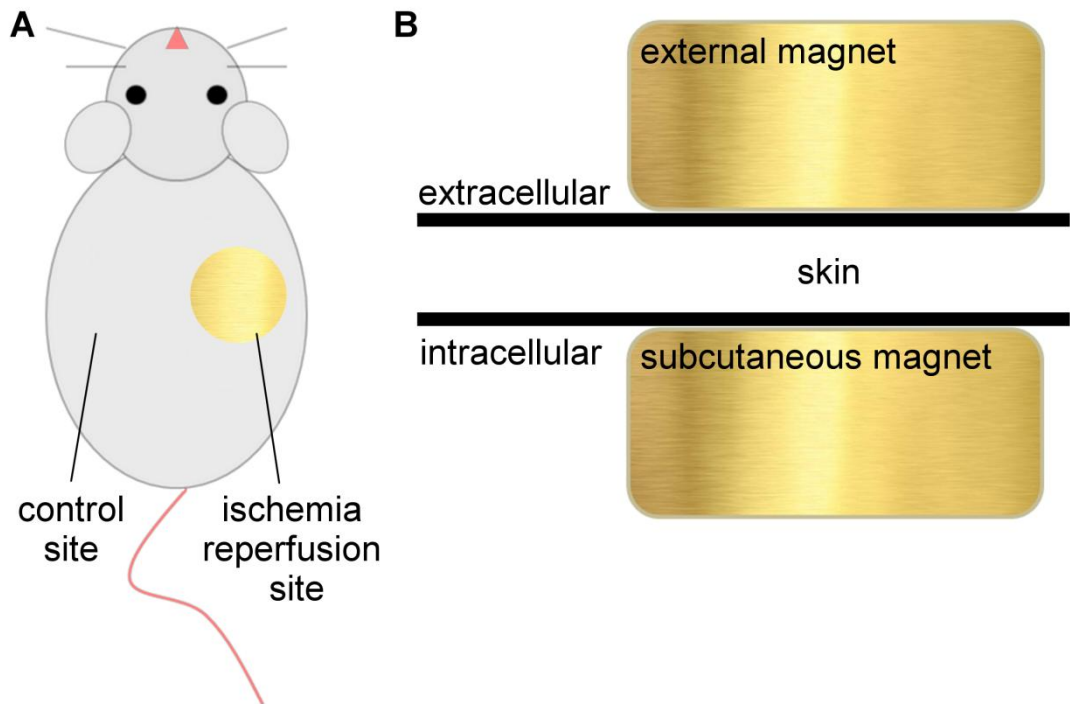


Figure 2.3 Ischemia reperfusion injury model

(A) *Ischemia reperfusion model.* The ischemic phase of the model is accomplished by applying a neodymium magnet over a region of skin in which another neodymium magnet has been subcutaneously implanted. The reperfusion phase occurs 1.5 hours after and is achieved by removing the external magnet. (B) *Cross-sectional view of the pressure model created using magnetic force.*

2.3.3 Tissue processing and cryosectioning

Immediately after euthanasia, the tissue of interest was carefully excised from the back of the mouse and laid on waxy cardboard to prevent the edges of the skin from rolling. The tissue was quartered into four separate wounds (figure 2.4A) before being submerged in 4% PFA at room temperature overnight. On the following day, the tissue was thoroughly washed with 1X PBS (minimum of three times for 1-2 hours) before being transferred into sucrose solution at 4°C overnight; 20% sucrose (VWR, Leicestershire, UK) with 0.1% sodium azide in 1X PBS.

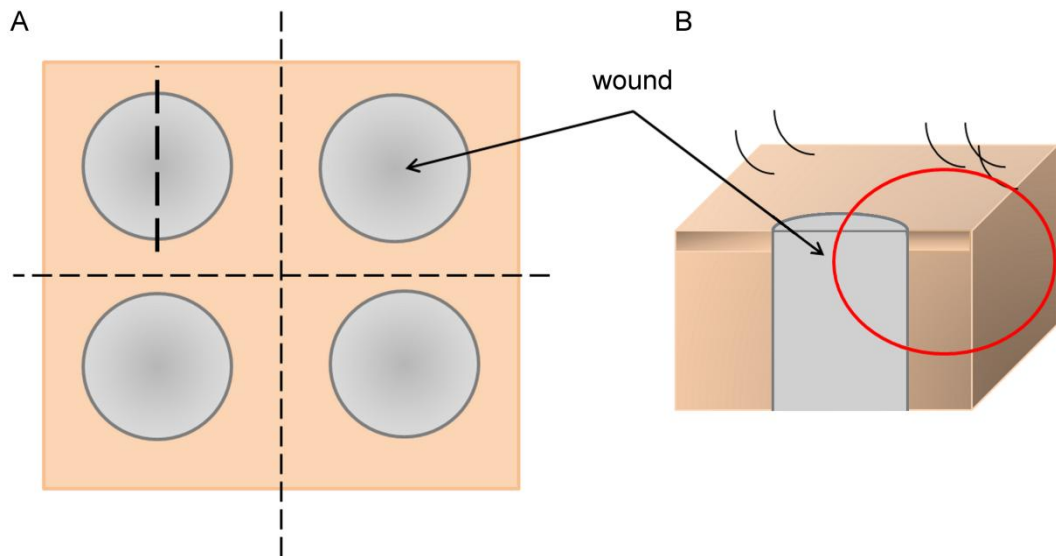


Figure 2.4 Tissue processing

(A) Back tissue from each mouse was removed and laid on waxy cardboard to prevent the skin edges from curling. Wounds are coloured grey. Scalpel lines are depicted as dashed black lines. The four wounds were quartered so that each wound could be carefully excised before being bisected. This was to ensure that the two wound edges in each wound would be visible when sectioning (B).

Before embedding, the circular back wounds or pressure sites were bisected (figure 2.4A). Half of the wound tissue was then placed in cryomolds in the same orientation before being embedded in OCT (Tissue Tek, Sakura Finetek, USA). The orientation would ensure that the two edges in each wound would be visible during cryosectioning (figure 2.4B). OCT is a well established medium for frozen specimens. Formulated of water soluble glycols and resins, OCT provides a convenient specimen matrix for cryostat sectioning at temperatures of -20°C . OCT is a viscous liquid at room temperature and a solid at temperatures of -10°C and below. The second half of the wound was kept for contingency and stored at -80°C . Tissues were cooled using dry-ice and stored at -80°C until cryosectioned.

Tissue samples were sectioned using a Leica Cryostat CM 1900 UV, (Leica, Milton Keys, UK) and mounted onto gelatine coated slides. Tissue samples destined for histology processing were cut at 5 μm thick, whereas tissue specimens for immunostaining were sectioned at 12 μm thick. Sectioned slides were stored at -20°C until processed.

2.3.4 Histology assay - Haematoxylin and Eosin stain

Slides were placed in the same orientation in a slide rack and allowed to acclimatise to room temperature for 5-10 min, before being rinsed well with dH_2O for 5 min. This was to ensure any excess OCT was rinsed away. Slides were then immersed in Haematoxylin stain for 30-45 sec followed by immediate rinse in continuous running tap water for 5 min to remove excess stain. Slides were then observed under a light microscope to assess over-staining (nuclei should be blue/purple whereas the cytoplasm should be clear). If the staining was too strong, the slides were dipped once into 0.3% acid alcohol (HCl in dH_2O), rinsed in running tap water and checked again. If the staining was too weak, the Haematoxylin staining run was repeated. Once the optimal stain had been achieved, slides were immersed in Eosin for 1 min. After a quick dip into tap water, the slides underwent a dehydration process (1 min in 70% EtOH, 2 min in 100% EtOH, a further 2 min in fresh 100% EtOH, 5 min in Xylene and a further 5 min in fresh Xylene). This is a delicate process and the timings are crucial. Too much dehydration will remove the Eosin stain, whereas too little dehydration will cause the tissue sample to fall apart. Slides were mounted onto glass coverslips using DePeX mounting medium (VWR, Leicestershire, UK) and allowed to dry at room temperature for at least 12 hours.

2.3.5 Immunostaining tissue

Slides were placed in a humidified, light protected, slide chamber and allowed to acclimatise to room temperature for 5-10 min. Tissue samples on the slides were subsequently covered with a few drops of 1X PBS for 5-10 min, to remove excess OCT. Slides were then placed in the same orientation in a slide rack and immersed in ice cold acetone for 5 min to fix and permeabilise the tissue. On removal, excess acetone was carefully wiped away and the tissue samples were circled using a wax pen. Tissue samples were covered with blocking solution (1M lysine, 1X PBS, 0.05% Triton X-100) and incubated. After 30 min, tissue was immunolabeled with a primary antibody diluted in blocking solution (refer to table 2.1 for dilutions and incubation periods). Negative controls were incubated overnight in blocking solution containing no primary antibody for the same time. Following removal of the primary antibody solution, cells were washed in triplicate using 1X PBS before incubation for one hour at room temperature with the secondary antibody (refer to table 2.2 for dilutions) diluted in blocking solution. A counter stain of Hoechst 33258 and 33342 (1:50,000) diluted in dH₂O was applied as a nuclear indicator. After a further three 1X PBS washes, the slides were coverslipped using Citiflour™ mounting medium and viewed under a confocal microscope (Upright SPE, Leica, Milton Keys, UK). All images were acquired using identical parameters and camera settings to allow for direct comparison of staining intensity.

2.3.6 Detailed analysis

2.3.6.1 Blood vessel leakiness

In order to assess whether Gap27 has an effect on the early immune response, blood vessel leakiness was analysed. Tissue samples were observed under a confocal microscope (Upright SPE, Leica, Milton Keys, UK). For each animal, at

least three optical section images were taken adjacent to the wound edge (site I), 200-400 nm away from the wound edge (site II) and 600-1000 nm from the wound edge (site III); see figure 2.5 for further details. Images were then uploaded to ImageJ for analysis. Total percentage of blood vessel leakiness in each field of view was measured. This data was then normalised within each animal back to the non-treated site as uniform FITC-BSA was not guaranteed.

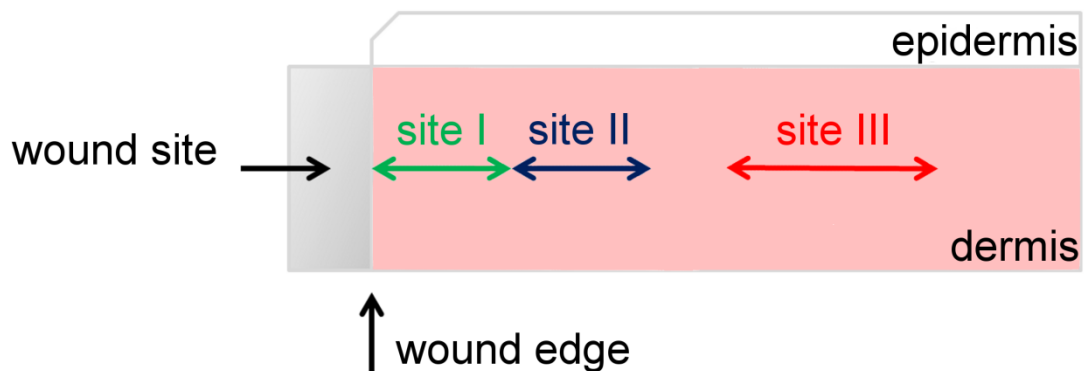


Figure 2.5 Regions of interest in blood vessel leakiness analysis

The cross section diagram of skin details the regions of interest measured in blood vessel leakiness analysis. Site I covers the dermis from the wound edge to 200 nm beyond the wound site. Site II covers the dermis 200-400 nm away from the wound edge. Site III covers the dermis 600-1000 nm away from the wound edge.

2.3.6.2 Inflammatory response

Haematoxylin and Eosin stained slides were used to assess the inflammatory response. Using identical parameters and camera settings images were taken with a light microscope (DMRE, Leica, Milton Keys, UK) before being uploaded onto ImageJ for analysis. Tissue was observed at the wound edge, distal to the wound edge and at blood vessels. Polymorphonuclear leukocytes were identified through high powered imaging of the tissue and leukocyte count per 1000 μm^2 was quantified.

2.3.6.3 Re-epithelialisation

Haematoxylin and Eosin stained slides were used to assess the re-epithelialisation rate. Using identical parameters and camera settings images were taken with a light microscope (DMRE, Leica, Milton Keys, UK) before being uploaded onto ImageJ for analysis. Re-epithelialisation was noted by measuring the distance from the top of the junctions between new and old epithelium to the leading edge of new epithelial growth on both sides of the wound in the epidermis. Measurements from both sides were averaged.

2.3.6.4 Connexin expression

Slides were immunolabeled for Cxs 26, 30, 43 and hemichannels to assess Gap27 effects during the early wound healing stages and slides were immunolabeled for Cx43 and hemichannels to assess Cx43 asODN effects on pressure wounds. Using identical parameters and camera settings images were screened using a light microscope (DMRE, Leica, Milton Keys, UK). Images were then taken for measurement using a confocal microscope (details below) before being uploaded onto ImageJ for analysis. In Gap27 dose response experiments, connexin profiles were measured within blood vessels, at the wound edge or adjacent to the wound edge, approximately 200-400 μm away from the wound (figure 2.6A). In pressure ulcer wound models, connexin profiles were measured at the pressure site, in tissue adjacent to the pressure site and in distal tissue (figure 2.6B). Connexin profiles were measured per nuclei within the epidermis and per 1000 μm^2 in the dermis.

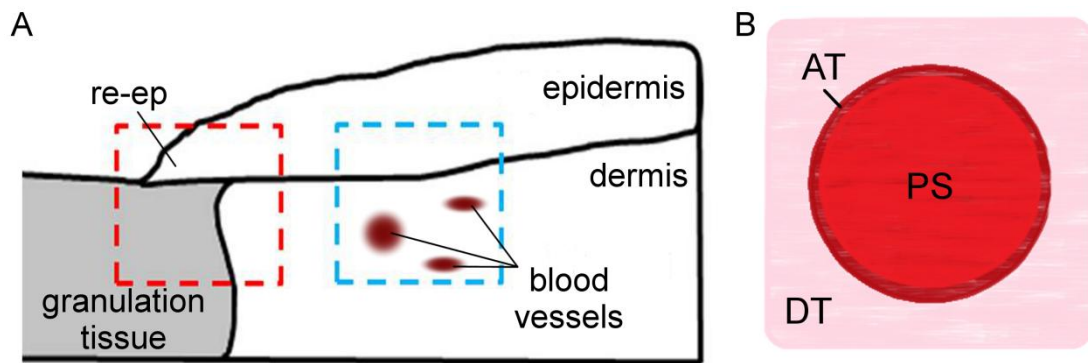


Figure 2.6 Regions of interest in connexin profiling

(A) *Punch biopsy wound.* The cross section diagram of skin details the regions of interest measured in *Gap27* dose response experiments. The red box indicates the wound edge whereas the blue box indicates an area adjacent to the wound edge, approximately 200-400 μm away from the wound. (B) *Ischemia reperfusion skin injury.* Diagram of a pressure site viewed from above indicates the areas of interest in connexin profiling. PS = Pressure site, AT = Adjacent tissue, DT = Distal tissue/non treated control site.

2.3.7 Confocal microscopy

In connexin profiling (*in vitro* and *in vivo*) single optical section images were taken using a Leica SPE confocal microscope using a 40X 1.2NA oil objective (*in vitro*) or a 60X 1.4NA oil objective (*in vivo*). Fluorophores were excited sequentially (Höchst using a 405 nm wavelength lasers, Alexa 488 using a 488nm wavelength laser and Alexa 568 using a 532 laser).

In blood vessel analysis single optical section images were taken using a Leica SPE confocal microscope using a 63X 1.4NA oil objective. Fluorophores were excited sequentially (Höchst using a 405 nm wavelength lasers, FITC-BSA using a 488nm wavelength laser and Alexa 568 using a 532 laser).

In FRAP analysis optical sections images, scanned in xyt mode, taken using a confocal microscope using a 63X water immersion apochromatic objective lens (NA, 0.9). FITC fluorophore was excited using a 488 nm wavelength.

All images were 8-bit greyscale at 1024 x 1024 pixels. Images were captured using a z-series frame average of four. All image acquisition settings remained identical between images in order to allow comparisons in image analysis.

2.3.8 Statistics

Statistical comparisons were made using either a one-way analysis of variance (ANOVA) or independent-samples t-test using SPSS Statistics™ (version 21, IBM). Data was tested for normality (Shapiro-Wilk test) and equal variances (Levene test) before statistical comparisons were carried out. In time-lapse experiments, the null hypothesis was rejected using a multivariate analysis of variance (MANOVA), The Dunnett post hoc test (against the control sample) or Tukey post hoc test were performed if data proved significant. All experiments were performed at least in triplicate. All data are presented as means \pm S.E.M. and n represents the number of repeats for each experiment indicated below each graph.

3. Gap27 mechanisms *in vitro*

3.1 Introduction

Gap junctions provide an essential route of communication that occurs in the majority of cells, tissues and organs in vertebrates. The exceptions to these cases include non-nucleated units such as platelets, red blood cells and skeletal muscle (Evans and Martin, 2002a). Previous work has consistently shown how gap junctions play fundamental roles in communication during the wound healing process (Goliger and Paul, 1995, Saitoh et al., 1997, Coutinho et al., 2003). A variety of cell types (including keratinocytes, fibroblasts and neutrophils) and tissue rely on complex communication through gap junctions and their connexins to ensure completion of wound healing (Coutinho et al., 2003, Brandner et al., 2004, Mori et al., 2006). By directly coupling neighbouring cells gap junctions provide a signalling highway for ions, small molecules and messages that are crucial in co-ordinating cellular activities during the stages of wound healing. Gap junctions are expressed in all cells linked with tissue repair and three key connexins (Cxs 26, 30 and 43) undergo dynamic changes to regulate the stages of wound closure (Coutinho et al., 2003). It has been noted in recent research that in chronic, non healing wounds Cx43 fails to down regulate at the wound edge and follow the natural sequence of events during wound closure (Brandner et al., 2004, Wang et al., 2007). Inhibiting Cx43 expression, using specific Cx43 asODN, can achieve significant improvement in wound repair (Qiu et al., 2003, Mori et al., 2006, Wang et al., 2007).

However, there are still very few pharmacological reagents that externally block this communication pathway in an acceptably specific manner without unwanted and non-specific effects. These include aliphatic alcohols (Guan et al., 1997, Cotrina et al., 1998b) and anaesthetics (Boitano et al., 1992), that although successfully

disrupt gap junction communication, do so by 'squeezing,' which is likely to modify other non-gap junction channels in the membrane. Other methods to disrupt gap junction communication involve using lipophilic aglycones (Taylor et al., 1998, Chaytor et al., 1999), which act indirectly to disrupt gap junction communication. The therapeutic answer to specific and external inhibition of hemichannel and gap junction based communication could lie in the development of the short synthetic connexin mimetic peptide Gap27 (Warner et al., 1995). Designed against Cx32 but also possessing homology to the second extracellular loop of Cx43, Gap27 has been extensively used to quickly and reversibly inhibit communication in gap junctions constructed of Cx43.

Connexin mimetic peptides, such as Gap27, have consistently been identified as effective inhibitors of gap junction based communication; however there is still some uncertainty on its mechanism of action. Several *in vitro* experimental studies into gap junction communication across a broad range of cells and tissues have resulted in three key theories on how connexin mimetic peptides can interrupt or inhibit this communication. These include the connexin mimetic peptide interacting with an unpaired connexon in the plasma membrane and therefore preventing connexons docking (figure 3.1A); interacting via the intracellular space within a gap junction resulting in its dissociation and ultimately leading to its internalisation (figure 3.1B); or interacting directly with a gap junction and altering its gating (figure 3.1C) (Berthoud et al., 2000, Evans and Boitano, 2001).

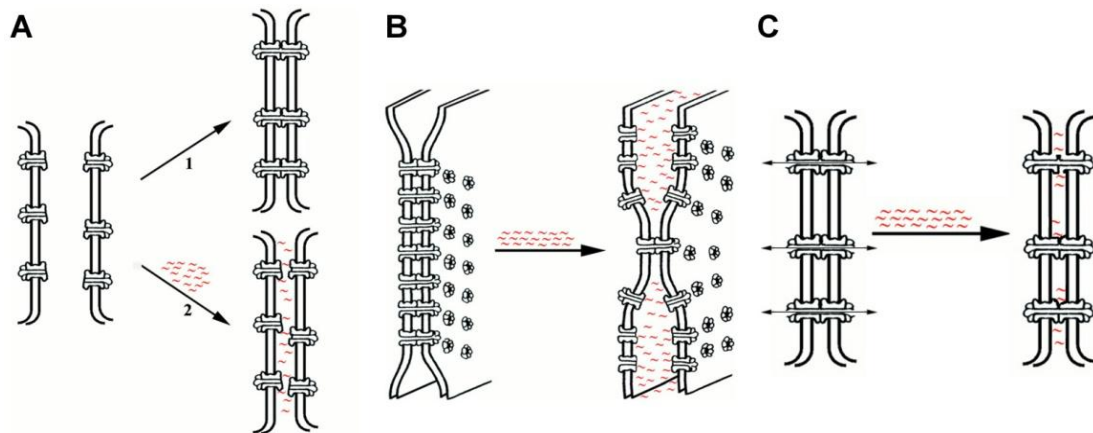


Figure 3.1 Proposed mechanisms of action of connexin mimetic peptides

(A) Diagram illustrating inhibition of docking. Gap junction channels are formed by docking of hemichannels from two neighbouring cells (arrow 1). In the presence of connexin mimetic peptide (depicted by red ~), docking is prevented (arrow 2). (B) Diagram illustrating dissociation of formed gap junctions. The presence of connexin mimetic peptides induces destabilization of established gap junction channels, leading to the undocking of hemichannels. (C) Diagram illustrating altered gating. Connexin mimetic peptides rapidly diffuse into the extracellular confines of gap junctions where the two hemichannels interact and alter channel gating. Diagrams adapted from *American Journal of Physiology Lung Cellular and Molecular Physiology* 279; L619-L622 (Berthoud et al., 2000) and *Biochemical Society Transactions* 29; 606-612 (Evans and Boitano, 2001).

Nonetheless in recent research it has been realized that connexin mimetic peptides show a huge potential in tackling connexin-based maladies and show promise in translational and therapeutic possibilities. For example, O'Carroll, Green and colleagues demonstrated that during an *in vitro* spinal cord injury, treatment with connexin mimetic peptides could significantly reduce the cell damage that occurs (O'Carroll et al., 2008) and more recently, cardiac protection has been noted when rat models of myocardial infarction are treated with connexin mimetic peptides (Hawat et al., 2012). Early work conducted by the Martin group has not only shown that connexin mimetic peptide Gap27 reduces gap junction communication in

Chapter 3 Gap27 mechanisms *in vitro*

human keratinocytes and fibroblast cells but has great potential in the wound healing environment (Wright et al., 2009, Pollok et al., 2011). The advantage of using connexin mimetic peptides such as Gap27 over Cx43 asODN (that specifically disrupts Cx43 protein production), is the unique time dependent properties that connexin mimetic peptides possess when disrupting either hemichannel or gap junction based communication.

Using skin cell cultures (immortal fibroblast cells derived from mouse; NIH 3T3 and immortalized keratinocyte cells derived from human; HaCat) the work presented in this chapter aims to build upon the current theories of Gap27 mechanism of action. This was achieved by characterizing the effect of Gap27 on connexin expression in these cells while exploring the mechanical effects of the connexin mimetic peptide in cell communication and *in vitro* models of wound healing.

Hypothesis – Gap27 will reduce communication and increase the migration rates in fibroblast and keratinocyte cells. There is no assumption that Gap27 will reduce connexin expression in these cell types.

3.2 Results

Gap27 incubation significantly reduced communication between fibroblast cells

For two hours confluent immortal NIH 3T3 fibroblast cells were treated with Gap27 (30 or 300 μM), scrambled peptide (300 μM) or left untreated (naive) prepared in complete OptiMEM. Cells were subsequently incubated with Calcein-AM and PI before FRAP was carried out. Fluorescence recovery was significantly reduced in cultures incubated in high (300 μM) concentrations of Gap27 in comparison to untreated (naive) cultures. There was no change in fluorescence recovery in cultures incubated in low (30 μM) concentrations of Gap27 or in scrambled peptide (figure 3.2)

Gap27 incubation significantly increased the rate of migration in fibroblast cells

Confluent NIH 3T3 fibroblast cells were subjected to an *in vitro* model of wound healing. Cultures were scratched before being treated with a single dose of Gap27 (10, 30, 100, 300 μM), scrambled peptide (100 μM) or left untreated (naive) prepared in complete OptiMEM. The rate of cell migration across the scratch wound increased in cultures incubated with high (100-300 μM) concentrations of Gap27 in comparison to untreated (naive) cultures. Incubation with scrambled peptide did not increase the rate of migration (figure 3.3).

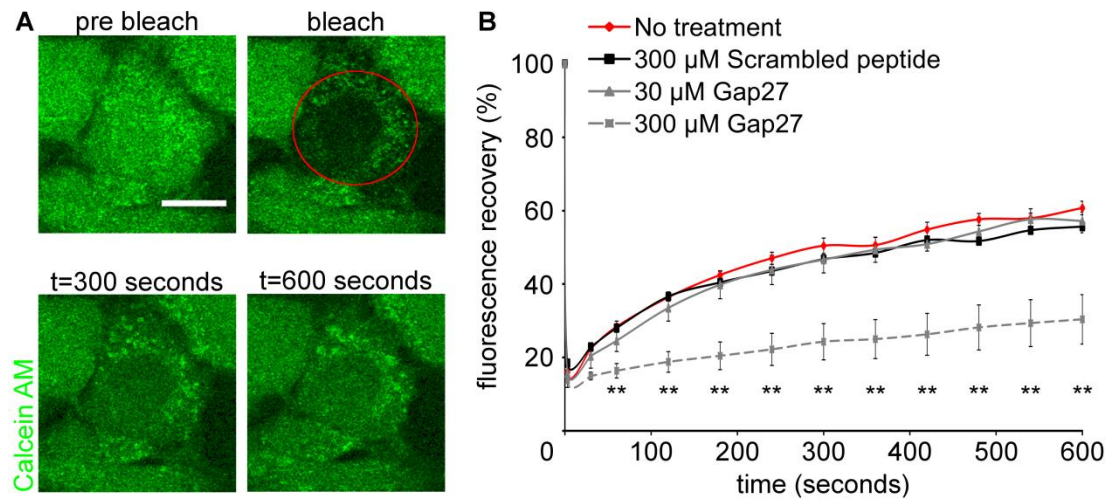


Figure 3.2 High concentrations of Gap27 significantly reduced gap junction communication in fibroblast cells

(A) The panels show representative images of Fluorescence Recovery after Photobleaching (FRAP). Cultures were incubated with Gap27 (30 or 300 μ M) or 300 μ M scrambled control peptide for two hours. A control of non-treatment was used. (B) Graph shows the recovery profiles of fluorescence. During incubation gap junction communication was significantly reduced between cells in 300 μ M Gap27. Statistical comparisons were made using a one-way analysis of variance (ANOVA). The null hypothesis was rejected using a multivariate analysis of variance (MANOVA) before statistical comparisons were carried out. The data is shown as the means \pm S.E.M. (Between non-treated cells and cells treated with 300 μ M Gap27 $n=3$, $**p<0.01$). Scale bar = 20 μ m, $t=$ time.

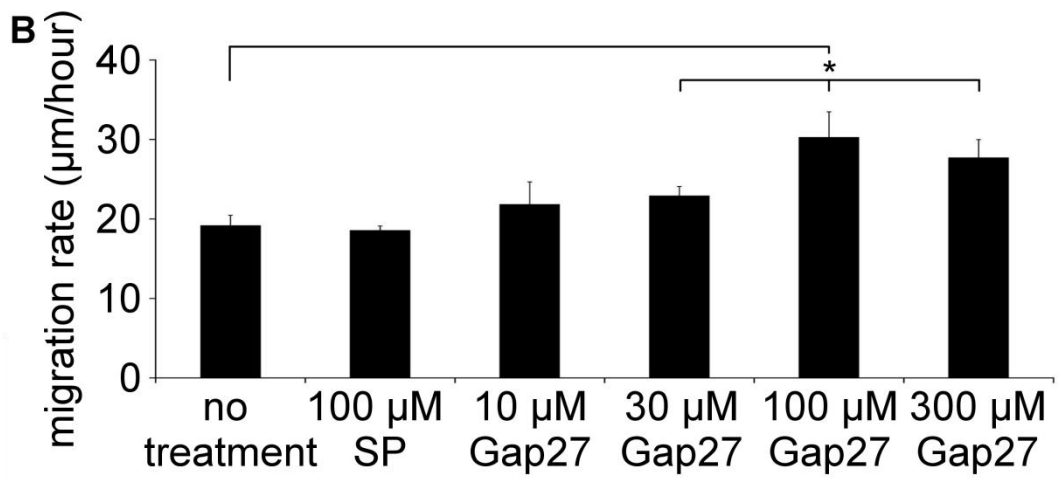
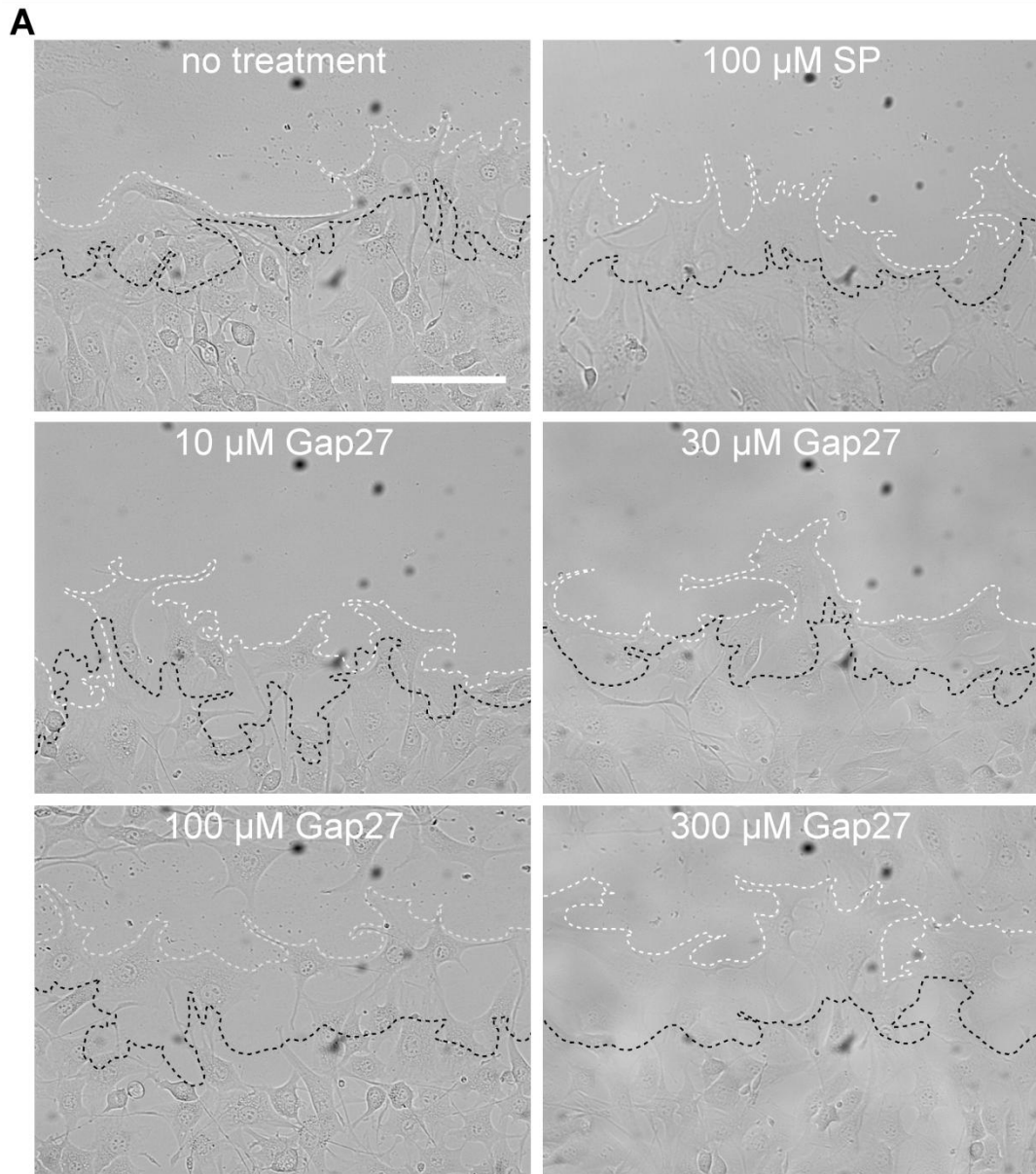


Figure 3.3 High concentrations of Gap27 significantly increased the rate of fibroblast cell migration

(A) The panels show representative images of scratch wounds during a migration assay. Confluent fibroblast cells were scratched and rinsed of any cell debris before being incubated with a single dose of 10, 30, 100 or 300 μM Gap27, 100 μM scrambled peptide or left untreated. The dashed black line indicates the leading edge of the scratch wound 1 hour after scratching. The dashed white line indicates the leading edge of the scratch wound 6 hours after scratching. (B) Graph shows the velocity of migration for all the aforementioned conditions. Cells incubated with higher (100-300 μM) concentrations of Gap27 migrated faster over the scratch wound. Statistical comparisons were made using a one-way analysis of variance (ANOVA). The data is shown as the means \pm S.E.M. ($n=4$, $*p\leq 0.05$). Scale bar = 100 μm . SP = Scrambled peptide.

Gap27 incubation significantly reduced Cx43 and connexin hemichannel expression in fibroblast cells

For two hours confluent NIH 3T3 fibroblast cells were treated with Gap27 (10, 30, 100 or 300 μM) scrambled peptide (100 μM) or left untreated (naive) prepared in complete OptiMEM. For six hour incubation periods, confluent NIH 3T3 fibroblast cells were treated with Gap27 (10, 30, 100 or 300 μM) scrambled peptide (100 μM) or left untreated (naive) prepared in complete OptiMEM and medium was replaced every two hours with fresh medium containing Gap27, scrambled peptide or naive OptiMEM. Cells were fixed and immunolabeled for Cx43 and nuclei before total pixel area per cell was quantified. Incubation of high (100-300 μM) concentrations of Gap27 for two hours and incubations with both low (10-30 μM) and high (100-300 μM) concentrations of Gap27 for six hours of continuous incubation significantly reduced Cx43 expression in fibroblast cells in comparison to untreated naive cultures. Incubation with scrambled peptide did not reduce Cx43 expression (figure 3.4).

Chapter 3 Gap27 mechanisms *in vitro*

Further analysis of Cx43 protein expression by Western blotting confirmed that Cx43 and phosphorylated isoforms of Cx43 decreased in confluent NIH 3T3 fibroblast cells after Gap27 treatment. Incubation of high (100-300 μM) concentrations of Gap27 for two hours and incubations with both low (30 μM) and high (100-300 μM) concentrations of Gap27 for six hours of continuous incubation significantly reduced Cx43 expression in fibroblast cells in comparison to untreated naive cultures (figure 3.5)

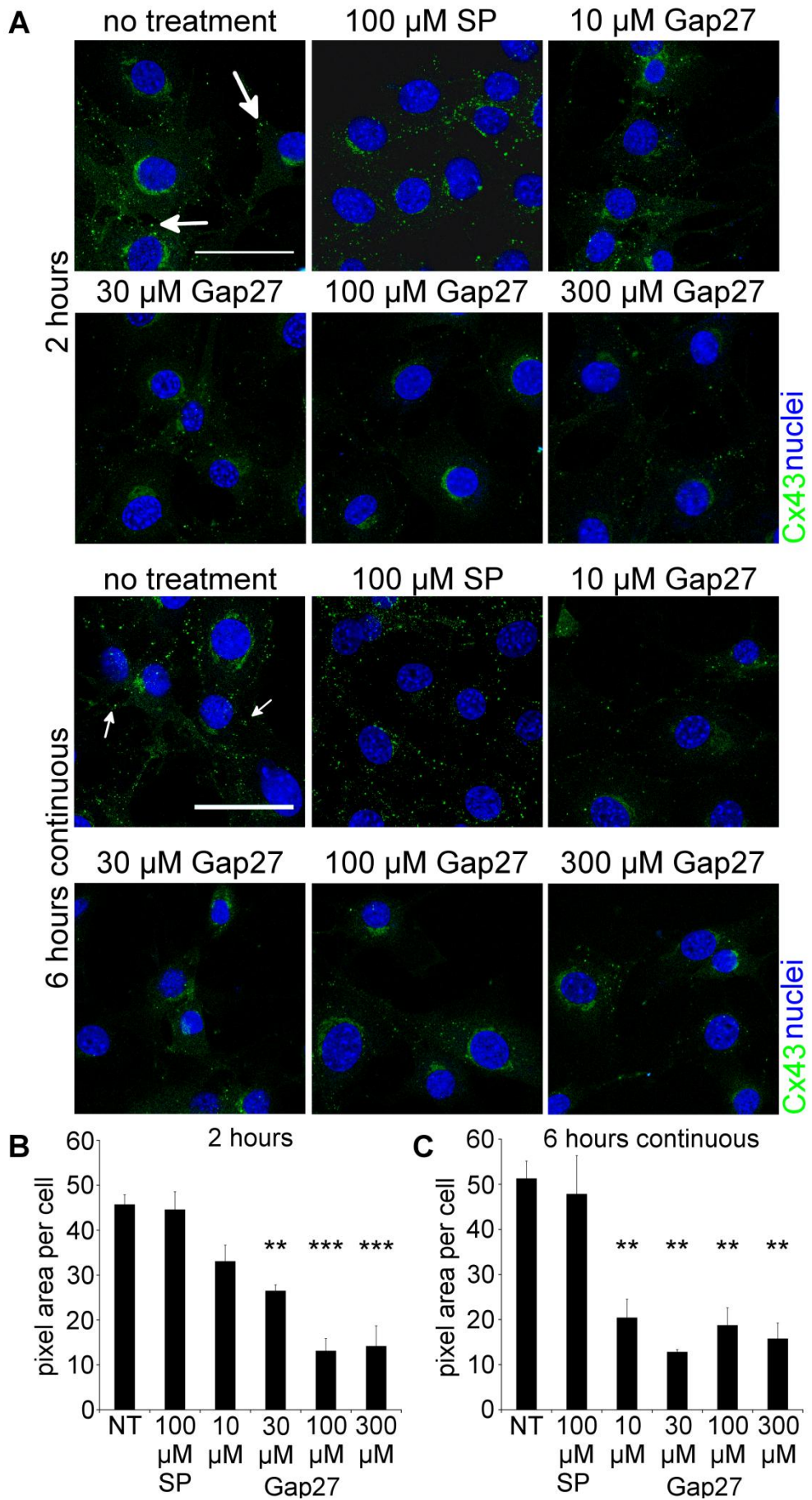


Figure 3.4 Effect of Gap27 on Cx43 expression in fibroblast cells; immunofluorescence analysis

(A) The panels show representative images of non-treated fibroblast cells and those that have been incubated with 100 μ M scrambled control peptide or increasing doses of Gap27 for either 2 hours or for 6 hours of continuous incubation (Gap27 replaced every 2 hours). A control of non-treatment was used. Cells were immunolabeled for Cx43 (green) and nuclei (blue), (B) Total pixel area per cell was quantified and the graph shows that higher doses (100-300 μ M) of Gap27 significantly reduced Cx43 expression in fibroblast cells after just two hours of incubation. (C) Total pixel area per cell was quantified and the graph shows that in continuous incubation both low (10-30 μ M) and high (100-300 μ M) doses of Gap27 significantly reduced Cx43 expression in fibroblast cells over 6 hours. Incubation with scrambled control peptide did not reduce Cx43 expression. Statistical comparisons were made using a one-way analysis of variance (ANOVA). The data are shown as the means \pm S.E.M. ($n=3$, ** $p<0.01$, *** $p<0.001$ against non-treated cells). White arrows indicate Cx43 expression. Scale bar = 50 μ m. NT = No treatment, SP = Scrambled peptide.

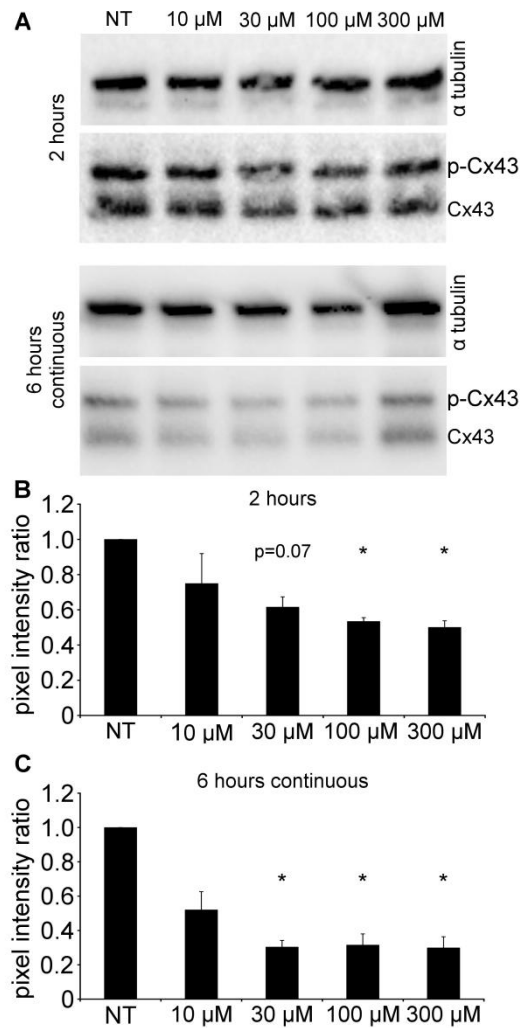


Figure 3.5 Effect of Gap27 on Cx43 expression in fibroblast cells; Western blot analysis

(A) Cx43 protein and phosphorylated isoforms (p-Cx43) expression in fibroblast cells during incubation with Gap27 was confirmed through Western blot analysis. The panels show representative blots. Alpha tubulin serves as a loading control housekeeping protein. (B) The intensity of the total protein was measured relative to the intensity of the housekeeping protein. The graph shows that higher doses of Gap27 (100-300 μ M) significantly reduced Cx43 protein expression in fibroblast cells after just two hours of incubation. (C) The graph shows that during 6 hours continuous incubation both low (30 μ M) and high (100-300 μ M) doses of Gap27 significantly reduced Cx43 expression in fibroblast cells over 6 hours. Statistical comparisons were made using a one-way analysis of variance (ANOVA). The data are shown as the means \pm S.E.M. ($n=3$, $*p<0.05$ against NT cells). NT = No treatment.

Chapter 3 Gap27 mechanisms *in vitro*

As above, for two hours confluent NIH 3T3 fibroblast cells were treated with Gap27 (10, 30, 100 or 300 μM) or left untreated (naive) prepared in complete OptiMEM. For six hour incubation periods, confluent NIH 3T3 fibroblast cells were treated with Gap27 (10, 30, 100 or 300 μM or left untreated (naive) prepared in complete OptiMEM and medium was replaced every two hours with fresh medium containing Gap27 or naive OptiMEM. Cells were fixed and immunolabeled for connexin hemichannels and nuclei before total pixel area per cell was quantified. Connexin hemichannel antibody is a custom made affinity purified antibody against a highly conserved portion of the first extracellular loop of Cx43. Incubation of high (30-300 μM) concentrations of Gap27 for two hours and incubations with both low (10-30 μM) and high (100-300 μM) concentrations of Gap27 for six hours of continuous incubation significantly reduced connexin hemichannel expression in fibroblast cells in comparison to untreated naive cultures (figure 3.6).

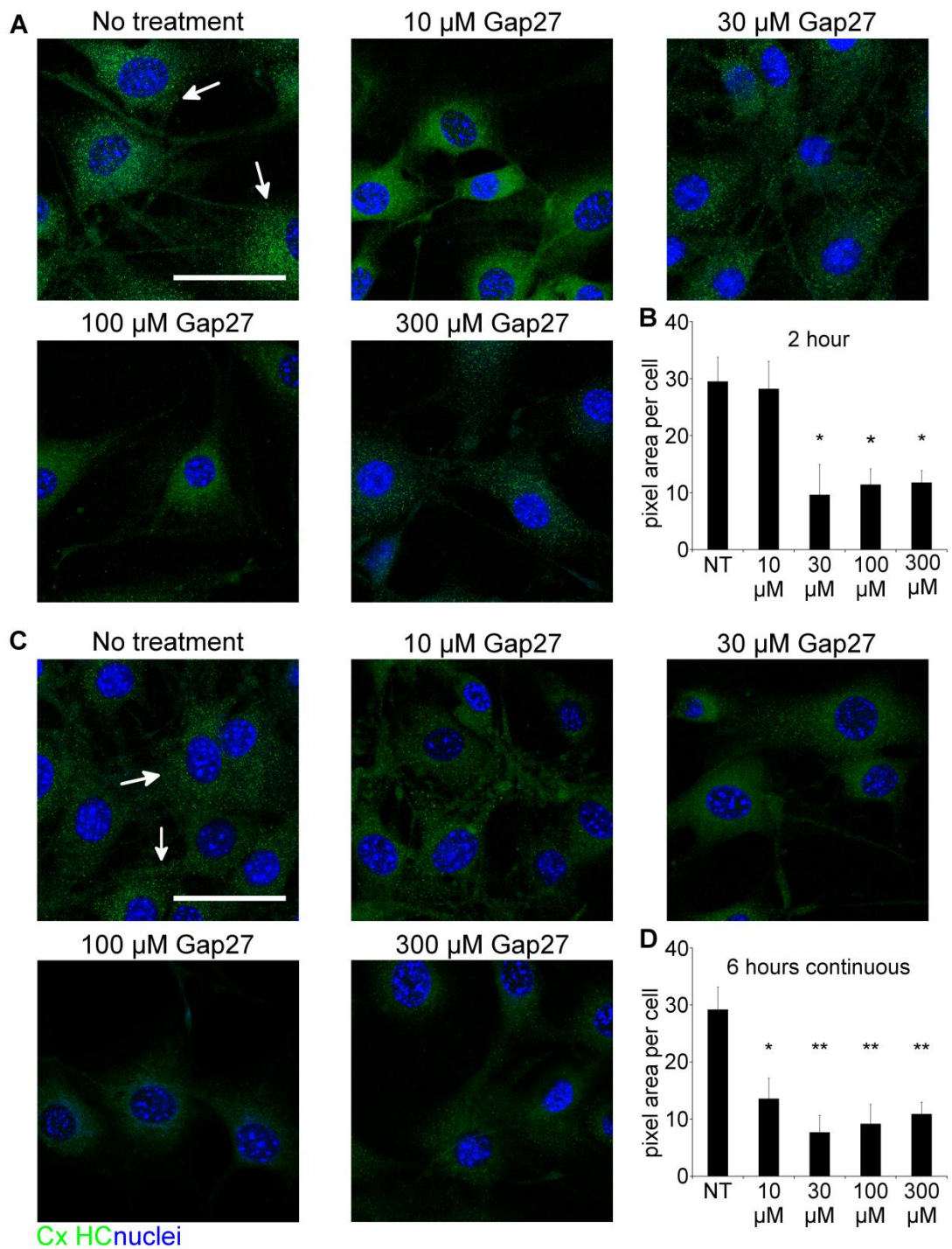


Figure 3.6 Effect of Gap27 on connexin hemichannel expression in fibroblast cells; immunofluorescence analysis

Chapter 3 Gap27 mechanisms *in vitro*

(A) The panels show representative images of non-treated fibroblast cells and those that have been incubated with increasing doses of Gap27 for 2 hours. A control of non-treatment was used. Cells were immunolabeled for hemichannels (green) and nuclei (blue). (B) Total pixel area per cell was quantified and the graph shows that mid to high doses (30-300 μM) of Gap27 significantly reduced hemichannel expression after just two hours of incubation. (C) The panels show representative images of non-treated cells and those that have been incubated with increasing doses of Gap27 for 6 hours of continuous incubation (Gap27 replaced every 2 hours). A control of non-treatment was used. Cells were immunolabeled for hemichannels (green) and nuclei (blue). (D) Total pixel area per cell was quantified and the graph shows that in continuous incubation both low (10-30 μM) and high (100-300 μM) doses of Gap27 significantly reduced hemichannel expression over 6 hours. Statistical comparisons were made using a one-way analysis of variance (ANOVA). The data are shown as the means \pm S.E.M. ($n=3$, $*p<0.05$, $**p<0.01$ against NT cells). White arrows indicate hemichannel expression. Scale bar = 50 μm . NT = No treatment.

Gap27 incubation significantly increased the rate of migration in keratinocyte cells

Confluent HaCaT keratinocyte cells were subjected to an *in vitro* model of wound healing as described above. Cultures were scratched before being treated with a single dose of Gap27 (10, 30, 100, 300 μM), scrambled peptide (100 μM) or left untreated (naive) prepared in complete OptiMEM. The rate of cell migration across the scratch wound significantly increased in cultures incubated with high (100-300 μM) concentrations of Gap27 in comparison to untreated (naive) cultures. Incubation with scrambled peptide did not increase the rate of migration (figure 3.7)

Gap27 incubation significantly reduced Cx43 expression in keratinocyte cells

As described above, for two hours confluent HaCaT keratinocyte cells were treated with Gap27 (10, 30, 100 or 300 μM) scrambled peptide (100 μM) or left untreated (naive) prepared in complete OptiMEM. For six hour incubation periods, confluent HaCaT keratinocyte cells were treated with Gap27 (10, 30, 100 or 300 μM) scrambled peptide (100 μM) or left untreated (naive) prepared in complete OptiMEM and medium was replaced every two hours with fresh medium containing Gap27, scrambled peptide or naive OptiMEM. Cells were fixed and immunolabeled for Cx43 and nuclei before total pixel area per cell was quantified. Incubation of high (100-300 μM) concentrations of Gap27 for two hours and incubations with both low (10-30 μM) and high (100-300 μM) concentrations of Gap27 for six hours of continuous incubation significantly reduced Cx43 expression in keratinocyte cells in comparison to untreated naive cultures. Incubation with scrambled peptide did not reduce Cx43 expression (figure 3.8).

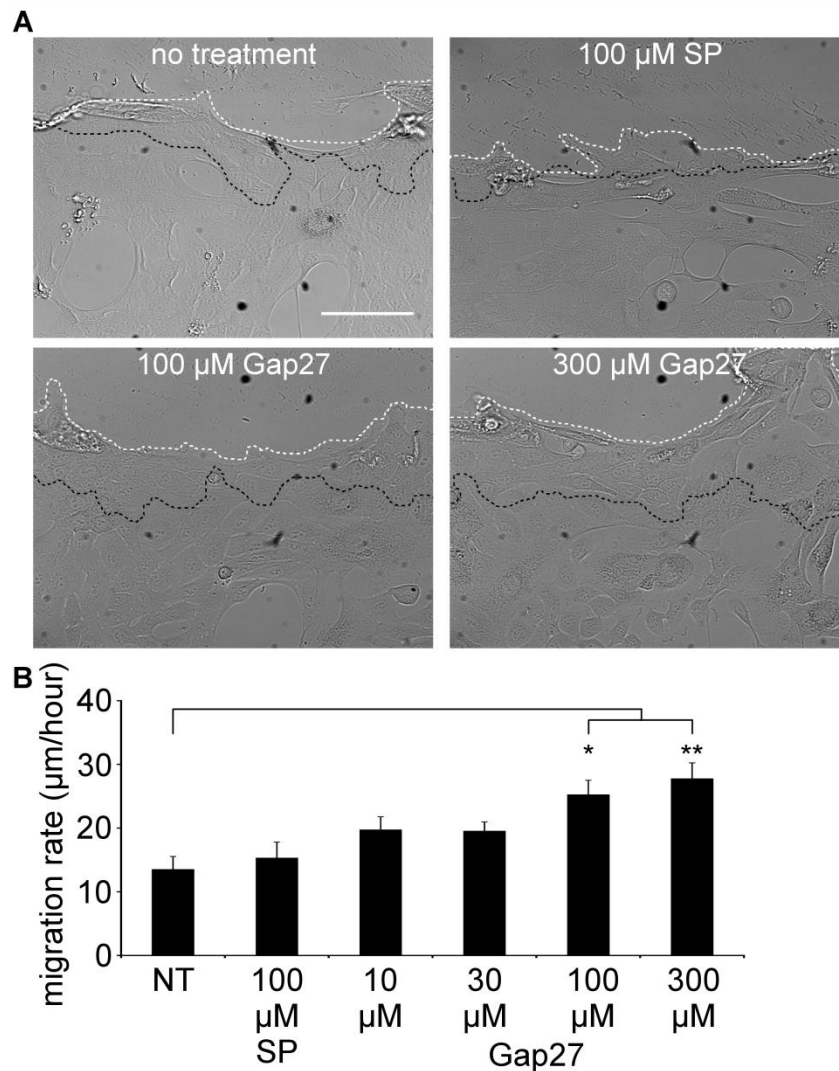


Figure 3.7 High concentrations of Gap27 significantly increased the rate of keratinocyte cell migration

(A) The panels show representative images of scratch wounds during a migration assay. Confluent keratinocyte cells were scratched and rinsed of any cell debris before being incubated with a single dose of 10, 30, 100 or 300 μM Gap27, 100 μM scrambled peptide or left untreated. The dashed black line indicates the leading edge of the scratch wound 1 hour after scratching. The dashed white line indicates the leading edge of the scratch wound 6 hours after scratching. (B) Graph shows the velocity of migration for all the aforementioned conditions. Cells incubated with higher (100-300 μM) concentrations of Gap27 migrated faster over the scratch wound. Statistical comparisons were made using a one-way analysis of variance (ANOVA). The data is shown as the means \pm S.E.M. ($n=4$, $*p<0.05$, $**p<0.01$). Scale bar = 100 μm . NT = No treatment, SP = Scrambled peptide.

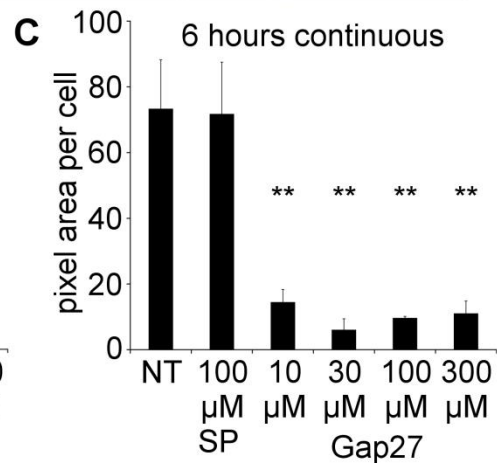
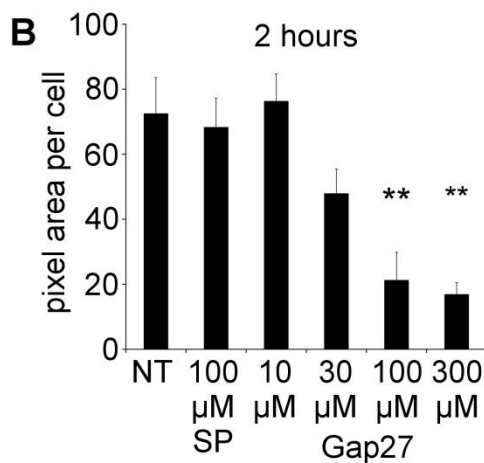
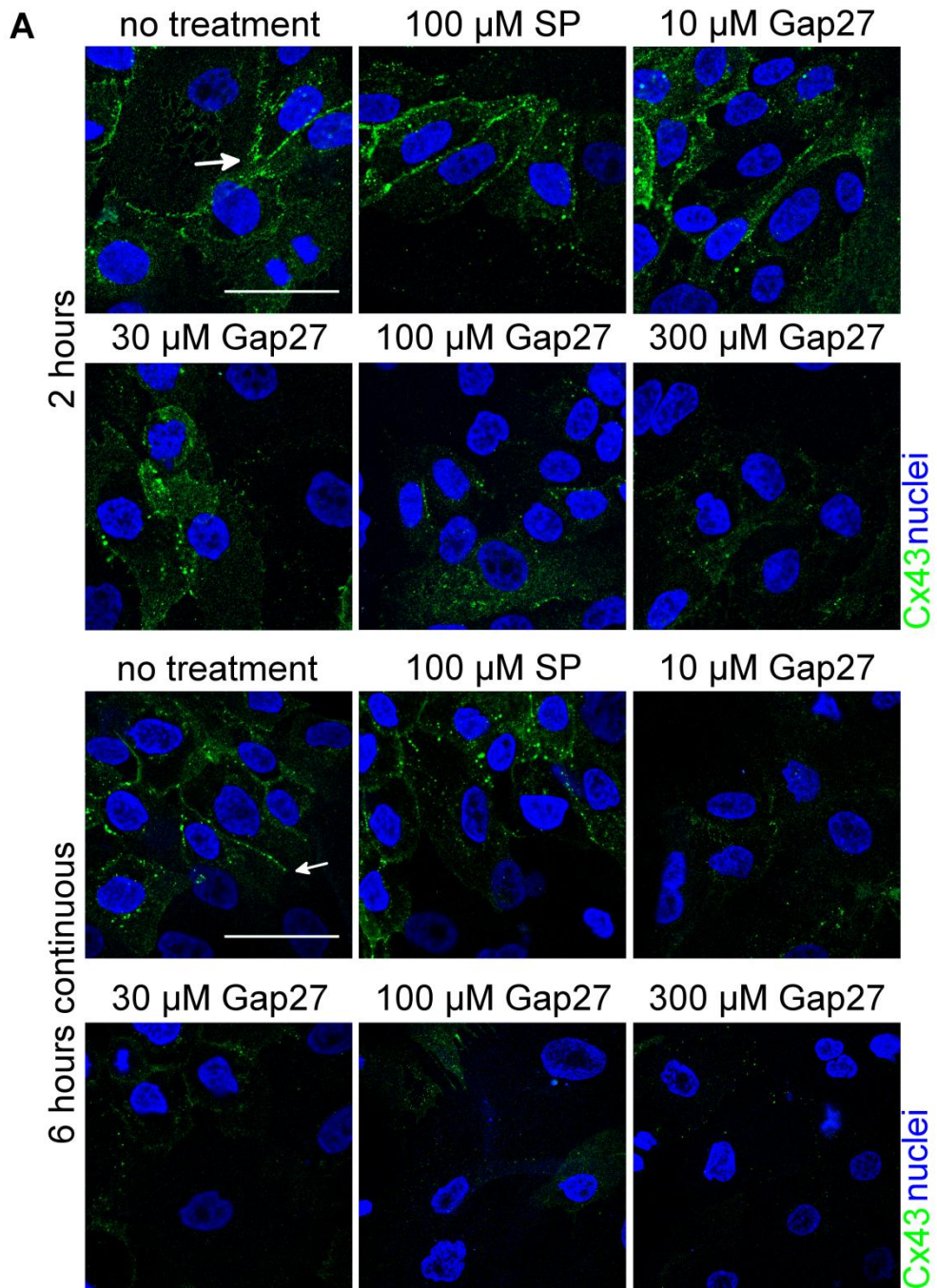


Figure 3.8 Effect of Gap27 on Cx43 expression in keratinocyte cells; immunofluorescence analysis

(A) The panels show representative images of non-treated keratinocyte cells and those that been incubated with 100 μM scrambled control peptide or increasing doses of Gap27 for either 2 hours or for 6 hours of continuous incubation (Gap27 replaced every 2 hours). A control of non-treatment was used. Cells were immunolabeled for Cx43 (green) and nuclei (blue), (B) Total pixel area per cell was quantified and the graph shows that higher doses (100-300 μM) of Gap27 significantly reduced Cx43 expression in keratinocyte cells after just two hours of incubation. (C) Total pixel area per cell was quantified and the graph shows that in continuous incubation both low (10-30 μM) and high (100-300 μM) doses of Gap27 significantly reduced Cx43 expression in keratinocyte cells over 6 hours. Incubation with scrambled control peptide did not reduce Cx43 expression. Statistical comparisons were made using a one-way analysis of variance (ANOVA). The data are shown as the means \pm S.E.M. ($n=3$, $**p<0.01$ against NT cells). White arrows indicate Cx43 expression. Scale bar = 50 μm . NT = No treatment, SP = Scrambled peptide.

Further analysis of Cx43 protein expression by Western blotting confirmed that Cx43 expression decreased in confluent HaCaT keratinocyte cells after Gap27 treatment. Incubation of high (100-300 μM) concentrations of Gap27 for two hours and incubations with both low (30 μM) and high (100-300 μM) concentrations of Gap27 for six hours of continuous incubation significantly reduced Cx43 expression in keratinocyte cells in comparison to untreated naive cultures (figure 3.9)

Continuous incubation with Gap27 significantly reduced Cxs 26 and 30 expressions in keratinocyte cells

For two hours confluent HaCaT keratinocyte cells were treated with Gap27 (10, 30, 100 or 300 μM) scrambled peptide (100 μM) or left untreated (naive) prepared in complete OptiMEM. For six hour incubation periods, confluent HaCaT keratinocyte cells were treated with Gap27 (10, 30, 100 or 300 μM) scrambled peptide (100 μM) or left untreated (naive) prepared in complete OptiMEM and medium was replaced every two hours with fresh medium containing Gap27, scrambled peptide or naive OptiMEM. Cells were fixed and immunolabeled for either Cx26 or Cx30 and nuclei before total pixel area per cell was quantified. Two hours of incubation in Gap27 did not significantly reduce Cx26 Cx30 in keratinocyte cells (figure 3.10). Incubation in both low (10-30 μM) and high (100-300 μM) concentrations of Gap27 for six hours of continuous incubation significantly reduced both Cx26 and Cx30 expression in keratinocyte cells in comparison to untreated naive cultures. Incubation with scrambled peptide did not reduce Cxs 26 and 30 expressions (figure 3.11).

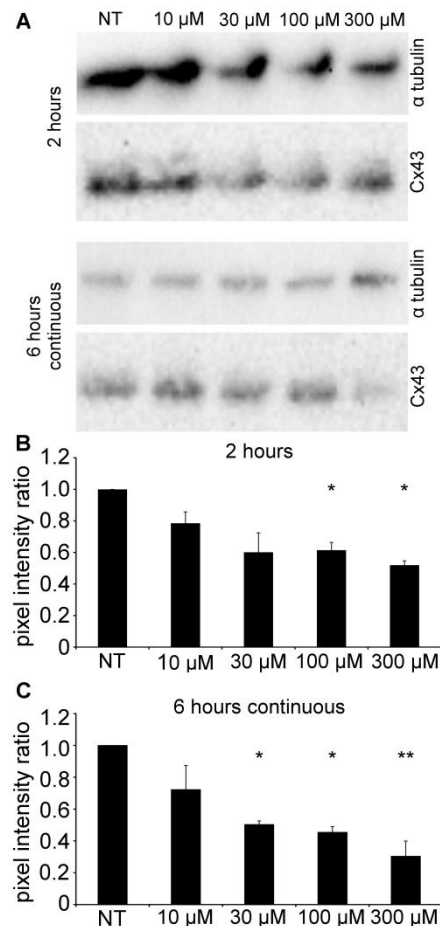


Figure 3.9 Effect of Gap27 on Cx43 expression in keratinocyte cells; Western blot analysis

(A) Cx43 protein expression in keratinocyte cells during incubation with Gap27 was confirmed through Western blot analysis. The panels show representative blots. Alpha tubulin serves as a loading control housekeeping protein. (B) The intensity of the protein of interest was measured relative to the intensity of the housekeeping protein. The graph shows that higher doses of Gap27 (100-300 μ M) significantly reduced Cx43 protein expression in keratinocyte cells after just two hours of incubation. (C) The graph shows that during 6 hours continuous incubation (Gap27 replaced every 2 hours) both low (30 μ M) and high (100-300 μ M) doses of Gap27 significantly reduced Cx43 expression in keratinocyte cells over 6 hours. Statistical comparisons were made using a one-way analysis of variance (ANOVA). The data are shown as the means \pm S.E.M. ($n=3$, $*p<0.05$, $**p<0.01$ against NT cells). NT = No treatment.

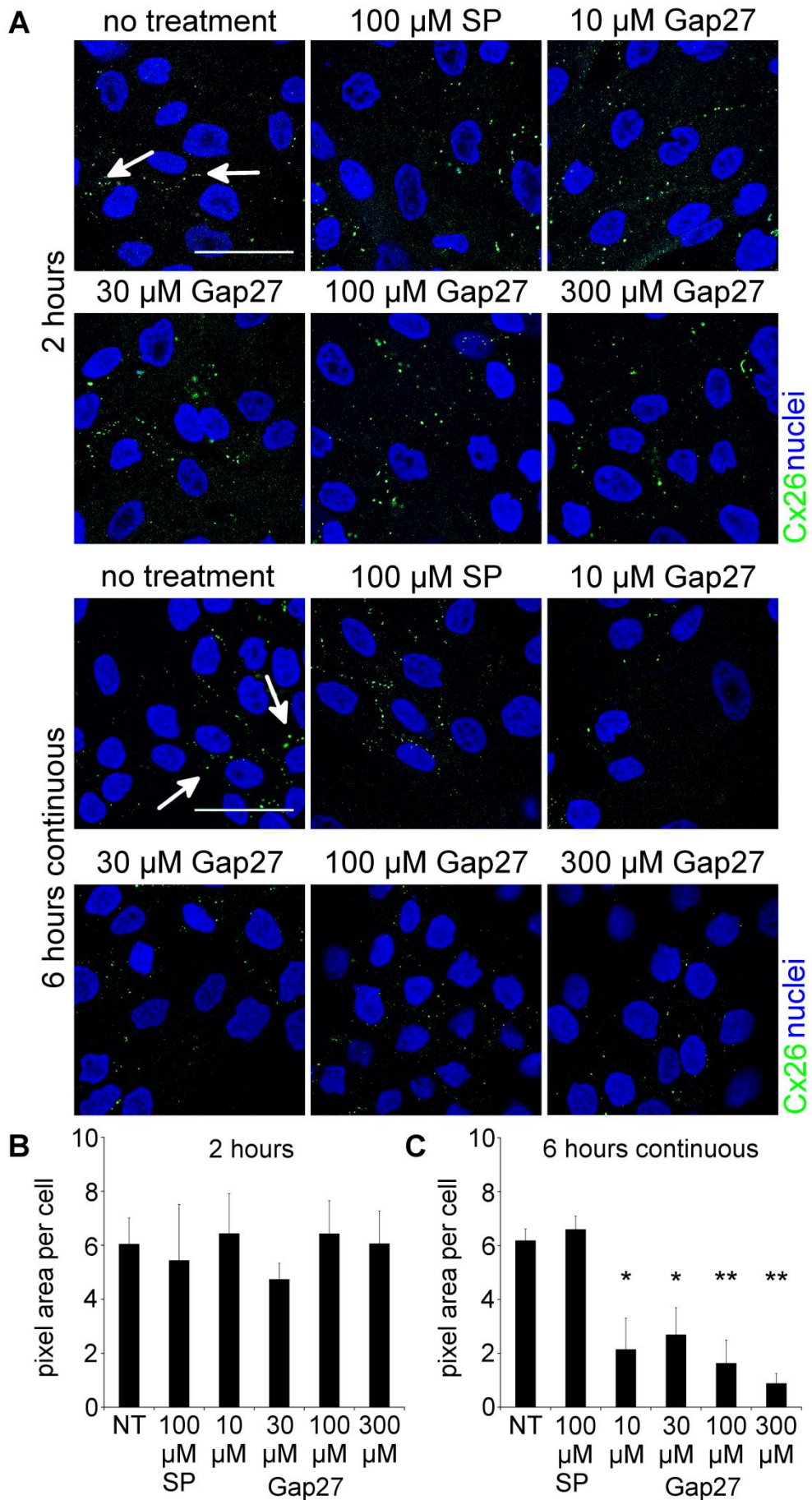


Figure 3.10 Effect of Gap27 on Cx26 expression in keratinocyte cells; immunofluorescence analysis

(A) The panels show representative images of non-treated keratinocyte cells and those that been incubated with 100 μ M scrambled control peptide or increasing doses of Gap27 for either 2 hours or for 6 hours of continuous incubation (Gap27 replaced every 2 hours). A control of non-treatment was used. Cells were immunolabeled for Cx26 (green) and nuclei (blue), (B) Total pixel area per cell was quantified and the graph shows that a short incubation period with Gap27 did not reduce Cx26 expression per cells. Incubation with scrambled peptide did not reduce Cx26 expression per cell. (C) Total pixel area per cell was quantified and the graph shows that in continuous incubation both low (10-30 μ M) and high (100-300 μ M) doses of Gap27 significantly reduced Cx26 expression in keratinocyte cells over 6 hours. Incubation with scrambled control peptide did not reduce Cx26 expression. Statistical comparisons were made using a one-way analysis of variance (ANOVA). The data are shown as the means \pm S.E.M. ($n=3$, $*p<0.05$, $**p<0.01$ against NT cells). White arrows indicate Cx26 expression. Scale bar = 50 μ m. NT = No treatment, SP = Scrambled peptide.

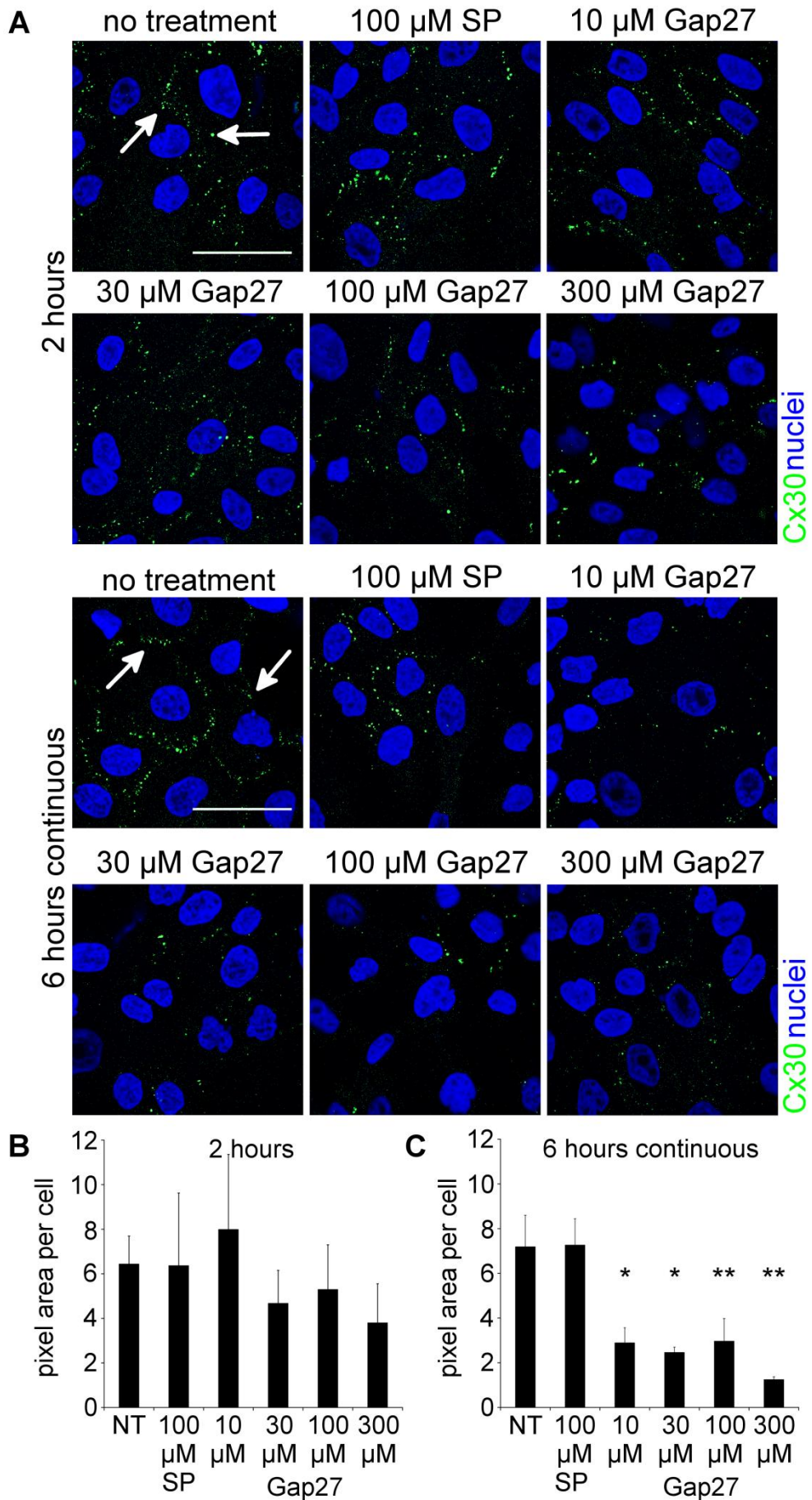


Figure 3.11 Effect of Gap27 on Cx30 expression in keratinocyte cells; immunofluorescence analysis

(A) The panels show representative images of non-treated keratinocyte cells and those that been incubated with 100 μ M scrambled control peptide or increasing doses of Gap27 for either 2 hours or for 6 hours of continuous incubation (Gap27 replaced every 2 hours). A control of non-treatment was used. Cells were immunolabeled for Cx30 (green) and nuclei (blue), (B) Total pixel area per cell was quantified and the graph shows that a short incubation period with Gap27 did not reduce Cx30 expression per cells. Incubation with scrambled peptide did not reduce Cx30 expression per cell. (C) Total pixel area per cell was quantified and the graph shows that in continuous incubation both low (10-30 μ M) and high (100-300 μ M) doses of Gap27 significantly reduced Cx30 expression in keratinocyte cells over 6 hours. Incubation with scrambled control peptide did not reduce Cx30 expression. Statistical comparisons were made using a one-way analysis of variance (ANOVA). The data are shown as the means \pm S.E.M. ($n=3$, $*p<0.05$, $**p<0.01$ against NT cells). White arrows indicate Cx30 expression. Scale bar = 50 μ m. NT = No treatment, SP = Scrambled peptide.

3.3 Discussion

Gap27 reduced gap junction communication

Functional assays of gap junctional communication mainly fall into two categories; the first measures the transfer of dye molecules between neighbouring cells whereas the second is designed to measure electrical currents carried by ions. FRAP was used to investigate the connectivity of neighbouring cells incubated in Gap27 by monitoring the diffusion of the fluorophore calcein between the connected cells. High concentrations of Gap27 significantly reduced gap junction communication in fibroblast cells after two hours of incubation (figure 3.2). Fibroblast cells left untreated or treated with either scrambled peptide or a tenfold lower dose of Gap27 showed no significant difference in communication.

Similar studies using dye transfer assays (where cells are injected with dyes with a typical weight of 500 Da that will comfortably transfer through communicating gap junctions) have shown that Gap27 significantly reduces communication in fibroblast like COS-7 cells (Dora et al., 1999, Chaytor et al., 1999) Schwann cells (Mambetisaeva et al., 1999) leukocyte cells (Oviedo-Orta et al., 2000), alveolar cells (Isakson et al., 2003) and HeLa cells transfected with Cx43-GFP (Berman et al., 2002). Incubation periods ranged from 15 minutes to a couple of hours in these studies but a consistent feature throughout was a high concentration of Gap27 (typically ranging between 130-500 μ M). As shown in the chapter, it is primarily high concentrations of Gap27 that will reduce gap junction communication.

Reduction in cell to cell gap junction communication was also seen in tracheal airway epithelial cells (Boitano and Evans, 2000) and primary ATII cells (Isakson et al., 2001) where high concentrations of Gap27 significantly reduced calcium waves in stimulated cells. Again, similar results were observed in rabbit mesenteric arterial

cells (Dora et al., 1999) and rat aortic smooth muscle cells (Kwak and Jongsma, 1999) where high concentrations of Gap27 reduced cellular conductance.

Gap27 increased the rate of migration

An *in vitro* model of wound healing was used to investigate mimetic peptide effects on cell migration rates and again it was the higher concentrations of Gap27 (100-300 μM) that had significant effects on increasing the rate of migration in both fibroblast (figure 3.3) and keratinocyte (figure 3.7) cells. Fibroblast and keratinocyte migration into the wound are crucial steps during the wound healing stages. Fibroblasts are recruited from several sources including circulating fibrocytes, bone marrow cells (Abe et al., 2001) and migrating fibroblasts from nearby unwounded dermis (Hinz, 2007). Within the maturing granulation tissue fibroblasts differentiate into α -SMA expressing myofibroblasts whose actin enable tissue contraction and help contract down the granulation tissue (Hinz et al., 2001a). Whereas keratinocyte cells achieve re-epithelialisation of the wound by crawling and migrating along the wound edge and aiding in ultimate wound closure. It was observed in the research presented in this chapter how both fibroblast and keratinocyte cell rates of migration were clearly increased by high concentrations of Gap27 and those cells left untreated or treated with either scrambled peptide or a lower dose of Gap27 had no significant difference in the rate of migration.

Conversely, studies of wound closure using rat fibroblast cells have shown that treatment using non-specific gap junction blockers heptanol and endosulpan led to a reduction in both fibroblast migration and collagen production (Ehrlich and Diez, 2003). However, as discussed previously, the use of non-specific blockers of gap junction communication can frequently lead to unwanted and non-specific effects. Using NIH 3T3 fibroblast cells that have been transduced with Cx43 specific shRNA construct in an *in vitro* scratch wound model, Mendoza-Naranjo and colleagues have shown that reducing Cx43 and Cx43 based gap junction communication

significantly increases the migration rate (Mendoza-Naranjo et al., 2012a). Further supportive studies carried out by the Martin group have shown how Gap27 incubation can significantly increase the rate of migration in a range of fibroblast and keratinocyte cell types. In both an *in vitro* organotypic culture (Kandyba et al., 2008) where primary mouse keratinocyte cells were seeded onto primary mouse dermal cells, and in primary human fibroblast and keratinocyte cells (Wright et al., 2009) Gap27 increased the rate of cell migration and the rate of *in vitro* wound closure. An acceleration of Gap27 migration was also observed in human fibroblast and keratinocyte cells that had their proliferation rates inhibited through pre-treatment by x-ray radiation (Pollok et al., 2011).

Typical total rates of migration, observed in cells involved in the studies carried out by the Martin group, ranged between 8-10 μm per hour in fibroblast cells and between 6-15 μm per hour in keratinocyte cells. Work presented in this research chapter (where migration rates were approximately 18-30 μm per hour in fibroblasts and 15-30 μm per hour in keratinocytes) highlight a difference in migration rates. However a closer observation into the scratch wound studies carried out by the Martin group reveal faster rates of migration in the first few hours of observation. Typically 20-25% of *in vitro* wounds had already closed in the first 6-12 hours of a 48-72 hours study. This initial burst of migration in the first few hours of observation supports the results I have presented in this chapter where migration rates were only observed for a six hour window, when migration rates in scratch wound assays are at their peak. Furthermore it was noted that peptide replenishment was only executed every 12 hours. Work carried out by Wright and colleagues have shown through dye transfer assays that the mimetic peptide Gap26M has a peak level of effectiveness 90 minutes post application, remaining at a similar level of effectiveness 5 hours post application before dropping significantly to control levels 8 to 24 hours post application (Wright et al., 2009). Although Gap26 aligns to a

region in the first extracellular loop of Cx43, whereas Gap27 aligns to a region within the second, one would expect the breakdown rate of a similar number of amino acids to be relatively comparable. One note of interest is that Gap26M is an amended version of Gap26 that has an acylated N-terminus to provide the connexin mimetic peptide with greater solubility and stability. Therefore the peak effectiveness level of unmodified connexin mimetic peptides may be sooner and last for less time. Thereby if the mimetic peptide effectiveness is thought to drop significantly 8 to 24 hours post application, this could explain the slower rates of migration seen in the work carried out by the Martin group. This is particularly noted in Wright and colleagues work where migration rates of human fibroblast cells appear to increase and plateau in turn over 72 hours which would correspond to reapplication of peptide every 12 hours (Wright et al., 2009). These periods of migration when peptide is replenished could correspond to a reduction in gap junction communication that is encouraging an increase in cell migration rates.

Gap27 reduced Cx43 and connexin hemichannel expression

Previous research discussed above together with work presented in this research chapter supports the consistent claim that connexin mimetic peptides are effective inhibitors of gap junction based communication. Novel work presented in this chapter also suggests that it is higher concentrations of Gap27 that effectively reduced this communication. However there is still some uncertainty on connexin mimetic peptide's mechanism of action and there are currently three key theories on how peptides can interrupt or inhibit gap junction communication as discussed in detail above (Berthoud et al., 2000, Evans and Boitano, 2001). The first includes the assumption that mimetic peptides may be interacting with unpaired connexons in the plasma membrane, ultimately preventing the docking of complementary hemichannels from neighbouring cells and thereby reducing the number of operational gap junction channels and gap junction communication. As connexins

have a rapid turnover, between 1 and 4 hours (Fallon and Goodenough, 1981, Traub et al., 1987), this mechanism of disruption can be achieved in a relatively short time. The second theory suggests that connexin mimetic peptides interact via the extracellular space within a gap junction resulting in the dissociation or 'undocking' of the channel and leading to its internalization and breakdown. This would also cause a reduction in the number of operational gap junction channels and ultimately reduce gap junction communication. Finally, the third theory hypothesises that mimetic peptides interact directly with gap junctions and alter their chemical gating, thus reducing gap junction communication.

In a novel discovery reported in this research chapter, it was observed that incubation with Gap27 significantly reduced Cx43 expression in both 3T3 fibroblast and HaCaT keratinocyte cells. This was shown by both immunostaining (figure 3.4 and figure 3.8) and in Western blot protein quantification assays (figure 3.5 and 3.9). A key observation made throughout these results was that in the short incubation period of two hours, only higher concentrations of Gap27 significantly reduced Cx43 expression. In the six hour incubation period, where Gap27 was replaced every two hours, both lower and high concentrations significantly reduced Cx43 expression.

A comparable report was made by O'Carroll, Green and colleagues when incubating *ex vivo* spinal cord segments in 'Peptide 5'; a 12 amino acid long short connexin mimetic peptide that corresponds to the second extracellular loop of Cx43 and overlaps with Gap27 by seven amino acids (O'Carroll et al., 2008). A markedly reduced expression of Cx43 was observed in cultures as shown by Western blot when compared to cells incubated in a control peptide. However until now there have been no more reports that support the claim that mimetic peptides have the ability to reduce Cx43 expression.

Berman and colleagues were the first to claim that connexin mimetic peptides decrease gap junction communication without disrupting their intrinsic structure (Berman et al., 2002). Using HeLa cells stably transfected with Cx43-GFP incubated in Gap27 for 90 minutes, they observed that Lucifer yellow dye transfer was reduced between connected cells, yet there was no significant difference in plaque number of Cx43 between untreated and treated cells. However, it should be noted that cells were also treated with sodium butyrate 18 hours before experiments were carried out to enhance protein expression and therefore cannot be fairly compared to natural Cx43 expression in cells. A similar study was carried out using an immortal smooth muscle cell line transfected with Cx43-GFP (Martin et al., 2005) to visualise trafficking of the protein to the cell membrane in cells treated with Gap26 or Gap27, or left untreated. Punctate staining of Cx43 was apparent in both sets of cells; however there was no visual difference in Cx43 expression. On the other hand, it must be mentioned that quantification was carried out 12 hours after Gap27 incubation and that during quantification there was no measurement of plaque area or number, only overall fluorescence. As detailed above, Gap27 is unlikely to be effective 12 hours after application due to its fragile structure and ease of degradation. In addition, quantification took place past the natural turnover time of connexins. Both studies claim that Gap27 doesn't reduce Cx43 expression but neither observed this in cells that naturally express this connexin.

Rat aortic smooth muscle cells, that do naturally express Cx43, were incubated in Gap27 for 4 hours before immunocytochemical analysis to determine Cx43 expression (Martin et al., 2005). Although it was reported that gap junction plaques in the plasma membrane remained intact with levels of fluorescence not differing significantly from control cells, there was an observed reduction in Cx43 expression shown in the fluorescent images and graphical data of this result. In this study, cells were incubated in complete DMEM supplemented with 10% foetal bovine serum and

it has been well documented how proteases within serum can rapidly digest and break down peptides, greatly reducing their half life. It is highly likely that after four hours of incubation, the peptide will no longer have an optimal effect on Cx43 expression in cells, as the peptide has been degraded in this serum supplemented medium. Another group, using primary keratinocyte cells, observed that although Gap27 significantly reduced gap junction communication as shown by reduction in dye transfer, the mimetic peptide did not reduce Cx43 expression. However, there was no quantification of Cx43 expression and only an illustrative observation was made (Wright et al., 2013).

This is the first detailed report exploring the dynamics of time and concentration effects of Gap27 on Cx43 expression. Research presented in this chapter has shown for the first time, using 3T3 fibroblast and HaCaT keratinocyte cells (that naturally express Cx43) in a time and concentration dependent protocol, that a high concentration of connexin mimetic peptide Gap27 significantly reduced Cx43 expression. This was coupled with high concentrations of Gap27 reducing gap junction communication and increasing the migration rate of cells.

It is unlikely that Gap27 reduced Cx43 through dissociation of already formed gap junctions, as once hemichannels have docked with their neighbouring hemichannels and accreted latterly in the plasma membrane, they are very difficult to tear apart (Evans and Boitano, 2001). The first and second extracellular loop domains of connexin proteins are the segments that are primarily involved in intercellular interactions during docking. Each domain has three conserved cysteine residues, joined by at least one disulfide bond between the loops. Docking between opposed hemichannels involves the interactions between the extracellular loops to complete a fully formed channel. This interaction subsequently provides a continuous wall of protein, functioning as a tight electrical and chemical seal (Unger et al. 1999). The construction of this sealed bridge is difficult to break and it is doubtful that Gap27 is

able to disrupt this connection. Indeed, it has been shown in research that explores the trafficking of connexin proteins using cells that are transfected with connexin-fluorophores that one of the two partner cells internalises a fully formed gap junction from both cells (Jordan et al., 2001) confirming that once formed, gap junctions are not likely to pull apart.

Because of the strong interaction between connexons and the difficulty to disrupt this link, early theories developed by Evans and Berthoud proposed that the primary action of mimetic peptides such as Gap27 was to mimetically bind to undocked hemichannels, before preventing the docking of connexons to form functional gap junctions (Berthoud et al., 2000, Boitano and Evans, 2000). Connexin mimetic peptide's high affinity to its counterpart sequence on the extracellular loop would compete with and prevent the docking of two connexin hemichannels, causing disruption to gap junction coupling. This would suggest an early effect of Gap27 was to inhibit hemichannel based communication before a later effect was to reduce or inhibit gap junction formation. This theory was supported by the results of a study using intravenous injections of fluorescently tagged Gap26 in a rat model of myocardial infarction. It was observed how the connexin mimetic peptide was able to reach the lateral membranes of cardiomyocytes and co-localise with Cx43, but remained absent from intercalated discs where gap junctions were formed. This demonstrated how Gap26 was able to interact with unopposed hemichannels but was unable to access the binding sites of connexons, on connexin extracellular loops, due to their engagement with their docked counterparts (Boengler et al., 2005).

Further work by Desplantez and colleagues, using an electrophysiological experiment with HeLa cells expressing Cx43 (Desplantez et al., 2012), demonstrated that Gap26 applied to non-contacting single cells inhibited hemichannel based currents whereas Gap26 applied to paired cells for a longer

incubation period inhibited gap junction communication, suggesting prevention of hemichannel docking. Recent work by Wang and colleagues, using patch clamp studies in HeLa cells transfected with Cx43 and pig ventricular myocytes endogenously expressing Cx43, has shown that incubation with connexin mimetic peptides can inhibit Cx43 hemichannel currents within minutes (Wang et al. 2013). These results further support that the primary function of connexin mimetic peptides are to interact with the extracellular loops of connexins, creating an inhibitory effect on hemichannel communication, before further incubation prevents these hemichannels from docking to their neighbours and ultimately inhibiting gap junction communication.

I propose an additional branch to this hypothesis that explains how both Cx43 and hemichannel expressions are reduced in two types of cells after Gap27 incubation. The theory proposes that after Gap27 has bound to the extracellular surface of a connexin, an increased rate of internalisation is triggered. However this theory needs further testing to validate its assumptions. One way in which this could be achieved is to use fluorescently tagged connexins together with fluorescently tagged mimetic peptides to view in real time the effects of connexin mimetic peptides on connexin turnover. The design of the experiments needs to take into consideration the short lifespan of a connexin and the degradation rate of connexin mimetic peptides.

Already there are successfully transfected cell lines with Cx43-GFP, that form functional gap junctions when compared to non-transfected cells of the same type (Jordan et al., 2001, Martin et al., 2001b, Martin et al., 2001a). These studies observe the trafficking and turnover of connexins from new connexin proteins into docked functional gap junctions before they are internalized at the end of their lifespan. However, there is no discretion in these observations between the new, forming connexins and the old, internalized connexins. FIAsh (Fluorescein

Arsenical Hairpin) – ReAsH (Resorufin-derived red fluorescent Arsenical Hairpin) FIAsh-ReAsH (Gaietta et al., 2002, Evans and Martin, 2002b) or DENDRA (derived from *Dendronephthya sp.*) (Bejarano et al., 2012) may provide alternatives to tackle this observation obstacle. FIAsh-ReAsH as connexin tags allows the distinction between old and new connexins. As a pulse labelling experiment, cells expressing a Cx43 tetracysteine (Cx43-TC) chimera are initially exposed to the membrane permeant non-fluorescent biarsenical derivative FLASH-EDT₂, resulting in a rapid binding to the tetracysteine motif before emitting light between 508-528 nm. As a result, trafficking of connexins labelled in this first hour can be monitored for the next 4-8 hours. Cell exposure to REASH-ED₂ creates a similar binding between the derivative and Cx43-TC, emitting light between 593-608 nm and will not stain the older connexins. Thus, a discrepancy between older and new connexins is achieved. Cells transfected with cDNA encoding Cx43-DENDRA will show Cx43 as green. Photo-switching using light pulses will convert this green into red and thereby also distinguish from new forming connexins in green. Thereby one could observe in real-time the potential docking of Gap27 onto old connexin plaques and monitor levels of possible internalized connexins from this incubation.

In all of the research reports discussed above, it has been thought that initially connexin mimetic peptides primarily interact with undocked hemichannels and at later incubation periods, prevent the docking of connexons to form functional gap junctions. The research presented in this chapter further enhances this theory by suggesting that in short incubation periods of two hours, only higher concentrations of Gap27 significantly reduced Cx43 expression and gap junction communication, whereas in six hour incubation periods, where Gap27 was replaced every two hours, both lower and high concentrations significantly reduced Cx43 expression. This suggests that continually incubating cells in Gap27 will result in the lower concentrations having similar effects in reducing connexin expression and perhaps

reducing gap junction communication, observed in cells incubated at higher concentrations. Further work using communication assays could further support this theory.

Using Gap27 to understand the conformation of connexons

Although substantial research in the gap junction field has confirmed that during gap junction formation the extracellular portions of connexons from opposing cells interact and dock to complete a fully formed channel (Laird 1996), the conformation of the connexons is still unknown. During connexon docking, it is still unclear as to whether extracellular loops line up heterotypic (ECL1 to ECL2) or homotypic (ECL1 to ECL1) as shown in more detail in figure 3.12A and B.

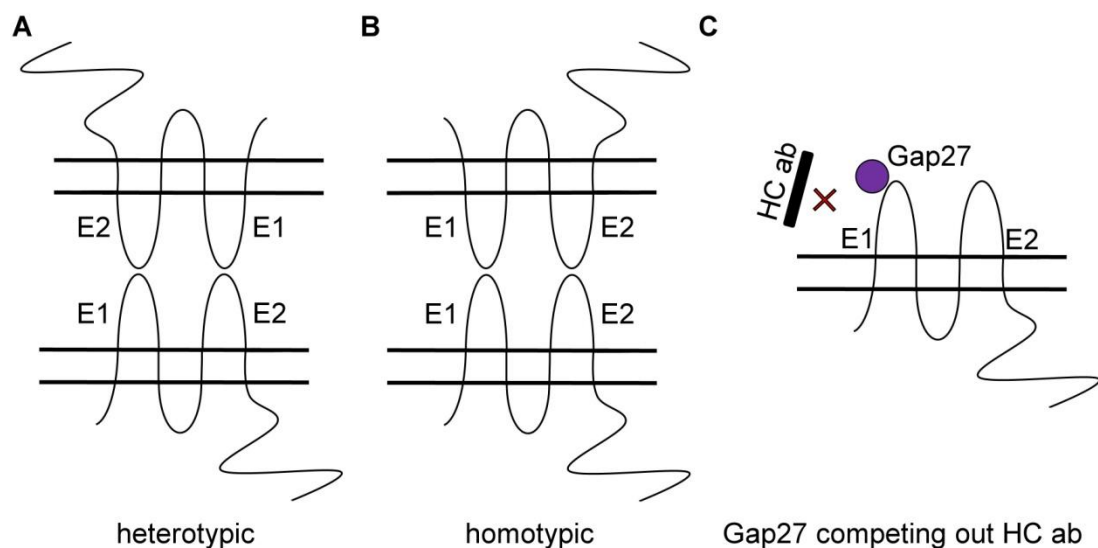


Figure 3.12 Conformation of gap junction connexons

(A) Figure depicting connexon docking in heterotypic conformation; ECL1 to ECL2. (B) Figure depicting connexon docking in homotypic conformation; ECL1 to ECL1. (C) Gap27 competing out the hemichannel domain in ECL1 thereby reducing connexin hemichannel staining. ECL = Extracellular loop. HC ab = Hemichannel antibody.

In this chapter, a custom made affinity purified antibody against a highly conserved portion of the 1st ECL of Cx43 was used to detect connexin hemichannels. One of a group of large antibodies that were raised against the first extracellular loop of Cx32 by Becker and colleagues (that were recognised by both Cxs 32 and 43) not only reduced gap junction communication but would also fail to immunostain gap junctions (Becker, Evans et al. 1995, Warner, Clements et al. 1995). These antibodies, larger in size but having a similar function to connexin mimetic peptides, delayed gap junction formation and reduced dye transfer between neighbouring cells.

The results presented here have shown that incubation in Gap27 reduced hemichannel expression as shown by immunofluorescence. This would suggest that Gap27 has competed out the hemichannel antibody domain in ECL1 and therefore connexons are docking in a heterotypic fashion (figure 3.12A and C). Results presented here further supports the theory of rotational staggers developed by Unger and colleagues (Unger et al. 1999). By using electron microscope and image analysis to examine gap junction formation, they noticed a 30° displacement between the rings of opposing alpha helices on two connexons forming a channel. They assumed that if the rough shape for a connexin is circular, this displacement proposes that the two hemichannels forming the channel were likely to be rotationally staggered with respect to each other. Further work is needed to confirm these observations, perhaps repeating the experiment using Gap26, the mimetic peptide that shares homology to the first extracellular loop of Cx43.

Gap27 reduced Cx26 and Cx30 expression in keratinocyte cells

Research presented in this chapter, has shown for the first time, using immortal keratinocyte cells, that naturally express Cxs 26 and 30 and can form functional gap junctions (Fitzgerald et al., 1994, Choung et al., 2011, Lee et al., 2012) in a time and

concentration dependent protocol that continuously incubating these cells in Gap27 can significantly reduce Cx26 and 30 (figure 3.10 and figure 3.11).

Connexin mimetic peptides Gap26 and Gap27 have mainly been used to inhibit Cx43 based communication; however there has been some question on their specificity. Work carried out by Martin and colleagues has shown that Gap27 can inhibit both Cxs 43 and 37 based communication, although Gap27 does share 100% homology with both these connexins (Martin et al., 2005). Gap26 incubation in HeLa cells transfected with single Cxs 43, 40 and 26 can significantly reduce dye transfer in these cells (Wright et al., 2009) when there is at a least three amino acid differences between Cxs 40 and 26 and Gap26. However Gap27 incubation with these cells only reduced Cx43 based communication suggesting that Gap27 is more Cx43 specific. Yet, these cells were only incubated in 50 μ M for 90 minutes and this low dose experiment may not reflect the results presented in this research chapter that continuous Gap27 incubation significantly reduced Cxs 26 and 30 in immortal keratinocyte cells. There are only three amino acid differences between Gap27 and human Cx26 and only two differences between Gap27 and human Cx30. This supports the results shown here as there is only a small divergence between the connexins and the connexin mimetic peptide. Further work using Western blot analysis could support these results.

Homo Sapiens Cx43

FLSRPTEKTIFIIFMLVSL

SRPTEKTIFII

183

Homo Sapiens Cx26

FVSRPTEKT**VFT**FMIAVSG

SRPTEKTIFII

183

Homo Sapiens Cx30

FISRPTEKT**VFT**IFMISASV

SRPTEKTIFII

183

Figure 3.13 Sequence alignments

Diagram shows the topology of Cxs 43, 26 and 30 between amino acid numbers 181 and 200. Connexin mimetic peptide Gap27 is given below each sequence. Amino acids coloured in red are non-alignments.

Conclusions

- Gap27 reduced communication in 3T3 fibroblast cells and increased migration rates in 3T3 fibroblast and HaCaT keratinocyte cells.
- Gap27 significantly reduced Cx43 expression in both 3T3 fibroblast and HaCaT keratinocyte cells.
- Gap27 also significantly reduced connexin hemichannel expression in 3T3 fibroblast cells.
- Continuous incubation with Gap27 significantly reduced Cxs 26 and 30 expressions in HaCaT keratinocyte cells.

In recent research it has been realized that connexin mimetic peptides show a huge potential in tackling connexin-based maladies. As Gap27 has unique time and concentration dependent properties when disrupting either hemichannel or gap junction based communication, this connexin mimetic peptide shows promise in translational and therapeutic possibilities in wound repair. The next chapter explores the potential of Gap27 in the wound healing environment using an *in vitro* model of wound healing.

4. Gap27 in wound healing

4.1 Introduction

Wound healing begins immediately after the body's protective barrier has become damaged and there are three classic stages of wound repair involved in its closure; the immediate inflammatory response, new tissue formation and remodelling. The immediate inflammatory response begins within moments of initial injury with a series of platelet aggregation, vasoconstriction and a release of pro-inflammatory signals. This is promptly followed by the recruitment of neutrophil leukocytes whose main role is to defend the host from the invasion by microbes. The migration of keratinocyte cells in the re-epithelialisation process and the migration of fibroblast cells and collagen deposition in granulation tissue formation govern the stage of tissue formation. This stage ultimately brings the wound margins closer together. Collagen continues to be synthesised (exceeding the rate of collagen degradation) in the tissue remodelling stage before the final process of scar resolution. This final stage can take between 6-12 months to complete fully, depending on the size and depth of the initial wound (Martin, 1997, Gurtner et al., 2008, Shaw and Martin, 2009). The highly complex sequence of events in skin wound healing relies heavily on the communication of signals released during the numerous, overlapping stages. Cell-to-cell communication is crucial in order for tissues to co-ordinate their processes and mounting evidence has shown that gap junctions and their connexin sub units play a pivotal role in the communication of these signals.

Gap junction communication within the skin is governed by at least ten different connexin subtypes. Within rodents, Cx43 is highly expressed in the differentiating strata spinosum, granulosum and basal in the epidermis and expressed in sebaceous glands, hair follicles and fibroblasts within the dermis. Both Cxs 26 and

30 are highly expressed in the differentiating strata spinosum and granulosum of rodent epidermis, whereas only hair follicles, sebaceous glands and sweat glands express Cx26 (Guo et al., 1992, Salomon et al., 1994, Butterweck et al., 1994, Tada and Hashimoto, 1997, Locke et al., 2000, Brandner et al., 2004, Kandyba et al., 2008).

These key connexins undergo dynamic changes and play integral roles during the wound healing process. In the immediate response of wound repair Cx43 protein expression is up-regulated in blood vessels, yet significantly down-regulated in leading edge tissue within the first day of wound closure. This protein switch-off is accompanied by a significant increase in the expression of Cxs 26 and 30 in the leading edge tissue, corresponding to the onset of re-epithelisation of epidermal keratinocytes and the migration of dermal fibroblasts. Upon the resolution of the wound, the expression profiles of these connexin proteins return to their normal pre-wound levels (Goliger and Paul, 1995, Saitoh et al., 1997, Coutinho et al., 2003).

In work developed by the Becker lab, it has been shown that transiently reducing Cx43 expression in acute wounds enhances the rate of wound closure in rodent models of wound healing (Qiu et al., 2003, Mori et al., 2006). Using a Cx43 specific asODN, a 30mer unmodified backbone antisense that targets to Cx43 mRNA and induces a Cx43 protein knockdown, it has been demonstrated that reducing this protein significantly accelerates the rate of wound closure. By comparing both physiological and cell biological aspects of tissue repair, it was confirmed how a single early application of Cx43 asODN to acute wounds dampened tissue swelling and the inflammatory response, promoted early keratinocyte and fibroblast cell migration and closed the wound gap earlier than wounds left un-treated. Wounds treated with Cx43 asODN showed rapid angiogenesis, increased myofibroblast differentiation, enhanced granulation tissue deposition and increased wound

contraction. These events occurred 2-3 days before normal wound healing stages and resulted in the wounds appearing less red and swollen with smaller and thinner scar tissue. Treated wounds also had a markedly reduced neutrophil and macrophage recruitment and decreased leukocyte infiltration. This was coupled with a reduction in mRNA expression of pro inflammatory chemokines ligand 2 and TNF- α in treated wounds. Both studies demonstrated that by targeting the early stages of wound closure using Cx43 asODN 'jump-started' the subsequent phases of acute wound healing.

In a similar study using Cx43 asODN in a rodent acute mechanical scrape corneal wound model, it was also demonstrated that a transient knockdown of Cx43 increased the rate of wound healing (Grupcheva et al., 2012). In comparison to control wounds, Cx43 asODN treatment decreased the wound area, reduced the inflammatory response and tissue oedema while increasing the rate of keratinocyte re-epithelialisation. In a further optic model of wound repair it was also shown that Cx43 asODN treatment increased the rate of wound repair in comparison to control wounds (Danesh-Meyer et al., 2008). Ischemia reperfusion injury was observed in this model, together with an increase in Cx43 expression that resulted in an increase in inflammation, capillary break down and cell death. Transiently knocking down Cx43 reduced the responses observed in ischemic reperfusion damage and increased cell viability. This healing response was also recorded in human eye injury, where as a result of severe ocular surface burns, corneal epithelial wounds can lead to blindness (Ormonde et al., 2012). Treatment with Cx43 asODN significantly reduced inflammation in injured eyes and complete and stable corneal re-epithelialisation was observed in all treated patients.

In another model of thermal injury, treatment with Cx43 asODN was tested in limiting burn extension damage (Coutinho et al., 2005). Using a rodent model, acute

thermal injuries were applied to the backs of these animals. Often burn damage spreads beyond the initial site of injury and this was noted with an increase in Cx43 expression within the surrounding tissue. A single application of Cx43 asODN significantly reduced this elevation of Cx43 and limited the extension of burn damage. This was achieved through reducing neutrophil infiltration, increasing keratinocyte re-epithelialisation and wound closure, ultimately resulting in reduced scarring and granulation tissue deposition and increased dermal appendage survival. This study demonstrated how initial thermal injury can rapidly spread to neighbouring cells via gap junctions and by reducing this communication through transient Cx43 knockdown, thermal damage extent is significantly reduced.

A comparable story was described in reports of rodent spinal cord injury (Cronin et al., 2008). In both models of compression injury and partial spinal cord transection, application of Cx43 asODN increased the rate of recovery. This was observed in treated animals scoring higher in behavioural tests of locomotion, having a reduction in tissue swelling and a decrease in blood vessel leakiness around the injury site. A more detailed investigation carried out by the same group using an *ex vivo* model of spinal cord trauma, revealed that Cx43 asODN treatment significantly reduced cell death and inhibited inflammation spreading from the site of injury to the neighbouring healthy tissue (Zhang et al., 2010a). These studies have supported the theory that in injured tissue gap junction protein Cx43 is transiently upregulated and spreads tissue damage to neighbouring healthy cells. Treatment with Cx43 asODN reduces this communication through transient Cx43 knockdown and maintained tissue viability.

Transient knockdown of Cx43 has also seen benefits in the chronic wound environment. In both human diabetic foot ulcers and STZ-induced diabetic rat lesions, Cx43 fails to down-regulate at the wound edge, as seen in normal acute

wounds 24 h after wounding. This sustained increase in Cx43 protein expression may be fundamental to the impaired healing found in diabetic foot ulcers. A single application of Cx43 asODN to a wound on STZ-induced diabetic rats was sufficient enough to prevent Cx43 up-regulation at the wound site. Treatment with Cx43 asODN was also able to prevent the formation of a bulb of non-migratory keratinocyte cells, restoring the healing rate back to normal and in some cases exceeding the rate of control re-epithelialisation (Wang et al., 2007).

Although it is becoming increasingly certain that Cx43 plays integral roles in both acute and chronic wound healing, it is still unclear whether these responses are attributed to the connexin hemichannels or gap junctions. Long term hemichannel and gap junction down-regulation can be achieved through topical application of Cx43 asODN; however the differences between gap junction communication and hemichannel signaling can be teased out by application of small connexin mimetic peptides. Synthetic connexin mimetic peptide Gap27 is currently being considered as a candidate to improve the rate of wound healing. As shown in the previous chapter, Gap27 has unique time and concentration dependent properties when disrupting gap junction based communication or reducing Cx43 expression in immortal fibroblast and keratinocyte cells. Gap27 can rapidly block hemichannels and prevent gap junction formation in short or low concentration periods, however, with longer or more concentrated incubation periods, Gap27 can inhibit gap junctional communication and reduce Cx43 expression. In recent research it has been realized that connexin mimetic peptides show a huge potential in tackling connexin-based maladies and increasing the rate of wound repair. However, this research has been limited to 2D cultures, 3D organotypic or *ex vivo* models of wound healing and to date, there have been no studies executed on *in vivo* models of wound healing to elucidate the potential of Gap27 as a wound healing remedy (Kandyba et al., 2008, Pollok et al., 2011).

Chapter 4 Gap27 in wound healing

Using a murine *in vivo* model of wound healing, the work presented in this chapter aims to investigate the ability of connexin mimetic peptide Gap27 to enhance the rate of wound closure. Detailed analysis was carried out on the effect of Gap27 during the initial stages of wound healing. This included an assessment on the inflammatory response and re-epithelialisation, while special attention was given to the connexin profiles in treated and non-treated tissue. Using Gap27 as a tool, a detailed exploration was carried out to determine the importance of hemichannel and gap junction based communication during wound repair.

Hypothesis – By reducing connexin based communication, Gap27 will enhance the early stages of wound closure.

4.2 Results

Gap27 significantly reduced blood vessel leakiness four hours after wounding

In order to assess whether Gap27 has an effect on the extravasation process during the early immune response, blood vessel leakiness was assessed as described in detail in the methods section. Blood vessel leakiness was more pronounced at the wound site (figure 4.1B) and significantly reduced further away from the wound edge. Total blood vessel leakiness was then quantified in all four wounds in site 1 (figure 4.1B) but as uniform FITC-BSA injection was not guaranteed, the data was normalised within each animal back to the non-treated site (figure 4.1E). Gap27 effects on blood vessel leakiness were compared with a positive control of Cx43 asODN (which has already been shown to reduce leakiness in wounded tissue). Application of Cx43 asODN and Gap27 significantly reduced the extent of blood vessel leakiness.

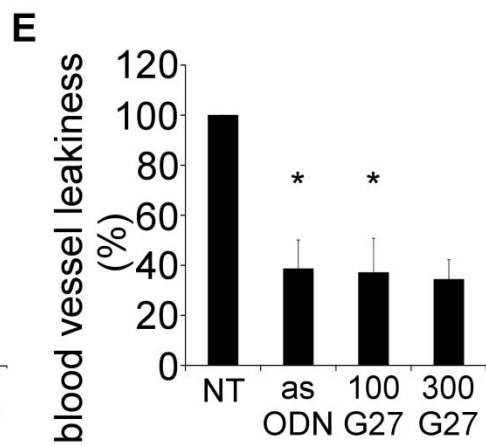
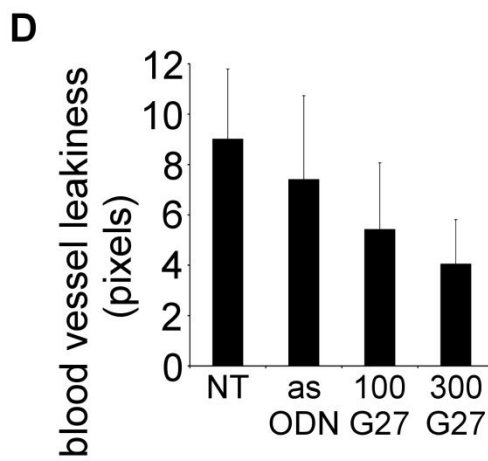
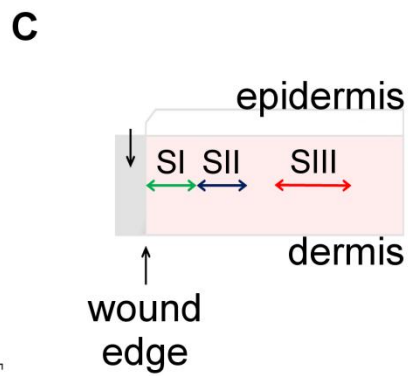
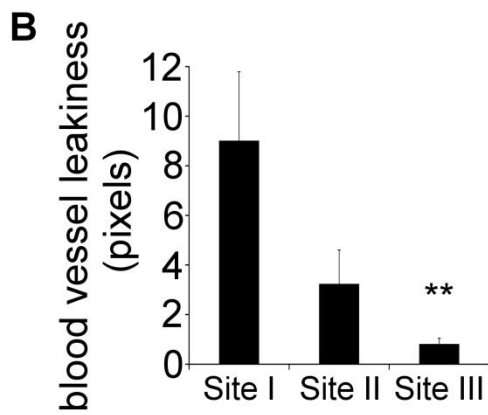
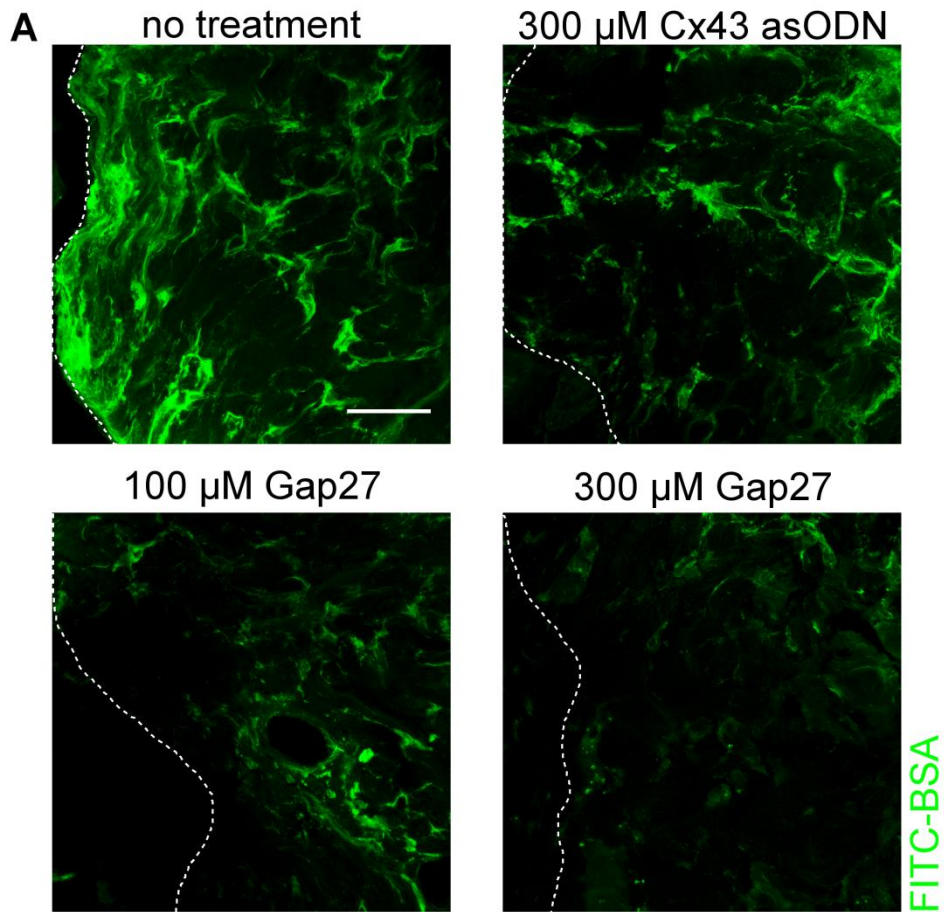


Figure 4.1 Gap27 significantly reduced blood vessel leakiness at the wound site, four hours after wounding

(A) The panels show representative images from site 1 of treated and non-treated wounds. FITC-BSA (green) Dashed white line indicated wound edge. (B) Total leakiness of the blood vessels was quantified in three sites relative to the wound and significantly reduced further away from the wound edge. (C) Diagram depicting sites of interest in blood vessel leakiness analysis. (D) Total leakiness of blood vessels was quantified in site 1. (E) This data was normalised within each animal back to the non-treated site as uniform injection of FITC-BSA was not guaranteed. Application of Cx43 asODN and Gap27 to the wound site significantly reduced the extent of blood vessel leakiness. Statistical comparisons were made using a one-way analysis of variance (ANOVA). Data was tested for normality (Shapiro-Wilk test) and equal variances (Levene test) before statistical comparisons were carried out. The data are shown as the means \pm S.E.M. ($n=7$, $*p<0.05$, $**p<0.01$ against Site 1 in B and NT tissue in E). Scale bar = 50 μ m. NT = No treatment, asODN = Cx43 antisense oligodeoxynucleotide, G27 = Gap27, SI = Site 1, SII = Site 2, SIII = Site 3

Gap27 significantly reduced Cx43 expression in blood vessels, four hours after wounding

Tissue slices were immunolabeled for Cx43 to assess what effect Gap27 had on this connexin's expression within and around leaking blood vessels. Gap27 significantly reduced Cx43 expression in and around the vasculature at the wound site four hours after wounding (figure 4.2).

Gap27 significantly reduced Cx43 and hemichannel expression at the wound edge, four hours after wounding

Tissue slices were immunolabeled for Cx43 and connexin hemichannels before being imaged at the wound edge and adjacent to the wound site, four hours after wounding. Within the epidermis, high concentrations of Gap27 significantly reduced Cx43 expression at the wound edge, whereas a lower concentration of Gap27 only markedly reduced Cx43 expression at the wound edge (figure 4.3B). Within the dermis, Cx43 expression significantly increased at the wound edge of non-treated tissue in comparison to sites adjacent to the wound. Treatment with Gap27 significantly reduced this expression at both the wound edge and adjacent to the wound (figure 4.3C). Similar results were observed in hemichannel expression. Both high and lower concentrations of Gap27 significantly reduced hemichannel expression within the epidermis at the wound edge (figure 4.4B). Within the dermis, hemichannel expression also significantly increased at the wound edge of non treated tissues in comparison to sites adjacent to the wound. Treatment with Gap27 significantly reduced this expression at both the wound edge and adjacent to the wound (figure 4.4C).

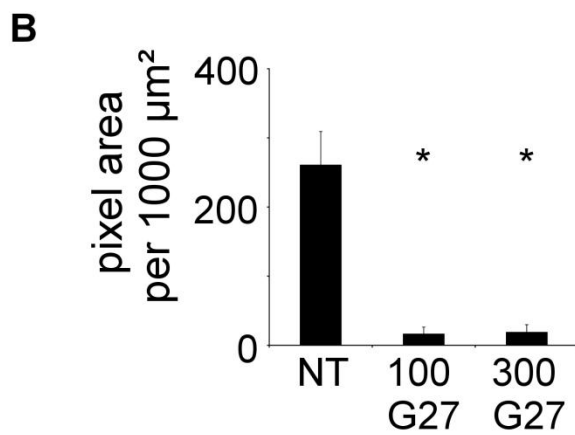
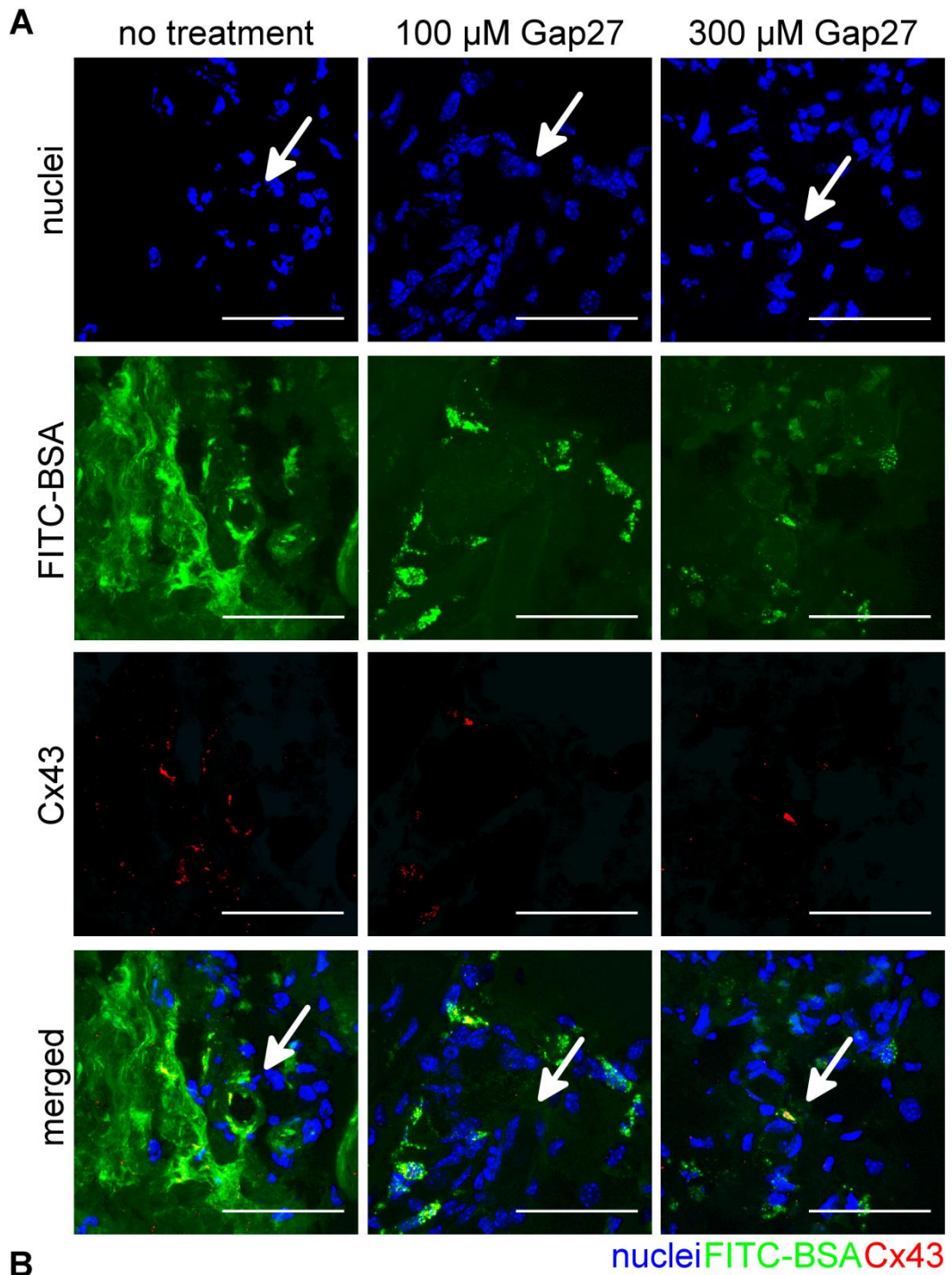


Figure 4.2 Gap27 significantly reduced Cx43 expression in blood vessels, four hours after wounding

(A) The panels show representative z series images of nuclei (blue) FITC-BSA (green) and Cx43 (red), in treated and non-treated tissue 4 hours after wounding. The images are merged in the lower panels. Blood vessels are indicated by a white arrow in the nuclei panels. (B) Total Cx43 area per 1000 μm^2 was quantified. Gap27 significantly reduced Cx43 expression in and around blood vessels. Statistical comparisons were made using a one-way analysis of variance (ANOVA). The data are shown as the means \pm S.E.M. ($n=5$, $*p<0.05$ against NT tissue). Scale bar = 50 μm . NT = No treatment, G27 = Gap27.

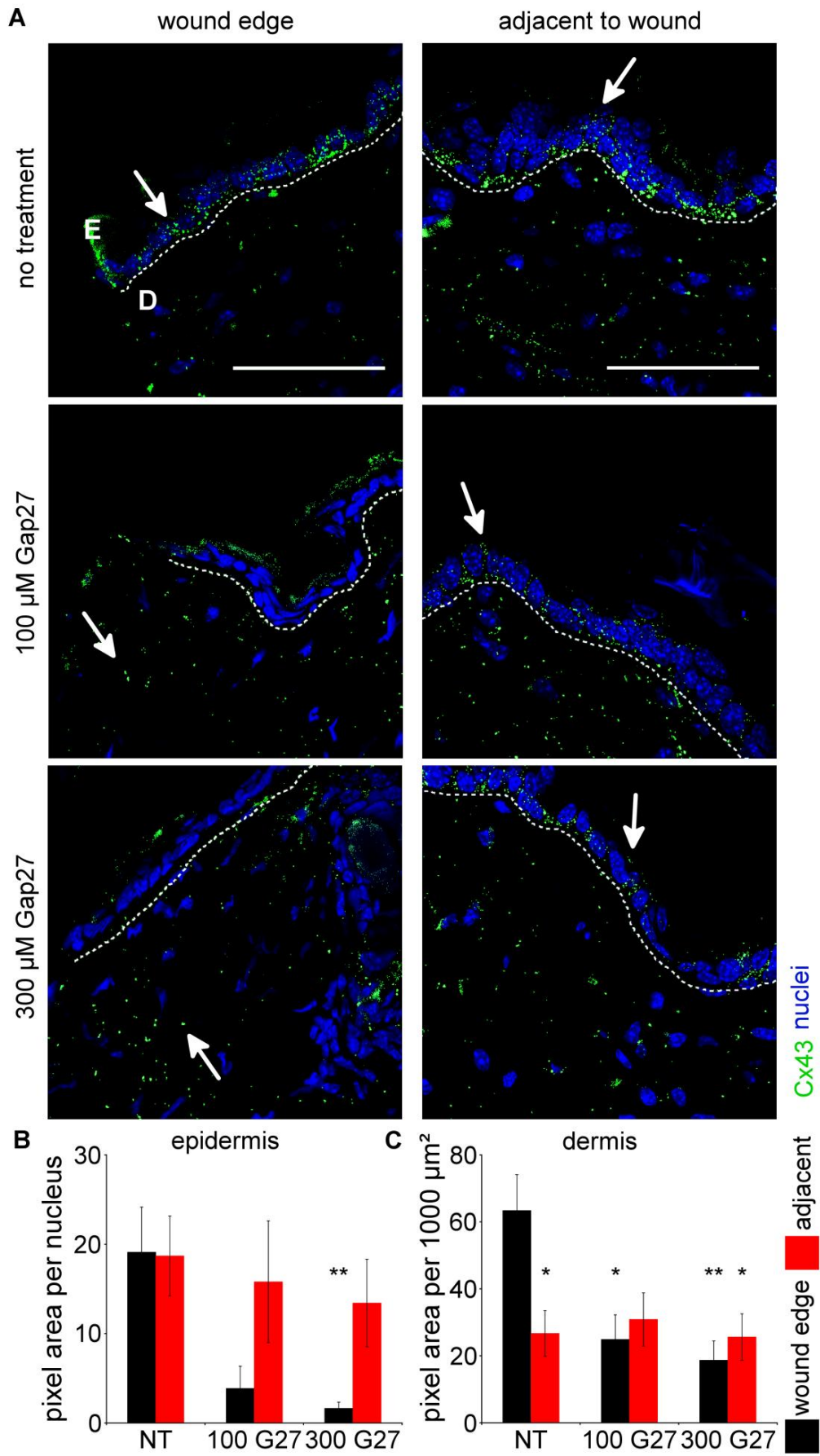


Figure 4.3 Gap27 significantly reduced Cx43 expression at the wound edge, four hours after wounding

(A) The panels show representative images of treated and non-treated tissue 4 hours after wounding. Tissue was immunolabeled for Cx43 (green) and nuclei (blue) and connexin profiles were measured at the wound edge or adjacent to the wound, approximately 200-400 μm away from the wound edge. The epidermis and the dermis are separated by a white dashed line. (B) Total pixel area per nucleus within the epidermis was quantified at the wound edge and adjacent to the wound edge. (C) Total pixel area per 1000 μm^2 within the dermis was also quantified at the wound edge and adjacent to the wound. Application of Gap27 to the wound site significantly reduced Cx43 at the wound edge in both the epidermis and dermis. Note that the 'no treatment-wound edge panel' has auto fluorescence which was not quantified. Statistical comparisons were made using a one-way analysis of variance (ANOVA). The data are shown as the means \pm S.E.M. ($n=5$, $*p<0.05$, $**p<0.01$ against NT wound edge tissue). White arrows indicate Cx43 expression. Scale bar = 50 μm . E = Epidermis, D = Dermis, NT = No treatment, G27 = Gap27.

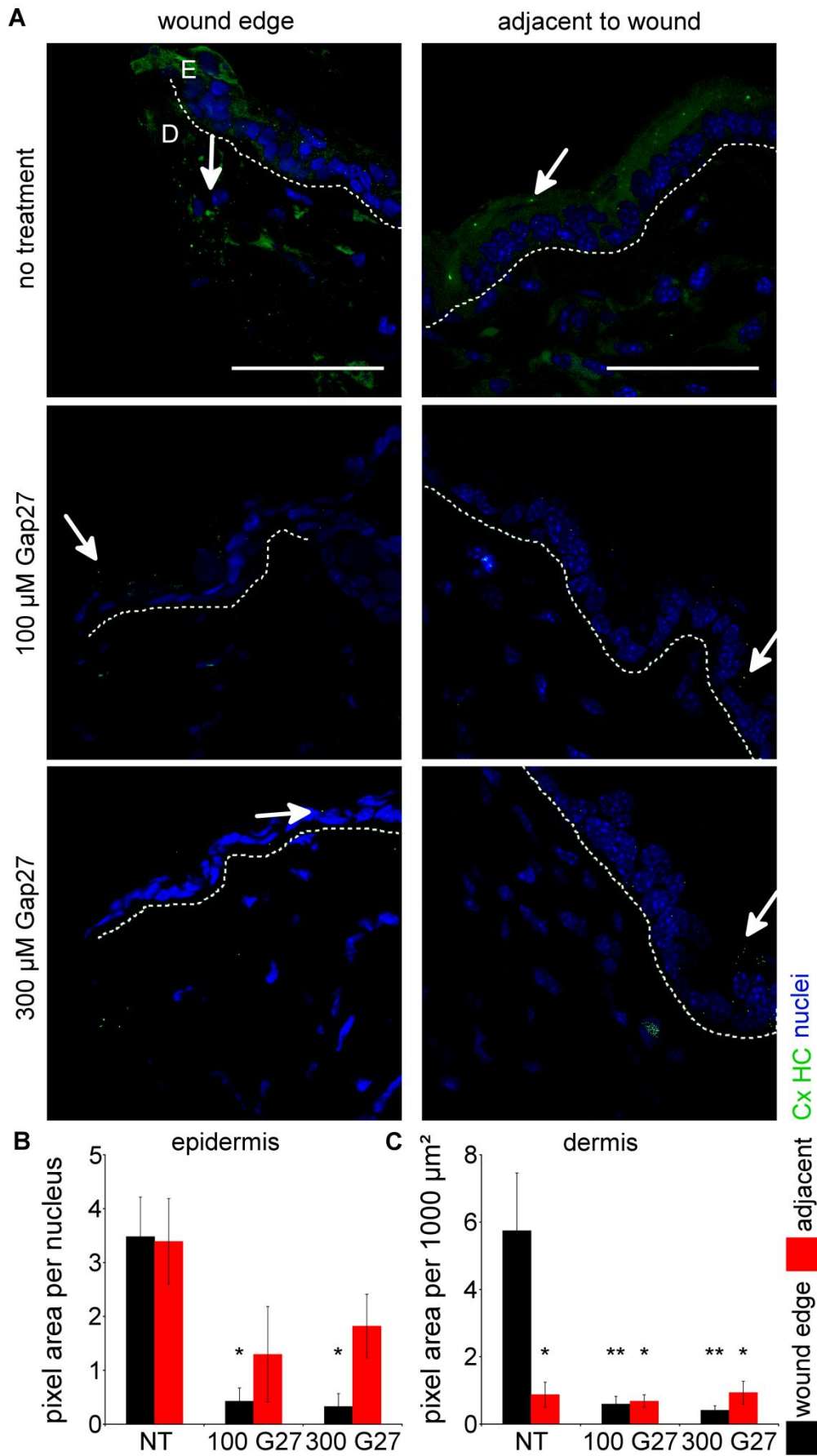


Figure 4.4 Gap27 significantly reduced connexin hemichannel expression at the wound edge, four hours after wounding

(A) The panels show representative images of treated and non-treated tissue 4 hours after wounding. Tissue was immunolabeled for connexin hemichannels (green) and nuclei (blue) and connexin profiles were measured at the wound edge or adjacent to the wound, approximately 200-400 μm away from the wound edge. The epidermis and the dermis are separated by a white dashed line. (B) Total pixel area per nucleus within the epidermis was quantified at the wound edge and adjacent to the wound edge. (C) Total pixel area per 1000 μm^2 within the dermis was also quantified at the wound edge and adjacent to the wound. Application of Gap27 to the wound site significantly reduced connexin hemichannel at the wound edge in both the epidermis and dermis. Note that the 'no treatment-wound edge panel' has auto fluorescence which was not quantified. Statistical comparisons were made using a one-way analysis of variance (ANOVA). The data are shown as the means \pm S.E.M. ($n=5$, $*p<0.05$, $**p<0.01$ against NT wound edge tissue). White arrows indicate hemichannel expression. Scale bar = 50 μm . E = Epidermis, D = Dermis, NT = No treatment, G27 = Gap27.

Gap27 significantly reduced the number of neutrophils in the dermis, twenty-four hours after wounding

Tissue was stained with Haematoxylin and Eosin to assess how treatment with Gap27 affected the number of neutrophils within the tissue, twenty four hours after wounding. Tissue was observed at the wound edge, distal to the wound and around wound edge blood vessels (figure 4.5A). Polymorphonuclear neutrophil leukocytes were identified through high powered imaging of the tissue (figure 4.5B) and leukocyte count per 1000 μm^2 was quantified. Gap27 significantly reduced polymorphonuclear neutrophil leukocyte count at the wound edge, distal to the wound and around wound edge blood vessels (figure 4.6).

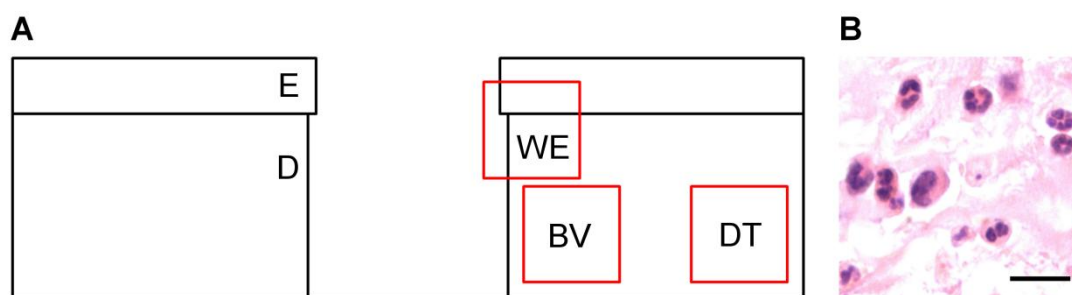


Figure 4.5 Regions of interest in polymorphonuclear leukocyte count

(A) The cross section diagram of skin details the regions of interest measured in leukocyte count. The red boxes indicate the wound edge dermis (WE), distal tissue approximately 200-400 μm away from the wound (DT) and tissue with wound edge dermal blood vessels (BV). E = Epidermis, D = Dermis, WE = Wound edge, DT = Distal tissue, BV = Blood vessels. (B) Example of polymorphonuclear neutrophils. Scale bar = 25 μm .

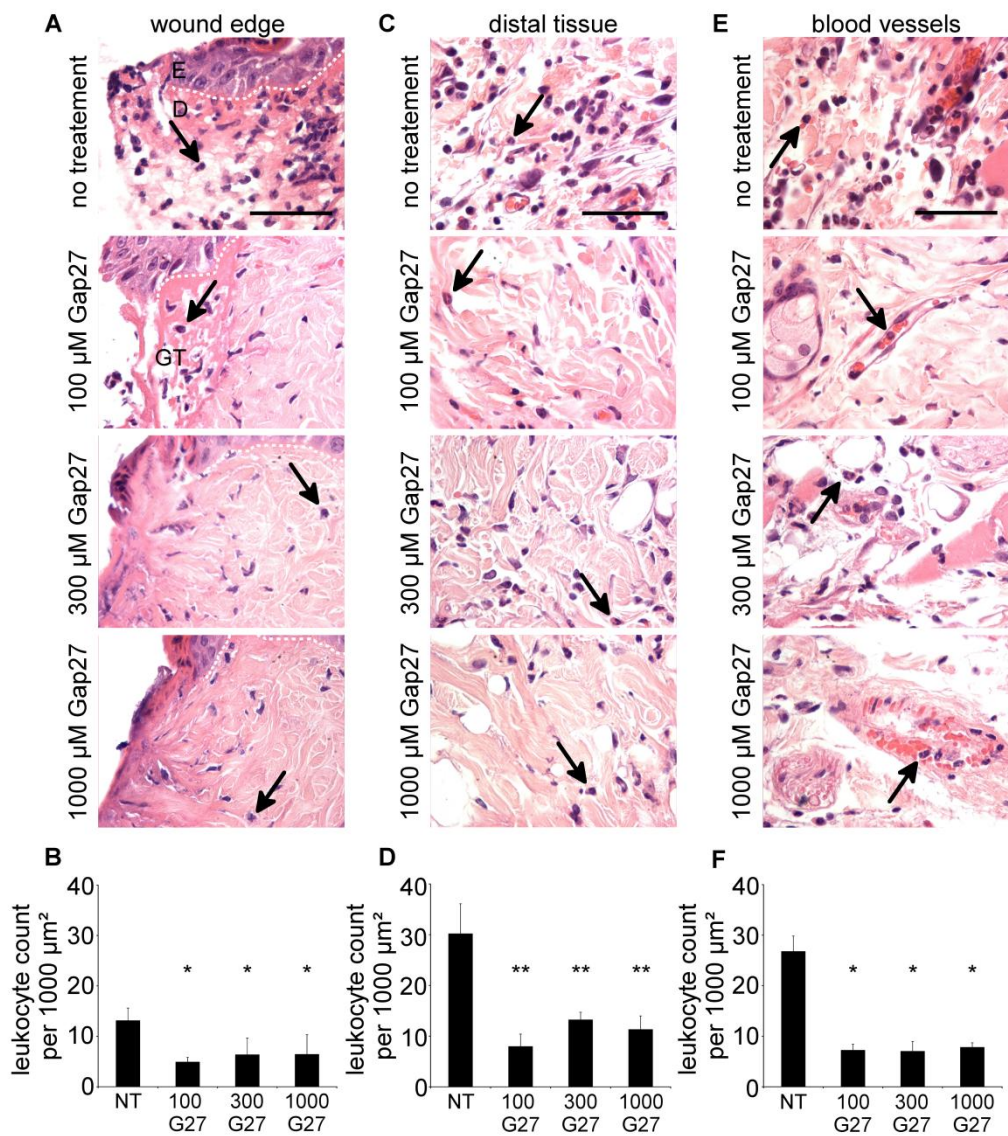


Figure 4.6 Gap27 significantly reduced the number of leukocytes in the dermis, twenty four hours after wounding

The panels show representative histological images of treated and non-treated tissue 24 hours after wounding. Tissue was observed at the wound edge (A), distal to the wound edge (C) and at blood vessels (E). Leukocyte count per 1000 μm^2 was quantified. Leukocyte neutrophils were identified by their multi-lobed nuclei (black arrows). At the wound edge (B), distal tissue (D) and surrounding blood vessels (F) Gap27 significantly reduced leukocyte count. Statistical comparisons were made using a one-way analysis of variance (ANOVA). The data are shown as the means \pm S.E.M. ($n=6$, * $p<0.05$, ** $p<0.01$ against NT tissue). Scale bar = 200 μm . E = Epidermis, D = Dermis, GT = Granulation tissue.

A low concentration of Gap27 increased re-epithelialisation twenty four hours after wounding

Tissue was stained with Haematoxylin and Eosin to assess the rate of re-epithelialisation (figure 4.7). Re-epithelialisation was noted by measuring the distance from the top of the junctions between new and old epithelium (black arrow in figure 4.7) to the leading edge of new epithelial growth on both sides of the wound in the epidermis. This is shown as a red-dashed line in the representative images in figure 4.7. Low concentrations of Gap27 significantly increased the extent of re-epithelialisation twenty four hours after wounding. In earlier preliminary studies, when tissue was collected three and seven days after wounding it was apparent that Gap27 did not have an any effect on the extent of re-epithelialisation in comparison to non-treated wounds in these later stages after wounding.

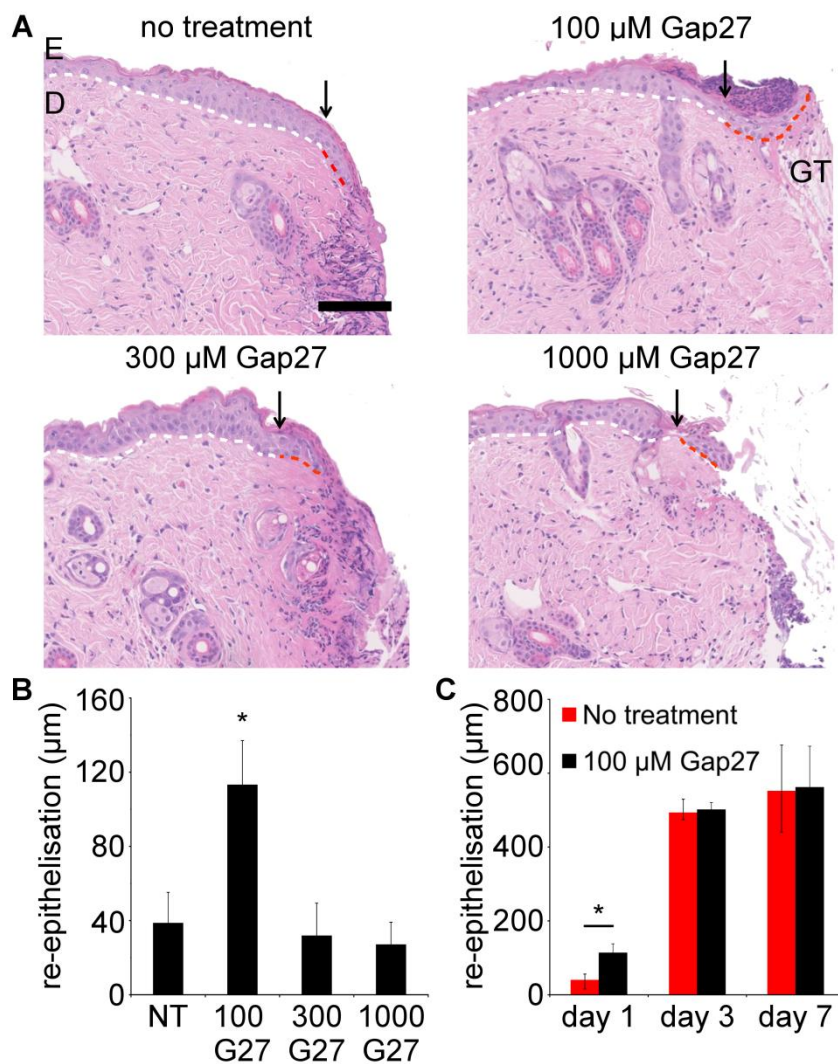


Figure 4.7 A low concentration of Gap27 significantly increased the extent of re-epithelialisation, twenty four hours after wounding

(A) The panels show representative histological images of treated and non-treated tissue 24 hours after wounding. The epidermis and the dermis are separated by a white dashed line. Wound edge is shown by a black arrow and new epidermal growth is shown as a red-dashed line. (B) Low concentrations of Gap27 significantly increased the extent of re-epithelialisation 24 hours after wounding. (C) Three and seven days after wounding Gap27 did not have any effect on the extent of re-epithelialisation in comparison to non-treated wounds in these later stages after wounding. Statistical comparisons were made using a one-way analysis of variance (ANOVA). The data are shown as the means \pm S.E.M. ($n=6$, $*p<0.05$ against NT tissue). Scale bar = 100 μ m. E = Epidermis, D = Dermis, GT = Granulation tissue, NT = No treatment, G27 = Gap27.

Connexin profiles in tissue 24 hours after wounding

Tissue slices were immunolabeled for Cxs 26, 30 and 43 and imaged at the wound edge and adjacent to the wound site, twenty four hours after wounding. Within the epidermis, Cx43 expression decreased at the wound edge. Treatment with Gap27 only slightly reduced this expression (figure 4.8B). A similar observation was noted in the dermis where Cx43 expression was also increased at the sites adjacent to the wound edge in comparison to the wound site. Again, treatment with Gap27 reduced this expression but was not deemed significant (figure 4.8C).

Cx26 expression within the epidermis markedly increased at the wound edge of non-treated tissue in comparison to sites adjacent to the wound. Gap27 did not have any effect on this connexin expression. There was no difference in Cx26 expression between treated and non-treated tissue in any region measured (figure 4.9). A comparable observation was noted in Cx30 expression within the dermis where protein levels were markedly increased at the wound edge of non-treated tissue in comparison to sites adjacent to the wound. However, Cx30 protein expression was much lower than Cx26 expression and there was no measurable quantity of Cx30 protein levels within the dermis (figure 4.10).

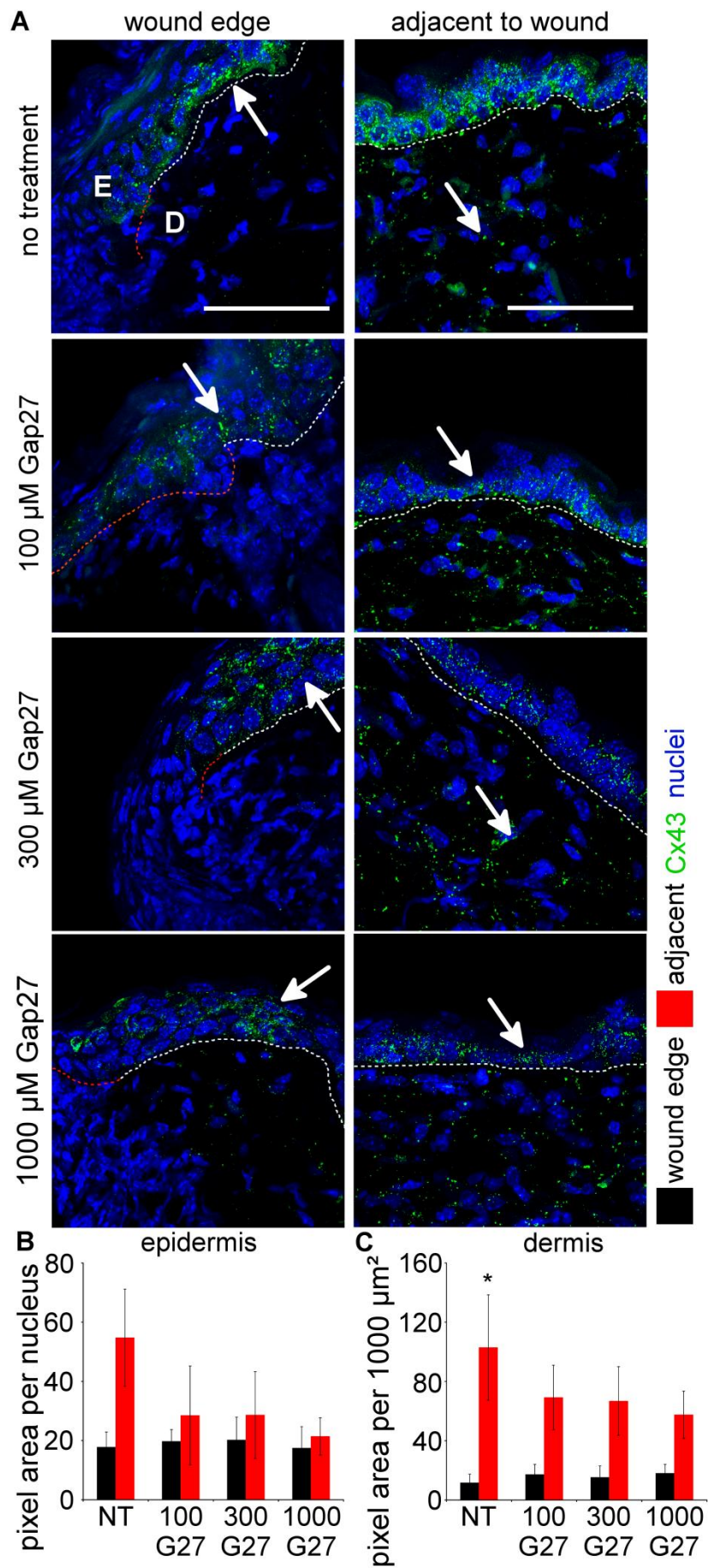


Figure 4.8 Gap27 did not significantly reduce Cx43 expression at the wound edge, twenty four hours after wounding

(A) The panels show representative images of treated and non-treated tissue 24 hours after wounding. Tissue was immunolabeled for Cx43 (green) and nuclei (blue) and connexin profiles were measured at the wound edge or adjacent to the wound, approximately 200-400 μm away from the wound edge. The epidermis and the dermis are separated by a white dashed line. New epidermal growth is shown as a red-dashed line. (B) Total pixel area per nucleus within the epidermis was quantified at the wound edge and adjacent to the wound edge. (C) Total pixel area per 1000 μm^2 within the dermis was also quantified at the wound edge and adjacent to the wound. Application of Gap27 to the wound site slightly reduced Cx43 adjacent to the wound in both the epidermis and dermis. Statistical comparisons were made using a one-way analysis of variance (ANOVA). The data are shown as the means \pm S.E.M. ($n=6$, $*p<0.05$ against NT wound edge tissue). White arrows indicate Cx43 expression. Scale bar = 50 μm . E = Epidermis, D = Dermis, NT = No treatment, G27 = Gap27.

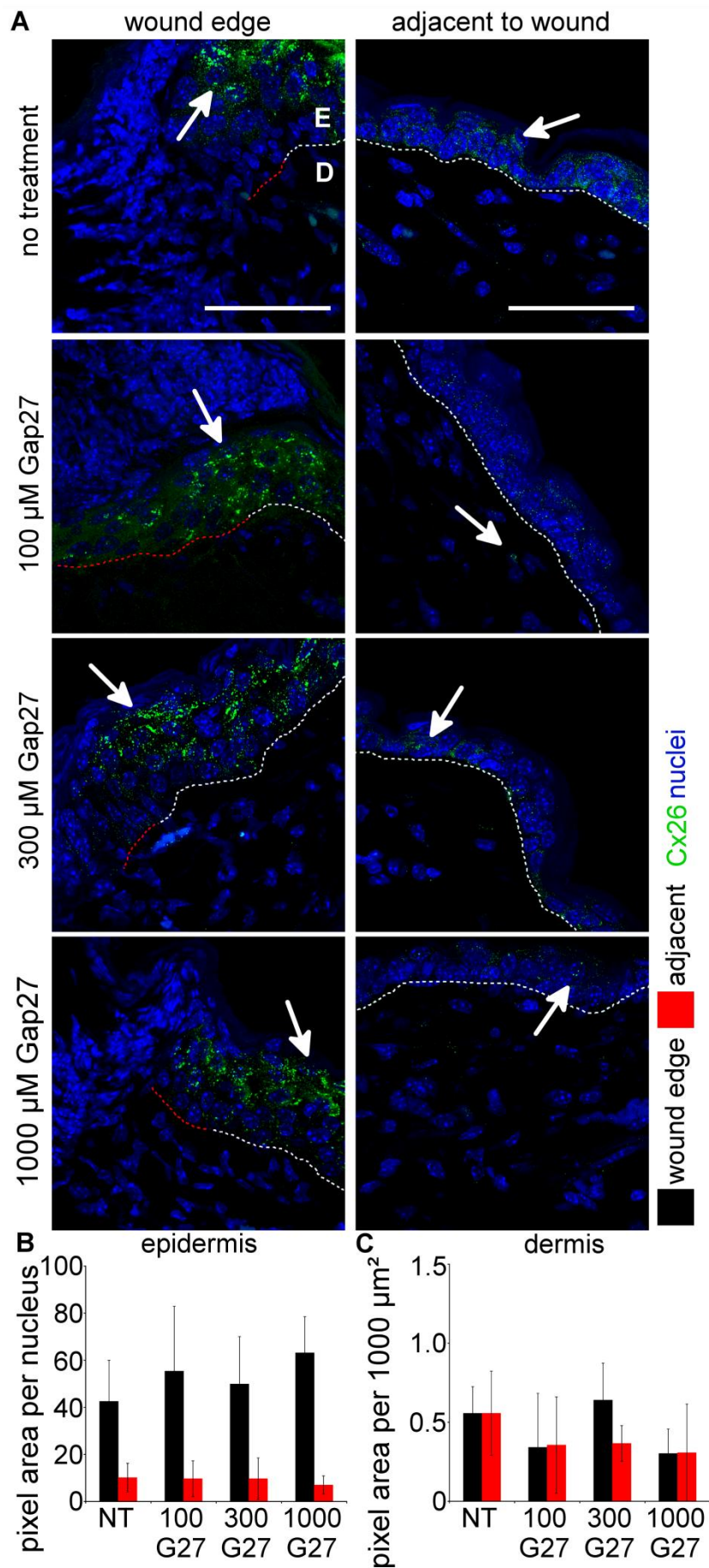


Figure 4.9 Gap27 did not significantly reduce Cx26 expression at the wound edge, twenty four hours after wounding

(A) The panels show representative images of treated and non-treated tissue 24 hours after wounding. Tissue was immunolabeled Cx26 (green) and nuclei (blue) and connexin profiles were measured at the wound edge or adjacent to the wound, approximately 200-400 μm away from the wound edge. The epidermis and the dermis are separated by a white dashed line. New epidermal growth is shown as a red dashed line. (B) Total pixel area per nucleus within the epidermis was quantified at the wound edge and adjacent to the wound edge. (C) Total pixel area per 1000 μm^2 within the dermis was also quantified at the wound edge and adjacent to the wound. After application of Gap27 to the wound site, there was no difference in Cx26 expression between treated and non-treated tissue in any region measured. The data are shown as the means \pm S.E.M. ($n=6$). White arrows indicate Cx26 expression. Scale bar = 50 μm . E = Epidermis, D = Dermis, NT = No treatment, G27 = Gap27.

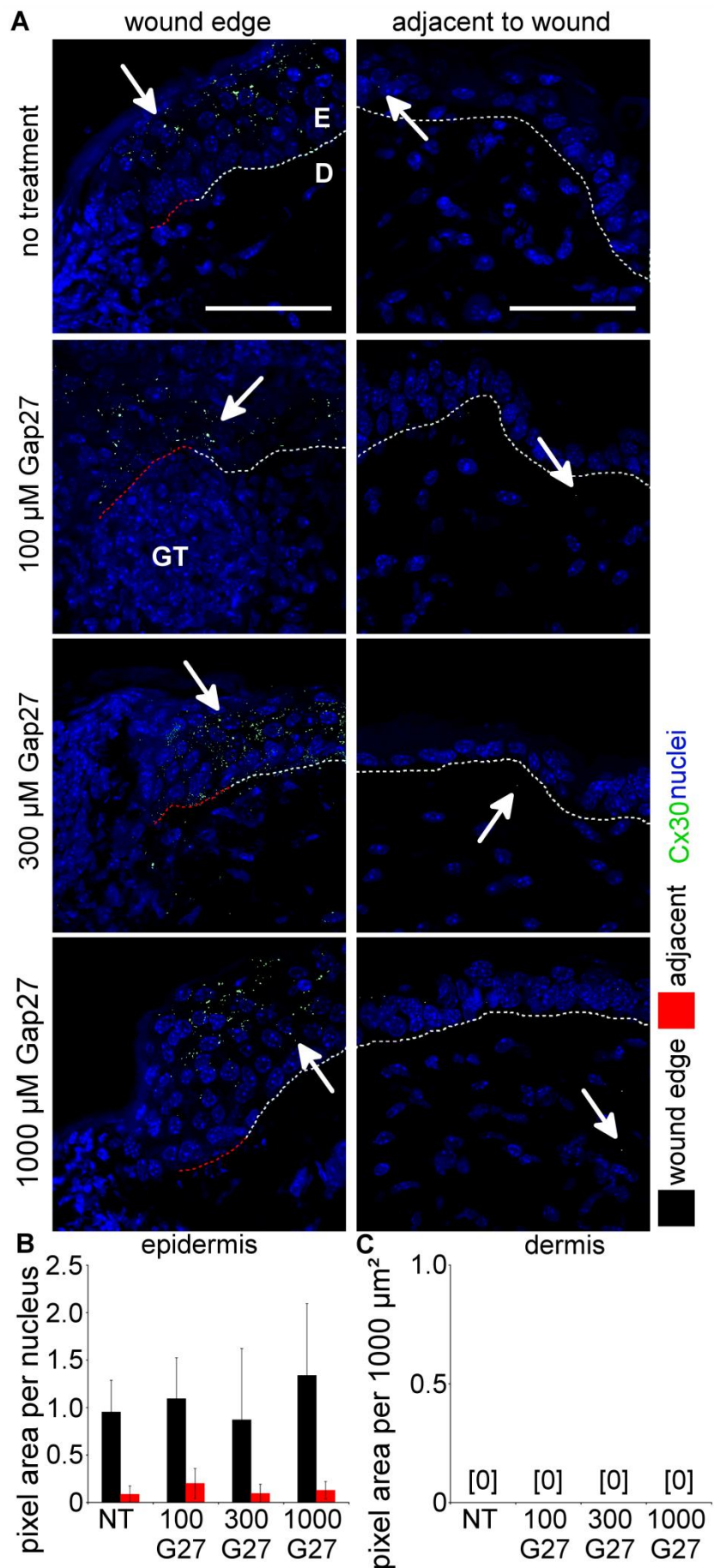


Figure 4.10 Gap27 did not significantly reduce Cx30 expression at the wound edge, twenty four hours after wounding

(A) The panels show representative images of treated and non-treated tissue 24 hours after wounding. Tissue was immunolabeled Cx30 (green) and nuclei (blue) and connexin profiles were measured at the wound edge or adjacent to the wound, approximately 200-400 μm away from the wound edge. The epidermis and the dermis are separated by a white dashed line. New epidermal growth is shown as a red dashed line. (B) Total pixel area per nucleus within the epidermis was quantified at the wound edge and adjacent to the wound edge. (C) Total pixel area per 1000 μm^2 within the dermis was also quantified at the wound edge and adjacent to the wound. After application of Gap27 to the wound site, there was no difference in Cx30 expression between treated and non-treated tissue the epidermis. There was no measurable quantity of Cx30 protein levels within the dermis. The data are shown as the means \pm S.E.M. (n=6). White arrows indicate Cx30 expression. Scale bar = 50 μm . E = Epidermis, D = Dermis, NT = No treatment, G27 = Gap27.

4.3 Discussion

Treatment with Gap27 significantly reduced blood vessel leakiness and dampened the inflammatory response

A crucial novel finding reported in this chapter was that the application of connexin mimetic peptide Gap27 to full thickness wounds significantly reduced blood vessel leakiness around the wound site (figure 4.1). The effects of Gap27 were compared with a positive control of Cx43 asODN treatment and a negative control of non-treated wounds. Blood vessel leakiness was more pronounced at the wound site and it was also noted that Cx43 expression was significantly increased in and around the blood vessels of the same site (figure 4.2).

Similar results were reported by De Bock, Leybeart and colleagues on investigating blood-brain barrier endothelial permeability in rats. They described how bradykinin, as an inflammatory stimulus, significantly increased endothelial permeability both *in vivo* and *in vitro* (De Bock et al., 2011, De Bock et al., 2012). Administration of Gap27 significantly reduced endothelial permeability in both environments. More recently, work carried out by Danesh-Meyer, Green and colleagues has also shown how Peptide 5 (a 12 amino acid long short connexin mimetic peptide that corresponds to the second extracellular loop of Cx43 and overlaps with Gap27 by seven amino acids) can also significantly reduce vascular leakage following retinal ischemia reperfusion (Danesh-Meyer et al., 2012). Another crucial observation reported in this chapter was that there was a correlation between blood vessel leakiness, Gap27 treatment and Cx43 expression. As blood vessel leakiness increased at the wound site four hours after wounding, it was observed that Cx43 expression was also significantly increased in and around the blood vessel. Treatment with Gap27 significantly reduced blood vessel leakiness and Cx43 expression (figure 4.2). Cx43 protein reduction after connexin mimetic peptide

incubation was also reported by O'Carroll, Green and colleagues when incubating *ex vivo* spinal cord segments in Peptide 5. A markedly reduced expression of Cx43 was observed in cultures through Western blot analysis when compared to cells incubated in a control peptide (O'Carroll et al., 2008). Cx43 reduction after Gap27 incubation was also presented in the first research chapter of this thesis, where it was reported that Gap27 incubation *in vitro* reduced Cx43 expression in immortal fibroblast and keratinocyte cells.

In a novel discovery reported in this chapter, it was observed that incubation with Gap27 significantly reduced the PMN leukocyte count at the wound edge, distal to the wound and around wound edge blood vessels, 24 hours after wounding (figure 4.6). In a comparable report given by Cronin, Becker and colleagues where rats were subjected to spinal cord injury, treatment with Cx43 asODN significantly rescued blood vessel leakiness by reducing the extravasation of FITC-BSA. They also noted how Cx43 asODN significantly reduced neutrophil recruitment to the site of injury. Transiently knocking down Cx43 in wounded tissue has previously shown to reduce neutrophil macrophage recruitment and decreased leukocyte infiltration in studies carried out by the same group (Qiu et al., 2003, Mori et al., 2006). Although it is apparent from these studies and the data reported here that connexins play a fundamental role during the early immune response, there is still some debate on how this happens.

Gap junctions, hemichannels and connexins have been identified in leukocytes and vasculature endothelial cells and there is mounting evidence of functional communication in homotypic and heterotypic populations of these cell types during the inflammatory response (Oviedo-Orta and Howard Evans, 2004). Human monocytes and macrophages have been reported to express Cx43 when activated with lipopolysaccharides (LPS). Although these cells could form functional gap

junctions, their communication was inhibited by the known gap junction communication inhibitor 18 α -Glycyrrhetic acid (Eugenín et al., 2003). Time dependent and bi-directional cross talk has also been observed between populations of PMNs and human umbilical vein endothelial cells (HUVECs) and this gap junction based communication was inhibited by Gap26 incubation (Zahler et al., 2003). Oviedo-Orta, Evans and colleagues were the first to note Cx43 expression in non-activated lymphocytes (Oviedo-Orta et al., 2000) however, incubation with either 18 α -Glycyrrhetic acid or Gap27 decreased dye transfer and therefore confirmed gap junction based communication between these cells.

In a study conducted by Oviedo-Orta, Evans and colleagues, trans-endothelial migration was investigated using an *in vitro* model of heterotypic populations of endothelial cells and lymphocytes in a chamber system (Oviedo-Orta et al., 2002). Interestingly pre-incubation with connexin mimetic peptides inhibited dye transfer between gap junctions but did not slow down the transmigration process, suggesting that connexin mimetic peptides did not have any affect in the adhesion stage of extravasation. Controversially, a study exploring the interaction between mouse endothelial cells and neutrophils *in vitro* reported that when incubated with Gap26, adhesion between these two cell types was significantly reduced (Sarieddine et al., 2009). These results, together with the data reported here, suggest that although not fully understood gap junctions and their connexins may have a heavy involvement in the complex sequence of events of the early inflammatory response.

Although neutrophils within early inflammatory response can provide the body's first active defensive mechanism against infectious disease and foreign material by having primary roles in killing invading microorganisms (Dovi et al., 2004), it is now thought that neutrophils may actually do more harm than good and retard wound closure (Martin and Leibovich, 2005). It has been reported that wounded guinea

pigs depleted of inflammatory cells in a sterile environment does not impair wound debridement, granulation tissue deposition or tissue repair (Simpson and Ross, 1972, Leibovich and Ross, 1975). Further studies using knockout models to reduce neutrophils in mice have demonstrated that dermal healing and collagen deposition is unaffected and that epidermal healing and wound closure was significantly faster than in control mice (Dovi et al., 2003, Dovi et al., 2004). Therefore, it seems that the chemokines released by neutrophils and actions of neutrophils within the tissue are either not essential or other cells are able to supply alternatives (Martin and Leibovich, 2005) and dampening down the inflammatory response and neutrophil invasion by reducing Cx43 based communication may be beneficial to the wound healing process, particularly in a chronic wound environment.

Treatment with low concentrations of Gap27 enhanced re-epithelialisation rates

Research presented in this chapter has shown for the first time, using an *in vivo* murine wound healing model, that a low concentration of Gap27 can enhance the extent of re-epithelialisation twenty fours after wounding. However, in a peculiar twist, higher concentrations of Gap27 did not enhance the re-epithelialisation rate beyond normal, non-treated control wounds (figure 4.7).

Cx43 dynamics during acute wound healing are tightly regulated to ensure successful wound closure. Cx43 is moderately expressed in the strata basal and spinosum in non-wounded tissue but upon wounding, Cx43 expression significantly drops at the wound edge within the first hours after barrier disruption. Until approximately four days later, Cx43 expression remains absent in all proliferative and regenerative areas within the epidermis. Cx43 expression then significantly up-regulates in the proliferating epidermis and remains elevated until six to seven days after wounding, when expression returns to pre-wounding levels (Coutinho et al.,

2003). Coutinho and colleagues theorised that this observed reduction of Cx43 expression in keratinocyte cells in the first few hours of wound healing, together with an observed increase in the proliferation marker Ki67⁺, is crucial in the transformation of leading edge keratinocyte cells into a migratory phenotype (Coutinho et al., 2003). Further work conducted by the same group has also shown that transient knockdown of Cx43 using Cx43 asODN can promote early keratinocyte migration, increase re-epithelialisation rates and close the wound gap earlier than wounds left untreated (Qiu et al., 2003, Mori et al., 2006, Wang et al., 2007). In a similar knock-out study, this time investigating residual connexin expression in mouse tail epidermis using a Cx43^{Cre-ER(T)/flox} mouse model, it was shown that a reduction in Cx43 expression was associated with the de-differentiation and mobilization of keratinocytes at the wound edge during the first couple of days after wounding (Kretz et al., 2003, Kretz et al., 2004). Reducing Cx43 in the mouse tail epidermis in this knock out mouse model promoted wound healing a day faster than wild-type control mice.

In the previous research chapter, it was observed how high concentrations of Gap27 significantly increased the rate of migration of immortal keratinocyte cells in an *in vitro* scratch wound assay. Early *in vitro* works conducted by the Martin group has also shown how connexin mimetic peptides Gap26 and Gap27 can increase the rate of migration in human keratinocyte cells (Wright et al., 2009, Pollok et al., 2011). Further studies using biologically relevant organotypic models of wound healing have shown a similar result (Kandyba et al., 2008, Pollok et al., 2011). In an *ex vivo* wound healing model using porcine skin, it has also been reported that Gap27 treatment significantly increased re-epithelialisation and that treated sections expressed significantly more Ki67⁺ in leading edge epidermal cells (Pollok et al., 2011). However, research presented in this chapter has shown that only a lower concentration of Gap27 can increase the rate of re-epithelialisation and keratinocyte

migration in an *in vivo* wound healing model (figure 4.7). This suggests that more than one element is at play in this stage of wound repair which has only been noted using an *in vivo* model of wound healing.

Perhaps the extra element in play is an involvement of hemichannel communication during re-epithelialisation. Long term hemichannel protein disruption can be achieved through topical application of Cx43 asODN and in murine knock out models. However the differences between gap junction communication and hemichannel signalling can be teased out by application of small connexin mimetic peptides such as Gap27. Connexin mimetic peptides can rapidly block hemichannels and prevent gap junction formation, however, with more concentrated incubation periods, Gap27 can inhibit also gap junctional communication. For many years it was thought that hemichannels remained in a permanently closed form, until docked with its counter partner from a neighboring cell. However, recent research has emerged that shows hemichannels can open in cultured cells and provide a signaling pathway between the cell's cytoplasm and the extracellular environment (Evans et al., 2006).

Recent studies have shown that ATP can be released from open Cx43 hemichannels (Stout et al., 2002, Eltzschig et al., 2006, Robertson et al., 2010, Orellana et al., 2012) and in a study using cultured neonatal keratinocytes that were briefly exposed to air, a robust long lasting ATP release was observed (Barr et al., 2013). Using this novel *in vitro* wound healing model, it was also noted that Cx43 mRNA significantly increased during this stress and that cell treatment with octanol and carbenoxolone significantly reduced ATP release. An additional study has also shown that during wound healing, platelets can release ATP that have the potential to expose the wounded epidermis to concentrations of ATP known to alter cellular functions (Pillai and Bikle, 1992). ATP released from Cx43 hemichannels can also

cause cell death by acting on purinergic P2X receptors (Stout et al., 2002), leading to cellular permeation pathways to large molecules and ultimately causing cell death through osmotic imbalance. It has been shown in both *in vitro* and *in vivo* models of wound healing that ATP release causes a reduction in keratinocyte number and epidermal thickness, a decrease in keratinocyte differentiation and a decline in barrier formation (Pillai and Bikle, 1992, Denda et al., 2002). Treatment with a P2X antagonist after wounding reversed these deleterious effects and accelerated barrier repair (Denda et al., 2002). Connexin mimetic peptides have also been shown to inhibit ATP release in a variety of cells in culture, including leukocytes (Eltzschig et al., 2006) , astroglial (Orellana et al., 2012) and endothelial cells (Robertson et al., 2010) by plugging open hemichannels.

As discussed in detail in the previous research chapter, it is thought that connexin mimetic peptides primarily interact with undocked hemichannels and at later incubation periods, prevent the docking of connexons to form functional gap junctions due to an increased rate of internalisation. The initial interaction of connexin mimetic peptides has been shown to block open hemichannels and prevent ATP release. Therefore it is possible to believe that ATP is being released in the early stages of wound healing, (from surrounding damaged tissue, migrating leukocytes, platelets or stressed keratinocyte cells) and that treatment with a low concentration of Gap27, as shown in the data reported here, could reduce ATP release and enhance the re-epithelialisation rate. Expanding this theory would suggest that higher concentrations of Gap27 would completely disrupt Cx43 based gap junction communication in keratinocytes, which in the case presented in this research chapter, failed to have any enhancement in re-epithelialisation rate beyond normal, non-treated control wounds. This would suggest that communication between keratinocyte cells is a critical component of wound healing and Defranco and colleagues confirmed this by showing that migrating cells in a scratch wound

assay retain functional gap junction communication (Defranco et al., 2008). However, the data reported in this chapter is contradictory to a number of reports that have described that reducing Cx43 protein expression using *in vivo* models of wound healing, increases the rate of re-epithelialisation (Qiu et al., 2003, Mori et al., 2006, Wang et al., 2007, Kretz et al., 2003). However, these studies reduced Cx43 expression through protein disruption (using knock out models or asODN), whereas Gap27 most likely reduces Cx43 expression and gap junction communication through increasing the internalisation rate of connexins. Therefore, perhaps disrupting Cx43 protein expression will influence a compensatory increase in another connexin and this was shown and supported by Kretz and colleagues in their Cx43^{Cre-ER(T)/flox} knock out mouse model. Animals with reduced Cx43 expression showed an increase in Cx30 expression in the epidermis (Kretz et al., 2003). This study would support the theory that cell to cell communication between migrating epidermis during wound repair is a critical component of wound healing and that a high concentration of Gap27 on a wound may disrupt this communication in such a way that is compensated by another connexin increase. Further immuno analysis investigation is required to support this theory.

Connexin mimetic peptides during wound repair

This chapter is the first to explore connexin profiles during wound repair after Gap27 treatment in an *in vivo* model of wound healing. During the first four hours of healing, a single dose of a high concentration of Gap27 significantly reduced Cx43 expression around the blood vasculature and within wound edge epidermis and dermis (figures 4.2 and 4.3). A single dose of lower concentrations only markedly reduced Cx43 expression within wound edge epidermis and dermis (figure 4.3). Similar results were observed on quantifying hemichannel expression where single doses of both high and low concentrations of Gap27 significantly reduced hemichannel expression in wound edge epidermis and dermis. A single dose of

Gap27 also significantly reduced hemichannel expression in the dermis adjacent to the wound (figure 4.4). Twenty four hours after wounding, a single dose of Gap27 only slightly reduced Cx43 expression at the wound edge (figure 4.8) whereas there was no effect on Cxs 26 and 30 after a single dose of Gap27 treatment at the same time (figures 4.9 and 4.10).

Comparable results were made in the previous research chapter where it was reported that a single dose of high concentrations of Gap27 significantly reduced Cx43 expression in immortal fibroblast and keratinocyte cells. Single doses of both high and low concentrations of Gap27 significantly reduced hemichannel expression in immortal fibroblast cells and only continuous incubation of Gap27 had any effect on the expression of Cxs 26 and 30 in immortal keratinocyte cells. It had been previously thought that Gap27 primarily interacts with undocked hemichannels and at later incubation periods or with higher concentrations, prevents the docking of connexons, thereby reducing connexin hemichannel and connexin gap junction based communication respectively. Work presented in the previous chapter built upon this theory by suggesting that after Gap27's initial hemichannel interaction, an increase in the internalisation rate was triggered. This would reduce antibody interaction with connexins and would explain how Cx43 and connexin hemichannel expression is reduced in the first few hours after initial Gap27 treatment, as shown in both the previous research chapter and in the data reported in this chapter.

By twenty four hours after wounding, it is clear that Gap27 no longer has a profound effect on reducing connexin expression. This may be due to the rapid turnover of connexins or as a result of peptide degradation in an *in vivo* system. Proteases within the animal will rapidly break down peptides, greatly reducing its half life and exonucleases within serum are also known to break down unmodified fragile components such as oligodeoxynucleotides (Shaw et al., 1991). Work carried out by

Chapter 4 Gap27 in wound healing

Wright and colleagues has also shown that the modified connexin mimetic peptide Gap26M has a peak level of effectiveness 90 minutes post application, remaining at a similar level of effectiveness 5 hours post application before dropping significantly to control levels 8 to 24 hours post application (Wright et al., 2009). To counteract the rapid breakdown, Gap27 was delivered within a Pluronic™ F-127 gel. This gel has thermo-reversible properties (can be liquid at temperatures between 0 and 4 °C but sets rapidly at body temperature), that acts as a slow release reservoir that has successfully enabled a constant topical delivery for several hours when used to deliver Cx43 asODN to wounds (Becker et al., 1999, Cronin et al., 2006). However, this delivery agent has not been adequate to successfully release the connexin mimetic peptide Gap27 over a long period of time in an *in vivo* model of wound healing and other delivery agents need to be considered. One such agent could be to use osmotic pumps that ensure a continuous delivery of the peptide over a defined study period. Subcutaneous implanted osmotic pumps delivering Gap27 were used to reduce Cx43 expression in bile-duct ligated livers within mice. Gap27 successfully reduced Cx43 expression in the liver, when compared to a scrambled peptide control, after two weeks of constant peptide delivery (Balasubramanian et al., 2013). No cardiotoxicity or any other adverse effects were noticed, making this delivery system a potential ideal route for connexin mimetic peptide treatment.

Conclusions

- During the first four hours of wounding, a single dose of Gap27 significantly reduced blood vessel leakiness at the wound edge and delayed leukocyte infiltration to the wounded tissue observed 24 hours later.
- Low concentrations of Gap27 significantly increased the rate of re-epithelisation.
- Gap27 significantly reduced Cx43 and connexin hemichannel expression in the early stages of wound healing.

In recent years it has been realised that connexin mimetic peptides show a huge potential in enhancing the rate of wound repair and novel research reported in this chapter has supported this capability. The next two chapters explore the prospects of Gap27 in reducing the spread of cell damage and death caused in tissue ischemia reperfusion injury, with a detailed analysis on the pressure ulcer.

5. Connexin based communication in ischemia reperfusion

5.1 Introduction

Research has consistently indicated the potential of connexin mimetic peptides in tackling connexin-based maladies. These prospects include enhancing the rate of wound repair in acute wounds (as demonstrated and expanded on in the previous research chapters) and reducing the spread of damage caused in tissue ischemia reperfusion injury. Tissue ischemia is caused by a restriction of blood supply to tissue, causing a severe shortage of oxygen, glucose and nutrients needed for cell survival. The majority of tissue injury often occurs during reperfusion; triggered by the return of blood supply during the restoration of circulation, causing inflammation and oxidative damage to the tissue that has been denied oxygen for a period of time. Often this damage spreads beyond the initial ischemic area as repeated or prolonged ischemia reperfusion injury can result in the spread of cell death by necrosis and apoptosis (Mustoe, 2004). As connexin, hemichannel and gap junction based communication play such essential roles within intact tissue and during the wound healing process, it is not surprising that connexins have been flagged to have possible roles in the spread of cell death and tissue damage during ischemia reperfusion injury (Cotrina et al., 1998a, García-Dorado et al., 2004, Thompson et al., 2006, Orellana et al., 2010).

Gap junction mediated tissue ischemia reperfusion injury has been identified in a number of organs including cardiac tissue during heart attacks (García-Dorado et al., 2004) and cerebral tissue during strokes (Frantseva et al., 2002a, Frantseva et

Chapter 5 Connexin based communication in ischemia reperfusion

al., 2002b). Repeated ischemia reperfusion injury in the skin during pressure ulcer formation, can also cause severe tissue damage similar to the damage formed in cerebral and cardiac ischemia reperfusion. Pressure ulcers develop on areas of the skin that have been deprived of oxygen flow for extended periods of time and are often seen in bed-ridden, wheelchair bound and elderly patients. Pressure ulcers are extremely debilitating and there are currently no effective treatments to reduce or reverse the spread of cell damage caused during ischemia reperfusion. It is estimated that up to 25% of elderly residents in long term geriatric wards will develop a pressure ulcer (Sen et al., 2009). This reflects a staggering cost of over £2 billion for the NHS every year (Bennett et al., 2004) and the medical need for an effective therapeutic will increase as the elderly population grows.

Already there is mounting evidence that connexin mimetic peptides may provide cardiac and neuronal tissue protection during ischemia reperfusion models of heart attacks and strokes. Using a model of cerebral ischemia in foetal sheep, Davidson and colleagues demonstrated that connexin mimetic peptide treatment could not only increase the survival rate of cells during ischemia reperfusion but also reduce seizure activity (Davidson et al., 2012b). Cardiac protection has also been noted when rat models of myocardial infarction are treated with connexin mimetic peptides (Hawat et al., 2012) and treatment with connexin mimetic peptide significantly reduced the infarct size by over sixty percent. To date, there has been no published work indicating that connexin mimetic peptides could reduce the extensive progressive damage often seen in pressure ulcers. The work presented in this research chapter and the next explores how gap junctions are involved in the spread of damage in pressure ulcers, with the ultimate aim of developing a therapy to reduce the damage and promote healing.

Chapter 5 Connexin based communication in ischemia reperfusion

Despite the growing evidence that marks connexin based communication as a key contributor to the spread of cell death in neighbouring cells after an ischemic insult, the mechanisms behind this spread of damage are still unclear. The “bystander effect” model suggests that death signals can spread laterally through gap junctions from dying cells into their healthy neighbouring cells (Mao et al., 2009, Danesh-Meyer et al., 2012, Zhang et al., 2013). However, some reports attribute cell death in ischemia reperfusion models to the opening of undocked gap junctions, release of ATP and activation of purinergic receptors (Thompson et al., 2006, Orellana et al., 2010, Poornima et al., 2012, Clarke et al., 2009). Understanding how cell death occurs and spreads will help in the development of a therapeutic to reduce spread of damage and the impact of ischemia reperfusion injury. A key step in this understanding will be to determine how dying cells communicate with non-ischemic neighbouring tissue.

Current research has repeatedly demonstrated the unique dose response of connexin mimetic peptides. At low doses, Gap27 has been shown to block open hemichannels but can target gap junctional intercellular communication at high doses and for longer incubation periods. Research presented in this chapter uses an *in vitro* model of ischemia reperfusion and the unique properties of connexin mimetic peptides to determine the role of Cx43 following ischemia reperfusion insult. Further investigative steps were taken to establish whether the apoptosis observed was related to gap junction communication or through the opening of hemichannels.

Hypothesis – Cx43 is involved in the spread of fibroblast cell death in an *in vitro* model of ischemia reperfusion and incubation with Gap27 will reduce the extent of cell loss.

5.2 Results

The *in vitro* model of ischemia reperfusion significantly reduced oxygen in culture media

To investigate the communication between cells during hypoxic stress, a well characterised model of *in vitro* ischemia reperfusion developed by Pringle and Sundstom was replicated using fibroblast cells (Pringle et al., 1997). Fibroblast cells were subjected to hypoxic conditions before reperfusion in an oxygen-glucose deprivation-reoxygenation (OGDR) insult. Partial pressure of oxygen within OGDR medium was measured using the fibre oxygen (FOXY) probe to confirm hypoxic conditions immediately after reperfusion (at OGD). In this model, the oxygen levels were reduced four times the normal environment (figure 5.1).

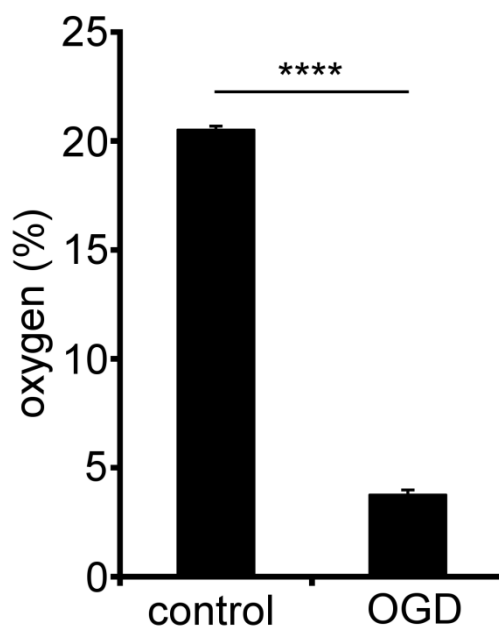


Figure 5.1 OGDR model of ischemia reperfusion reduced O₂ in culture media

Graph shows oxygen percentage levels in medium that has undergone Oxygen Glucose Deprivation stress in comparison to non-treated control medium. The data are shown as the means \pm S.E.M. ($n=5$, **** $p<0.0001$). OGDR = Oxygen glucose deprivation.

OGDR significantly decreased cell viability

Fibroblast cells were subjected to OGDR as described above. Control samples were left in control medium in atmospheric conditions. Cell viability was assessed using a standard MTT assay. OGDR significantly reduced cell viability over 24 hours in 3T3 wild type fibroblast cells (figure 5.2A). Upon experimental replication, using Cx43 shRNA transduced fibroblast cells (a transduced cell line where the majority of Cx43 has been knocked down), no reduction in cell viability was observed (figure 5.2C). OGDR significantly reduced cell viability in fibroblast cells transduced with empty vectors, in a similar result to fibroblast cells (figure 5.2B)

Cx43, p-Cx43 and hemichannel expression significantly increased in fibroblast cells during OGDR

OGDR stress was induced in fibroblast cells as before. Control samples were again left in control medium in atmospheric conditions. Cells were fixed and immunolabeled for Cx43 and hemichannels before total pixel area per cell was quantified. Both Cx43 and hemichannel expressions significantly increased per cell during OGDR stress over 24 hours in comparison to control samples (figure 5.3). Further analysis of Cx43 protein expression by Western blotting confirmed that total Cx43 expression increased over 24 hours during OGDR stress in comparison to control cells (figure 5.4 C1, Cii). A similar pattern was observed in cells transduced with empty vectors (figure 5.4 Ai, Aii, Cii). However, as would be expected, there was no significant increase observed in total Cx43 expression in Cx43 shRNA transduced fibroblast cells during OGDR upon immuno (figure 5.4 Bi) and Western blot analysis (figure 5.4 Civ). No increase in connexin hemichannel expression was observed in the same cell type (figure 5.4 Bii).

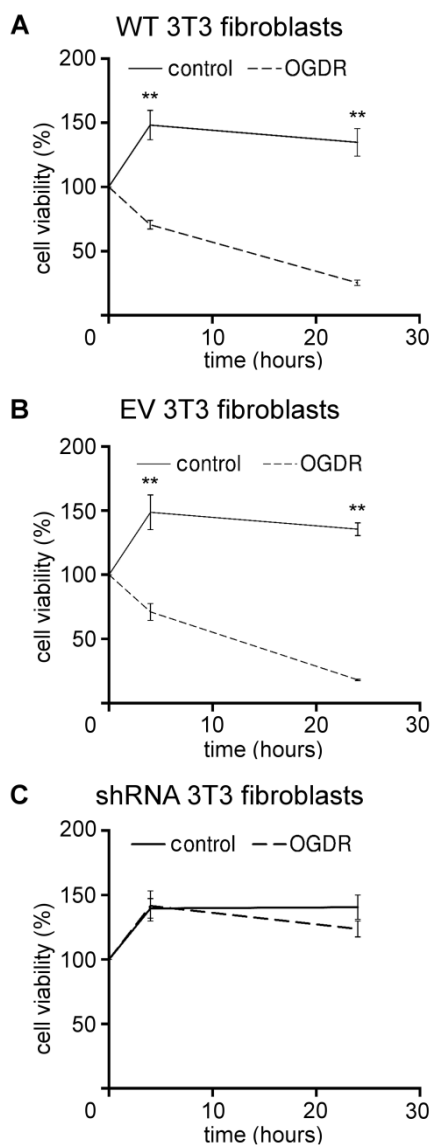


Figure 5.2 Cell viability significantly reduced in wild-type and PSupp 3T3 fibroblast cells during OGDR stress

Wild-type 3T3 fibroblast cells were subjected to OGDR stress for 24 hours. Cell viability was assessed using a MTT assay in both OGDR stressed cells and control cells. Cell viability decreased in wild-type 3T3 fibroblast cells (A) and cells virally transduced with empty vector PSupp (B) during OGDR stress over 24 hours. Cell viability was unaffected in cells transduced with shRNA-Cx43 (C) during OGDR stress. Statistical comparisons were made using an independent-samples *t*-test. The null hypothesis was rejected using a multivariate analysis of variance (MANOVA). The data is shown as the means \pm S.E.M. ($n=3$, $*p<0.05$). WT = Wild-type, EV = Empty vector, PSupp, shRNA = Cx43shRNA, OGDR = Oxygen glucose deprivation reoxygenation.

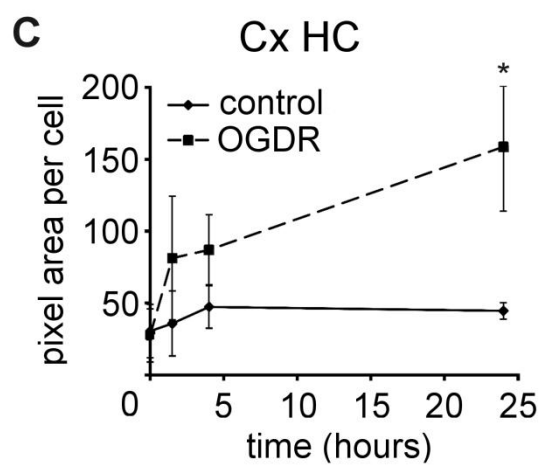
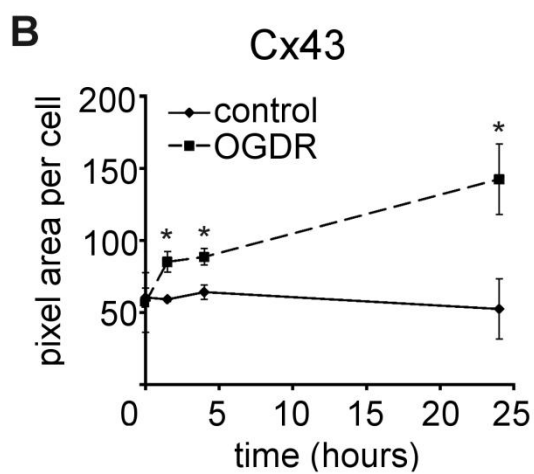
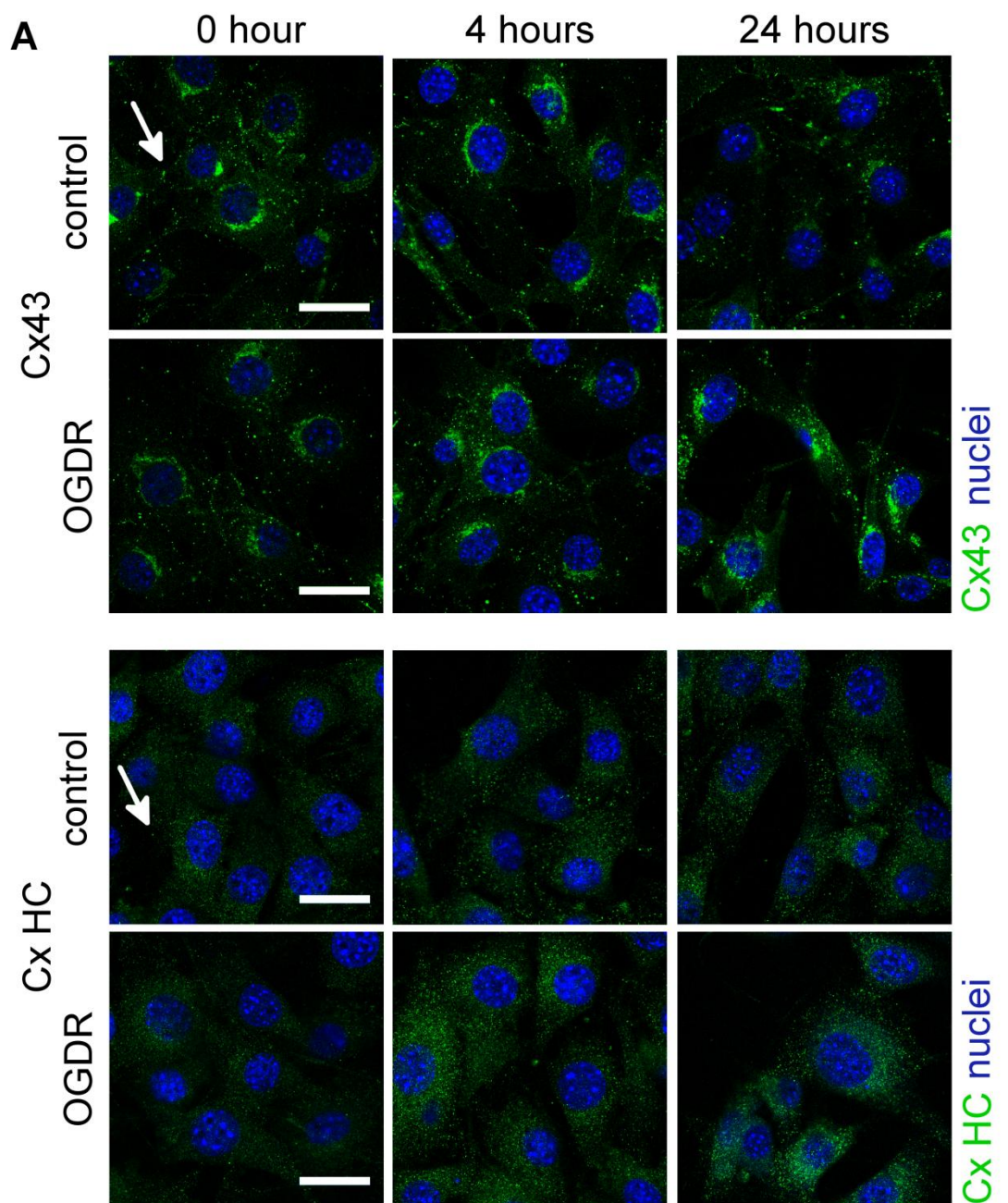


Figure 5.3 Cx43 and connexin hemichannel expression in wild-type fibroblast cells significantly increased during OGDR stress

(A) The panels show representative images of control 3T3 fibroblast cells and those that have undergone OGDR stress for twenty-four hours. Cells were immunolabeled for Cx43 or connexin hemichannels (green) and nuclei (blue). Total Cx43 pixel area per cell (B) and total connexin hemichannel area per cell (C) were quantified. Both Cx43 and connexin hemichannel expression significantly increased throughout OGDR stress over 24 hours. Statistical comparisons were made using an independent-samples *t*-test. The null hypothesis was rejected using a multivariate analysis of variance (MANOVA). The data is shown as the means \pm S.E.M. ($n=4$, $*p<0.05$). White arrows indicate Cx43 or connexin hemichannel expression. Scale bar = 20 μ m. OGDR = Oxygen glucose deprivation reoxygenation

Chapter 5 Connexin based communication in ischemia reperfusion

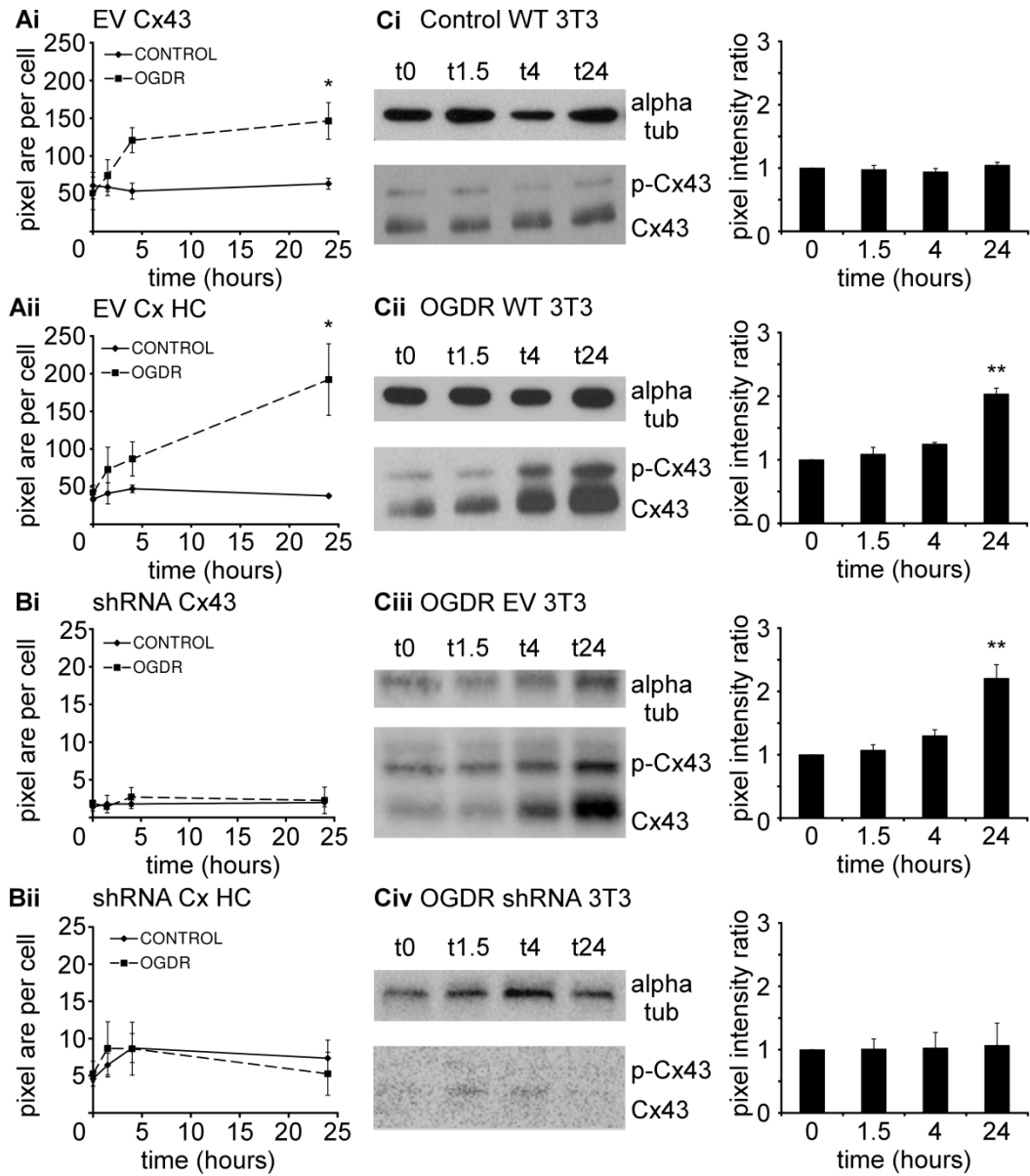


Figure 5.4 Cx43, p-Cx43 and connexin hemichannel expression in PSupp transduced cells significantly increased during OGDR stress

3T3 fibroblast cells virally transduced with empty vector PSupp were subjected to OGDR stress for 24 hours. Cells were immunolabeled for Cx43 and hemichannels and total pixel area per cell was measured. Total Cx43 pixel area per cell (Ai) and hemichannel pixel area per cell (Aii) significantly increased throughout OGDR stress. 3T3 fibroblast cells virally transduced with shRNA-Cx43 were also subjected to OGDR stress for twenty four hours. Total Cx43 pixel area per cell (Bi) and hemichannel pixel area per cell (Bii) did not change throughout OGDR stress. Total Cx43 protein expression during OGDR stress was confirmed through Western blot analysis. Pixel intensity of the bands was measured and the intensity of the protein of interest was measured relative to the intensity of the housekeeping protein. Alpha tubulin served as a loading control. (Ci) There was no significant change in Cx43 protein quantification in control wild-type 3T3 fibroblast cells over 24 hours. During OGDR stress, Cx43 protein expression in wild-type 3T3 cells (Cii) and in cells transduced with empty vector PSupp (Ciii) significantly increased after 24 hours of OGDR stress. (Civ) There was little Cx43 protein expression in cells transduced with shRNA-Cx43, which did not significantly change over 24 hours of OGDR stress. Immunoanalysis statistical comparisons were made using an independent t-test. The data are shown as the means \pm S.E.M. (n=4, *p<0.05). Western blot statistical comparisons were made using a one-way analysis of variance (ANOVA). The data are shown as the means \pm S.E.M. (n=3, **p<0.01). EV = Empty vector, PSupp, shRNA = Cx43shRNA, HC = Hemichannel, WT = Wild-type, OGDR = Oxygen glucose deprivation reoxygenation.

Non confluent cells labelled for PI during OGDR stress

To assess hemichannel activity during OGDR stress, PI uptake was observed and measured in low confluence fibroblast cells as described in detail in the methods section (figure 5.5). OGDR stress caused hemichannels to open and increase propidium iodide uptake. Incubation with connexin mimetic peptide Gap27 significantly reduced PI uptake by plugging open hemichannels.

OGDR induced a bystander effect observed by PI uptake

To explore the possible “bystander effect” between cells during OGDR stress, propidium iodide uptake and transfer was observed over 24 hours as described in detail in the methods section (figure 5.6 and movie 1 – supplementary disc). PI will enter cells through open hemichannels and is therefore small enough to pass to neighbouring cells via gap junction communication Wild-type 3T3 fibroblast cells were grown to confluence to ensure gap junction formation between neighbouring cells (Behringer et al., 2012). OGDR caused PI uptake in random, non-contacting cells. From these initial cells, a wave of PI uptake was observed in neighbouring cells. Incubation with Gap27 significantly reduced PI labelling. High and low concentrations of Gap27 reduced PI labelling in OGDR stressed cells up to 18 hours after reperfusion. However, only higher concentrations of Gap27 reduced PI labelling 21-24 hours after reperfusion.

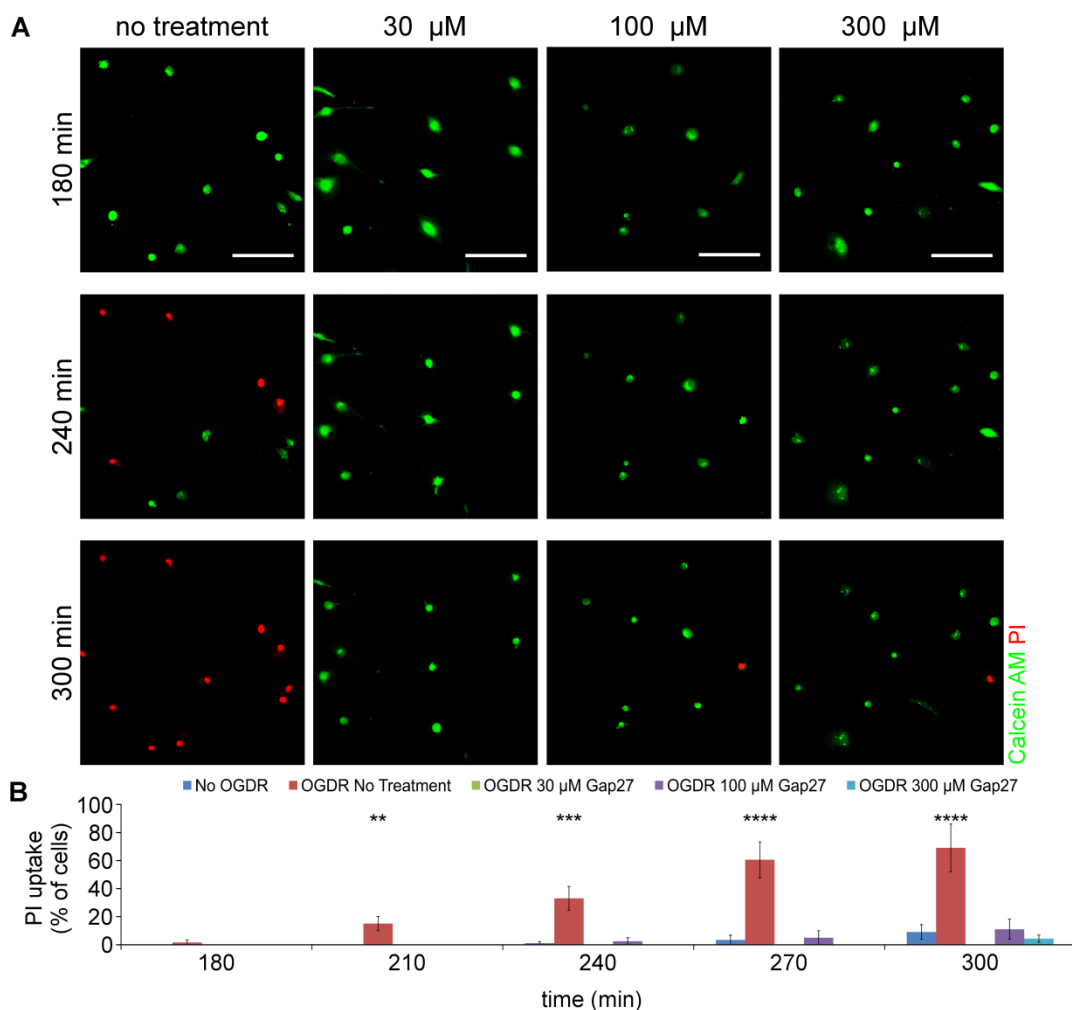


Figure 5.5 PI uptake after OGDR stress was reduced by Gap27 incubation

(A) The panels show representative images of wild-type fibroblast cells that have undergone OGDR stress. Cells were incubated with Calcein AM (green) and propidium iodide (PI). (B) Graph shows percentage of cells that have taken up PI. Non confluent cells labelled for PI during OGDR stress. Gap27 significantly reduced PI uptake. The Statistical comparisons were made using a one-way analysis of variance (ANOVA). The null hypothesis was rejected using a multivariate analysis of variance (MANOVA). The data is shown as the means \pm S.E.M. ($n=4$, $**p<0.01$, $***p<0.001$, $****p<0.0001$ against No OGDR). Scale bar = 100 μ m. PI = Propidium iodide, OGDR = Oxygen glucose deprivation reoxygenation.

Chapter 5 Connexin based communication in ischemia reperfusion

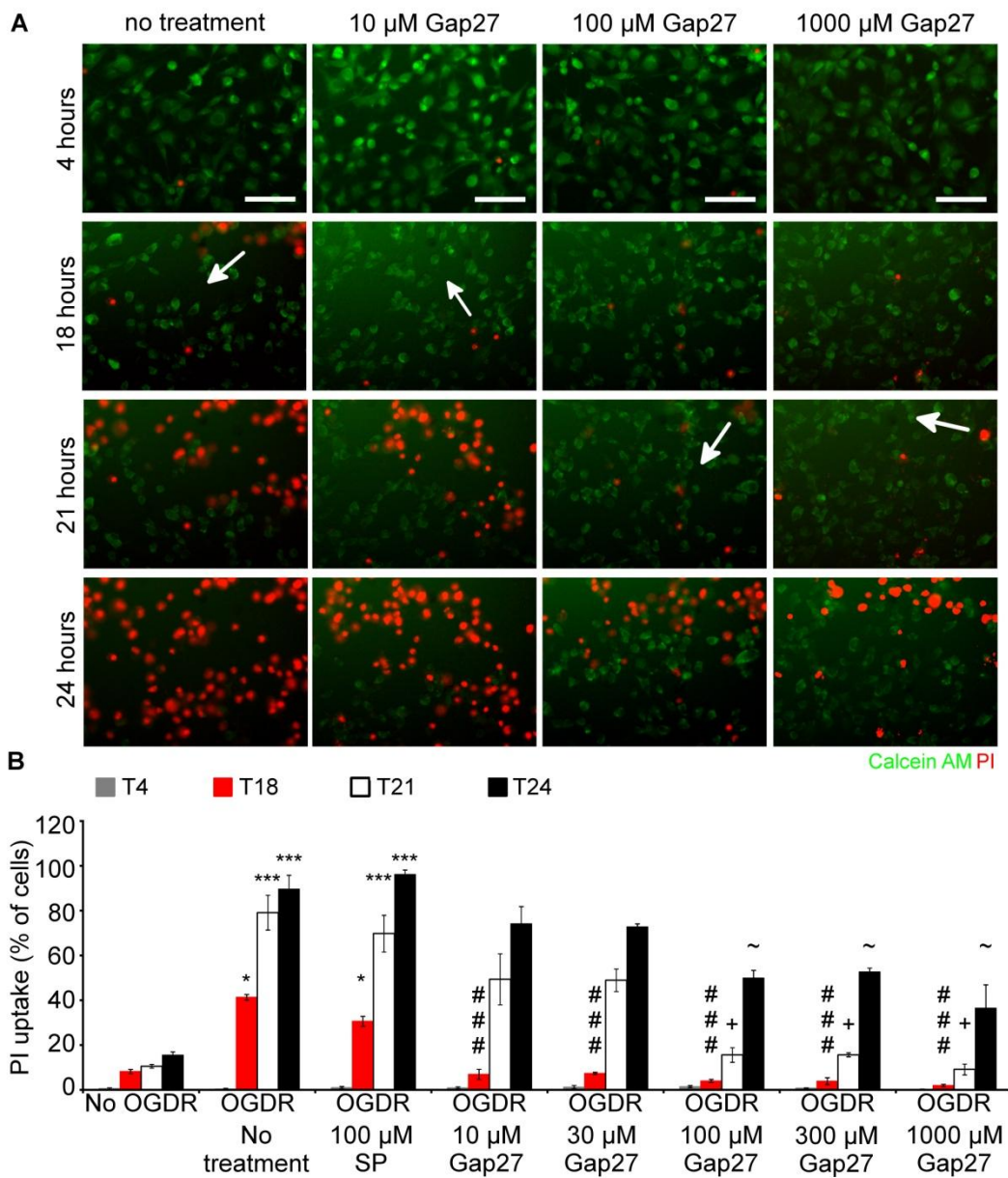


Figure 5.6 Hemichannels open during OGDR stress before wave of PI uptake in neighbouring cells occurs

(A) The panels show representative images of wild type 3T3 fibroblast cells that have undergone OGDR stress for 24 hours. Cells were then incubated with Calcein AM (green) and propidium iodide (PI) (red). Cells undergoing OGDR took up PI randomly before contacting neighbouring cells were labelled with PI. The white arrows indicate the direction of PI uptake. Incubation with high concentrations of Gap27 significantly reduced PI labelling.

(B) Graph shows percentage of cells that are labelled with PI after 4 (grey bars) 18 (red bars) 21 (white bars) and 24 (black bars) hours after OGDR stress. Statistical comparisons were made using a one-way analysis of variance (ANOVA). The data are shown as the means \pm S.E.M. ($n=4$, No OGDR versus OGDR No treatment and OGDR 100 μ M * $p<0.05$, *** $p<0.001$; OGDR No treatment versus OGDR treated cells at T18 #### $p<0.001$; OGDR No treatment versus OGDR treated cells at T21 + $p<0.05$; OGDR No treatment versus OGDR treated cells at T24 ~ $p<0.05$). Scale bar = 100 μ m. PI = Propidium iodide, SP = Scrambled peptide. OGDR = Oxygen glucose deprivation reoxygenation

Blocking downstream processes of ATP release did not prevent reduction in cell viability

Under stress, Cx43 hemichannels will open and release ATP which will act upon purinergic receptors. To assess the downstream processes of ATP release during OGDR stress, purinergic receptor antagonists were used. Wild-type 3T3 fibroblast cells were subjected to OGDR insult and were treated with 100 μ M Suramin upon reperfusion (a general, non-specific P2Y and P2X purinergic receptor antagonist) whereas control samples were left in control medium in atmospheric conditions. Suramin was first used as a specific antagonist for P2 purinergic receptor by Dunn and colleagues (Dunn and Blakeley, 1988) and was quickly identified as an antagonist for both P2Y and P2X purinergic receptors within a couple of years (Kennedy, 1990, Hoyle et al., 1990). Cell viability was assessed using a standard MTT assay. OGDR significantly reduced cell viability over 24 hour in wild type 3T3 fibroblast cell. Treatment with Suramin salts did not prevent the decrease in cell viability (figure 5.7A).

Cultures were again subjected to OGDR insult as described above and after 1.5 hours of oxygen glucose deprivation, cells were subjected to reperfusion. Cells were then incubated with Calcein-AM and PI. Test samples were treated with a single incubation of 300 μ M Gap27, 2 or 20 μ M Brilliant Blue G (BBG) or left untreated (naive OptiMEM). BBG is a selective antagonist of P2Y purinergic receptors (Eschke et al., 2002, León et al., 2006, Díaz-Hernández et al., 2009). After 24 hours of reperfusion, 90% of untreated cells had taken up PI. Incubation in Gap27 significantly reduced PI uptake to 53%. Treatment with high and low concentrations of BBG did not significantly reduce PI uptake (figure 5.7B).

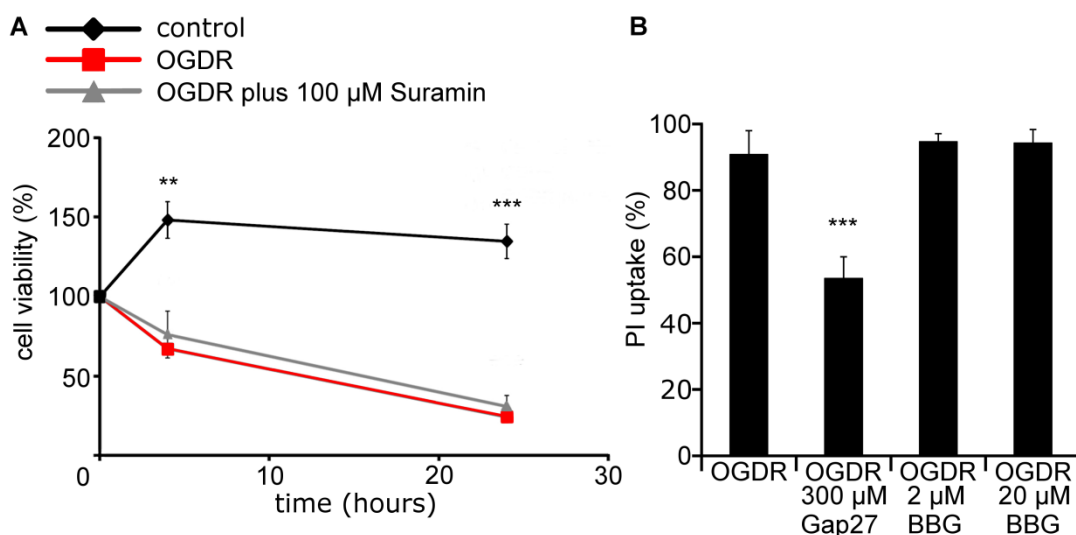


Figure 5.7 Blocking purinergic signalling did not prevent the reduction in cell viability during OGDR stress

(A) Wild type fibroblast cells were subjected to OGDR stress for 24 hours. Cell viability was assessed using a MTT assay in OGDR stressed cells, (un-treated and treated with 100 μ M Suramin salts) and control cells. The graph shows that by antagonistically blocking purinergic receptors with Suramin salts (a general, non-specific P2Y and P2X purinergic receptor antagonist) did not prevent a decrease in cell viability. (B) Cells were subjected to OGDR stress for twenty fours and incubated with Calcein-AM and propidium iodide (PI). The graph shows percentage of cells that have taken up PI after twenty-four hours of OGDR stress. Selectively antagonistically blocking P2Y purinergic receptors with Brilliant Blue G (BBG) did not prevent a decrease in PI uptake. MTT statistical comparisons were made using a one-way analysis of variance (ANOVA). The null hypothesis was rejected using a multivariate analysis of variance (MANOVA). The data is shown as the means \pm S.E.M. ($n=4$, ** $p<0.01$, *** $p<0.001$). PI uptake statistical comparisons were also made using a one-way analysis of variance (ANOVA). The data is shown as the means \pm S.E.M. ($n=4$, *** $p<0.001$ against OGDR no treatment). OGDR = Oxygen glucose deprivation reoxygenation.

Communication between fibroblast cells increased during OGDR stress.

To further explore the possible “bystander effect” between cells during OGDR, communication was assessed using Fluorescent Recovery after Photobleaching (FRAP). During OGDR stress, communication between cells significantly increased in comparison to control cells. Incubation with Gap27 significantly reduced this communication. Higher concentrations of Gap27 in OGDR stressed cells reduced communication beyond control cell levels (figure 5.8).

Reducing Cx43 decreased cell death following OGDR stress

Wild-type 3T3 fibroblast cells and Cx43 shRNA transduced fibroblast cells were subjected to OGDR insult. Cultures were then incubated with Calcein-Am and PI and were treated with a high concentration of Gap27 upon reperfusion. After 24 hours of reperfusion, 90% of untreated wild-type 3T3 fibroblast cells had taken up PI. Cx43 shRNA transduced fibroblast cells had significantly reduced PI uptake at 29% whereas wild-type 3T3 fibroblast cells incubated in a high concentration of Gap27 also had a significantly reduce PI uptake of 42% (figure 5.9A).

In addition, wild-type 3T3 fibroblast cells were subjected to OGDR insult as described above and were treated with 30 or 300 μ M Gap27 upon reperfusion whereas control samples were left in control medium in atmospheric conditions. Cell viability was assessed using a standard MTT assay. Cell viability significantly decreased in wild-type 3T3 fibroblast cells during OGDR stress over 24 hours but this cell death was not observed in cells treated with a high concentration of Gap27 (figure 5.9B).

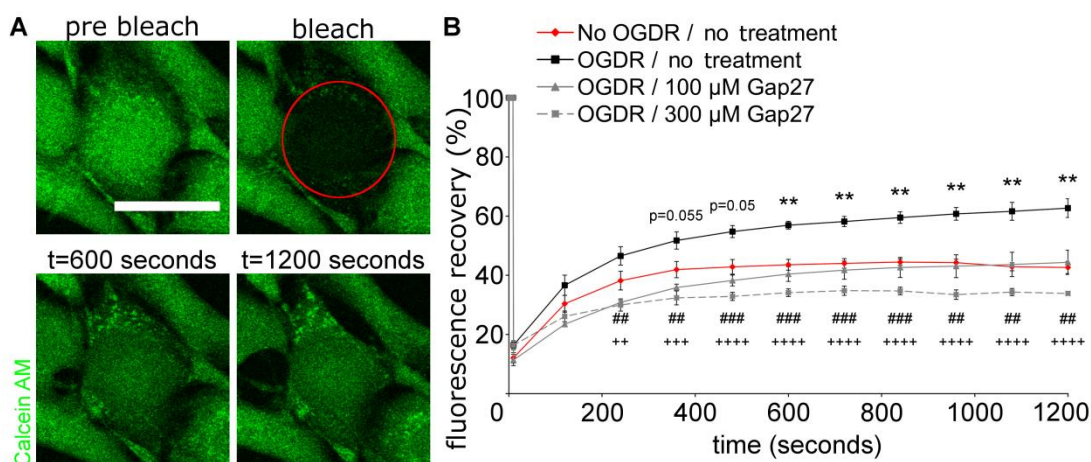


Figure 5.8 Communication between wild-type fibroblast cells significantly increased during OGDR stress

(A) The panels show representative images of Fluorescence Recovery after Photobleaching (FRAP). (B) Graph shows the recovery profiles of fluorescence. OGDR stress significantly increased the recovery rate in comparison to control cells. During OGDR stress, communication was significantly reduced in cells in higher concentrations of Gap27. Statistical comparisons were made using a one-way analysis of variance (ANOVA). The null hypothesis was rejected using a multivariate analysis of variance (MANOVA). The data is shown as the means \pm S.E.M. ($n=4$, between OGDR stress and control non-treated cells ** $p<0.01$; between OGDR stress and OGDR plus 100 μ M Gap27 ## $p<0.01$, ### $p<0.001$; between OGDR stress and OGDR plus 300 μ M ++ $p<0.01$, +++ $p<0.001$, ++++ $p<0.0001$). Scale bar = 25 μ m. OGDR = Oxygen glucose deprivation reoxygenation, t = time.

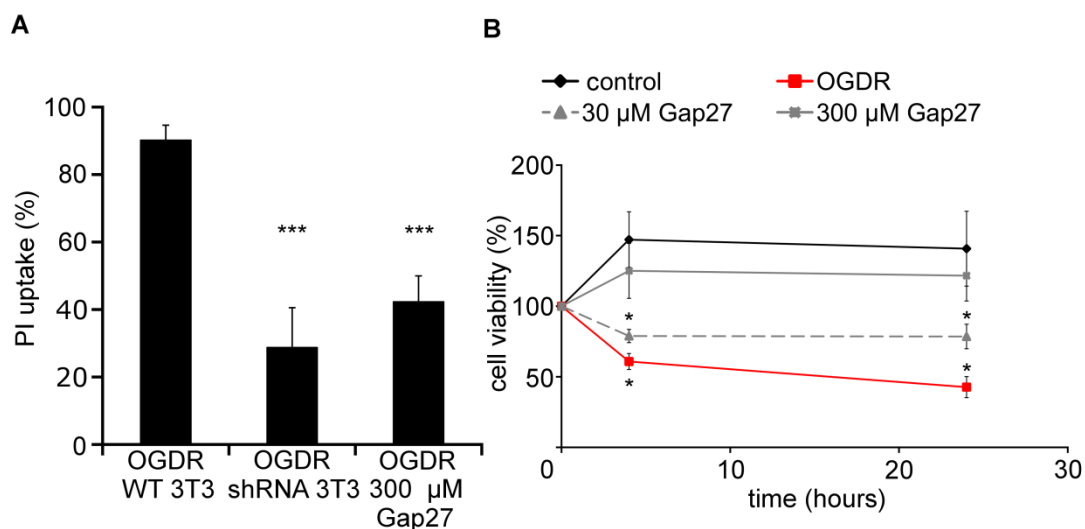


Figure 5.9 Reducing Cx43 during OGDR reduced cell death

(A) Wild type 3T3 fibroblast cells were subjected to OGDR stress for 24 hours and incubated with Calcein-AM and propidium iodide (PI). The graph shows the percentage of cells that have taken up PI after 24 hours of OGDR stress. 3T3 fibroblast cells virally transduced with shRNA-Cx43 and 3T3 fibroblast wild type cells treated with 300 μM Gap27 had significantly fewer cells take up PI in comparison to control cells subjected to OGDR stress. (B) Cells were subjected to OGDR stress for 24 hours. Cell viability was assessed using a MTT assay in OGDR stressed cells, (un-treated and treated with 30 or 300 μM Gap27 and control cells). Cell viability decreased in control cells during OGDR stress over 24 hours. This cell death was not seen in cells treated with a high concentration of Gap27. Statistical comparisons were made using a one-way analysis of variance (ANOVA). In the MTT time lapse experiment the null hypothesis was rejected using a multivariate analysis of variance (MANOVA). The data is shown as the means ± S.E.M. (n=4, *p<0.05, ***p<0.001). PI = Propidium iodide, OGDR = Oxygen glucose deprivation reoxygenation, WT = Wild type, shRNA = Cx43shRNA.

5.3 Discussion

OGDR decreased cell viability

In order to assess and investigate the communication between 3T3 fibroblast cells during hypoxic stress, a well characterised *in vitro* model of ischemia reperfusion was used. Oxygen and glucose deprivation, followed by reoxygenation, was achieved by closely following the *in vitro* model of ischemia reperfusion developed by Pringle and Sundstom (Pringle et al., 1997). By replicating this protocol, medium oxygen levels were reduced four times the normal environment in the data reported in this chapter (figure 5.1).

Similar examples of *in vitro* ischemia models have been used in rat embryonic fibroblast cell lines (Stoler et al., 1992, Gardner et al., 2003, Manotham et al., 2004), cardiac fibroblasts (Chen et al., 2004) and nasal polyp fibroblasts (Cohen et al., 2011). In these examples, only oxygen and nutrient deprivation was achieved. Other approaches to accomplish oxygen and nutrient deprivation have included using coverslip hypoxia; whereby cells are grown as a monolayer before a glass coverslip is placed over the culture. This creates a localized diffusion barrier reducing nutrients and oxygen transfer (Pitts and Toombs, 2004). Chemical anoxia has also been used to reduce nutrient and oxygen levels in cultures (Rentsch et al., 2007, Contreras et al., 2002). Models of oxygen and nutrient deprivation, followed by reoxygenation, have been repeated using hippocampal slice cultures (Laake et al., 1999, Frantseva et al., 2002b) and utilised in rat endothelial cells (Anderson et al., 1995) astrocyte cell lines (Orellana et al., 2010, Wang et al., 2013b) and in NIH 3T3 cells (Chen et al., 1999).

In the *in vitro* model of ischemia reperfusion employed in this chapter, OGDR significantly reduced cell viability over 24 hours in 3T3 wild type fibroblast cells (figure 5.2A). A similar observation was made by Pringle and colleagues upon

Chapter 5 Connexin based communication in ischemia reperfusion

analysis of cell death through PI uptake (Pringle et al., 1997). Hypoxia was induced for 60 minutes before reoxygenation insult took place. They reported a significant increase in PI uptake between 12 and 24 hours after reoxygenation, however the majority of PI labelling did not occur until 24 hours post reperfusion. They also noted that there was a progressive spread of cell death and damage from the ischemic area to surrounding cells. A comparable report was made by Laake and colleagues, again using hippocampal slice cultures (Laake et al., 1999) where a significant increase of PI labelling was observed 24 hours after reoxygenation. In a similar report using NIH 3T3 cells, DNA fragmentation and chromatin condensation were observed upon reperfusion (Chen et al., 1999). Both are indicative of cell death.

In an interesting twist in the same study, NIH 3T3 cells left in continuous anoxia for 48 hours did not show a decrease in cell viability (Chen et al., 1999). This has also been observed in nasal fibroblasts that were left in continuous hypoxic conditions for 12 or 24 hours using an *in vitro* model of ischemia (Cohen et al., 2011) and in rat endothelial fibroblast cells, where cell viability remained constant after 48 hours in a similar *in vitro* model of continuous anoxia (Stoler et al., 1992). This would suggest that it is the reoxygenation element of ischemia reperfusion stress that is responsible for the increase in the number of apoptotic cells and a reduction in cell viability. The oxidative injury during reoxygenation is thought to be a central mechanism in cellular damage and death, affecting most organisms and tissues after anoxic stress (Chen et al., 1999). Reactive Oxygen Species (ROS) are released in post anoxic reoxygenation (Caraceni et al., 1995) which can trigger Caspase 3 and 9 in hypoxia/reoxygenation induced apoptosis (Ho et al., 2006). Attenuating Caspase activation by introducing a catalase reduces apoptosis, indicating an important role for ROS in hypoxic/reoxygenation stress. Further studies using mouse retinal endothelial cells in an OGDR model of ischemia reperfusion reported progressive endothelial cell injury during the period of substrate

Chapter 5 Connexin based communication in ischemia reperfusion replenishment (Rieger et al., 2002). Addition of superoxide scavengers and oxidase inhibitors induced cell protection, and reduced apoptosis; further supporting the important and damaging roles of reactive oxidative species during ischemia reperfusion cell death.

Cx43 and connexin hemichannel expression increased correlating with a decrease in cell viability during OGDR

In a novel discovery, the data in the chapter reports a significant increase in Cx43, Cx43 phosphorylated isoforms and connexin hemichannels in 3T3 fibroblast cells during 24 hours of reoxygenation as supported by immuno and Western blot analysis (figure 5.3, 5.3Ci). This increase in protein expression correlated with a decrease in cell viability over the same 24 hour period (figure 5.2A). Upon repeating the experiment, using a transduced cell line where the majority of Cx43 has been knocked down, no reduction in cell viability was observed (figure 5.2B). Cells transduced with empty vectors served as a negative control and in a similar pattern to wild-type 3T3 fibroblast cells, Cx43 and connexin hemichannels expression increased in correlation with a reduction in cell viability (figure 5.2C, figure 5.4Ai, Aii and Ciii). These results strongly suggest that Cx43 plays a significant role in spreading cell death and damage during reoxygenation in an *in vitro* model of ischemia reperfusion.

Comparable studies using cortical astrocytes in culture models of ischemia reperfusion have also reported that upon reoxygenation an increase in cell surface expression of Cx43 was observed and correlated with a decrease in cell viability (Orellana et al., 2010). A recent study performed by Wang and colleagues, using an astrocytic cell line in a model of OGDR, also reported that Cx43 expression significantly increased during reoxygenation, whereas cell viability significantly reduced in the same time period (Wang et al., 2013b). An increase in Cx43 plaque

Chapter 5 Connexin based communication in ischemia reperfusion

size has also been described in similar circumstances (Cotrina et al., 1998a). Beardslee and colleagues have reported a marked increase in phosphorylated isoforms of Cx43 in reperfused adult rat hearts (Beardslee et al., 2000) whereas Turner and colleagues described how Cx43 became profoundly dephosphorylated during hypoxic conditions and was completely rephosphorylated within 30 minutes of reoxygenation (Turner et al., 2004). However, in prolonged ischemia it has been noted that phosphorylated isoforms markedly decrease (Clarke et al., 2009, Beardslee et al., 2000). Although the biological consequences of specific changes in Cx43 phosphorylation during chronic ischemia are not understood in detail, it has been suggested that there is a likely correlation with cellular uncoupling (Beardslee et al., 2000).

Organotypic hippocampal slices that underwent OGDR were reported to have significant cell death over a 48 hour period. Treatment with carbenoxalone (a non-specific inhibitor of gap junction communication) or Cx43 asODN significantly decreased cell death within the tissue during OGDR stress (Frantseva et al., 2002b). Apoptosis during metabolic inhibition was again noted in a human glial cell line transduced with Cx43 (Huang et al., 2001). Reducing Cx43 during the stress of ischemia reperfusion prevented the reduction of cell death. Despite the growing evidence in the literature discussed above, together with the data reported in this chapter, that marks Cx43 as a key contributor to the spread of cell death and damage after an ischemic insult, the mechanisms behind this damage are still unclear.

Contributors of cell death during OGDR

Some reports attribute cell death in ischemic reperfusion models to the opening of undocked gap junctions, releasing ATP and reducing cell viability through the activation of purinergic receptors. However, other reports suggest that the

Chapter 5 Connexin based communication in ischemia reperfusion

“bystander effect” model is in play during hypoxia-reoxygenation apoptosis, as cell death signals spread laterally through gap junctions from dying cells into their healthy neighbours. In order to understand the contribution of hemichannels and gap junction based communication during hypoxic stress and reoxygenation insult, two methods of examination were used. The first was to distinguish between hemichannel and gap junction communication through different confluence levels of fibroblast cells whereas the second was to employ the connexin mimetic peptide Gap27 as a tool, as it has consistently shown to have a unique dose and time response during incubation. At low doses, Gap27 has been shown to block open hemichannels but can also target gap junctional intercellular communication at high doses and for longer incubation periods.

Here it is shown that non-confluent cells subject to OGDR stress and treated with Gap27 do not label with PI (figure 5.5). However, in confluent cells subjected to the same insult, PI labelling initially occurs in random, non-contacting cells, before a wave of PI labelling was observed in neighbours (figure 5.6 and supplementary movies). High concentrations of Gap27 significantly reduced PI uptake. Although it is clear that Cx43 plays a role in communication and cell death during OGDR stress, it is still uncertain as to the mechanisms involved. This is discussed in more detail in the following sections.

Cell death through hemichannel communication

For many decades it was thought that hemichannels remained in a permanent closed state, until docked with their partners from a neighbouring cell, to avoid influencing cell death. However, recent research has shown how hemichannels can open under stress and provide a signalling pathway between the cytoplasm of the cell and the extracellular environment (Evans et al., 2006). To assess hemichannel activity during OGDR stress, PI labelling was observed in low confluence 3T3

Chapter 5 Connexin based communication in ischemia reperfusion

fibroblast cells (figure 5.5). It was noted that OGDR insult caused cells to label with PI; indicating that cells were either dying, opening their hemichannels or both. Treatment with Gap27 reduced this dye uptake. If Cx43 based communication wasn't involved, incubation in Gap27 would have made no difference in PI labelling during OGDR stress; heavily suggesting that hemichannel opening is involved during reperfusion insults.

Similar observations were made in models of ischemia reperfusion using metabolic inhibition. Both cardiac ventricular myocyte and rat cortical astrocyte cultures opened their hemichannels during reperfusion stress as shown by electrophysiological analysis and dye uptake (John et al., 1999, Contreras et al., 2002). Cells subjected to oxidative stress, via ROS application or through a lowered redox potential, also demonstrated hemichannel opening (Ramachandran et al., 2007, Retamal et al., 2007). A comparable report was made by Shintani-Ishida and colleagues upon subjecting rat neonatal cardiomyocytes to OGDR stress. They observed that hemichannels opened during the reperfusion period and that incubation with Gap26 reduced dye uptake.

It is still unclear as to whether surface hemichannels have similar permeability properties to gap junctions formed of the same connexins, however it is becoming increasingly apparent that hemichannels possess bi-directional properties as shown by dye uptake and ATP release (Evans et al., 2006). Research by Clarke and colleagues has demonstrated how cardiac myocytes undergoing ischemic stress release ATP, whereas treatment with Gap26 significantly abolishes this release (Clarke et al., 2009). Eltzschig and colleagues have demonstrated that polymorphonuclear leukocyte cells release ATP from Cx43 hemichannels (Eltzschig et al., 2006) whereas Stout and colleagues have described similar results in astrocytes (Stout et al., 2002). Orriss and colleagues demonstrated that during

Chapter 5 Connexin based communication in ischemia reperfusion

hypoxic stress osteoblasts released ATP (Orriss et al., 2009) while Orellana and contemporaries have also described how astrocytes subjected to hypoxia in high glucose increased cell permeabilisation via Cx43 hemichannels (Orellana et al., 2011). Not only was there a reported increase in dye uptake, an increase in ATP release and a reduction in cell viability were also observed. During stress, ATP release has been inhibited by connexin mimetic peptides in endothelial cells (Braet et al., 2003a, Braet et al., 2003b, Leybaert et al., 2003), polymorphonuclear leukocytes (Eltzschig et al., 2006) and HeLa cells transduced with Cx43 (Wang et al., 2012).

ATP released from Cx43 hemichannels has been shown to mediate calcium wave signalling in astrocyte cultures (Stout et al., 2002), epithelial cells (Pearson et al., 2005) and in HeLa cells transduced with Cx43 (Cotrina et al., 1998b, Verma et al., 2009). Upon disrupting Cx43 based communication, by either using wild-type HeLa cells that have no connexin expression (Verma et al., 2009) or through incubation with gap junction communication inhibitors (Stout et al., 2002) calcium propagation is reduced, suggesting connexin participation in calcium signalling is likely. High concentrations of calcium release can lead to cell death in a generation of pathological calcium signals, which result in compromising calcium homeostatic machinery, mitochondrial dysfunction, a release of pro-apoptotic factors and the activation of calcium dependent degrading enzymes (Verkhatsky, 2008). Although ATP released from Cx43 hemichannels has been shown to influence cell death through the mediation of calcium signalling, reduced cell viability can also be caused through ATP activation of purinergic signals.

Purinergic receptors are found in almost all mammalian tissues and are a family of plasma membrane molecules that respond to the release of adenosine (P1 receptors) or ATP (P2 receptors). P2 receptors can be further divided into five

Chapter 5 Connexin based communication in ischemia reperfusion

subclasses, P2X, P2Y, P2Z, P2U and P2T, which can be grouped into metabotropic receptors (P2Y, P2U and P2T) and ionotropic receptors (P2X and P2Z). P2Y purinergic receptors are metabotropic G-protein coupled receptors and their activation leads to phospholipase C activation, the generation of IP₃ and an increase in cytosolic calcium (Baroja-Mazo et al., 2013). Brief ATP stimulation on P2X purinergic receptors, particularly P2X7 purinergic receptors, induces the opening of non-selective cation-carrying pores, leading to a Ca²⁺ and Na⁺ influx and K⁺ efflux and resulting in the depolarisation of the plasma membrane (Di Virgilio et al., 1998, Pelegrin, 2011). Prolonged and repetitive ATP stimulation on P2X7 purinergic receptors leads to the opening of a non-selective “large pore” that is permeable to higher molecular weight molecules up to 900 Daltons (Di Virgilio et al., 1998, Pelegrin, 2011, Baroja-Mazo et al., 2013). Virgiono and colleagues reported how prolonged activation of P2X7 receptors with ATP resulted in the pore size increasing from 0.8nm to 3.5nm (Virgilio et al., 1999). This caused an osmotic balance, plasma membrane depolarisation, swelling and disaggregation of the cytoskeletal network and ultimately cell death as shown in lymphocytes (Di Virgilio et al., 1989, Di Virgilio et al., 1998, Tsukimoto et al., 2005) and both normal and diabetic human fibroblast cells (Solini et al., 2004). Fibroblasts cells have been shown to express P2Y and P2X purinergic receptors (Giovannardi et al., 1992, Solini et al., 1999, Burnstock and Verkhratsky, 2009, Knight, 2009) but predominately express P2X7 receptors (Knight, 2009).

To assess the downstream processes of ATP release during OGDR stress, purinergic receptor antagonists were employed. OGDR significantly reduced cell viability over 24 hours whereas treatment with Suramin did not prevent the decrease in cell viability (figure 5.7A). Further work was carried out to investigate whether the P2X7 pore was involved in the reduction of cell viability during OGDR stress (figure 5.7B). After 24 hours of reperfusion 90% of untreated cells had labelled with PI,

Chapter 5 Connexin based communication in ischemia reperfusion

whereas treatment with both high and low concentrations of BBG did not significantly reduce PI uptake. The results presented here would suggest that although hemichannels are opening in 3T3 fibroblasts during OGDR stress and potentially releasing ATP, this release is not enough to induce cell death. Blocking ATP purinergic receptors by using Suramin and BBG was not enough to save the reduction in cell viability. Interestingly, incubation in a high concentration of Gap27 significantly reduced PI uptake to 53%. As described in detail before, it is high concentrations of mimetic peptides that have been shown to reduce gap junction communication between confluent cells. It is possible that incubation in Gap27 was inhibiting the bystander effect in connected cells and this theory was explored further.

Cell death through gap junction communication

The “bystander effect” model suggests that death signals can spread laterally through gap junctions from dying cells into their healthy neighbours. The term was first used by Nagasawa and colleagues to explain the phenomenon in which un-irradiated cells exhibited the effects of radiation as a direct result of signals received from damaged irradiated neighbours (Nagasawa et al., 2002, Little et al., 2002). In cells that were genetically or chemically gap-junction compromised, less damage spread to neighbours (Azzam et al., 2001). Further reports of the bystander effect have been observed in Herpes Simplex Virus – Thymidine Kinases gene therapy for colorectal cancer (McMasters et al., 1998, Burrows et al., 2002, Sanson et al., 2002) and it was reported that expression of Cx43 based gap junctions were necessary components of the bystander effect in human colon tumour cells. A close correlation between Cx43 gap junction based communication and an increase in the consequences of the bystander effects was noted. Gap junction mediated spread of cell death has also been documented in models of *in vitro* metabolic stress (Lin et al., 1998, Cotrina et al., 1998a, Nodin et al., 2005), rodent models of stroke injury

Chapter 5 Connexin based communication in ischemia reperfusion

(Frantseva et al., 2002b, Rawanduzy et al., 1997, Zhang et al., 2013), rodent models of cardiac ischemia reperfusion injury (Mao et al., 2005, Mao et al., 2009) rodent models of spinal cord injury (Cronin et al., 2008) and rodent models of retinal ischemia injury (Danesh-Meyer et al., 2012).

To explore the possible bystander effect between confluent cells during OGDR stress, PI uptake and transfer was observed over 24 hours (figure 5.6 and movie 1 – supplementary disc). Research presented in this chapter has already demonstrated how non-confluent cells in OGDR stress open their hemichannels and label with PI. Treatment with Gap27 plugs open hemichannels and significantly reduced PI labelling. However, it was observed that PI uptake in confluent cells subjected to the same insult followed a different pattern. OGDR insult initially caused PI uptake in random, non-contacting untreated cells 18 hours after reperfusion. From these initial cells, a wave of PI uptake was observed in neighbouring cells until 90% of cells observed were labelled with PI, 24 hours after reperfusion. Cx43 shRNA transduced fibroblast cells, that underwent the same hypoxic stress, had significantly reduced PI uptake to 29% at 24 hours after reperfusion whereas wild-type 3T3 fibroblast cells incubated in a high concentration of Gap27 also had a significantly reduced PI uptake (figure 5.6 and 5.9A). This data further contributes to the mounting evidence that Cx43 based communication is involved during ischemic reperfusion stress in culture models and that by reducing communication by either removing Cx43 or inhibiting gap junction communication, PI labelling is reduced in cells undergoing OGDR stress.

Further evidence of increased gap junction based communication between neighbouring cells during OGDR insults was observed using FRAP analysis (figure 5.8). Communication between cells significantly increased during OGDR stress and incubation with Gap27 significantly reduced this communication. Similar results

Chapter 5 Connexin based communication in ischemia reperfusion

were observed by Lin and colleagues when investigating whether gap junctions propagated trans-cellular signals during metabolic stress (Lin et al., 1998). By also using FRAP analysis they observed how gap junctions remained open during metabolic stress, which correlated with an increase in cell death. Cell treatment using the non-specific gap junction blocker Octanol both reduced cell communication and cell death during metabolic insult.

Research presented in a previous chapter in this thesis has shown how higher concentrations of Gap27 significantly reduced communication between neighbouring cells, with further studies showing that Gap27 significantly reduced communication in fibroblast like COS-7 cells (Chaytor et al., 1999, Dora et al., 1999), Schwann cells (Mambetisaeva et al., 1999), leukocyte cells (Oviedo-Orta et al., 2000), alveolar cells (Isakson et al., 2003) and HeLa cells transduced with Cx43 (Berman et al., 2002). Incubation concentrations of Gap27 in these investigations typically ranged between 130 and 500 μM , supporting the theory that primarily higher concentrations of Gap27 will significantly reduce gap junction communication. In a novel report presented in this research chapter 3T3 fibroblast cells were once again subjected to OGDR stress before being treated with a low (30 μM) or high (300 μM) concentration of Gap27 upon reperfusion (figure 5.9B). As reported before, cell viability significantly decreased in untreated cells during OGDR insult whereas treatment with Gap27 prevented this reduction in cell death. However, it was only treatment in higher concentrations of Gap27 that significantly prevented a reduction in cell viability observed during OGDR stress. This would suggest that communication (and therefore the consequences of the bystander effect) is being significantly reduced during OGDR stress with a higher concentration of Gap27, which ultimately prevents a reduction in cell viability.

Chapter 5 Connexin based communication in ischemia reperfusion

A controversial study carried out by Decrock and colleagues using glioma cells transduced with Cx43 reported that gap junctions contributed to the spread of apoptosis in an area close to where apoptosis was initially triggered (Decrock et al., 2009). However, hemichannels also promoted cell death beyond this area. Long incubation periods with Gap27 (targeting gap junction based communication) reduced apoptosis in both area 1 (close to the apoptotic region) and area 2 (further beyond this region) whereas short incubation periods with Gap27 (targeting open hemichannels) only reduced apoptosis in area 2. However, this work was not carried out under ischemic reperfusion stress, which may explain the difference in connexin based spread of cell death and damage presented in this chapter (reperfusion stress triggers hemichannel opening before gap junction communication promotes a reduction in cell viability).

Conclusions

- During Oxygen-Glucose Deprivation Reoxygenation (OGDR) stress, 3T3 fibroblast cell viability decreased in correlation with an increase in Cx43, phosphorylated Cx43 isoforms and connexin hemichannel expressions.
- Non confluent 3T3 fibroblast cells labelled with Propidium Iodide (PI) during OGDR stress.
- Blocking downstream processes of ATP release did not prevent reduction 3T3 fibroblast cell viability.
- Communication between fibroblast cells increased during OGDR stress.
- Reducing Cx43 expression using Cx43 shRNA transduced 3T3 fibroblast cells or reducing gap junction based communication prevented this reduction in cell viability.

Further studies to build upon the research presented in this chapter would include an observation in calcium movement during OGDR stress. It is been theorised that during the bystander effect an apoptotic signal is transferred via gap junction communication between dying cells and healthy neighbouring cells (Cusato et al., 2003). Krutovskikh and colleagues hypothesise that calcium ions are the most probable cell killing signal that pass between gap junctions (Krutovskikh et al., 2002) as also shown by Isakson and colleagues in investigating mechanically perturbed rat alveolar cells (Krutovskikh et al., 2002). They observed an increase in calcium wave propagation from stressed cells to healthy neighbouring cells that was inhibited by Gap27 incubation. Therefore it is likely that calcium signals are promoting apoptosis between dying cells to healthy neighbours via gap junctions in the bystander effect observed in OGDR stress in this research chapter. The next chapter further explores the role of Cx43 based spread of cell death and damage using an *in vivo* model of pressure ulcers in mice.

6. The role of Cx43 in a model of pressure ulcers

6.1 Introduction

In the previous chapter it was reported that Cx43 based communication was heavily involved in the spread of fibroblast cell death and damage in an *in vitro* model of ischemia reperfusion. The research presented in this chapter further investigates the role of Cx43 and hemichannels in a murine model of pressure ulcers.

Pressure ulcers can be caused by either prolonged or repeated incidents of ischemia reperfusion in the skin. They are often found on bony prominences and are classed as chronic wounds. Chronic wounds are those that do not heal in an orderly set of phases nor in a predictable amount of time in the way that most acute wounds do. As chronic wounds take an unusually long time to heal, do not heal properly or constantly re-occur, independence and quality of life of the sufferer is compromised. A large percentage of chronic wounds fall into three main categories; diabetic foot ulcers, venous leg ulcers and pressure ulcers (Mustoe, 2004).

Pressure ulcers are an enormous economic burden to health services across the globe. It is estimated that there are currently 7.4 million people with pressure ulcers in the world and every year over 400,000 new patients will develop a pressure ulcer in the UK (Bennett et al., 2004). Approximations currently suggest that this is costing the NHS over £2bn a year in nursing, dressings, support and complication costs (Bennett et al., 2004). The incidence of pressure ulcers among hospital patients is between 4 and 20% whereas approximately 25% of patients resident in long-term geriatric wards will develop a pressure ulcer (Bennett et al., 2004, Sen et al., 2009).

Chapter 6 The role of Cx43 in a model of pressure ulcers

Improvements in Western civilization health care, living standards and socio-economic status means that more and more people are now living to an older age (Wicke et al., 2009). Between the years 2000 and 2020 the UK population of over 65's is forecast to increase by 23% from 9.2 million to 11.3 million. This will mean that over a fifth of the UK's population will be over 65 by 2020 (Bennett et al., 2004). As the global elderly population continues to grow, so will the number of pressure ulcers. The staggering financial burden will only get bigger and therefore the need for an effective pressure ulcer treatment is paramount.

Pressure ulcers are attributed to ischemia reperfusion injury, caused by the return of blood to tissues that has encountered a period of oxygen deprivation. Local oxygen tensions are crucial during the wound healing process as oxygen has roles within the inflammatory response (producing toxic oxidants to tackle infection), fibroblast proliferation, collagen and biological energy equivalents production (Tandara and Mustoe, 2004). During wound healing there is an increase in energy demand and oxygen aids in the production of ATP that is needed for processes such as aerobic glycolysis, citric acid cycle and oxidation of fatty acids (Schreml et al., 2010). Tissue hypoxia profoundly impairs and delays wound healing and it has been shown that lower extremities with a partial oxygen pressure of less than 30 mmHg will fail to heal (Mustoe et al., 2006). However, it has been observed in cardiac and neuronal models of ischemia reperfusion that the majority of tissue damage often occurs during the reoxygenation phase (Miyazaki et al., 1987, García-Dorado et al., 1989, Rawanduzy et al., 1997). While reperfusion may be necessary to reduce the irreversible cellular injury caused by tissue hypoxia, reperfusion can also cause additional tissue impairment (Mustoe, 2004). Indeed, most pressure ulcer damage occurs due to the repetitive nature of ischemic reperfusion in patients. As described by Mustoe, most critically ill patients or patients with impaired mobility are often placed on a strict turning regime (Mustoe et al., 2006). In fact, advice from a leading

Chapter 6 The role of Cx43 in a model of pressure ulcers

pressure ulcer prevention advisory panel recommends that a patient is repositioned every 2-6 hours depending on the severity of the injury (EPUAP, 2009). While good intentions are intended, the cyclic intervals of variable blood flow caused by this regime may have further detrimental clinical effects.

Vulnerable patients who will develop pressure ulcers are those who suffer from impaired mobility or sensation, such as the elderly, wheelchair bound or bedridden. Pressure ulcers are also extremely common in long term hospitalised patients. Pressure induced ischemia occurs when the patient is recumbent which is then followed by hyperaemia when a change in patient position provides a return of blood flow (Mustoe, 2004). The return of blood supply during the restoration of circulation causes inflammation and oxidative damage to the tissue, which often spreads beyond the initial ischemic area. Healthcare professionals use a grading system to describe the severity of pressure ulcer damage and often the higher the grade diagnosed means a more severe injury to the skin and underlying tissue (EPUAP, 2009). People with the highest grade of pressure ulcer, grade 4, have a high risk of developing a life threatening infection as they suffer full skin thickness loss that exposes the bone or muscle.

At present, our understanding of how these chronic wounds occur and why they take longer than average to heal is incomplete. Recent research has identified gap junction mediate ischemia reperfusion injury in the cardiac (García-Dorado et al., 2004) and cerebral tissue (Frantseva et al., 2002b), however there has been no published investigation (human or rodent based) into the role of gap junction based communication in the pressure ulcer. Using an *in vivo* model of pressure ulcers developed by Thomas Mustoe, this chapter examines the role of Cx43, hemichannels and gap junctions during ischemia reperfusion injury in the skin.

Chapter 6 The role of Cx43 in a model of pressure ulcers

Hypothesis – Cx43 propagates cell injury and death during ischemia reperfusion injury in murine skin.

6.2 Results

Development of an ischemia reperfusion model in murine skin

In order to create an early stage pressure ulcer model, a surgical procedure adapted from a protocol developed by Thomas Mustoe was implemented (Reid et al., 2004) as described in detail in the methods section. Tissue was observed at the three key sites (figure 6.1C) the pressure site (PS), adjacent to the pressure site (AT) and in distal tissue (DT). Initial observations confirmed that magnet pressure caused greater damage at the pressure site and in areas adjacent to the pressure site after 1.5 hours of ischemia followed by 24 hours of reperfusion (figure 6.1B). The European Pressure Ulcer Advisory Panel categorizes early stage pressure ulcers in humans as intact skin with non-blanchable redness which can develop into partial thickness loss of dermis in later stages (EPUAP, 2009). Macroscopic and histological observations of murine skin that had undergone ischemic reperfusion injury confirmed similar findings. Tissue breakdown was noted along with an increase in inflammatory cells within the tissue. Application of Cx43 asODN at the wound site greatly reduced the extent of damage (figure 6.1B).

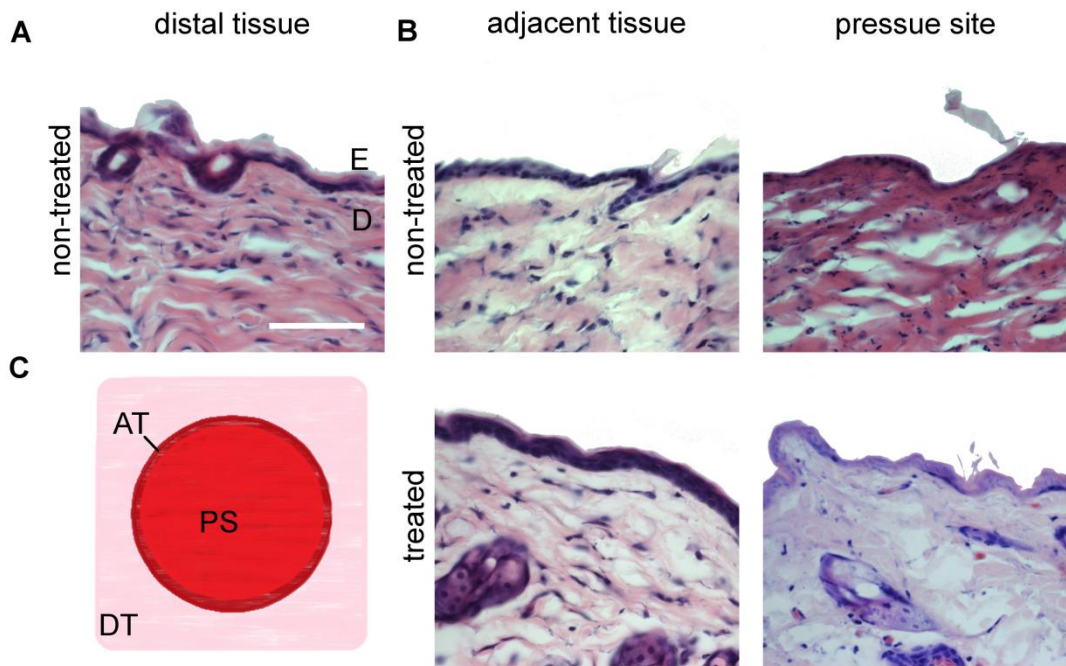


Figure 6.1 The skin ischemia reperfusion model caused tissue damage at the pressure site

(A) The panel shows a representative histological image of tissue that has not been subjected to pressure. (B) The panels show representative histological images of tissue that has been subjected to 1.5 hours of pressure followed by relief for 24 hours. Tissue was either treated with Cx43 asODN or left untreated. Pressure caused greater tissue damage at the pressure site and in areas adjacent to the pressure site. Application of Cx43 asODN at the wound site greatly reduced the extent of damage. (C) Diagram indicates areas of interest around the pressure site. $n=5$, Scale bar = 150 μm . PS = Pressure site, AT = Adjacent tissue, DT = Distal tissue, E= Epidermis, D=Dermis

Cx43 and connexin hemichannel expression significantly increased after ischemia reperfusion

Cx43 and connexin hemichannel expression profiles were examined in three key sites; the pressure site, adjacent to the pressure site and in distal tissue. Within the epidermis, Cx43 and connexin hemichannel expression did not differ at the pressure site in comparison to the distal tissue (figure 6.2A, Ci and figure 6.3A, Ci) four hours after pressure relief. However, Cx43 expression significantly increased at the pressure site in the upper dermis four hours after pressure relief (figure 6.2A, Cii) and connexin hemichannel expression significantly increased at the pressure site in both the upper and lower dermis four hours after pressure relief (figure 6.3A, B, Cii, Ciii) Application with Cx43 asODN at the pressure site significantly reduced the increase in both Cx43 and connexin hemichannel expression.

Twenty four hours after pressure relief, Cx43 and hemichannel expression within the epidermis still did not differ at the pressure site in comparison to the distal tissue (figure 6.4A, Ci and figure 6.5B). Cx43 expression significantly increased at the pressure site in both the upper and lower dermis twenty four hours after pressure relief (figure 6.4A, B, Cii, Ciii). However there was no significant change in connexin hemichannel expression within the dermis at the pressure site or surrounding tissue, twenty four hours after pressure relief (figure 6.5B and C).

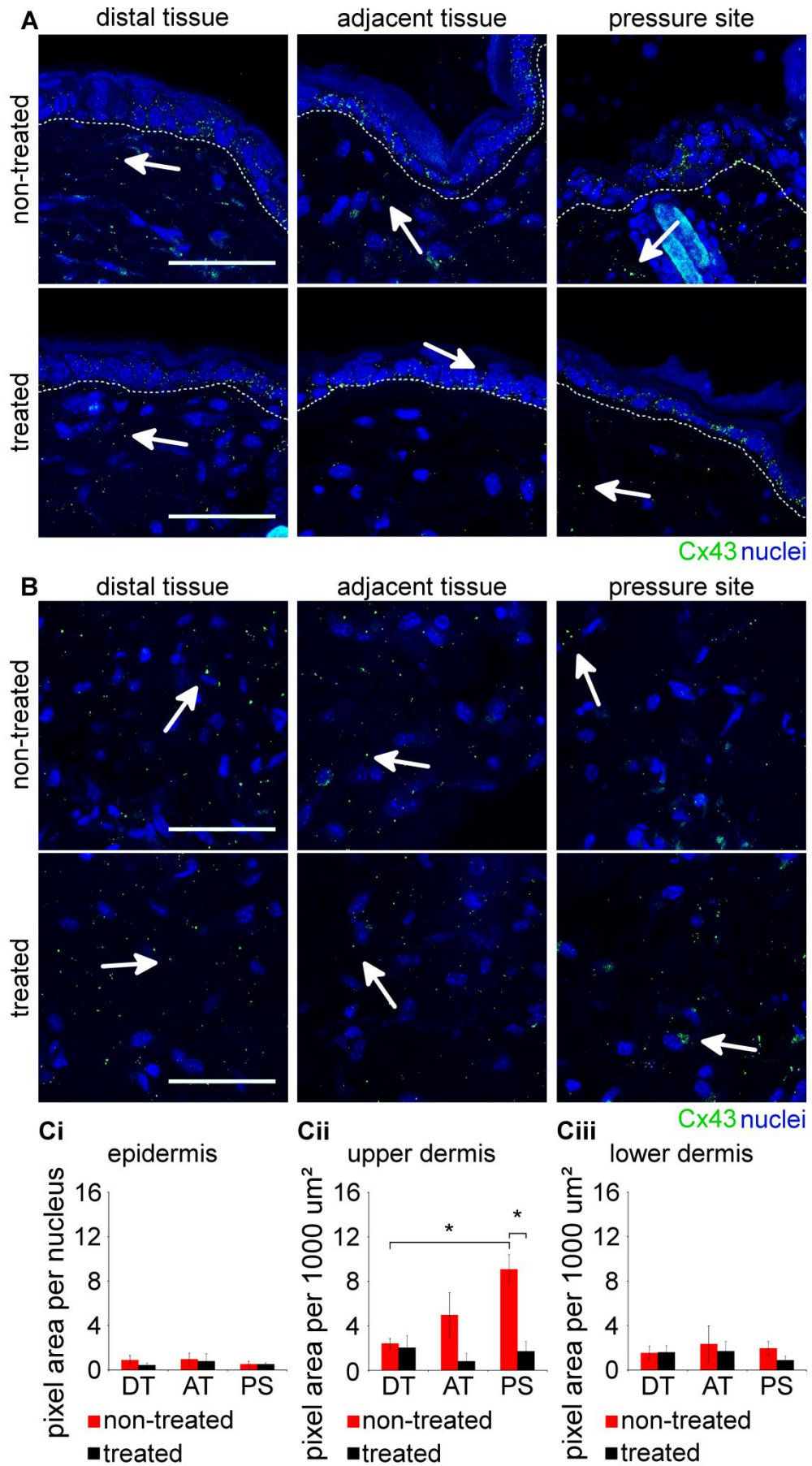


Figure 6.2 Cx43 expression in the skin ischemia reperfusion model four hours after pressure relief

The panels show representative images of epidermis tissue (A) and dermal tissue (B) that has not been subjected to pressure (distal and adjacent tissue) and tissue that has been subjected to 1.5 hours of pressure followed by relief for 4 hours (pressure site). Tissue was either treated with Cx43 asODN or left untreated. Tissue was immunolabeled for Cx43 (green) and nuclei (blue). The epidermis and dermis are separated by a white dashed line. (C) Total pixel area per nucleus within the epidermis was quantified. Cx43 expression did not differ at the pressure site in comparison to distal tissue. Total pixel area per 1000 μm^2 within the upper (D) and lower (E) dermis was quantified. Cx43 expression significantly increased at the pressure site in the upper dermis. Application of Cx43 asODN at the wound site significantly reduced this increase. Statistical comparisons were made using a one-way analysis of variance (ANOVA). The data are shown as the means \pm S.E.M. ($n=5$, $*p<0.05$). White arrows indicate Cx43 expression. Scale bar = 50 μm . E = epidermis, D = Dermis, DT = Distal tissue, AT = Adjacent tissue, PS = Pressure site.

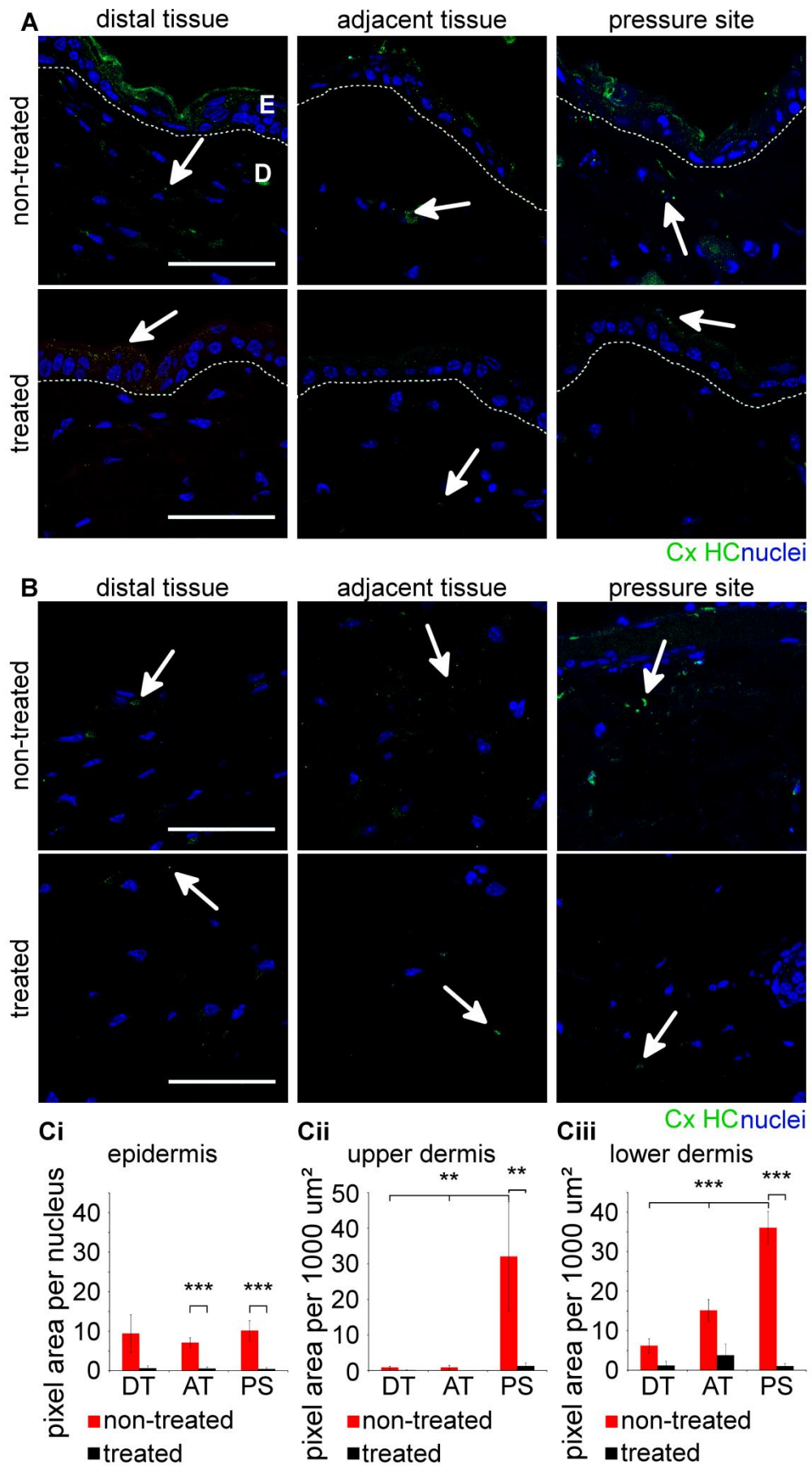


Figure 6.3 Connexin hemichannel expression in the skin ischemia reperfusion model four hours after pressure relief

The panels show representative images of epidermis tissue (A) and dermal tissue (B) that has not been subjected to pressure (distal and adjacent tissue) and tissue that has been subjected to 1.5 hours of pressure followed by relief for 4 hours (pressure site). Tissue was either treated with Cx43 asODN or left untreated. Tissue was immunolabeled for connexin hemichannels (green) and nuclei (blue). The epidermis and dermis are separated by a white dashed line. (C) Total pixel area per nucleus within the epidermis was quantified. Connexin hemichannel expression did not differ at the pressure site in comparison to distal tissue Total pixel area per 1000 μm^2 within the upper (D) and lower (E) dermis was quantified. Connexin hemichannel expression markedly increased in the both upper and lower dermis. Application of Cx43 asODN at the wound site significantly reduced this increase. Statistical comparisons were made using a one-way analysis of variance (ANOVA). The data are shown as the means \pm S.E.M. ($n=5$, $**p<0.01$, $***p<0.001$). White arrows indicate hemichannel expression. Scale bar = 50 μm . E = epidermis, D = Dermis, DT = Distal tissue, AT = Adjacent tissue, PS = Pressure site, Cx HC = Connexin hemichannel.

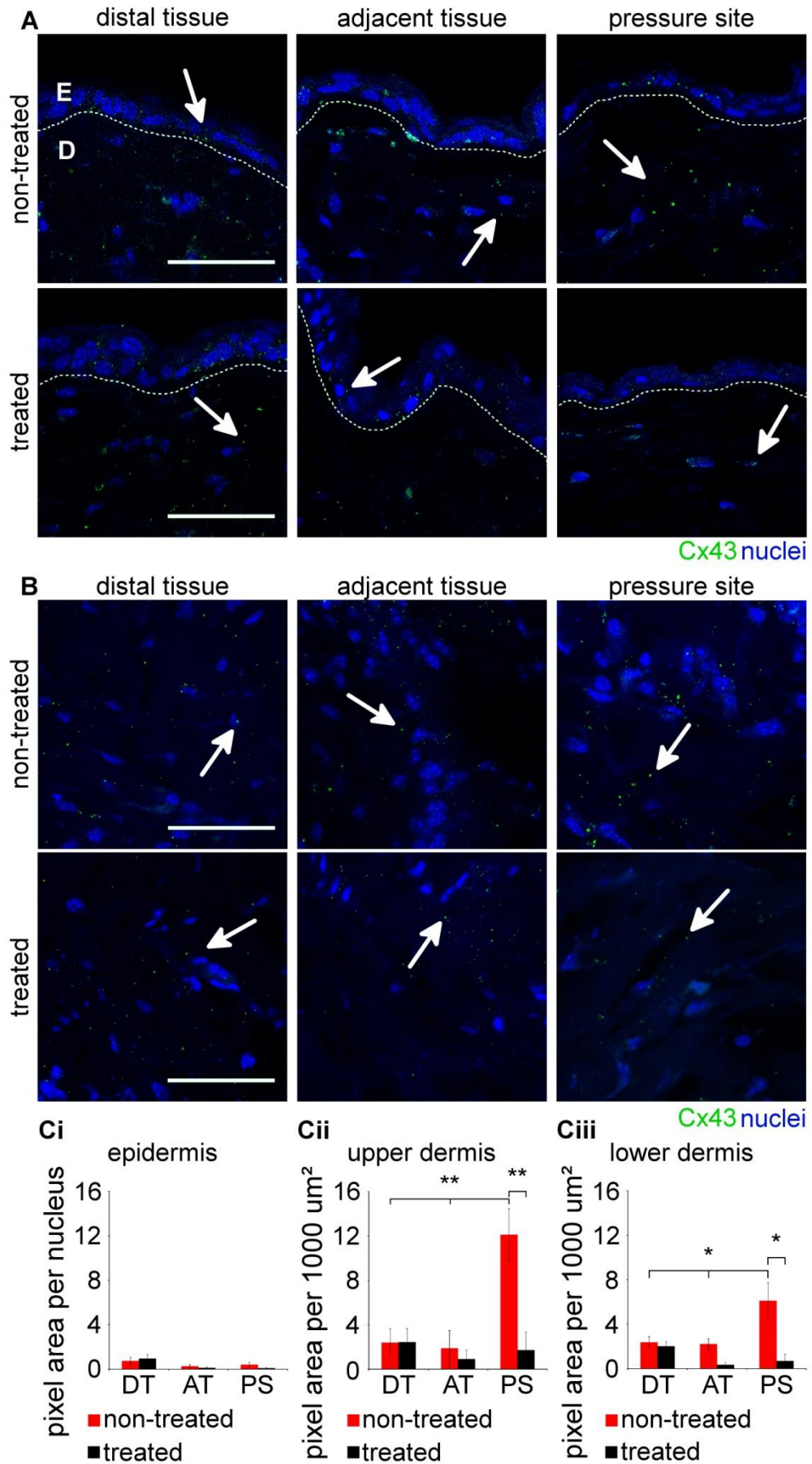


Figure 6.4 Cx43 expression in the skin ischemia reperfusion model twenty four hours after pressure relief

The panels show representative images of epidermis tissue (A) and dermal tissue (B) that has not been subjected to pressure (distal and adjacent tissue) and tissue that has been subjected to 1.5 hours of pressure followed by relief for 24 hours (pressure site). Tissue was either treated with Cx43 asODN or left untreated. Tissue was immunolabeled for Cx43 (green) and nuclei (blue). The epidermis and dermis are separated by a white dashed line. (C) Total pixel area per nucleus within the epidermis was quantified. Cx43 expression did not differ at the pressure site in comparison to distal tissue Total pixel area per 1000 μm^2 within the upper (D) and lower (E) dermis was quantified. Cx43 expression significantly increased in both upper and lower dermis. Again, application of Cx43 asODN at the wound site significantly reduced this increase. Statistical comparisons were made using a one-way analysis of variance (ANOVA). White arrows indicate Cx43 expression. The data are shown as the means \pm S.E.M. ($n=5$, $*p<0.05$, $**p<0.01$). Scale bar = 50 μm . E = epidermis, D = Dermis, DT = Distal tissue, AT = Adjacent tissue, PS = Pressure site.

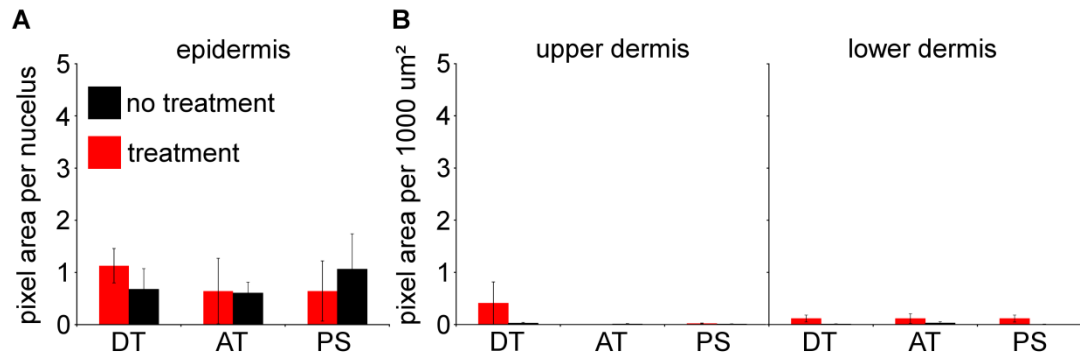


Figure 6.5 Connexin hemichannel expression in the skin ischemia reperfusion model twenty four hours after pressure relief

Tissue was either subjected to 1.5 hours of pressure followed by relief for 24 hours or left un-pressurised. Tissue was then either treated with Cx43 asODN or left untreated. (A) Total connexin hemichannel pixel area per nucleus within the epidermis was quantified. There was no significant change in connexin hemichannel expression at the pressure site or surrounding tissue. (B) Total connexin hemichannel pixel area per 1000 μm^2 within the upper and the lower dermis was quantified. There was no significant change in connexin hemichannel expression at the pressure site or surrounding tissue. Statistical comparisons were made using a one-way analysis of variance (ANOVA). The data are shown as the means \pm S.E.M. ($n=5$). PS = Pressure site, AT = Adjacent tissue, DT = Distal tissue.

Blood vessel leakiness significantly increased at the pressure site.

Thirty minutes before the mice were euthanized, 200 μ l of 1.5% FITC-BSA was injected into the tail vein of each mouse, to assess vascular permeability of the pressure site. Blood vessel leakiness was assessed in three key sites; the pressure site, adjacent to the pressure site and in distal tissue. Blood vessel leakiness significantly increased at the pressure site in comparison to the distal tissue 4 hours after reperfusion (figure 6.6). Leakiness also significantly increased at the pressure site and markedly increased in tissue adjacent to the pressure site 24 hours after reperfusion, in comparison to the distal tissue (figure 6.7). Application of Cx43 asODN at the wound site significantly reduced the extent of blood vessel leakiness at both time points.

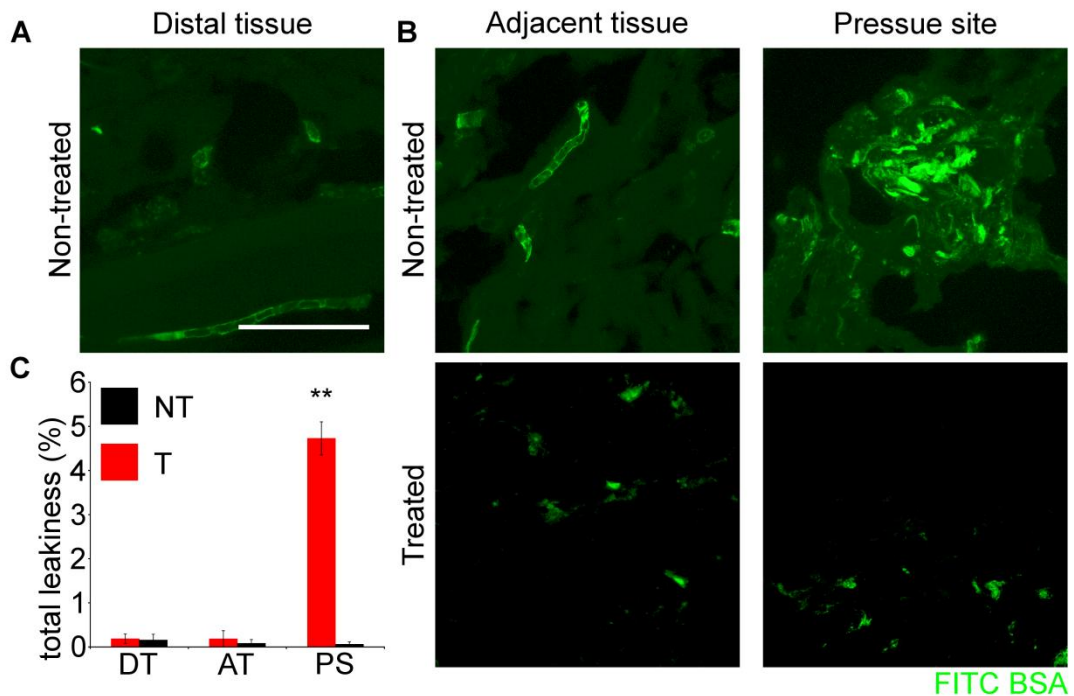


Figure 6.6 Blood vessel leakiness significantly increased at the pressure site four hours after pressure relief

Mice were intravenously injected with FITC fluorophore conjugated with Bovine Serum Albumin (FITC-BSA). (A) The panel shows a representative image of tissue that has not been subjected to pressure. FITC-BSA (green). (B) The panels show representative images of tissue that has been subjected to 1.5 hours of pressure followed by 4 hours of relief. Tissue was either treated with Cx43 asODN or left untreated. (C) Total leakiness of blood vessels was quantified. Blood vessel leakiness significantly increased at the pressure site in comparison to distal tissue. Application of Cx43 asODN at the wound site significantly reduced the extent of leakiness. Statistical comparisons were made using a one-way analysis of variance (ANOVA). The data are shown as the means \pm S.E.M. ($n=5$, $*p<0.05$, $**p<0.01$). Scale bar = 20 μ m. PS = Pressure site, AT = Adjacent tissue, DT = Distal tissue, NT = Non treated, T = Treated.

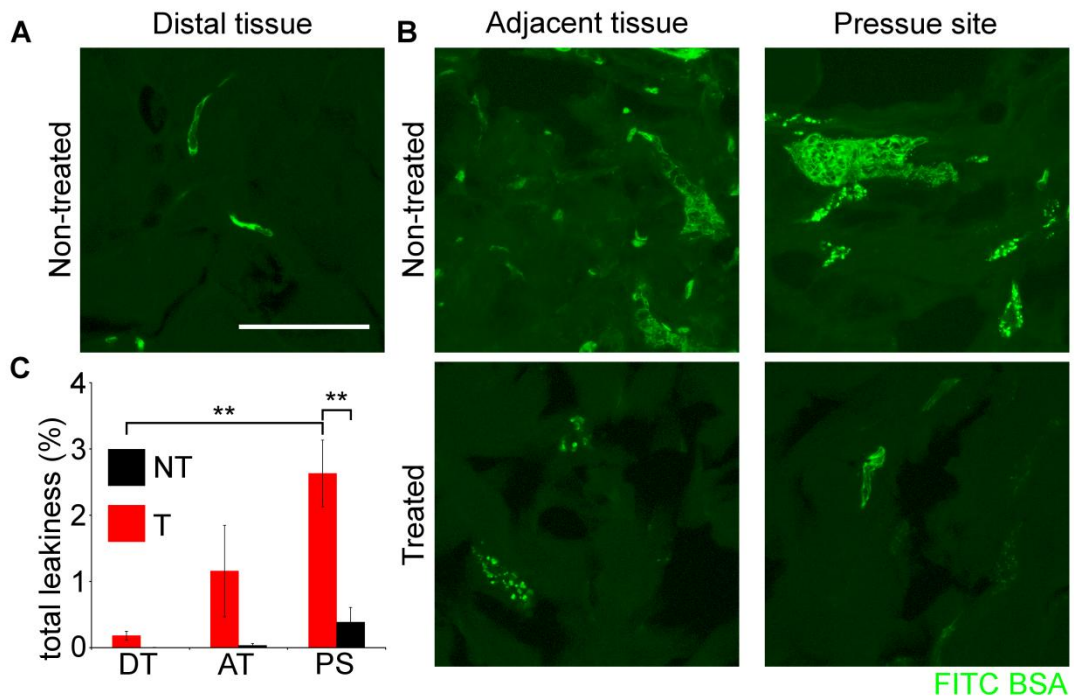


Figure 6.7 Blood vessel leakiness further increased at and beyond the pressure site twenty four hours after pressure relief

Mice were intravenously injected with FITC fluorophore conjugated with Bovine Serum Albumin (FITC-BSA). (A) The panel shows a representative image of tissue that has not been subjected to pressure. FITC-BSA (green). (B) The panels show representative images of tissue that have been subjected to 1.5 hours of pressure followed by relief for 24 hours. Tissue was either treated with Cx43 asODN or left untreated. (C) Total leakiness of the tissue was quantified. Blood vessel leakiness significantly increased at the pressure site and in surrounding tissue. Application of Cx43 asODN at the wound site significantly reduced the extent of leakiness. . Statistical comparisons were made using a one-way analysis of variance (ANOVA). Data was tested for normality (Shapiro-Wilk test) and equal variances (Levene test) before statistical comparisons were carried out. The data are shown as the means \pm S.E.M. (n=5, *p<0.05). Scale bar = 20 μ m. PS = Pressure site, AT = Adjacent tissue, DT = Distal tissue, NT = Non treated, T = Treated.

Leukocyte count significantly increased at the pressure site.

The inflammatory response was assessed four and twenty four hours after pressure relief. Tissue was observed in three key sites; the pressure site, adjacent to the pressure site and in distal tissue. Polymorphonuclear neutrophil leukocytes were identified through high powered imaging of the tissue and leukocyte count per 1000 μm^2 was quantified. Leukocyte numbers were significantly greater at the pressure site in comparison to distal tissue four and twenty four hours after pressure relief (figure 6.8 and 6.9) and markedly increased in tissue adjacent to the tissue site in comparison to distal tissue twenty four hours after pressure relief (figure 6.9). Application of Cx43 asODN at the wound site significantly reduced leukocyte numbers at both time points.

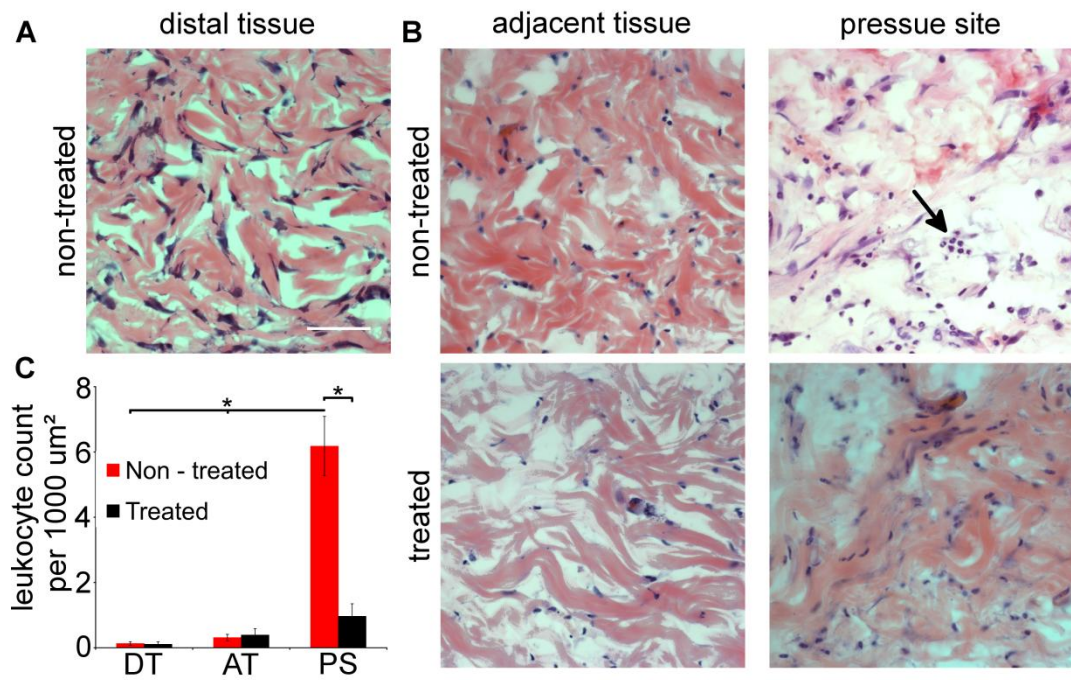


Figure 6.8 The number of leukocytes significantly increased at the pressure site, four hours after pressure relief

(A) The panel shows a representative histological image of tissue that has not been subjected to pressure. (B) The panels show representative histological images of tissue that has been subjected to 1.5 hours of pressure followed by relief for 4 hours. Tissue was either treated with Cx43 asODN or placebo delivery gel only. (C) Leukocyte count per 1000 μm² was quantified. Leukocyte neutrophils were identified by their multi-lobed nuclei (black arrow). Leukocyte numbers were significantly greater at the pressure site. Application of Cx43 asODN at the wound site significantly reduced the leukocyte number. Statistical comparisons were made using a one-way analysis of variance (ANOVA). The data are shown as the means ± S.E.M. (n=5, *p<0.05). Scale bar = 100 μm. PS = Pressure site, AT = Adjacent tissue, DT = Distal tissue.

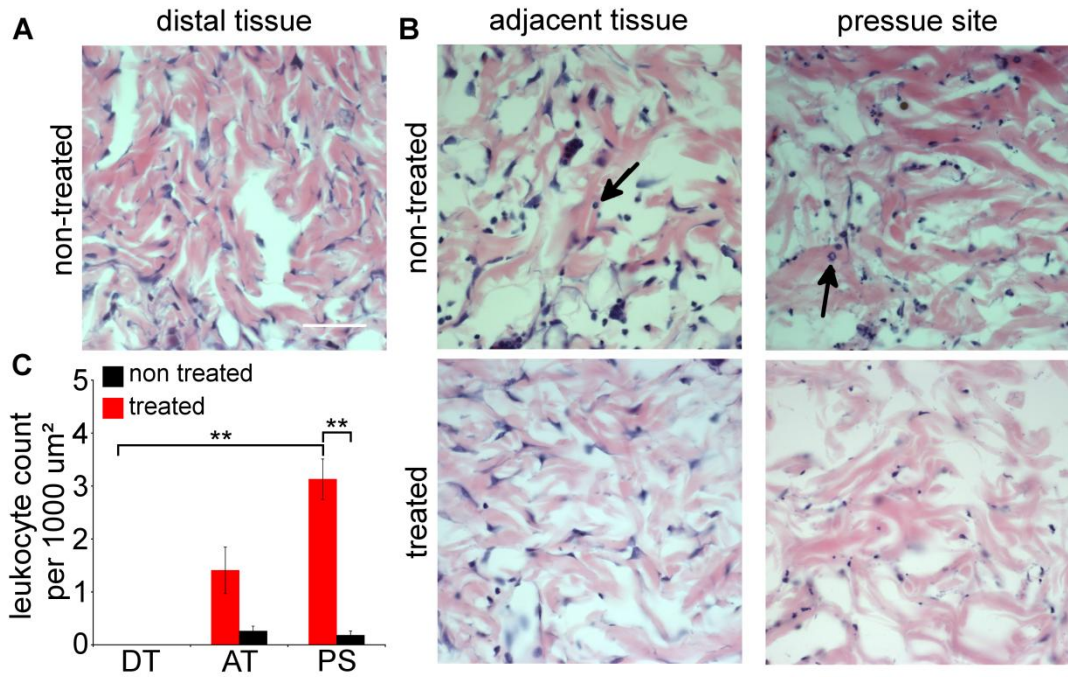


Figure 6.9 The number of leukocytes significantly increased at the pressure site, twenty-four hours after pressure relief

(A) The panel shows a representative histological image of tissue that has not been subjected to pressure. (B) The panels show representative histological images of tissue that have been subjected to 1.5 hours of pressure followed by relief for 24 hours. Tissue was either treated with Cx43 asODN or placebo delivery gel only. (C) Leukocyte count per 1000 μm^2 was quantified. Leukocyte neutrophils were identified by their multi-lobed nuclei (black arrows). Leukocyte numbers were significantly greater at the pressure site and in the surrounding tissue. Application of Cx43 asODN to the pressure site significantly reduced the leukocyte number. Statistical comparisons were made using a one-way analysis of variance (ANOVA). The data are shown as the means \pm S.E.M. ($n=5$, $**p<0.01$). Scale bar = 100 μm . PS = Pressure site, AT = Adjacent tissue, DT = Distal tissue.

6.3 Discussion

Replicating pressure ulcers

In this research chapter an *in vivo* ischemic reperfusion model was used to recreate an early stage pressure ulcer. Ischemia was executed for 1.5 hours whereas reperfusion was implemented for 4 or 24 hours. Initial observations confirmed damage to the skin 24 hours after reperfusion in comparison to non-pressured skin (figure 6.1). This was noted as tissue breakdown and an increase in inflammatory cells within the tissue. Similar observations were made by Peirce and colleagues who used a comparable pressure ulcer model on rat skin (Peirce et al., 2000). Not only was tissue injury reported in skin subjected to one cycle of ischemia reperfusion, but rats subjected to multiple or prolonged ischemia reperfusion cycles had progressively more tissue damage. Parallel studies have also reported that repeated cycles of ischemia reperfusion injury can cause a significant increase in skin damage in mouse (Reid et al., 2004) and rat (Jiang et al., 2011) skin.

Connexins in ischemia reperfusion

The data presented in this chapter reported that after just four hours of ischemia relief, Cx43 expression significantly increased in the sub-epidermal dermis at the pressure site in comparison to control distal tissue (figure 6.2 A and Cii). Within twenty fours of ischemia relief, Cx43 expression had significantly increased throughout the entire dermal layer at the pressure site in comparison to distal tissue (figure 6.3 A, B, Cii and D). An increase in Cx43 expression has also been noted in models of myocardial ischemia (Hatanaka et al., 2004) and focal ischemic stroke (Haupt et al., 2007). Nakase and colleagues also reported an increase in Cx43 expression in tissue samples from humans who had suffered from fatal strokes (Nakase et al., 2006) whereas Danesh-Mayer and colleagues additionally reported an increase in Cx43 in astrocytes and vascular endothelial cells in a rat model of

Chapter 6 The role of Cx43 in a model of pressure ulcers

retinal ischemia (Danesh-Meyer et al., 2012). They also noted that this increase correlated with an increase in retinal ganglion cell death.

For many years it has been theorised that physical interaction between cells is an important factor in the progression of tissue necrosis during ischemia reperfusion models (Ganote and Humphrey, 1985, García-Dorado et al., 1989). Rawanduzy noted that the extent of ischemic injury often does not occur immediately after arterial occlusion but that infarction expands over time in a step wise manner (Rawanduzy et al., 1997). This could explain the spread of Cx43 expression progressing across the dermal tissue within the pressure site, 24 hours after pressure relief. This increase in Cx43 expression also correlated with an increase in observed tissue damage (figure 6.1). An interesting observation made in the data presented in this research chapter was that after an initial increase in connexin hemichannel expression throughout the dermal layer four hours after pressure relief (figure 6.4A, B, Cii and D); there was no significant observed increase in connexin hemichannel expression twenty four later (figure 6.5B and C). This follows a similar pattern observed and reported in the previous research chapter where gap junction communication was far more detrimental in the spread of cell death than hemichannel based communication and suggests a more involved role for Cx43 gap junction based communication during the spread of tissue damage after pressure relief in this murine model of pressure ulcers.

Treatment with Cx43 asODN markedly reduced the extent of damage observed twenty four after ischemia relief. Comparable results have been reported in cardiac models of ischemic reperfusion (Mao et al., 2005, Mao et al., 2009) and in rodent stroke models (Rawanduzy et al., 1997) where reducing gap junction based communication using aliphatic alcohols significantly reduced the extent of infarct size. Treating hippocampal brain slices that underwent oxygen glucose deprivation,

Chapter 6 The role of Cx43 in a model of pressure ulcers

with carbenoxolone also significantly reduced gap coupling and neuronal cell death (de Pina-Benabou et al., 2005). In the model of rat retinal ischemia reperfusion injury, treatment with connexin mimetic peptide 'Peptide 5' also significantly reduced retinal ganglion cell death (Danesh-Meyer et al., 2012).

Throughout this thesis, the importance of Cx43 based communication during the wound healing process has been heavily discussed and it has been shown that by transiently reducing Cx43 expression in acute (Qiu et al., 2003, Mori et al., 2006) and chronic wounds (Wang et al., 2007) enhances the rate of wound closure in rodent models of wound healing. Coutinho and colleagues have also investigated the spread of cell death in burn injuries and its link with Cx43 expression (Coutinho et al., 2005). Burns create a lot of internal damage and this injury can spread to neighbouring cells. They reported a significant increase in Cx43 two to four days after the initial thermal injury and treatment with Cx43 asODN significantly reduced this expression and limited the spread of thermal damage. Treatment with Cx43 asODN significantly improved the wound appearance and the rate of wound closure. Reducing Cx43 also significantly reduced the number of leukocytes within the damaged tissue.

The inflammatory response during skin ischemia reperfusion

Data presented in this research chapter noted that ischemia reperfusion injury within the skin had a profound effect on the immune system. FITC-BSA was used to ascertain the extent of blood vessel leakiness at the pressure site and in surrounding tissue. It was reported that leakiness significantly increased at the ischemic reperfusion site four hours after ischemia relief (figure 6.6) and that leakiness continued to spread to adjacent tissue twenty four hours later (figure 6.7). Treatment with Cx43 asODN significantly reduced the extent of blood vessel leakiness at both time points (figures 6.6 and 6.7). Again, a comparable report was

Chapter 6 The role of Cx43 in a model of pressure ulcers

made in the retinal ischemia reperfusion model where treatment with Peptide 5 significantly reduced blood vessel leakiness in retinal tissue (Danesh-Meyer et al., 2012).

FITC-BSA blood vessel leakiness studies are often used to investigate vascular permeability events such as extravasation. This inflammatory response process involves the recruitment of circulating leukocytes to actively leak from blood vessels, through the vascular endothelium, into the wound site. Here it is reported that ischemic reperfusion injury in mouse skin significantly increased the number of leukocytes in the injured tissue four hours after pressure relief (figure 6.8) and that leukocyte count was further significantly increased in both pressure site tissue and adjacent tissue twenty four hours later (figure 6.9). Increased leukocyte infiltration has also been observed in other models of skin pressure ulcers using magnet compression (Reid et al., 2004, Jiang et al., 2011). Once again, treatment with Cx43 significantly reduced the extent of leukocyte infiltration (figures 6.8 and 6.9). Early application of Cx43 asODN to acute wounds also dampens down the inflammatory response, eventually leading to earlier wound closure (Qiu et al., 2003, Mori et al., 2006).

Connexin mimetic peptides as therapeutics in pressure ulcers

Connexin mimetic peptides have already been employed in reducing the extent of tissue damage in cardiac (Hawat et al., 2010, Hawat et al., 2012) and neuronal (Davidson et al., 2012b, Davidson et al., 2012a, Davidson et al., 2013) models of ischemia reperfusion. However, in both research groups, low concentrations of connexin mimetic peptides were used to successfully reduce infarct size by blocking open hemichannels. Although infarct size did not reduce beyond 60%, clearly leaving some room for improvement. Recent work by Wang and colleagues has shown successful blocking of open hemichannels in both *in vitro* and *in vivo* models

Chapter 6 The role of Cx43 in a model of pressure ulcers

of ischemia reperfusion through treatment with a nonapeptide Gap19 (Wang et al., 2013a). By mimetically binding to the cytoplasmic loop of Cx43, Gap19 prevents intramolecular CT-CL interactions and thereby inhibits hemichannels. In their cardiac *in vivo* model of ischemia reperfusion, infarct size reduced to 51.2%, compared to 63.8% in vehicle-treated control animals; a reduction of only approximately one-fifth. Surely by increasing the concentration of connexin mimetic peptide in these models would further reduce the extent of cell and tissue damage during ischemia reperfusion. However, this is not the case in cardiac and neuronal tissue as disrupting gap junction communication can disrupt key electrical cell-cell interactions. Indeed, in studies carried out by Davidson and colleagues, higher concentrations of Peptide 5 caused a greater secondary increase in brain cell swelling and mortality in foetal sheep subjected to carotid artery ischemia reperfusion (Davidson et al., 2012a). Studies using Cx43 knockout mice in models of neuronal ischemia reperfusion have also shown greater brain injury during this tissue stress (Nakase et al., 2004). However, no such electrical coupling is required for tissue viability in the skin; therefore high concentrations of Gap27 during ischemic reperfusion damage could successfully reduce the extent of injury.

Conclusions

- Ischemia reperfusion injury in the backs of mice correlated with an increase in Cx43 expression and connexin hemichannel expression.
- Blood vessel leakiness and leukocyte count significantly increased at the pressure site.
- Treatment with Cx43 asODN significantly reduced Cx43 and connexin hemichannel expression with correlated with a decrease in the extent to tissue damage and a reduced inflammatory response.

As *in vivo* peptide investigation is still in the preliminary stages, there was some uncertainty as to the concentration of Gap27 treatment to use in the model of pressure ulcers. Therefore, the decision was made to employ Cx43 asODN in the initial study to completely reduce Cx43 based communication in the pressure ulcer model. The results reported here suggest that Cx43 based gap junction communication is responsible for the spread of tissue damage during ischemia reperfusion in the skin, therefore a high concentrations of Gap27 if most likely needed to have the same therapeutic effects.

7. General discussion

The skin is the largest organ in the body and can regenerate effectively, even after considerable damage has occurred. Having roles as a defensive barrier between the body and the external world its long term integrity is essential and therefore a thorough understanding of the processes involved in its repair is extremely important. Wound healing occurs through an overlying sequence of events that can roughly be divided into three key overlapping stages; the immediate inflammatory response, new tissue formation and remodelling (Martin 1997, Gurtner, Wener et al. 2008). The highly complex sequence of events in skin wound healing relies heavily on the communication of signals released during these stages and cell-to-cell communication is crucial in order for the tissues to co-ordinate their processes. Mounting evidence now supports the theory that gap junctions play a pivotal role in the communication of these signals.

Salomon and colleagues in 1988 described how cells in normal and differentiated skin communicate with each other through gap junctions (Salomon, Sauret et al. 1988). Gap junctions are specialised connections that provide a regulated pathway linking the cytoplasm of adjacent cells and allow molecular signals to pass freely between the two. Each gap junction is made of two connexons, or hemichannels, from opposing cells, which in turn are composed of six protein subunits called connexins. To date, 20 connexin genes have been identified in rodents and 21 in humans, with at least ten detectable within the skin.

Three key connexins undergo dynamic changes and play integral roles during the wound healing process. Within the first few hours of wound closure, during the immediate inflammatory response, Cx43 protein expression is significantly up-

regulated in blood vessels, yet significantly down-regulated in the leading edge tissue. This protein switch-off is accompanied by a significant increase in the expression of Cxs 26 and 30 in the leading edge tissue, corresponding to the onset of re-epithelialisation of epidermal keratinocytes and the migration of dermal fibroblasts. Upon the resolution of the wound, the expression profiles of these connexins proteins return to their pre-wound levels (Goliger and Paul 1995, Saitoh, Oyamada et al. 1997, Coutinho, Qiu et al. 2003).

In recent years it has been realised that Cx43 protein dynamics during acute wound healing are tightly regulated to ensure successful closure of the wound. Of late, a promising therapeutic that could enhance the rate of acute and chronic wound healing has emerged as a Cx43 specific antisense oligodeoxynucleotide (Cx43 asODN) that targets Cx43 mRNA and induces a Cx43 protein knockdown. This ODN has proven successful in promoting accelerated wound healing and appears to 'jump start' the subsequent phases of wound closure (Qiu, Coutinho et al. 2003, Mori, Power et al. 2006, Wang, Lincoln et al. 2007). When immediately applied to a rodent skin wound, Cx43 asODN rapidly reduces Cx43 protein expression in wound edge keratinocytes, fibroblasts and blood vessels within two hours of wounding; nearly a complete day faster than in un-treated wounds (Qiu, Coutinho et al. 2003, Mori, Power et al. 2006). Early application of Cx43 asODN to acute wounds dampens tissue swelling and the inflammatory response, promotes early keratinocyte and fibroblast cell migration and closes the wound gap earlier than wounds left un-treated. Wounds treated with Cx43 asODN appear less red and swollen and rapidly reduce in size, resulting in smaller and thinner scar tissue.

Although it is becoming increasingly certain that Cx43 plays an integral role in wound healing, it is still unclear whether these responses are attributed to hemichannel or gap junction based communication. Long term hemichannel down-

regulation can be achieved through the topical application of Cx43 asODN; however it was realised that the differences between gap junction communication and hemichannel signalling can be teased out by the application of small connexin mimetic peptides. Acting on the extracellular loops of connexins, these peptides can rapidly block hemichannel communication and prevent gap junction formation. However, with longer or more concentrated incubation periods, connexin mimetic peptides can inhibit gap junction communication. Additionally, in recent years it has been noted that connexin mimetic peptides show a huge potential in tackling connexin-based maladies and show promise in translational and therapeutic possibilities. These prospects include enhancing the rate of wound repair and reducing the spread of damage caused in tissue ischemia reperfusion.

The general aim of this thesis was to further explore the role and potential therapeutic implications of the connexin mimetic peptide Gap27 in both *in vitro* and *in vivo* models of wound healing while contributing to the characterisation of this mimetic peptide. In the first instance, owing to the encouraging work conducted by the Martin group that has shown the therapeutic possibilities of Gap27 using *in vitro* and *ex vivo* wound healing models (Wright, van Steensal et al. 2009, Pollok, Pfeiffer et al. 2011), it was hypothesised that application of Gap27 to *in vitro* and *in vivo* models of wound healing would increase the rate of migration in fibroblast and keratinocyte cells and enhance the earlier stages of wound repair. Using functional assays of Gap27, data presented in Chapter 3 demonstrated how high concentrations of Gap27 reduced communication in fibroblast cells and increased the rate of migration in both fibroblast and keratinocyte cells. Further investigations in Chapter 4 explored for the first time, using a murine model of wound healing, the ability of Gap27 to enhance the rate of wound repair. During the first four hours of wounding, a single dose of Gap27 significantly reduced blood vessel leakiness at the wound edge and delayed leukocyte infiltration to the wounded tissue observed

24 hours later. It was also reported that low concentrations of Gap27 significantly increased the rate of re-epithelialisation 24 hours after wounding. It was theorised that during wounding, ATP is released through open hemichannels and that treatment with a low concentration of Gap27 could reduce this release through blocking these open hemichannels. This ultimately enhanced the rate of re-epithelialisation. It was clear that 24 hours after wounding Gap27 no longer had any effect on the rate of wound healing. This was most likely due to peptide degradation.

A need exists to prolong a release of rapidly metabolised connexin mimetic peptides and further investigations are required to find a suitable delivery agent. One such agent could be to use osmotic pumps that ensure a continuous delivery of the peptide over a defined study period. Subcutaneous implanted osmotic pumps delivering Gap27 were used to reduce Cx43 expression in bile-duct ligated livers within mice. Gap27 successfully reduced Cx43 expression in the liver, when compared to a scrambled peptide control, after two weeks of constant peptide delivery (Balasubramaniyan, Dhar et al. 2013). No cardiotoxicity or any other adverse effects were noticed, making this delivery system a potential ideal route for connexin mimetic peptide treatment. Another delivery agent that is currently being considered to supply a controlled delivery of biomaterials and drugs, including connexin mimetic peptides, is sodium alginate microcapsules (Moore et al., 2013).

As discussed previously, recent work conducted by the Becker group has shown by inhibiting Cx43 expression during wound repair, the rate of wound healing significantly increases (Qiu, Couthinho et al. 2003, Mori, Power et al. 2006, Wang, Lincoln et al. 2007). Work presented in Chapter 4 has shown that different concentrations of Gap27 can reduce either hemichannel or gap junction based communication and this connexin mimetic peptide has proven beneficial in the earlier stages of wound healing. Not only were these initial hypotheses confirmed,

research presented in Chapters 3 and 4 also shows for the first time that Gap27 significantly reduced Cx43 expression in fibroblast cells, keratinocyte cells and murine tissue. This was confirmed using immunostaining and Western blot analysis. In Chapter 3 it was also shown that Gap27 significantly reduced connexin hemichannel expression in fibroblast cells although some care must be excised with these conclusions. It is possible that the two difference antibodies are staining for connexins regardless of their conformation as a hemichannel or gap junction unit. A double immunostain of Cx43 and connexin hemichannel should be carried out to confirm if Gap27 reduced both connexin hemichannels and Cx43 gap junctions. Gap27 also significantly reduced Cx26 and 30 expressions in keratinocyte cells after continuous incubation in Gap27. It had previously been thought that connexin mimetic peptides primarily interact with undocked hemichannels and at later incubation periods, prevent the docking of connexons, thereby reducing hemichannels and gap junction based communication respectively (Evans and Boitano 2001). Work presented in Chapter 5 initially confirmed that Gap27 could block hemichannel communication. To assess hemichannel activity during cell stress, PI uptake was observed and measured in low confluence fibroblast cells.

The stress caused hemichannels to open and increase PI uptake whereas incubation in Gap27 significantly reduced PI uptake by plugging open hemichannels. Based on the research demonstrated in Chapters 3 and 4 an additional theory was proposed to explain how Cx43 and hemichannel expression were reduced in fibroblasts, keratinocytes and murine tissue after Gap27 incubation. The theory suggests that after Gap27 has bound to the extracellular surface of a connexon (and blocked hemichannel activity); an increased rate of internalisation is triggered (figure 7.1). However, as discussed in detail previously, this theory needs further testing to validate its assumptions. One way in which this could be achieved is to use fluorescently tagged connexins together with fluorescently tagged mimetic peptides

to view in real time the effects of connexin mimetic peptides on connexin turnover. The design of the experiments needs to take into consideration the short lifespan of a connexin and the degradation rate of connexin mimetic peptides.

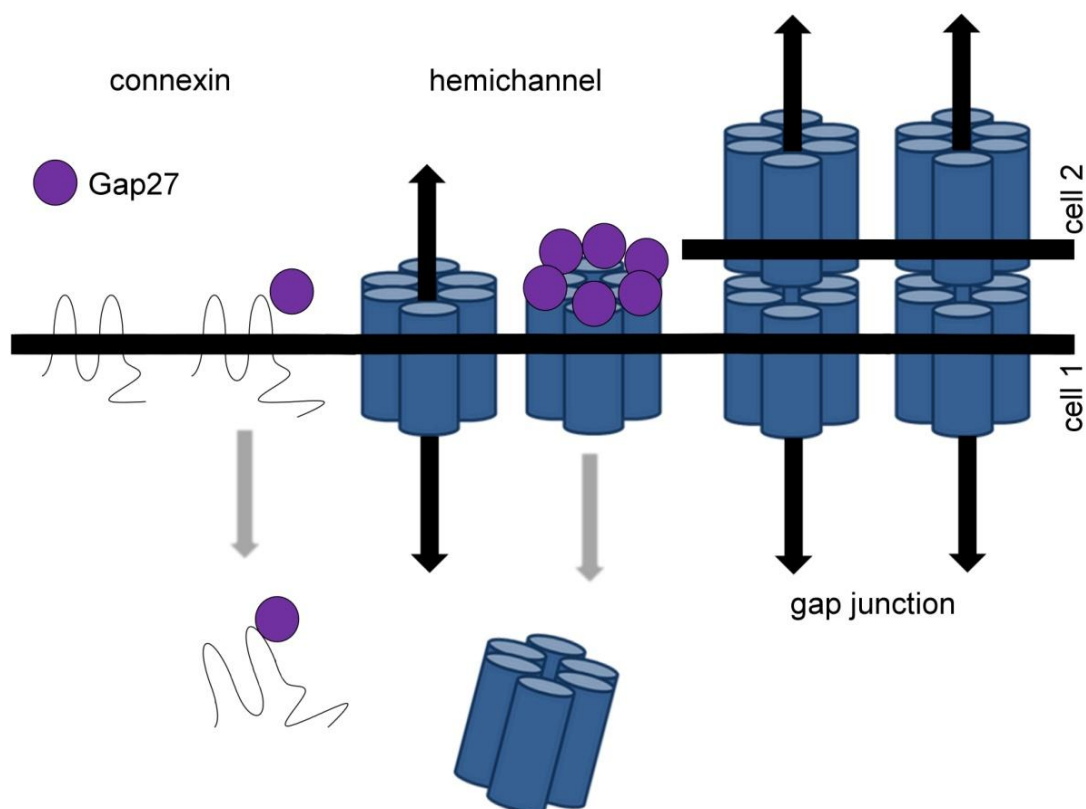


Figure 7.1 Increased rate of internalisation theory

This simplified diagram illustrates the theory that Gap27 increased the rate of internalisation of connexins and connexons and thereby reduced gap junction based communication. Gap27 primarily binds with the extracellular surface of a connexon and blocks hemichannel activity. This early interaction triggers an increased rate of internalisation and thereby reduced the amount of connexin or connexon to form functional gap junctions.

Work presented in Chapters 3 and 4 has nonetheless supported the realisation of connexin mimetic peptide's capability in enhancing the rate of wound repair. The next two chapters explored how fibroblast cells and tissue communicated during ischemic reperfusion stress. Due to the growing evidence that marks Cx43 as a key

contributor to the spread of cell death in cardiac and cerebral ischemic stress, it was hypothesised that Cx43 would also be responsible in the propagation of cell injury and death in ischemic reperfusion injury in the skin.

Tissue ischemia injury is a major medical problem that plagues a number of organs and is caused by a restriction of blood supply to the tissue, causing severe shortage of oxygen, glucose and other nutrients needed for survival. Tissue ischemia is common in cardiac, cerebral and skin tissue; however most of the damage occurs upon reperfusion. This is when the blood supply returns in a restoration of circulation and causes inflammation and oxidative damage to the tissue that has been denied oxygen flow for a period of time. Often this damage spread beyond the initial ischemia area.

Gap junction mediated tissue ischemia reperfusion injury has been identified in a number of organs including cardiac tissue during heart attacks (García-Dorado, Rodríguez-Sinovas et al. 2004) and cerebral tissue during strokes (Frantseva, Kokarovtseva et al. 2002, Frantseva, Kokarovtseva et al. 2002). Repeated ischemia reperfusion injury in the skin during pressure ulcer formation, can also cause severe tissue damage similar to the damage formed in cerebral and cardiac ischemia reperfusion. Despite the growing evidence that marks connexin based communication as a key contributor to the spread of cell death in neighbouring cells after an ischemic reperfusion insult, the mechanisms behind this spread of damage are still unclear. The “bystander effect” model suggests that death signals can spread laterally through gap junctions from dying cells into their healthy neighbouring cells (Mao, Chen et al. 2009, Danesh-Meyer, Kerr et al. 2012, Zhang, Li et al. 2013). However, some reports attribute cell death in ischemia reperfusion models to the opening of undocked gap junctions, release of ATP and activation of purinergic receptors that result in cell death (Thompson, Zhou et al. 2006, Clarke,

Williams et al. 2009, Orellana, Hernández et al. 2010, Poornima, Madhupriya et al. 2012). Understanding how cell death occurs and spreads will help in the development of a therapeutic to reduce spread of damage and the impact of ischemia reperfusion injury.

Using an *in vitro* model of ischemia reperfusion injury (oxygen glucose deprivation reoxygenation; OGDR) research in Chapter 5 explored how dying fibroblast cells communicated during an ischemic reperfusion stress. In a novel observation it was observed that OGDR stress significantly decreased cell viability in correlation with an increase in Cx43, phosphorylated Cx43 isoforms and connexin hemichannel expression. Reducing Cx43 expression in Cx43 shRNA transduced fibroblast cells prevented the reduction in cell viability; thereby contributing to the theory that Cx43 based communication is heavily involved in spreading cell death signals during this model of *in vitro* ischemic reperfusion stress. Further investigations into the communication mechanisms behind OGDR influenced cell death revealed that although ATP may be released through open hemichannels during this insult, it is not enough to promote cell death. However, communication between neighbouring cells propagated a cell death signal that is blocked by reducing Cx43 or inhibiting gap junction based communication using Gap27.

Building upon this work, Chapter 6 further investigated the role of Cx43 and hemichannels in a murine model of pressure ulcers. This type of chronic wound can be caused by either prolonged or repeated incidences of ischemia reperfusion in the skin. They are often found on bony prominences on elderly or bed ridden patients. Recent research has identified gap junction mediated ischemia reperfusion injury in the cardiac (García-Dorado, Rodríguez-Sinovas et al. 2004) and cerebral tissue (Frantseva, Kokarovtseva et al. 2002, Frantseva, Kokarovtseva et al. 2002) however, until now, there has been no investigations into the role of gap junction based

communication in the pressure ulcer. In this chapter it was reported that ischemia reperfusion injury on the back of mice associated with an increase in Cx43 expression and an elevated inflammatory response. Treatment with Cx43 asODN significantly reduced Cx43 expression (and thereby Cx43 based communication), decreased the extent of tissue damage and dampened down the inflammatory response.

Conclusions

The potential therapeutic implications of the wound healing properties of connexin mimetic peptides are exciting, novel and promising. Work presented in this thesis has further explored the roles and therapeutic properties of the connexin mimetic peptide Gap27 in both *in vitro* and *in vivo* models of wound healing. In a novel discovery, it was reported here that Gap27 reduced Cxs 43, 26 and 30 and connexin hemichannel expressions. Gap27 also increased the rate of wound healing in the early stages of wound closure. With further investigations to find a suitable delivery agent that could prolong the effects of Gap27, there is huge potential for this mimetic peptide to become a major therapeutic competitor in connexin based maladies and wound repair.

Research presented in the final results chapters of this thesis illustrate how Cx43 is associated with spreading cell death and damage as shown using an *in vitro* model of ischemia reperfusion. In a novel discovery, it was also reported how Cx43 propagates cell injury and death shown using an *in vivo* model of ischemia reperfusion on mouse skin. This compelling research builds upon the expanding mountain of evidence that gap junctions, hemichannels and connexins play an integral role in tissue injury and repair.

Bibliography

- AASEN, T. & IZPISÚA BELMONTE, J. C. 2010. Isolation and cultivation of human keratinocytes from skin or plucked hair for the generation of induced pluripotent stem cells. *Nat Protoc*, 5, 371-82.
- ABDULLAH, K. M., LUTHRA, G., BILSKI, J. J., ABDULLAH, S. A., REYNOLDS, L. P., REDMER, D. A. & GRAZUL-BILSKA, A. T. 1999. Cell-to-cell communication and expression of gap junctional proteins in human diabetic and nondiabetic skin fibroblasts: effects of basic fibroblast growth factor. *Endocrine*, 10, 35-41.
- ABE, R., DONNELLY, S. C., PENG, T., BUCALA, R. & METZ, C. N. 2001. Peripheral blood fibrocytes: differentiation pathway and migration to wound sites. *J Immunol*, 166, 7556-62.
- ADAMS, R. H. & ALITALO, K. 2007. Molecular regulation of angiogenesis and lymphangiogenesis. *Nat Rev Mol Cell Biol*, 8, 464-78.
- ANDERSEN, L. 1980. Cell junctions in squamous epithelium during wound healing in palatal mucosa of guinea pigs. *Scand J Dent Res*, 88, 328-39.
- ANDERSON, G. R., VOLPE, C. M., RUSSO, C. A., STOLER, D. L. & MILORO, S. M. 1995. The anoxic fibroblast response is an early-stage wound healing program. *J Surg Res*, 59, 666-74.
- AZZAM, E. I., DE TOLEDO, S. M. & LITTLE, J. B. 2001. Direct evidence for the participation of gap junction-mediated intercellular communication in the transmission of damage signals from alpha -particle irradiated to nonirradiated cells. *Proc Natl Acad Sci U S A*, 98, 473-8.
- BALASUBRAMANIAN, V., DHAR, D. K., WARNER, A. E., VIVIEN LI, W. Y., AMIRI, A. F., BRIGHT, B., MOOKERJEE, R. P., DAVIES, N. A., BECKER, D. L. & JALAN, R. 2013. Importance of Connexin-43 based gap junction in cirrhosis and acute-on-chronic liver failure. *J Hepatol*, 58, 1194-200.
- BAO, L., SAMUELS, S., LOCOVEI, S., MACAGNO, E. R., MULLER, K. J. & DAHL, G. 2007. Innexins form two types of channels. *FEBS Lett*, 581, 5703-8.
- BARANOVA, A., IVANOV, D., PETRASH, N., PESTOVA, A., SKOBLOV, M., KELMANSON, I., SHAGIN, D., NAZARENKO, S., GERAYMOVYCH, E., LITVIN, O., TIUNOVA, A., BORN, T. L., USMAN, N., STAROVEROV, D., LUKYANOV, S. & PANCHIN, Y. 2004. The mammalian pannexin family is homologous to the invertebrate innexin gap junction proteins. *Genomics*, 83, 706-16.
- BAROJA-MAZO, A., BARBERÀ-CREMADES, M. & PELEGRÍN, P. 2013. The participation of plasma membrane hemichannels to purinergic signaling. *Biochim Biophys Acta*, 1828, 79-93.
- BARR, T. P., ALBRECHT, P. J., HOU, Q., MONGIN, A. A., STRICHARTZ, G. R. & RICE, F. L. 2013. Air-stimulated ATP release from keratinocytes occurs through connexin hemichannels. *PLoS One*, 8, e56744.
- BEARDSLEE, M. A., LERNER, D. L., TADROS, P. N., LAING, J. G., BEYER, E. C., YAMADA, K. A., KLÉBER, A. G., SCHUESSLER, R. B. & SAFFITZ, J. E. 2000. Dephosphorylation and intracellular redistribution of ventricular connexin43 during electrical uncoupling induced by ischemia. *Circ Res*, 87, 656-62.
- BECKER, D. L., EVANS, W. H., GREEN, C. R. & WARNER, A. 1995. Functional analysis of amino acid sequences in connexin43 involved in intercellular communication through gap junctions. *J Cell Sci*, 108 (Pt 4), 1455-67.
- BECKER, D. L., MCGONNELL, I., MAKARENKOVA, H. P., PATEL, K., TICKLE, C., LORIMER, J. & GREEN, C. R. 1999. Roles for alpha 1 connexin in

- morphogenesis of chick embryos revealed using a novel antisense approach. *Dev Genet*, 24, 33-42.
- BECKER, D. L., THRASIVOULOU, C. & PHILLIPS, A. R. 2012. Connexins in wound healing; perspectives in diabetic patients. *Biochim Biophys Acta*, 1818, 2068-75.
- BEHRINGER, E. J., SOCHA, M. J., POLO-PARADA, L. & SEGAL, S. S. 2012. Electrical conduction along endothelial cell tubes from mouse feed arteries: confounding actions of glycyrrhetic acid derivatives. *Br J Pharmacol*, 166, 774-87.
- BEJARANO, E., GIRAO, H., YUSTE, A., PATEL, B., MARQUES, C., SPRAY, D. C., PEREIRA, P. & CUERVO, A. M. 2012. Autophagy modulates dynamics of connexins at the plasma membrane in a ubiquitin-dependent manner. *Mol Biol Cell*, 23, 2156-69.
- BENNETT, G., DEALEY, C. & POSNETT, J. 2004. The cost of pressure ulcers in the UK. *Age Ageing*, 33, 230-5.
- BENNETT, M. V., ZHENG, X. & SOGIN, M. L. 1994. The connexins and their family tree. *Soc Gen Physiol Ser*, 49, 223-33.
- BENTZEN, S. M. 2006. Preventing or reducing late side effects of radiation therapy: radiobiology meets molecular pathology. *Nat Rev Cancer*, 6, 702-13.
- BERGOFFEN, J., SCHERER, S. S., WANG, S., SCOTT, M. O., BONE, L. J., PAUL, D. L., CHEN, K., LENSCH, M. W., CHANCE, P. F. & FISCHBECK, K. H. 1993. Connexin mutations in X-linked Charcot-Marie-Tooth disease. *Science*, 262, 2039-42.
- BERMAN, R. S., MARTIN, P. E., EVANS, W. H. & GRIFFITH, T. M. 2002. Relative contributions of NO and gap junctional communication to endothelium-dependent relaxations of rabbit resistance arteries vary with vessel size. *Microvasc Res*, 63, 115-28.
- BERSE, B., BROWN, L. F., VAN DE WATER, L., DVORAK, H. F. & SENGER, D. R. 1992. Vascular permeability factor (vascular endothelial growth factor) gene is expressed differentially in normal tissues, macrophages, and tumors. *Mol Biol Cell*, 3, 211-20.
- BERTHOUD, V. M., BEYER, E. C. & SEUL, K. H. 2000. Peptide inhibitors of intercellular communication. *Am J Physiol Lung Cell Mol Physiol*, 279, L619-22.
- BEVANS, C. G., KORDEL, M., RHEE, S. K. & HARRIS, A. L. 1998. Isoform composition of connexin channels determines selectivity among second messengers and uncharged molecules. *J Biol Chem*, 273, 2808-16.
- BEVILACQUA, L. M., SIMON, A. M., MAGUIRE, C. T., GEHRMANN, J., WAKIMOTO, H., PAUL, D. L. & BERUL, C. I. 2000. A targeted disruption in connexin40 leads to distinct atrioventricular conduction defects. *J Interv Card Electrophysiol*, 4, 459-67.
- BOASSA, D., AMBROSI, C., QIU, F., DAHL, G., GAJETTA, G. & SOSINSKY, G. 2007. Pannexin1 channels contain a glycosylation site that targets the hexamer to the plasma membrane. *J Biol Chem*, 282, 31733-43.
- BOENGLER, K., DODONI, G., RODRIGUEZ-SINOVAS, A., CABESTRERO, A., RUIZ-MEANA, M., GRES, P., KONIETZKA, I., LOPEZ-IGLESIAS, C., GARCIA-DORADO, D., DI LISA, F., HEUSCH, G. & SCHULZ, R. 2005. Connexin 43 in cardiomyocyte mitochondria and its increase by ischemic preconditioning. *Cardiovasc Res*, 67, 234-44.
- BOITANO, S., DIRKSEN, E. R. & EVANS, W. H. 1998. Sequence-specific antibodies to connexins block intercellular calcium signaling through gap junctions. *Cell Calcium*, 23, 1-9.
- BOITANO, S., DIRKSEN, E. R. & SANDERSON, M. J. 1992. Intercellular propagation of calcium waves mediated by inositol trisphosphate. *Science*, 258, 292-5.

- BOITANO, S. & EVANS, W. H. 2000. Connexin mimetic peptides reversibly inhibit Ca(2+) signaling through gap junctions in airway cells. *Am J Physiol Lung Cell Mol Physiol*, 279, L623-30.
- BRAET, K., ASPESLAGH, S., VANDAMME, W., WILLECKE, K., MARTIN, P. E., EVANS, W. H. & LEYBAERT, L. 2003a. Pharmacological sensitivity of ATP release triggered by photoliberation of inositol-1,4,5-trisphosphate and zero extracellular calcium in brain endothelial cells. *J Cell Physiol*, 197, 205-13.
- BRAET, K., VANDAMME, W., MARTIN, P. E., EVANS, W. H. & LEYBAERT, L. 2003b. Photoliberating inositol-1,4,5-trisphosphate triggers ATP release that is blocked by the connexin mimetic peptide gap 26. *Cell Calcium*, 33, 37-48.
- BRANDNER, J. M., HOUDEK, P., HÜSING, B., KAISER, C. & MOLL, I. 2004. Connexins 26, 30, and 43: differences among spontaneous, chronic, and accelerated human wound healing. *J Invest Dermatol*, 122, 1310-20.
- BRANES, M. C., CONTRERAS, J. E. & SÁEZ, J. C. 2002. Activation of human polymorphonuclear cells induces formation of functional gap junctions and expression of connexins. *Med Sci Monit*, 8, BR313-23.
- BRIGHTMAN, M. W. & REESE, T. S. 1969. Junctions between intimately apposed cell membranes in the vertebrate brain. *J Cell Biol*, 40, 648-77.
- BROWN, J. & KIERLAND, R. R. 1966. Erythrokeratoderma variabilis. Report of three cases and review of the literature. *Arch Dermatol*, 93, 194-201.
- BRUNO, G. & LANDI, A. 2011. Epidemiology and costs of diabetes. *Transplant Proc*, 43, 327-9.
- BRUZZONE, R., HORMUZDI, S. G., BARBE, M. T., HERB, A. & MONYER, H. 2003. Pannexins, a family of gap junction proteins expressed in brain. *Proc Natl Acad Sci U S A*, 100, 13644-9.
- BRUZZONE, S., GUIDA, L., ZOCCHI, E., FRANCO, L. & DE FLORA A 2001. Connexin 43 hemi channels mediate Ca²⁺-regulated transmembrane NAD⁺ fluxes in intact cells. *FASEB J*, 15, 10-12.
- BURNSTOCK, G. & VERKHRATSKY, A. 2009. Evolutionary origins of the purinergic signalling system. *Acta Physiol (Oxf)*, 195, 415-47.
- BURROWS, F. J., GORE, M., SMILEY, W. R., KANEMITSU, M. Y., JOLLY, D. J., READ, S. B., NICHOLAS, T. & KRUSE, C. A. 2002. Purified herpes simplex virus thymidine kinase retroviral particles: III. Characterization of bystander killing mechanisms in transfected tumor cells. *Cancer Gene Ther*, 9, 87-95.
- BUTTERWECK, A., ELFGANG, C., WILLECKE, K. & TRAUB, O. 1994. Differential expression of the gap junction proteins connexin45, -43, -40, -31, and -26 in mouse skin. *Eur J Cell Biol*, 65, 152-63.
- CARACENI, P., RYU, H. S., VAN THIEL, D. H. & BORLE, A. B. 1995. Source of oxygen free radicals produced by rat hepatocytes during postanoxic reoxygenation. *Biochim Biophys Acta*, 1268, 249-54.
- CAVANI, A., ZAMBRUNO, G., MARCONI, A., MANCA, V., MARCHETTI, M. & GIANNETTI, A. 1993. Distinctive integrin expression in the newly forming epidermis during wound healing in humans. *J Invest Dermatol*, 101, 600-4.
- CHAYTOR, A. T., MARTIN, P. E., EVANS, W. H., RANDALL, M. D. & GRIFFITH, T. M. 1999. The endothelial component of cannabinoid-induced relaxation in rabbit mesenteric artery depends on gap junctional communication. *J Physiol*, 520 Pt 2, 539-50.
- CHEN, K., LI, D., ZHANG, X., HERMONAT, P. L. & MEHTA, J. L. 2004. Anoxia-reoxygenation stimulates collagen type-I and MMP-1 expression in cardiac fibroblasts: modulation by the PPAR-gamma ligand pioglitazone. *J Cardiovasc Pharmacol*, 44, 682-7.
- CHEN, Y. C., TSAI, S. H., LIN-SHIAU, S. Y. & LIN, J. K. 1999. Elevation of apoptotic potential by anoxia hyperoxia shift in NIH3T3 cells. *Mol Cell Biochem*, 197, 147-59.

- CHOUNG, Y. H., CHOI, S. J., JOO, J. S., LEE, J. B., LEE, H. K. & LEE, S. J. 2011. Green tea prevents down-regulation of gap junction intercellular communication in human keratinocytes treated with PMA. *Eur Arch Otorhinolaryngol*, 268, 885-92.
- CLARKE, T. C., WILLIAMS, O. J., MARTIN, P. E. & EVANS, W. H. 2009. ATP release by cardiac myocytes in a simulated ischaemia model: inhibition by a connexin mimetic and enhancement by an antiarrhythmic peptide. *Eur J Pharmacol*, 605, 9-14.
- COHEN, S., EFRAIM, A. N., LEVI-SCHAFFER, F. & ELIASHAR, R. 2011. The effect of hypoxia and cyclooxygenase inhibitors on nasal polyp derived fibroblasts. *Am J Otolaryngol*, 32, 564-73.
- COMMON, J. E., O'TOOLE, E. A., LEIGH, I. M., THOMAS, A., GRIFFITHS, W. A., VENNING, V., GRABCZYNSKA, S., PERIS, Z., KANSKY, A. & KELSELL, D. P. 2005. Clinical and genetic heterogeneity of erythrokeratoderma variabilis. *J Invest Dermatol*, 125, 920-7.
- CONTRERAS, J. E., SÁNCHEZ, H. A., EUGENIN, E. A., SPEIDEL, D., THEIS, M., WILLECKE, K., BUKAUSKAS, F. F., BENNETT, M. V. & SÁEZ, J. C. 2002. Metabolic inhibition induces opening of unapposed connexin 43 gap junction hemichannels and reduces gap junctional communication in cortical astrocytes in culture. *Proc Natl Acad Sci U S A*, 99, 495-500.
- COTRINA, M. L., KANG, J., LIN, J. H., BUENO, E., HANSEN, T. W., HE, L., LIU, Y. & NEDERGAARD, M. 1998a. Astrocytic gap junctions remain open during ischemic conditions. *J Neurosci*, 18, 2520-37.
- COTRINA, M. L., LIN, J. H., ALVES-RODRIGUES, A., LIU, S., LI, J., AZMI-GHADIMI, H., KANG, J., NAUS, C. C. & NEDERGAARD, M. 1998b. Connexins regulate calcium signaling by controlling ATP release. *Proc Natl Acad Sci U S A*, 95, 15735-40.
- COUTINHO, P., QIU, C., FRANK, S., TAMBER, K. & BECKER, D. 2003. Dynamic changes in connexin expression correlate with key events in the wound healing process. *Cell Biol Int*, 27, 525-41.
- COUTINHO, P., QIU, C., FRANK, S., WANG, C. M., BROWN, T., GREEN, C. R. & BECKER, D. L. 2005. Limiting burn extension by transient inhibition of Connexin43 expression at the site of injury. *Br J Plast Surg*, 58, 658-67.
- CRONIN, M., ANDERSON, P. N., COOK, J. E., GREEN, C. R. & BECKER, D. L. 2008. Blocking connexin43 expression reduces inflammation and improves functional recovery after spinal cord injury. *Mol Cell Neurosci*, 39, 152-60.
- CRONIN, M., ANDERSON, P. N., GREEN, C. R. & BECKER, D. L. 2006. Antisense delivery and protein knockdown within the intact central nervous system. *Front Biosci*, 11, 2967-75.
- CRUCIANI, V. & MIKALSEN, S. O. 2006. The vertebrate connexin family. *Cell Mol Life Sci*, 63, 1125-40.
- CUSATO, K., ZAKEVICIUS, J. & RIPPS, H. 2003. An experimental approach to the study of gap-junction-mediated cell death. *Biol Bull*, 205, 197-9.
- DAHL, G. & HARRIS, A. L. 2009. *Chapter 12 Pannexins or Connexins*, Humana Press.
- DAHL, G. & LOCOVEI, S. 2006. Pannexin: to gap or not to gap, is that a question? *IUBMB Life*, 58, 409-19.
- DAHL, G., NONNER, W. & WERNER, R. 1994. Attempts to define functional domains of gap junction proteins with synthetic peptides. *Biophys J*, 67, 1816-22.
- DAHL, G., WERNER, R., LEVINE, E. & RABADAN-DIEHL, C. 1992. Mutational analysis of gap junction formation. *Biophys J*, 62, 172-80; discussion 180-2.

- DANESH-MEYER, H. V., HUANG, R., NICHOLSON, L. F. & GREEN, C. R. 2008. Connexin43 antisense oligodeoxynucleotide treatment down-regulates the inflammatory response in an in vitro interphase organotypic culture model of optic nerve ischaemia. *J Clin Neurosci*, 15, 1253-63.
- DANESH-MEYER, H. V., KERR, N. M., ZHANG, J., EADY, E. K., O'CARROLL, S. J., NICHOLSON, L. F., JOHNSON, C. S. & GREEN, C. R. 2012. Connexin43 mimetic peptide reduces vascular leak and retinal ganglion cell death following retinal ischaemia. *Brain*, 135, 506-20.
- DASGUPTA, C., MARTINEZ, A. M., ZUPPAN, C. W., SHAH, M. M., BAILEY, L. L. & FLETCHER, W. H. 2001. Identification of connexin43 (alpha1) gap junction gene mutations in patients with hypoplastic left heart syndrome by denaturing gradient gel electrophoresis (DGGE). *Mutat Res*, 479, 173-86.
- DAVIDSON, J. O., GREEN, C. R., NICHOLSON, L. F., BENNET, L. & GUNN, A. J. 2012a. Deleterious effects of high dose connexin 43 mimetic Peptide infusion after cerebral ischaemia in near-term fetal sheep. *Int J Mol Sci*, 13, 6303-19.
- DAVIDSON, J. O., GREEN, C. R., NICHOLSON, L. F., BENNET, L. & GUNN, A. J. 2013. Connexin hemichannel blockade is neuroprotective after, but not during, global cerebral ischemia in near-term fetal sheep. *Exp Neurol*, 248, 301-8.
- DAVIDSON, J. O., GREEN, C. R., NICHOLSON, L. F., O'CARROLL, S. J., FRASER, M., BENNET, L. & GUNN, A. J. 2012b. Connexin hemichannel blockade improves outcomes in a model of fetal ischemia. *Ann Neurol*, 71, 121-32.
- DE BOCK, M., CULOT, M., WANG, N., BOL, M., DECROCK, E., DE VUYST, E., DA COSTA, A., DAUWE, I., VINKEN, M., SIMON, A. M., ROGIERS, V., DE LEY, G., EVANS, W. H., BULTYNCK, G., DUPONT, G., CECHELLI, R. & LEYBAERT, L. 2011. Connexin channels provide a target to manipulate brain endothelial calcium dynamics and blood-brain barrier permeability. *J Cereb Blood Flow Metab*, 31, 1942-57.
- DE BOCK, M., CULOT, M., WANG, N., DA COSTA, A., DECROCK, E., BOL, M., BULTYNCK, G., CECHELLI, R. & LEYBAERT, L. 2012. Low extracellular Ca²⁺ conditions induce an increase in brain endothelial permeability that involves intercellular Ca²⁺ waves. *Brain Res*, 1487, 78-87.
- DE PINA-BENABOU, M. H., SZOSTAK, V., KYROZIS, A., REMPE, D., UZIEL, D., URBAN-MALDONADO, M., BENABOU, S., SPRAY, D. C., FEDEROFF, H. J., STANTON, P. K. & ROZENTAL, R. 2005. Blockade of gap junctions in vivo provides neuroprotection after perinatal global ischemia. *Stroke*, 36, 2232-7.
- DECROCK, E., DE VUYST, E., VINKEN, M., VAN MOORHEM, M., VRANCKX, K., WANG, N., VAN LAEKEN, L., DE BOCK, M., D'HERDE, K., LAI, C. P., ROGIERS, V., EVANS, W. H., NAUS, C. C. & LEYBAERT, L. 2009. Connexin 43 hemichannels contribute to the propagation of apoptotic cell death in a rat C6 glioma cell model. *Cell Death Differ*, 16, 151-63.
- DEFRANCO, B. H., NICKEL, B. M., BATY, C. J., MARTINEZ, J. S., GAY, V. L., SANDULACHE, V. C., HACKAM, D. J. & MURRAY, S. A. 2008. Migrating cells retain gap junction plaque structure and function. *Cell Commun Adhes*, 15, 273-88.
- DENDA, M., INOUE, K., FUZIWARA, S. & DENDA, S. 2002. P2X purinergic receptor antagonist accelerates skin barrier repair and prevents epidermal hyperplasia induced by skin barrier disruption. *J Invest Dermatol*, 119, 1034-40.

- DESPLANTEZ, T., VERMA, V., LEYBAERT, L., EVANS, W. H. & WEINGART, R. 2012. Gap26, a connexin mimetic peptide, inhibits currents carried by connexin43 hemichannels and gap junction channels. *Pharmacol Res*, 65, 546-52.
- DEVRIES, S. H. & SCHWARTZ, E. A. 1992. Hemi-gap-junction channels in solitary horizontal cells of the catfish retina. *J Physiol*, 445, 201-30.
- DI VIRGILIO, F., BRONTE, V., COLLAVO, D. & ZANOVELLO, P. 1989. Responses of mouse lymphocytes to extracellular adenosine 5'-triphosphate (ATP). Lymphocytes with cytotoxic activity are resistant to the permeabilizing effects of ATP. *J Immunol*, 143, 1955-60.
- DI VIRGILIO, F., CHIOZZI, P., FALZONI, S., FERRARI, D., SANZ, J. M., VENKETARAMAN, V. & BARICORDI, O. R. 1998. Cytolytic P2X purinoceptors. *Cell Death Differ*, 5, 191-9.
- DI, W. L., MONYPENNY, J., COMMON, J. E., KENNEDY, C. T., HOLLAND, K. A., LEIGH, I. M., RUGG, E. L., ZICHA, D. & KELSELL, D. P. 2002. Defective trafficking and cell death is characteristic of skin disease-associated connexin 31 mutations. *Hum Mol Genet*, 11, 2005-14.
- DIEZ, J. A., AHMAD, S. & EVANS, W. H. 1999. Assembly of heteromeric connexons in guinea-pig liver en route to the Golgi apparatus, plasma membrane and gap junctions. *Eur J Biochem*, 262, 142-8.
- DORA, K. A., MARTIN, P. E., CHAYTOR, A. T., EVANS, W. H., GARLAND, C. J. & GRIFFITH, T. M. 1999. Role of heterocellular Gap junctional communication in endothelium-dependent smooth muscle hyperpolarization: inhibition by a connexin-mimetic peptide. *Biochem Biophys Res Commun*, 254, 27-31.
- DOVI, J. V., HE, L. K. & DIPIETRO, L. A. 2003. Accelerated wound closure in neutrophil-depleted mice. *J Leukoc Biol*, 73, 448-55.
- DOVI, J. V., SZPADERSKA, A. M. & DIPIETRO, L. A. 2004. Neutrophil function in the healing wound: adding insult to injury? *Thromb Haemost*, 92, 275-80.
- DUNN, P. M. & BLAKELEY, A. G. 1988. Suramin: a reversible P2-purinoceptor antagonist in the mouse vas deferens. *Br J Pharmacol*, 93, 243-5.
- DÍAZ-HERNÁNDEZ, M., DÍEZ-ZAERA, M., SÁNCHEZ-NOGUEIRO, J., GÓMEZ-VILLAFUERTES, R., CANALS, J. M., ALBERCH, J., MIRAS-PORTUGAL, M. T. & LUCAS, J. J. 2009. Altered P2X7-receptor level and function in mouse models of Huntington's disease and therapeutic efficacy of antagonist administration. *FASEB J*, 23, 1893-906.
- EHRlich, H. P. & DIEZ, T. 2003. Role for gap junctional intercellular communications in wound repair. *Wound Repair Regen*, 11, 481-9.
- ELTZSCHIG, H. K., ECKLE, T., MAGER, A., KÜPER, N., KARCHER, C., WEISSMÜLLER, T., BOENGLER, K., SCHULZ, R., ROBSON, S. C. & COLGAN, S. P. 2006. ATP release from activated neutrophils occurs via connexin 43 and modulates adenosine-dependent endothelial cell function. *Circ Res*, 99, 1100-8.
- EPUAP, E. P. U. A. P. 2009. Pressure ulcer prevention: quick reference guide.
- ESCHKE, D., WÜST, M., HAUSCHILDT, S. & NIEBER, K. 2002. Pharmacological characterization of the P2X(7) receptor on human macrophages using the patch-clamp technique. *Naunyn Schmiedebergs Arch Pharmacol*, 365, 168-71.
- EUGENÍN, E. A., BRAÑES, M. C., BERMAN, J. W. & SÁEZ, J. C. 2003. TNF-alpha plus IFN-gamma induce connexin43 expression and formation of gap junctions between human monocytes/macrophages that enhance physiological responses. *J Immunol*, 170, 1320-8.
- EVANS, W. H. & BOITANO, S. 2001. Connexin mimetic peptides: specific inhibitors of gap-junctional intercellular communication. *Biochem Soc Trans*, 29, 606-12.

- EVANS, W. H., BULTYNCK, G. & LEYBAERT, L. 2012. Manipulating connexin communication channels: use of peptidomimetics and the translational outputs. *J Membr Biol*, 245, 437-49.
- EVANS, W. H., DE VUYST, E. & LEYBAERT, L. 2006. The gap junction cellular internet: connexin hemichannels enter the signalling limelight. *Biochem J*, 397, 1-14.
- EVANS, W. H. & MARTIN, P. E. 2002a. Gap junctions: structure and function (Review). *Mol Membr Biol*, 19, 121-36.
- EVANS, W. H. & MARTIN, P. E. 2002b. Lighting up gap junction channels in a flash. *Bioessays*, 24, 876-80.
- FALER, B. J., MACSATA, R. A., PLUMMER, D., MISHRA, L. & SIDAWY, A. N. 2006. Transforming growth factor-beta and wound healing. *Perspect Vasc Surg Endovasc Ther*, 18, 55-62.
- FALK, M. M., BUEHLER, L. K., KUMAR, N. M. & GILULA, N. B. 1997. Cell-free synthesis and assembly of connexins into functional gap junction membrane channels. *EMBO J*, 16, 2703-16.
- FALLON, R. F. & GOODENOUGH, D. A. 1981. Five-hour half-life of mouse liver gap-junction protein. *J Cell Biol*, 90, 521-6.
- FARAG, Y. M. & GABALLA, M. R. 2011. Diabetes: an overview of a rising epidemic. *Nephrol Dial Transplant*, 26, 28-35.
- FITZGERALD, D. J., FUSENIG, N. E., BOUKAMP, P., PICCOLI, C., MESNIL, M. & YAMASAKI, H. 1994. Expression and function of connexin in normal and transformed human keratinocytes in culture. *Carcinogenesis*, 15, 1859-65.
- FLANAGAN, M. 2003. Wound measurement: can it help us to monitor progression to healing? *J Wound Care*, 12, 189-94.
- FORGE, A., BECKER, D., CASALOTTI, S., EDWARDS, J., MARZIANO, N. & NEVILL, G. 2003a. Gap junctions in the inner ear: comparison of distribution patterns in different vertebrates and assesment of connexin composition in mammals. *J Comp Neurol*, 467, 207-31.
- FORGE, A., MARZIANO, N. K., CASALOTTI, S. O., BECKER, D. L. & JAGGER, D. 2003b. The inner ear contains heteromeric channels composed of cx26 and cx30 and deafness-related mutations in cx26 have a dominant negative effect on cx30. *Cell Commun Adhes*, 10, 341-6.
- FRANCIS, D., STERGIPOULOS, K., EK-VITORÍN, J. F., CAO, F. L., TAFFET, S. M. & DELMAR, M. 1999. Connexin diversity and gap junction regulation by pH. *Dev Genet*, 24, 123-36.
- FRANTSEVA, M. V., KOKAROVTSSEVA, L., NAUS, C. G., CARLEN, P. L., MACFABE, D. & PEREZ VELAZQUEZ, J. L. 2002a. Specific gap junctions enhance the neuronal vulnerability to brain traumatic injury. *J Neurosci*, 22, 644-53.
- FRANTSEVA, M. V., KOKAROVTSSEVA, L. & PEREZ VELAZQUEZ, J. L. 2002b. Ischemia-induced brain damage depends on specific gap-junctional coupling. *J Cereb Blood Flow Metab*, 22, 453-62.
- FRIEDENSTEIN, A. J., CHAILAKHJAN, R. K. & LALYKINA, K. S. 1970. The development of fibroblast colonies in monolayer cultures of guinea-pig bone marrow and spleen cells. *Cell Tissue Kinet*, 3, 393-403.
- FUCHS, E. 2008. Skin stem cells: rising to the surface. *J Cell Biol*, 180, 273-84.
- GABBIANI, G., CHAPONNIER, C. & HÜTTNER, I. 1978. Cytoplasmic filaments and gap junctions in epithelial cells and myofibroblasts during wound healing. *J Cell Biol*, 76, 561-8.
- GAIETTA, G., DEERINCK, T. J., ADAMS, S. R., BOUWER, J., TOUR, O., LAIRD, D. W., SOSINSKY, G. E., TSIEN, R. Y. & ELLISMAN, M. H. 2002. Multicolor and electron microscopic imaging of connexin trafficking. *Science*, 296, 503-7.

- GANOTE, C. E. & HUMPHREY, S. M. 1985. Effects of anoxic or oxygenated reperfusion in globally ischemic, isovolumic, perfused rat hearts. *Am J Pathol*, 120, 129-45.
- GARCÍA-DORADO, D., RODRÍGUEZ-SINOVAS, A. & RUIZ-MEANA, M. 2004. Gap junction-mediated spread of cell injury and death during myocardial ischemia-reperfusion. *Cardiovasc Res*, 61, 386-401.
- GARCÍA-DORADO, D., THÉROUX, P., DESCO, M., SOLARES, J., ELIZAGA, J., FERNANDEZ-AVILÉS, F., ALONSO, J. & SORIANO, J. 1989. Cell-to-cell interaction: a mechanism to explain wave-front progression of myocardial necrosis. *Am J Physiol*, 256, H1266-73.
- GARDNER, L. B., LI, F., YANG, X. & DANG, C. V. 2003. Anoxic fibroblasts activate a replication checkpoint that is bypassed by E1a. *Mol Cell Biol*, 23, 9032-45.
- GARLICK, J. A. & TAICHMAN, L. B. 1994. Fate of human keratinocytes during reepithelialization in an organotypic culture model. *Lab Invest*, 70, 916-24.
- GILCHREST, B. A., KARASSIK, R. L., WILKINS, L. M., VRABEL, M. A. & MACIAG, T. 1983. Autocrine and paracrine growth stimulation of cells derived from human skin. *J Cell Physiol*, 117, 235-40.
- GIOVANNARDI, S., RACCA, C., BERTOLLINI, L., STURANI, E. & PERES, A. 1992. P2Y purinoceptors in normal NIH 3T3 and in NIH 3T3 overexpressing c-ras. *Exp Cell Res*, 202, 398-404.
- GIRO, M. G., OIKARINEN, A. I., OIKARINEN, H., SEPHEL, G., UITTO, J. & DAVIDSON, J. M. 1985. Demonstration of elastin gene expression in human skin fibroblast cultures and reduced tropoelastin production by cells from a patient with atrophoderma. *J Clin Invest*, 75, 672-8.
- GOLDBERG, G. S., LAMPE, P. D., SHEEDY, D., STEWART, C. C., NICHOLSON, B. J. & NAUS, C. C. 1998. Direct isolation and analysis of endogenous transjunctional ADP from Cx43 transfected C6 glioma cells. *Exp Cell Res*, 239, 82-92.
- GOLDBERG, G. S., VALIUNAS, V. & BRINK, P. R. 2004. Selective permeability of gap junction channels. *Biochim Biophys Acta*, 1662, 96-101.
- GOLIGER, J. A. & PAUL, D. L. 1994. Expression of gap junction proteins Cx26, Cx31.1, Cx37, and Cx43 in developing and mature rat epidermis. *Dev Dyn*, 200, 1-13.
- GOLIGER, J. A. & PAUL, D. L. 1995. Wounding alters epidermal connexin expression and gap junction-mediated intercellular communication. *Mol Biol Cell*, 6, 1491-501.
- GOODENOUGH, D. A., GOLIGER, J. A. & PAUL, D. L. 1996. Connexins, connexons, and intercellular communication. *Annu Rev Biochem*, 65, 475-502.
- GOODENOUGH, D. A. & REVEL, J. P. 1970. A fine structural analysis of intercellular junctions in the mouse liver. *J Cell Biol*, 45, 272-90.
- GOTTFRIED, I., LANDAU, M., GLASER, F., DI, W. L., OPHIR, J., MEVORAH, B., BEN-TAL, N., KELSELL, D. P. & AVRAHAM, K. B. 2002. A mutation in GJB3 is associated with recessive erythrokeratoderma variabilis (EKV) and leads to defective trafficking of the connexin 31 protein. *Hum Mol Genet*, 11, 1311-6.
- GRUPCHEVA, C. N., LAUX, W. T., RUPENTHAL, I. D., MCGHEE, J., MCGHEE, C. N. & GREEN, C. R. 2012. Improved corneal wound healing through modulation of gap junction communication using connexin43-specific antisense oligodeoxynucleotides. *Invest Ophthalmol Vis Sci*, 53, 1130-8.
- GUAN, X., CRAVATT, B. F., EHRING, G. R., HALL, J. E., BOGER, D. L., LERNER, R. A. & GILULA, N. B. 1997. The sleep-inducing lipid oleamide deconvolutes gap junction communication and calcium wave transmission in glial cells. *J Cell Biol*, 139, 1785-92.

- GUO, H., ACEVEDO, P., PARSA, F. D. & BERTRAM, J. S. 1992. Gap-junctional protein connexin 43 is expressed in dermis and epidermis of human skin: differential modulation by retinoids. *J Invest Dermatol*, 99, 460-7.
- GURTNER, G. C., WERNER, S., BARRANDON, Y. & LONGAKER, M. T. 2008. Wound repair and regeneration. *Nature*, 453, 314-21.
- HAAPASALMI, K., ZHANG, K., TONNESEN, M., OLERUD, J., SHEPPARD, D., SALO, T., KRAMER, R., CLARK, R. A., UITTO, V. J. & LARJAVA, H. 1996. Keratinocytes in human wounds express alpha v beta 6 integrin. *J Invest Dermatol*, 106, 42-8.
- HARDING, K. & QUEEN, D. 2010. Chronic wounds and their management and prevention is a significant public health issue. *Int Wound J*, 7, 125-6.
- HARDING, K. G., MORRIS, H. L. & PATEL, G. K. 2002. Science, medicine and the future: healing chronic wounds. *BMJ*, 324, 160-3.
- HASLETT, C. 1992. Resolution of acute inflammation and the role of apoptosis in the tissue fate of granulocytes. *Clin Sci (Lond)*, 83, 639-48.
- HATANAKA, K., KAWATA, H., TOYOFUKU, T. & YOSHIDA, K. 2004. Down-regulation of connexin43 in early myocardial ischemia and protective effect by ischemic preconditioning in rat hearts in vivo. *Jpn Heart J*, 45, 1007-19.
- HAUPT, C., WITTE, O. W. & FRAHM, C. 2007. Up-regulation of Connexin43 in the glial scar following photothrombotic ischemic injury. *Mol Cell Neurosci*, 35, 89-99.
- HAWAT, G., BENDERDOUR, M., ROUSSEAU, G. & BAROUDI, G. 2010. Connexin 43 mimetic peptide Gap26 confers protection to intact heart against myocardial ischemia injury. *Pflugers Arch*, 460, 583-92.
- HAWAT, G., HÉLIE, P. & BAROUDI, G. 2012. Single intravenous low-dose injections of connexin 43 mimetic peptides protect ischemic heart in vivo against myocardial infarction. *J Mol Cell Cardiol*, 53, 559-66.
- HINZ, B. 2007. Formation and function of the myofibroblast during tissue repair. *J Invest Dermatol*, 127, 526-37.
- HINZ, B., CELETTA, G., TOMASEK, J. J., GABBIANI, G. & CHAPONNIER, C. 2001a. Alpha-smooth muscle actin expression upregulates fibroblast contractile activity. *Mol Biol Cell*, 12, 2730-41.
- HINZ, B., MASTRANGELO, D., ISELIN, C. E., CHAPONNIER, C. & GABBIANI, G. 2001b. Mechanical tension controls granulation tissue contractile activity and myofibroblast differentiation. *Am J Pathol*, 159, 1009-20.
- HO, F. Y., TSANG, W. P., KONG, S. K. & KWOK, T. T. 2006. The critical role of caspases activation in hypoxia/reoxygenation induced apoptosis. *Biochem Biophys Res Commun*, 345, 1131-7.
- HOYLE, C. H., KNIGHT, G. E. & BURNSTOCK, G. 1990. Suramin antagonizes responses to P2-purinoceptor agonists and purinergic nerve stimulation in the guinea-pig urinary bladder and taenia coli. *Br J Pharmacol*, 99, 617-21.
- HUANG, R., LIU, Y. G., LIN, Y., FAN, Y., BOYNTON, A., YANG, D. & HUANG, R. P. 2001. Enhanced apoptosis under low serum conditions in human glioblastoma cells by connexin 43 (Cx43). *Mol Carcinog*, 32, 128-38.
- HUANG, Y., GRINSPAN, J. B., ABRAMS, C. K. & SCHERER, S. S. 2007. Pannexin1 is expressed by neurons and glia but does not form functional gap junctions. *Glia*, 55, 46-56.
- HÜBNER, G., BRAUCHLE, M., SMOLA, H., MADLENER, M., FÄSSLER, R. & WERNER, S. 1996. Differential regulation of pro-inflammatory cytokines during wound healing in normal and glucocorticoid-treated mice. *Cytokine*, 8, 548-56.
- HÜLSER, D. F. & PETERS, J. H. 1971. Intercellular communication in phytohemagglutinin-induced lymphocyte agglutinates. *Eur J Immunol*, 1, 494-5.

- HÜLSER, D. F. & PETERS, J. H. 1972. Contact cooperation in stimulated lymphocytes. II. Electrophysiological investigations on intercellular communication. *Exp Cell Res*, 74, 319-26.
- IOSSA, S., MARCIANO, E. & FRANZÉ, A. 2011. GJB2 Gene Mutations in Syndromic Skin Diseases with Sensorineural Hearing Loss. *Curr Genomics*, 12, 475-785.
- ISAKSON, B. E., EVANS, W. H. & BOITANO, S. 2001. Intercellular Ca²⁺ signaling in alveolar epithelial cells through gap junctions and by extracellular ATP. *Am J Physiol Lung Cell Mol Physiol*, 280, L221-8.
- ISAKSON, B. E., SEEDORF, G. J., LUBMAN, R. L., EVANS, W. H. & BOITANO, S. 2003. Cell-cell communication in heterocellular cultures of alveolar epithelial cells. *Am J Respir Cell Mol Biol*, 29, 552-61.
- JARA, P. I., BORIC, M. P. & SÁEZ, J. C. 1995. Leukocytes express connexin 43 after activation with lipopolysaccharide and appear to form gap junctions with endothelial cells after ischemia-reperfusion. *Proc Natl Acad Sci U S A*, 92, 7011-5.
- JEFFCOATE, W. J. & HARDING, K. G. 2003. Diabetic foot ulcers. *Lancet*, 361, 1545-51.
- JIANG, L. P., TU, Q., WANG, Y. & ZHANG, E. 2011. Ischemia-reperfusion injury-induced histological changes affecting early stage pressure ulcer development in a rat model. *Ostomy Wound Manage*, 57, 55-60.
- JOHN, S. A., KONDO, R., WANG, S. Y., GOLDBERGER, J. I. & WEISS, J. N. 1999. Connexin-43 hemichannels opened by metabolic inhibition. *J Biol Chem*, 274, 236-40.
- JORDAN, K., CHODOCK, R., HAND, A. R. & LAIRD, D. W. 2001. The origin of annular junctions: a mechanism of gap junction internalization. *J Cell Sci*, 114, 763-73.
- KAMIBAYASHI, Y., OYAMADA, M., OYAMADA, Y. & MORI, M. 1993. Expression of gap junction proteins connexin 26 and 43 is modulated during differentiation of keratinocytes in newborn mouse epidermis. *J Invest Dermatol*, 101, 773-8.
- KANDYBA, E. E., HODGINS, M. B. & MARTIN, P. E. 2008. A murine living skin equivalent amenable to live-cell imaging: analysis of the roles of connexins in the epidermis. *J Invest Dermatol*, 128, 1039-49.
- KANTER, H. L., SAFFITZ, J. E. & BEYER, E. C. 1992. Cardiac myocytes express multiple gap junction proteins. *Circ Res*, 70, 438-44.
- KENNEDY, C. 1990. P1- and P2-purinoceptor subtypes--an update. *Arch Int Pharmacodyn Ther*, 303, 30-50.
- KIKUCHI, T., KIMURA, R. S., PAUL, D. L., TAKASAKA, T. & ADAMS, J. C. 2000. Gap junction systems in the mammalian cochlea. *Brain Res Brain Res Rev*, 32, 163-6.
- KNIGHT, G. 2009. *Purinergic receptors*, Elsevier.
- KOBAYASHI, H., AIBA, S., YOSHINO, Y. & TAGAMI, H. 2003. Acute cutaneous barrier disruption activates epidermal p44/42 and p38 mitogen-activated protein kinases in human and hairless guinea pig skin. *Exp Dermatol*, 12, 734-46.
- KONDO, R. P., WANG, S. Y., JOHN, S. A., WEISS, J. N. & GOLDBERGER, J. I. 2000. Metabolic inhibition activates a non-selective current through connexin hemichannels in isolated ventricular myocytes. *J Mol Cell Cardiol*, 32, 1859-72.
- KRETZ, M., EUWENS, C., HOMBACH, S., ECKARDT, D., TEUBNER, B., TRAUB, O., WILLECKE, K. & OTT, T. 2003. Altered connexin expression and wound healing in the epidermis of connexin-deficient mice. *J Cell Sci*, 116, 3443-52.
- KRETZ, M., MAASS, K. & WILLECKE, K. 2004. Expression and function of connexins in the epidermis, analyzed with transgenic mouse mutants. *Eur J Cell Biol*, 83, 647-54.

- KRUTOVSKIKH, V. A., PICCOLI, C. & YAMASAKI, H. 2002. Gap junction intercellular communication propagates cell death in cancerous cells. *Oncogene*, 21, 1989-99.
- KUMAR, N. M. & GILULA, N. B. 1992. Molecular biology and genetics of gap junction channels. *Semin Cell Biol*, 3, 3-16.
- KWAK, B. R. & JONGSMA, H. J. 1999. Selective inhibition of gap junction channel activity by synthetic peptides. *J Physiol*, 516 (Pt 3), 679-85.
- LAAKE, J. H., HAUG, F. M., WIELOCH, T. & OTTERSEN, O. P. 1999. A simple in vitro model of ischemia based on hippocampal slice cultures and propidium iodide fluorescence. *Brain Res Brain Res Protoc*, 4, 173-84.
- LAI, C. P., BECHBERGER, J. F., THOMPSON, R. J., MACVICAR, B. A., BRUZZONE, R. & NAUS, C. C. 2007. Tumor-suppressive effects of pannexin 1 in C6 glioma cells. *Cancer Res*, 67, 1545-54.
- LAING, J. G., TADROS, P. N., WESTPHALE, E. M. & BEYER, E. C. 1997. Degradation of connexin43 gap junctions involves both the proteasome and the lysosome. *Exp Cell Res*, 236, 482-92.
- LAIRD, D. W. 1996. The life cycle of a connexin: gap junction formation, removal, and degradation. *J Bioenerg Biomembr*, 28, 311-8.
- LAIRD, D. W. 2006. Life cycle of connexins in health and disease. *Biochem J*, 394, 527-43.
- LANDESMAN, Y., WHITE, T. W., STARICH, T. A., SHAW, J. E., GOODENOUGH, D. A. & PAUL, D. L. 1999. Innexin-3 forms connexin-like intercellular channels. *J Cell Sci*, 112 (Pt 14), 2391-6.
- LARSEN, W. J. & TUNG, H. N. 1978. Origin and fate of cytoplasmic gap junctional vesicles in rabbit granulosa cells. *Tissue Cell*, 10, 585-98.
- LAW, L. Y., ZHANG, W. V., STOTT, N. S., BECKER, D. L. & GREEN, C. R. 2006. In vitro optimization of antisense oligodeoxynucleotide design: an example using the connexin gene family. *J Biomol Tech*, 17, 270-82.
- LEE, H. J., SOHN, E. J., LEE, E. O., KIM, J. H., LEE, M. H. & KIM, S. H. 2012. Inhibition of Connexin 26/43 and Extracellular-Regulated Kinase Protein Plays a Critical Role in Melatonin Facilitated Gap Junctional Intercellular Communication in Hydrogen Peroxide-Treated HaCaT Keratinocyte Cells. *Evid Based Complement Alternat Med*, 2012, 589365.
- LEIBOVICH, S. J. & ROSS, R. 1975. The role of the macrophage in wound repair. A study with hydrocortisone and antimacrophage serum. *Am J Pathol*, 78, 71-100.
- LEVY, J. A., WEISS, R. M., DIRKSEN, E. R. & ROSEN, M. R. 1976. Possible communication between murine macrophages oriented in linear chains in tissue culture. *Exp Cell Res*, 103, 375-85.
- LEYBAERT, L., BRAET, K., VANDAMME, W., CABOOTER, L., MARTIN, P. E. & EVANS, W. H. 2003. Connexin channels, connexin mimetic peptides and ATP release. *Cell Commun Adhes*, 10, 251-7.
- LEÓN, D., HERVÁS, C. & MIRAS-PORTUGAL, M. T. 2006. P2Y1 and P2X7 receptors induce calcium/calmodulin-dependent protein kinase II phosphorylation in cerebellar granule neurons. *Eur J Neurosci*, 23, 2999-3013.
- LIN, J. H., WEIGEL, H., COTRINA, M. L., LIU, S., BUENO, E., HANSEN, A. J., HANSEN, T. W., GOLDMAN, S. & NEDERGAARD, M. 1998. Gap-junction-mediated propagation and amplification of cell injury. *Nat Neurosci*, 1, 494-500.
- LITTLE, J. B., AZZAM, E. I., DE TOLEDO, S. M. & NAGASAWA, H. 2002. Bystander effects: intercellular transmission of radiation damage signals. *Radiat Prot Dosimetry*, 99, 159-62.

- LOCKE, D., PERUSINGHE, N., NEWMAN, T., JAYATILAKE, H., EVANS, W. H. & MONAGHAN, P. 2000. Developmental expression and assembly of connexins into homomeric and heteromeric gap junction hemichannels in the mouse mammary gland. *J Cell Physiol*, 183, 228-37.
- LOCOVEI, S., BAO, L. & DAHL, G. 2006. Pannexin 1 in erythrocytes: function without a gap. *Proc Natl Acad Sci U S A*, 103, 7655-9.
- LOEWENSTEIN, W. R., NAKAS, M. & SOCOLAR, S. J. 1967. Junctional membrane uncoupling. Permeability transformations at a cell membrane junction. *J Gen Physiol*, 50, 1865-91.
- LURIA, E. A., PANASYUK, A. F. & FRIEDENSTEIN, A. Y. 1971. Fibroblast colony formation from monolayer cultures of blood cells. *Transfusion*, 11, 345-9.
- MACNEIL, S. 2007. Progress and opportunities for tissue-engineered skin. *Nature*, 445, 874-80.
- MADISON, K. C. 2003. Barrier function of the skin: "la raison d'être" of the epidermis. *J Invest Dermatol*, 121, 231-41.
- MAMBETISAEVA, E. T., GIRE, V. & EVANS, W. H. 1999. Multiple connexin expression in peripheral nerve, Schwann cells, and Schwannoma cells. *J Neurosci Res*, 57, 166-75.
- MANOTHAM, K., TANAKA, T., MATSUMOTO, M., OHSE, T., INAGI, R., MIYATA, T., KUROKAWA, K., FUJITA, T., INGELFINGER, J. R. & NANGAKU, M. 2004. Transdifferentiation of cultured tubular cells induced by hypoxia. *Kidney Int*, 65, 871-80.
- MAO, H. J., CHEN, B. P., REN, G. Y., JIN, J. S., FAN, F. Y., GAO, Q., BRUCE, I. & XIA, Q. 2005. The Effects of Heptanol on Electrical Coupling during Ischemia in the Perfused Isolated Rat Heart. *Conf Proc IEEE Eng Med Biol Soc*, 1, 122-5.
- MAO, H. J., CHEN, B. P., YU, T. N., YE, Z. G., YUAN, X. G. & XIA, Q. 2009. [Effect of gap junction on the cardioprotection of ischemic postconditioning in rat heart]. *Zhongguo Ying Yong Sheng Li Xue Za Zhi*, 25, 60-4.
- MARTIN, P. 1997. Wound healing--aiming for perfect skin regeneration. *Science*, 276, 75-81.
- MARTIN, P. & LEIBOVICH, S. J. 2005. Inflammatory cells during wound repair: the good, the bad and the ugly. *Trends Cell Biol*, 15, 599-607.
- MARTIN, P. E., BLUNDELL, G., AHMAD, S., ERRINGTON, R. J. & EVANS, W. H. 2001a. Multiple pathways in the trafficking and assembly of connexin 26, 32 and 43 into gap junction intercellular communication channels. *J Cell Sci*, 114, 3845-55.
- MARTIN, P. E., COLEMAN, S. L., CASALOTTI, S. O., FORGE, A. & EVANS, W. H. 1999. Properties of connexin26 gap junctional proteins derived from mutations associated with non-syndromal hereditary deafness. *Hum Mol Genet*, 8, 2369-76.
- MARTIN, P. E., ERRINGTON, R. J. & EVANS, W. H. 2001b. Gap junction assembly: multiple connexin fluorophores identify complex trafficking pathways. *Cell Commun Adhes*, 8, 243-8.
- MARTIN, P. E., WALL, C. & GRIFFITH, T. M. 2005. Effects of connexin-mimetic peptides on gap junction functionality and connexin expression in cultured vascular cells. *Br J Pharmacol*, 144, 617-27.
- MARTINEZ, F. O., GORDON, S., LOCATI, M. & MANTOVANI, A. 2006. Transcriptional profiling of the human monocyte-to-macrophage differentiation and polarization: new molecules and patterns of gene expression. *J Immunol*, 177, 7303-11.
- MARZIANO, N. K., CASALOTTI, S. O., PORTELLI, A. E., BECKER, D. L. & FORGE, A. 2003. Mutations in the gene for connexin 26 (GJB2) that cause hearing loss have a dominant negative effect on connexin 30. *Hum Mol Genet*, 12, 805-12.

- MCGUCKIN, M., WATERMAN, R., BROOKS, J., CHERRY, G., PORTEN, L., HURLEY, S. & KERSTEIN, M. D. 2002. Validation of venous leg ulcer guidelines in the United States and United Kingdom. *Am J Surg*, 183, 132-7.
- MCMASTERS, R. A., SAYLORS, R. L., JONES, K. E., HENDRIX, M. E., MOYER, M. P. & DRAKE, R. R. 1998. Lack of bystander killing in herpes simplex virus thymidine kinase-transduced colon cell lines due to deficient connexin43 gap junction formation. *Hum Gene Ther*, 9, 2253-61.
- MENDOZA-NARANJO, A., CORMIE, P., SERRANO, A. E., HU, R., O'NEILL, S., WANG, C. M., THRASIVOULOU, C., POWER, K. T., WHITE, A., SERENA, T., PHILLIPS, A. R. & BECKER, D. L. 2012a. Targeting Cx43 and N-cadherin, which are abnormally upregulated in venous leg ulcers, influences migration, adhesion and activation of Rho GTPases. *PLoS One*, 7, e37374.
- MENDOZA-NARANJO, A., CORMIE, P., SERRANO, A. E., WANG, C. M., THRASIVOULOU, C., SUTCLIFFE, J. E., GILMARTIN, D. J., TSUI, J., SERENA, T. E., PHILLIPS, A. R. & BECKER, D. L. 2012b. Overexpression of the gap junction protein Cx43 as found in diabetic foot ulcers can retard fibroblast migration. *Cell Biol Int*, 36, 661-7.
- MIYAZAKI, S., FUJIWARA, H., ONODERA, T., KIHARA, Y., MATSUDA, M., WU, D. J., NAKAMURA, Y., KUMADA, T., SASAYAMA, S. & KAWAI, C. 1987. Quantitative analysis of contraction band and coagulation necrosis after ischemia and reperfusion in the porcine heart. *Circulation*, 75, 1074-82.
- MOORE, K., AMOS, J., DAVIS, J., GOURDIE, R. & POTTS, J. D. 2013. Characterization of polymeric microcapsules containing a low molecular weight peptide for controlled release. *Microsc Microanal*, 19, 213-26.
- MORI, L., BELLINI, A., STACEY, M. A., SCHMIDT, M. & MATTOLI, S. 2005. Fibrocytes contribute to the myofibroblast population in wounded skin and originate from the bone marrow. *Exp Cell Res*, 304, 81-90.
- MORI, R., POWER, K. T., WANG, C. M., MARTIN, P. & BECKER, D. L. 2006. Acute downregulation of connexin43 at wound sites leads to a reduced inflammatory response, enhanced keratinocyte proliferation and wound fibroblast migration. *J Cell Sci*, 119, 5193-203.
- MOULIN, V. 1995. Growth factors in skin wound healing. *Eur J Cell Biol*, 68, 1-7.
- MURANDO, M. & DEALEY, C. 2013. The use of granulated sugar to treat two pressure ulcers. *Wounds International*, 1.
- MUSIL, L. S. & GOODENOUGH, D. A. 1991. Biochemical analysis of connexin43 intracellular transport, phosphorylation, and assembly into gap junctional plaques. *J Cell Biol*, 115, 1357-74.
- MUSIL, L. S. & GOODENOUGH, D. A. 1993. Multisubunit assembly of an integral plasma membrane channel protein, gap junction connexin43, occurs after exit from the ER. *Cell*, 74, 1065-77.
- MUSTOE, T. 2004. Understanding chronic wounds: a unifying hypothesis on their pathogenesis and implications for therapy. *Am J Surg*, 187, 65S-70S.
- MUSTOE, T. A., O'SHAUGHNESSY, K. & KLOETERS, O. 2006. Chronic wound pathogenesis and current treatment strategies: a unifying hypothesis. *Plast Reconstr Surg*, 117, 35S-41S.
- NAGASAWA, H., CREMESTI, A., KOLESNICK, R., FUKS, Z. & LITTLE, J. B. 2002. Involvement of membrane signaling in the bystander effect in irradiated cells. *Cancer Res*, 62, 2531-4.
- NAGATA, M., TAKENAKA, H., SHIBAGAKI, R. & KISHIMOTO, S. 1999. Apoptosis and p53 protein expression increase in the process of burn wound healing in guinea-pig skin. *Br J Dermatol*, 140, 829-38.
- NAKASE, T., SÖHL, G., THEIS, M., WILLECKE, K. & NAUS, C. C. 2004. Increased apoptosis and inflammation after focal brain ischemia in mice lacking connexin43 in astrocytes. *Am J Pathol*, 164, 2067-75.

- NAKASE, T., YOSHIDA, Y. & NAGATA, K. 2006. Enhanced connexin 43 immunoreactivity in penumbral areas in the human brain following ischemia. *Glia*, 54, 369-75.
- NAUS, C. C., HEARN, S., ZHU, D., NICHOLSON, B. J. & SHIVERS, R. R. 1993. Ultrastructural analysis of gap junctions in C6 glioma cells transfected with connexin43 cDNA. *Exp Cell Res*, 206, 72-84.
- NHS 2013. Venous leg ulcer and wound healing. AQP VLU&WH Core & Reference Group, NHS.
- NISHII, K., KUMAI, M. & SHIBATA, Y. 2001. Regulation of the epithelial-mesenchymal transformation through gap junction channels in heart development. *Trends Cardiovasc Med*, 11, 213-8.
- NODIN, C., NILSSON, M. & BLOMSTRAND, F. 2005. Gap junction blockage limits intercellular spreading of astrocytic apoptosis induced by metabolic depression. *J Neurochem*, 94, 1111-23.
- O'CARROLL, S. J., ALKADHI, M., NICHOLSON, L. F. & GREEN, C. R. 2008. Connexin 43 mimetic peptides reduce swelling, astrogliosis, and neuronal cell death after spinal cord injury. *Cell Commun Adhes*, 15, 27-42.
- OGAWA, M., LARUE, A. C. & DRAKE, C. J. 2006. Hematopoietic origin of fibroblasts/myofibroblasts: Its pathophysiologic implications. *Blood*, 108, 2893-6.
- OKADA, A., TOMASETTO, C., LUTZ, Y., BELLOCQ, J. P., RIO, M. C. & BASSET, P. 1997. Expression of matrix metalloproteinases during rat skin wound healing: evidence that membrane type-1 matrix metalloproteinase is a stromal activator of pro-gelatinase A. *J Cell Biol*, 137, 67-77.
- ORELLANA, J. A., FROGER, N., EZAN, P., JIANG, J. X., BENNETT, M. V., NAUS, C. C., GIAUME, C. & SÁEZ, J. C. 2011. ATP and glutamate released via astroglial connexin 43 hemichannels mediate neuronal death through activation of pannexin 1 hemichannels. *J Neurochem*, 118, 826-40.
- ORELLANA, J. A., HERNÁNDEZ, D. E., EZAN, P., VELARDE, V., BENNETT, M. V., GIAUME, C. & SÁEZ, J. C. 2010. Hypoxia in high glucose followed by reoxygenation in normal glucose reduces the viability of cortical astrocytes through increased permeability of connexin 43 hemichannels. *Glia*, 58, 329-43.
- ORELLANA, J. A., SÁEZ, P. J., CORTÉS-CAMPOS, C., ELIZONDO, R. J., SHOJI, K. F., CONTRERAS-DUARTE, S., FIGUEROA, V., VELARDE, V., JIANG, J. X., NUALART, F., SÁEZ, J. C. & GARCÍA, M. A. 2012. Glucose increases intracellular free Ca²⁺ in tanocytes via ATP release through connexin 43 hemichannels. *Glia*, 60, 53-68.
- ORMONDE, S., CHOU, C. Y., GOOLD, L., PETSOGLOU, C., AL-TAIE, R., SHERWIN, T., MCGHEE, C. N. & GREEN, C. R. 2012. Regulation of connexin43 gap junction protein triggers vascular recovery and healing in human ocular persistent epithelial defect wounds. *J Membr Biol*, 245, 381-8.
- ORRIS, I. R., KNIGHT, G. E., UTTING, J. C., TAYLOR, S. E., BURNSTOCK, G. & ARNETT, T. R. 2009. Hypoxia stimulates vesicular ATP release from rat osteoblasts. *J Cell Physiol*, 220, 155-62.
- OVIEDO-ORTA, E., ERRINGTON, R. J. & EVANS, W. H. 2002. Gap junction intercellular communication during lymphocyte transendothelial migration. *Cell Biol Int*, 26, 253-63.
- OVIEDO-ORTA, E., GASQUE, P. & EVANS, W. H. 2001. Immunoglobulin and cytokine expression in mixed lymphocyte cultures is reduced by disruption of gap junction intercellular communication. *FASEB J*, 15, 768-74.
- OVIEDO-ORTA, E. & HOWARD EVANS, W. 2004. Gap junctions and connexin-mediated communication in the immune system. *Biochim Biophys Acta*, 1662, 102-12.

- OVIEDO-ORTA, E., HOY, T. & EVANS, W. H. 2000. Intercellular communication in the immune system: differential expression of connexin40 and 43, and perturbation of gap junction channel functions in peripheral blood and tonsil human lymphocyte subpopulations. *Immunology*, 99, 578-90.
- PANCHIN, Y. V. 2005. Evolution of gap junction proteins--the pannexin alternative. *J Exp Biol*, 208, 1415-9.
- PAUL, D. L. 1986. Molecular cloning of cDNA for rat liver gap junction protein. *J Cell Biol*, 103, 123-34.
- PAUL, D. L., EBIHARA, L., TAKEMOTO, L. J., SWENSON, K. I. & GOODENOUGH, D. A. 1991. Connexin46, a novel lens gap junction protein, induces voltage-gated currents in nonjunctional plasma membrane of *Xenopus* oocytes. *J Cell Biol*, 115, 1077-89.
- PEARSON, R. A., DALE, N., LLAUDET, E. & MOBBS, P. 2005. ATP released via gap junction hemichannels from the pigment epithelium regulates neural retinal progenitor proliferation. *Neuron*, 46, 731-44.
- PEIRCE, S. M., SKALAK, T. C. & RODEHEAVER, G. T. 2000. Ischemia-reperfusion injury in chronic pressure ulcer formation: a skin model in the rat. *Wound Repair Regen*, 8, 68-76.
- PELEGRIN, P. 2011. Many ways to dilate the P2X7 receptor pore. *Br J Pharmacol*, 163, 908-11.
- PHELAN, P., BACON, J. P., DAVIES, J. A., STEBBINGS, L. A., TODMAN, M. G., AVERY, L., BAINES, R. A., BARNES, T. M., FORD, C., HEKIMI, S., LEE, R., SHAW, J. E., STARICH, T. A., CURTIN, K. D., SUN, Y. A. & WYMAN, R. J. 1998. Innexins: a family of invertebrate gap-junction proteins. *Trends Genet*, 14, 348-9.
- PILLAI, S. & BIKLE, D. D. 1992. Adenosine triphosphate stimulates phosphoinositide metabolism, mobilizes intracellular calcium, and inhibits terminal differentiation of human epidermal keratinocytes. *J Clin Invest*, 90, 42-51.
- PITTINGER, M. F., MACKAY, A. M., BECK, S. C., JAISWAL, R. K., DOUGLAS, R., MOSCA, J. D., MOORMAN, M. A., SIMONETTI, D. W., CRAIG, S. & MARSHAK, D. R. 1999. Multilineage potential of adult human mesenchymal stem cells. *Science*, 284, 143-7.
- PITTS, J. D. 1998. The discovery of metabolic co-operation. *Bioessays*, 20, 1047-51.
- PITTS, K. R. & TOOMBS, C. F. 2004. Coverslip hypoxia: a novel method for studying cardiac myocyte hypoxia and ischemia in vitro. *Am J Physiol Heart Circ Physiol*, 287, H1801-12.
- POLACEK, D., BECH, F., MCKINSEY, J. F. & DAVIES, P. F. 1997. Connexin43 gene expression in the rabbit arterial wall: effects of hypercholesterolemia, balloon injury and their combination. *J Vasc Res*, 34, 19-30.
- POLACEK, D., LAL, R., VOLIN, M. V. & DAVIES, P. F. 1993. Gap junctional communication between vascular cells. Induction of connexin43 messenger RNA in macrophage foam cells of atherosclerotic lesions. *Am J Pathol*, 142, 593-606.
- POLLOK, S., PFEIFFER, A. C., LOBMANN, R., WRIGHT, C. S., MOLL, I., MARTIN, P. E. & BRANDNER, J. M. 2011. Connexin 43 mimetic peptide Gap27 reveals potential differences in the role of Cx43 in wound repair between diabetic and non-diabetic cells. *J Cell Mol Med*, 15, 861-73.
- POORNIMA, V., MADHUPRIYA, M., KOOTAR, S., SUJATHA, G., KUMAR, A. & BERA, A. K. 2012. P2X7 receptor-pannexin 1 hemichannel association: effect of extracellular calcium on membrane permeabilization. *J Mol Neurosci*, 46, 585-94.

- PRINGLE, A. K., IANNOTTI, F., WILDE, G. J., CHAD, J. E., SEELEY, P. J. & SUNDSTROM, L. E. 1997. Neuroprotection by both NMDA and non-NMDA receptor antagonists in in vitro ischemia. *Brain Res*, 755, 36-46.
- QIU, C., COUTINHO, P., FRANK, S., FRANKE, S., LAW, L. Y., MARTIN, P., GREEN, C. R. & BECKER, D. L. 2003. Targeting connexin43 expression accelerates the rate of wound repair. *Curr Biol*, 13, 1697-703.
- RAFFETTO, J. D., MENDEZ, M. V., MARIEN, B. J., BYERS, H. R., PHILLIPS, T. J., PARK, H. Y. & MENZOIAN, J. O. 2001. Changes in cellular motility and cytoskeletal actin in fibroblasts from patients with chronic venous insufficiency and in neonatal fibroblasts in the presence of chronic wound fluid. *J Vasc Surg*, 33, 1233-41.
- RAHMAN, S. & EVANS, W. H. 1991. Topography of connexin32 in rat liver gap junctions. Evidence for an intramolecular disulphide linkage connecting the two extracellular peptide loops. *J Cell Sci*, 100 (Pt 3), 567-78.
- RAMACHANDRAN, S., XIE, L. H., JOHN, S. A., SUBRAMANIAM, S. & LAL, R. 2007. A novel role for connexin hemichannel in oxidative stress and smoking-induced cell injury. *PLoS One*, 2, e712.
- RANA, S. & DRINGEN, R. 2007. Gap junction hemichannel-mediated release of glutathione from cultured rat astrocytes. *Neurosci Lett*, 415, 45-8.
- RANSFORD, G. A., FREGIEN, N., QIU, F., DAHL, G., CONNER, G. E. & SALATHE, M. 2009. Pannexin 1 contributes to ATP release in airway epithelia. *Am J Respir Cell Mol Biol*, 41, 525-34.
- RAWANDUZY, A., HANSEN, A., HANSEN, T. W. & NEDERGAARD, M. 1997. Effective reduction of infarct volume by gap junction blockade in a rodent model of stroke. *J Neurosurg*, 87, 916-20.
- REAUME, A. G., DE SOUSA, P. A., KULKARNI, S., LANGILLE, B. L., ZHU, D., DAVIES, T. C., JUNEJA, S. C., KIDDER, G. M. & ROSSANT, J. 1995. Cardiac malformation in neonatal mice lacking connexin43. *Science*, 267, 1831-4.
- REID, R. R., SULL, A. C., MOGFORD, J. E., ROY, N. & MUSTOE, T. A. 2004. A novel murine model of cyclical cutaneous ischemia-reperfusion injury. *J Surg Res*, 116, 172-80.
- RENTSCH, M. L., OSSUM, C. G., HOFFMANN, E. K. & PEDERSEN, S. F. 2007. Roles of Na⁺/H⁺ exchange in regulation of p38 mitogen-activated protein kinase activity and cell death after chemical anoxia in NIH3T3 fibroblasts. *Pflugers Arch*, 454, 649-62.
- RETAMAL, M. A., SCHALPER, K. A., SHOJI, K. F., BENNETT, M. V. & SAEZ, J. C. 2007. Opening of connexin 43 hemichannels is increased by lowering intracellular redox potential. *Proc Natl Acad Sci U S A*, 104, 8322-7.
- REVEL, J. P. & KARNOVSKY, M. J. 1967. Hexagonal array of subunits in intercellular junctions of the mouse heart and liver. *J Cell Biol*, 33, C7-C12.
- RICHARD, G. 2000. Connexins: a connection with the skin. *Exp Dermatol*, 9, 77-96.
- RICHARD, G. 2005. Connexin disorders of the skin. *Clin Dermatol*, 23, 23-32.
- RICHARD, G., LIN, J. P., SMITH, L., WHYTE, Y. M., ITIN, P., WOLLINA, U., EPSTEIN, E., HOHL, D., GIROUX, J. M., CHARNAS, L., BALE, S. J. & DIGIOVANNA, J. J. 1997. Linkage studies in erythrokeratodermias: fine mapping, genetic heterogeneity and analysis of candidate genes. *J Invest Dermatol*, 109, 666-71.
- RICHARD, G., SMITH, L. E., BAILEY, R. A., ITIN, P., HOHL, D., EPSTEIN, E. H., DIGIOVANNA, J. J., COMPTON, J. G. & BALE, S. J. 1998. Mutations in the human connexin gene GJB3 cause erythrokeratoderma variabilis. *Nat Genet*, 20, 366-9.
- RIEGER, J. M., SHAH, A. R. & GIDDAY, J. M. 2002. Ischemia-reperfusion injury of retinal endothelium by cyclooxygenase- and xanthine oxidase-derived superoxide. *Exp Eye Res*, 74, 493-501.

- ROBERTSON, J., LANG, S., LAMBERT, P. A. & MARTIN, P. E. 2010. Peptidoglycan derived from *Staphylococcus epidermidis* induces Connexin43 hemichannel activity with consequences on the innate immune response in endothelial cells. *Biochemical Journal*, 432, 133-143.
- SAEZ, J. C., BERTHOUD, V. M., BRANES, M. C., MARTINEZ, A. D. & BEYER, E. C. 2003. Plasma membrane channels formed by connexins: their regulation and functions. *Physiol Rev*, 83, 1359-400.
- SAITOH, M., OYAMADA, M., OYAMADA, Y., KAKU, T. & MORI, M. 1997. Changes in the expression of gap junction proteins (connexins) in hamster tongue epithelium during wound healing and carcinogenesis. *Carcinogenesis*, 18, 1319-28.
- SALOMON, D., MASGRAU, E., VISCHER, S., ULLRICH, S., DUPONT, E., SAPPINO, P., SAURAT, J. H. & MEDA, P. 1994. Topography of mammalian connexins in human skin. *J Invest Dermatol*, 103, 240-7.
- SALOMON, D., SAURAT, J. H. & MEDA, P. 1988. Cell-to-cell communication within intact human skin. *J Clin Invest*, 82, 248-54.
- SANSON, M., MARCAUD, V., ROBIN, E., VALÉRY, C., STURTZ, F. & ZALC, B. 2002. Connexin 43-mediated bystander effect in two rat glioma cell models. *Cancer Gene Ther*, 9, 149-55.
- SARIEDDINE, M. Z., SCHECKENBACH, K. E., FOGLIA, B., MAASS, K., GARCIA, I., KWAK, B. R. & CHANSON, M. 2009. Connexin43 modulates neutrophil recruitment to the lung. *J Cell Mol Med*, 13, 4560-70.
- SCHERER, S. S. & KLEOPA, K. A. 2012. X-linked Charcot-Marie-Tooth disease. *J Peripher Nerv Syst*, 17 Suppl 3, 9-13.
- SCHREML, S., SZEIMIES, R. M., PRANTL, L., KARRER, S., LANDTHALER, M. & BABILAS, P. 2010. Oxygen in acute and chronic wound healing. *Br J Dermatol*, 163, 257-68.
- SCHRÖDER, J. M. 1995. Cytokine networks in the skin. *J Invest Dermatol*, 105, 20S-24S.
- SEN, C. K., GORDILLO, G. M., ROY, S., KIRSNER, R., LAMBERT, L., HUNT, T. K., GOTTRUP, F., GURTNER, G. C. & LONGAKER, M. T. 2009. Human skin wounds: a major and snowballing threat to public health and the economy. *Wound Repair Regen*, 17, 763-71.
- SEPHEL, G. C. & DAVIDSON, J. M. 1986. Elastin production in human skin fibroblast cultures and its decline with age. *J Invest Dermatol*, 86, 279-85.
- SHAW, J. E., SICREE, R. A. & ZIMMET, P. Z. 2010. Global estimates of the prevalence of diabetes for 2010 and 2030. *Diabetes Res Clin Pract*, 87, 4-14.
- SHAW, J. P., KENT, K., BIRD, J., FISHBACK, J. & FROEHLER, B. 1991. Modified deoxyoligonucleotides stable to exonuclease degradation in serum. *Nucleic Acids Res*, 19, 747-50.
- SHAW, T. J. & MARTIN, P. 2009. Wound repair at a glance. *J Cell Sci*, 122, 3209-13.
- SHINTANI-ISHIDA, K., UEMURA, K. & YOSHIDA, K. 2007. Hemichannels in cardiomyocytes open transiently during ischemia and contribute to reperfusion injury following brief ischemia. *Am J Physiol Heart Circ Physiol*, 293, H1714-20.
- SIDDIQUI, A. R. & BERNSTEIN, J. M. 2010. Chronic wound infection: facts and controversies. *Clin Dermatol*, 28, 519-26.
- SIMON, A. M., GOODENOUGH, D. A. & PAUL, D. L. 1998. Mice lacking connexin40 have cardiac conduction abnormalities characteristic of atrioventricular block and bundle branch block. *Curr Biol*, 8, 295-8.
- SIMPSON, D. M. & ROSS, R. 1972. The neutrophilic leukocyte in wound repair a study with antineutrophil serum. *J Clin Invest*, 51, 2009-23.

- SMITH, R. S., SMITH, T. J., BLIEDEN, T. M. & PHIPPS, R. P. 1997. Fibroblasts as sentinel cells. Synthesis of chemokines and regulation of inflammation. *Am J Pathol*, 151, 317-22.
- SOLINI, A., CHIOZZI, P., MORELLI, A., ADINOLFI, E., RIZZO, R., BARICORDI, O. R. & DI VIRGILIO, F. 2004. Enhanced P2X7 activity in human fibroblasts from diabetic patients: a possible pathogenetic mechanism for vascular damage in diabetes. *Arterioscler Thromb Vasc Biol*, 24, 1240-5.
- SOLINI, A., CHIOZZI, P., MORELLI, A., FELLIN, R. & DI VIRGILIO, F. 1999. Human primary fibroblasts in vitro express a purinergic P2X7 receptor coupled to ion fluxes, microvesicle formation and IL-6 release. *J Cell Sci*, 112 (Pt 3), 297-305.
- SPRINGER, T. A. 1994. Traffic signals for lymphocyte recirculation and leukocyte emigration: the multistep paradigm. *Cell*, 76, 301-14.
- STEBBINGS, L. A., TODMAN, M. G., PHELAN, P., BACON, J. P. & DAVIES, J. A. 2000. Two Drosophila innexins are expressed in overlapping domains and cooperate to form gap-junction channels. *Mol Biol Cell*, 11, 2459-70.
- STOLER, D. L., ANDERSON, G. R., RUSSO, C. A., SPINA, A. M. & BEERMAN, T. A. 1992. Anoxia-inducible endonuclease activity as a potential basis of the genomic instability of cancer cells. *Cancer Res*, 52, 4372-8.
- STOUT, C. E., COSTANTIN, J. L., NAUS, C. C. & CHARLES, A. C. 2002. Intercellular calcium signaling in astrocytes via ATP release through connexin hemichannels. *J Biol Chem*, 277, 10482-8.
- SUBAK-SHARPE, H., BÜRK, R. R. & PITTS, J. D. 1969. Metabolic co-operation between biochemically marked mammalian cells in tissue culture. *J Cell Sci*, 4, 353-67.
- SYBALSKA, E. H. & SZYBALSKI, W. 1962. Genetics of human cress line. IV. DNA-mediated heritable transformation of a biochemical trait. *Proc Natl Acad Sci U S A*, 48, 2026-34.
- SÁEZ, J. C., CONNOR, J. A., SPRAY, D. C. & BENNETT, M. V. 1989a. Hepatocyte gap junctions are permeable to the second messenger, inositol 1,4,5-trisphosphate, and to calcium ions. *Proc Natl Acad Sci U S A*, 86, 2708-12.
- SÁEZ, J. C., GREGORY, W. A., WATANABE, T., DERMETZEL, R., HERTZBERG, E. L., REID, L., BENNETT, M. V. & SPRAY, D. C. 1989b. cAMP delays disappearance of gap junctions between pairs of rat hepatocytes in primary culture. *Am J Physiol*, 257, C1-11.
- TADA, J. & HASHIMOTO, K. 1997. Ultrastructural localization of gap junction protein connexin 43 in normal human skin, basal cell carcinoma, and squamous cell carcinoma. *J Cutan Pathol*, 24, 628-35.
- TANDARA, A. A. & MUSTOE, T. A. 2004. Oxygen in wound healing--more than a nutrient. *World J Surg*, 28, 294-300.
- TAYLOR, H. J., CHAYTOR, A. T., EVANS, W. H. & GRIFFITH, T. M. 1998. Inhibition of the gap junctional component of endothelium-dependent relaxations in rabbit iliac artery by 18-alpha glycyrrhetic acid. *Br J Pharmacol*, 125, 1-3.
- THEILGAARD-MÖNCH, K., KNUDSEN, S., FOLLIN, P. & BORREGAARD, N. 2004. The transcriptional activation program of human neutrophils in skin lesions supports their important role in wound healing. *J Immunol*, 172, 7684-93.
- THOMPSON, R. J., ZHOU, N. & MACVICAR, B. A. 2006. Ischemia opens neuronal gap junction hemichannels. *Science*, 312, 924-7.
- TRAUB, O., LOOK, J., PAUL, D. & WILLECKE, K. 1987. Cyclic adenosine monophosphate stimulates biosynthesis and phosphorylation of the 26 kDa gap junction protein in cultured mouse hepatocytes. *Eur J Cell Biol*, 43, 48-54.

- TREXLER, E. B., BUKAUSKAS, F. F., BENNETT, M. V., BARGIELLO, T. A. & VERSELIS, V. K. 1999. Rapid and direct effects of pH on connexins revealed by the connexin46 hemichannel preparation. *J Gen Physiol*, 113, 721-42.
- TSUKIMOTO, M., HARADA, H., IKARI, A. & TAKAGI, K. 2005. Involvement of chloride in apoptotic cell death induced by activation of ATP-sensitive P2X7 purinoceptor. *J Biol Chem*, 280, 2653-8.
- TURNER, M. S., HAYWOOD, G. A., ANDREKA, P., YOU, L., MARTIN, P. E., EVANS, W. H., WEBSTER, K. A. & BISHOPRIC, N. H. 2004. Reversible connexin 43 dephosphorylation during hypoxia and reoxygenation is linked to cellular ATP levels. *Circ Res*, 95, 726-33.
- UEHARA, Y. & BURNSTOCK, G. 1970. Demonstration of "gap junctions" between smooth muscle cells. *J Cell Biol*, 44, 215-7.
- VALENCIA, I. C., FALABELLA, A., KIRSNER, R. S. & EAGLSTEIN, W. H. 2001. Chronic venous insufficiency and venous leg ulceration. *J Am Acad Dermatol*, 44, 401-21; quiz 422-4.
- VAN KEMPEN, M. J. & JONGSMA, H. J. 1999. Distribution of connexin37, connexin40 and connexin43 in the aorta and coronary artery of several mammals. *Histochem Cell Biol*, 112, 479-86.
- VAN STEENSEL, M. A. 2004. Gap junction diseases of the skin. *Am J Med Genet C Semin Med Genet*, 131C, 12-9.
- VANDEN ABEELE, F., BIDAUX, G., GORDIENKO, D., BECK, B., PANCHIN, Y. V., BARANOVA, A. V., IVANOV, D. V., SKRYMA, R. & PREVARSKAYA, N. 2006. Functional implications of calcium permeability of the channel formed by pannexin 1. *J Cell Biol*, 174, 535-46.
- VANDERSTEEN, P. R. & MULLER, S. A. 1971. Erythrokeratoderma variabilis. An enzyme histochemical and ultrastructural study. *Arch Dermatol*, 103, 362-70.
- VEENSTRA, R. D. 1996. Size and selectivity of gap junction channels formed from different connexins. *J Bioenerg Biomembr*, 28, 327-37.
- VERKHRATSKY, A. 2008. *Calcium and cell death*, Netherlands, Springer.
- VERMA, V., HALLETT, M. B., LEYBAERT, L., MARTIN, P. E. & EVANS, W. H. 2009. Perturbing plasma membrane hemichannels attenuates calcium signalling in cardiac cells and HeLa cells expressing connexins. *Eur J Cell Biol*, 88, 79-90.
- VIRGINIO, C., MACKENZIE, A., NORTH, R. A. & SURPRENANT, A. 1999. Kinetics of cell lysis, dye uptake and permeability changes in cells expressing the rat P2X7 receptor. *J Physiol*, 519 Pt 2, 335-46.
- WAGNER, R. W. 1994. Gene inhibition using antisense oligodeoxynucleotides. *Nature*, 372, 333-5.
- WALLER, J. M. & MAIBACH, H. I. 2005. Age and skin structure and function, a quantitative approach (I): blood flow, pH, thickness, and ultrasound echogenicity. *Skin Res Technol*, 11, 221-35.
- WANG, C. M., LINCOLN, J., COOK, J. E. & BECKER, D. L. 2007. Abnormal connexin expression underlies delayed wound healing in diabetic skin. *Diabetes*, 56, 2809-17.
- WANG, N., DE BOCK, M., ANTOONS, G., GADICHERLA, A. K., BOL, M., DECROCK, E., EVANS, W. H., SIPIDO, K. R., BUKAUSKAS, F. F. & LEYBAERT, L. 2012. Connexin mimetic peptides inhibit Cx43 hemichannel opening triggered by voltage and intracellular Ca²⁺ elevation. *Basic Res Cardiol*, 107, 304.

- WANG, N., DE VUYST, E., PONSARTS, R., BOENGLER, K., PALACIOS-PRADO, N., WAUMAN, J., LAI, C. P., DE BOCK, M., DECROCK, E., BOL, M., VINKEN, M., ROGIERS, V., TAVERNIER, J., EVANS, W. H., NAUS, C. C., BUKAUSKAS, F. F., SIPIDO, K. R., HEUSCH, G., SCHULZ, R., BULTYNCK, G. & LEYBAERT, L. 2013a. Selective inhibition of Cx43 hemichannels by Gap19 and its impact on myocardial ischemia/reperfusion injury. *Basic Res Cardiol*, 108, 309.
- WANG, X., MA, A., ZHU, W., ZHU, L., ZHAO, Y., XI, J., ZHANG, X. & ZHAO, B. 2013b. The role of connexin 43 and hemichannels correlated with the astrocytic death following ischemia/reperfusion insult. *Cell Mol Neurobiol*, 33, 401-10.
- WARNER, A., CLEMENTS, D. K., PARIKH, S., EVANS, W. H. & DEHAAN, R. L. 1995. Specific motifs in the external loops of connexin proteins can determine gap junction formation between chick heart myocytes. *J Physiol*, 488 (Pt 3), 721-8.
- WATANABE, A. 1958. The interaction of electrical activity among neurons of lobster cardiac ganglion. *Jpn J Physiol*, 8, 305-18.
- WEIDMANN, S. 1969. Electrical coupling between myocardial cells. *Prog Brain Res*, 31, 275-81.
- WHITE, T. W. 2003. Nonredundant gap junction functions. *News Physiol Sci*, 18, 95-9.
- WHITE, T. W., DEANS, M. R., KELSELL, D. P. & PAUL, D. L. 1998. Connexin mutations in deafness. *Nature*, 394, 630-1.
- WICKE, C., BACHINGER, A., COERPER, S., BECKERT, S., WITTE, M. B. & KÖNIGSRÄINER, A. 2009. Aging influences wound healing in patients with chronic lower extremity wounds treated in a specialized Wound Care Center. *Wound Repair Regen*, 17, 25-33.
- WILD, S., ROGLIC, G., GREEN, A., SICREE, R. & KING, H. 2004. Global prevalence of diabetes: estimates for the year 2000 and projections for 2030. *Diabetes Care*, 27, 1047-53.
- WRIGHT, C. S., BERENDS, R. F., FLINT, D. J. & MARTIN, P. E. 2013. Cell motility in models of wounded human skin is improved by Gap27 despite raised glucose, insulin and IGFBP-5. *Exp Cell Res*, 319, 390-401.
- WRIGHT, C. S., VAN STEENSEL, M. A., HODGINS, M. B. & MARTIN, P. E. 2009. Connexin mimetic peptides improve cell migration rates of human epidermal keratinocytes and dermal fibroblasts in vitro. *Wound Repair Regen*, 17, 240-9.
- WRIGHT, J. A., RICHARDS, T. & BECKER, D. L. 2012. Connexins and diabetes. *Cardiol Res Pract*, 2012, 496904.
- YANO, S., KOMINE, M., FUJIMOTO, M., OKOCHI, H. & TAMAKI, K. 2004. Mechanical stretching in vitro regulates signal transduction pathways and cellular proliferation in human epidermal keratinocytes. *J Invest Dermatol*, 122, 783-90.
- YE, Z. C., WYETH, M. S., BALTAN-TEKKOK, S. & RANSOM, B. R. 2003. Functional hemichannels in astrocytes: a novel mechanism of glutamate release. *J Neurosci*, 23, 3588-96.
- YEN, M. R. & SAIER, M. H. 2007. Gap junctional proteins of animals: the innexin/pannexin superfamily. *Prog Biophys Mol Biol*, 94, 5-14.
- ZÄHLER, S., HOFFMANN, A., GLOE, T. & POHL, U. 2003. Gap-junctional coupling between neutrophils and endothelial cells: a novel modulator of transendothelial migration. *J Leukoc Biol*, 73, 118-26.
- ZHANG, J., O'CARROLL, S. J., WU, A., NICHOLSON, L. F. & GREEN, C. R. 2010a. A model for ex vivo spinal cord segment culture--a tool for analysis of injury repair strategies. *J Neurosci Methods*, 192, 49-57.

- ZHANG, L., HUO, W., GAO, X. H., MA, L., XIU, Y., ZHENG, S., HONG, Y. & CHEN, H. D. 2010b. Familial erythrokeratoderma variabilis with pustular lesions: a new variant? *Acta Derm Venereol*, 90, 274-8.
- ZHANG, L., LI, Y. M., JING, Y. H., WANG, S. Y., SONG, Y. F. & YIN, J. 2013. Protective effects of carbenoxolone are associated with attenuation of oxidative stress in ischemic brain injury. *Neurosci Bull*, 29, 311-20.
- ZHANG, P., ZHANG, X., BROWN, J., VISTISEN, D., SICREE, R., SHAW, J. & NICHOLS, G. 2010c. Global healthcare expenditure on diabetes for 2010 and 2030. *Diabetes Res Clin Pract*, 87, 293-301.

Appendix I

Abbreviations

3D	3 dimensional
°C	degrees Celsius
µg	microgram
µl	microlitre
µm	micrometer
µM	micromole
α	alpha
α-SMA	smooth muscle actin
ADP	adenosine diphosphate
ANOVA	one way analysis of variance
asODN	antisense oligodeoxynucleotide
ATP	adenosine triphosphate
ADP	adenosine diphosphate
β	beta
BBG	brilliant blue G
bFGF	basic fibroblast growth factor
bn	billion
BSA	Bovine serum albumin
Ca²⁺	Calcium ion
calcein-AM	calcein acetomethoxy ester
cAMP	cyclic adenosine monophosphate
CL	cytoplasmic loop
CO₂	Carbon dioxide
CT	carboxyl terminus
Cx	connexin
dH₂O	deionised water
Da	Daltons
DAMP	damage associated molecular pattern molecule

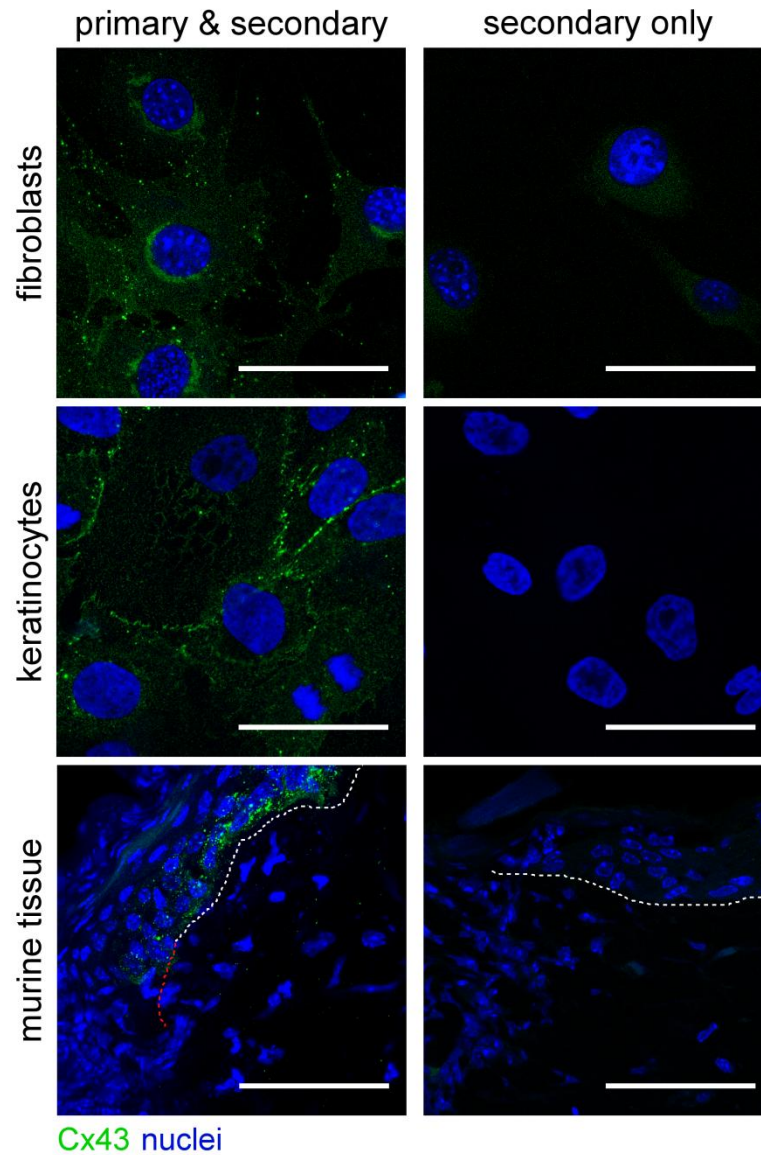
DBS	donor bovine serum
DENDRA	Derived from <i>Dendronephthya sp.</i>
DMEM	Dulbecco's modified essential medium
DNA	deoxyribonucleic acid
EL	extracellular loop
ECL	enhanced chemiluminescence
ER	endoplasmic reticulum
EtOH	Ethanol
EPUAP	European Pressure Ulcer Advisory Panel
EVK	erythrokeratoderma variabilis
FACS	fluorescence-activated cell sorting
FDA	Food and Drug Administration
FGF	fibroblast growth factor
FGF-2	fibroblast growth factor 2
FITC-BSA	fluorescein isothiocyanate conjugated to Bovine serum albumin
FOXY	fibre optic oxygen
FIAsH	Fluorescein Arsenical Hairpin
FRAP	fluorescence recovery after photobleaching
g	grams
GFP	green fluorescent protein
GJB1	gene coding for Cx32
GJB2	gene coding for Cx26
GJB3	gene coding for Cx31
gt	goat
h	hour
HaCaT	Human adult low Calcium Temperature keratinocytes
HSC	haematopoietic stem cell
hc	hemichannel
HeLa	Henrietta Lacks cells
HCl	Hydrochloric acid
HID	Hystrix-like Ichthyosis deafness
HRP	horseradish peroxidase
HSC	haematopoietic stem cell

HUVECs	human umbilical vein endothelial cells
ICR	Institute of Cancer Research
IL	interleukin
IP₃	inositol triphosphate
JNK	jun N-terminal kinase
K⁺	Potassium ion
KID	keratitis ichthyosis deafness
l	litre
LED	light emitting diode
m	meter
M	Mole
M	transmembrane loop
MANOVA	multivariate analysis of variance
MAPK	mitogen activated protein kinases
MSC	mesenchymal stem cell
mg	milligram
min	minute
ml	millilitre
mm	millimetre
mM	millimole
MMP	matrix metalloproteinase
mRNA	messenger ribonucleic acid
MSC	mesenchymal stem cell
MTT	3-(4,5-Dimethylthiazol-2-Yl)-2,5-Diphenyltetrazolium Bromide
MW	molecular weight
n	sample number
N₂	Nitrogen
NaCl	Sodium Chloride
NAD	nicotinamide adenine dinucleotide
NHS	National Health Service
NIH 3T3	fibroblasts
NT	amino terminus
OCT	optimal cutting temperature

OGDR	oxygen glucose deprivation reoxygenation
OptiMEM	opti-minimal essential medium
PBS	phosphate buffered saline
PFA	paraformaldehyde
pH	power of Hydrogen
PI	propidium iodide
rb	rabbit
ReAsH	Resorufin-derived red fluorescent Arsenical Hairpin
RIPA	radio-immunoprecipitation assay
RNA	ribonucleic acid
ROI	region of interest
RT-PCR	reverse transcription polymerase chain reaction
SAPK	stress activated protein kinase
SDS	sodium dodecyl sulphate
SDS-PAGE	sodium dodecyl sulphate polyacrylamide gel electrophoresis
SEM	standard error from the mean
shRNA	short hairpin ribonucleic acid
STZ	streptozotocin
TGF-β	transforming growth factor beta
U	units
UV	ultraviolet
V	Volts
VEGF	vascular endothelial growth factor
vWF	von Willebrand factor

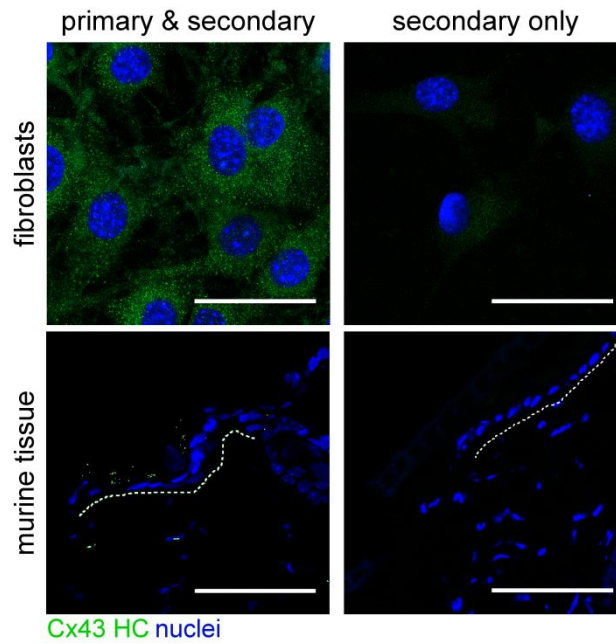
Appendix II

Supplementary figures



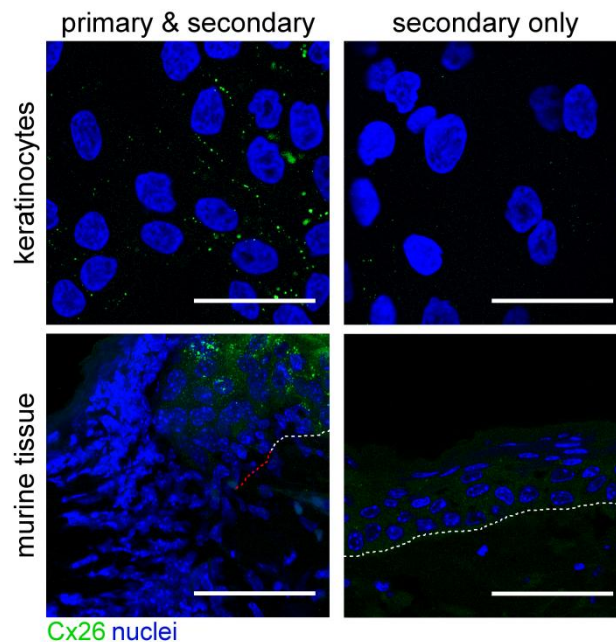
Supplementary 1 - Immunofluorescence staining of Cx43

Panels are representative of staining and second antibody control staining of Cx43 in NIH 3T3 fibroblast cells, HaCaT keratinocyte cells and murine epidermal and upper dermal tissue. Tissue was immunolabeled Cx43 (green) and nuclei (blue).⁷



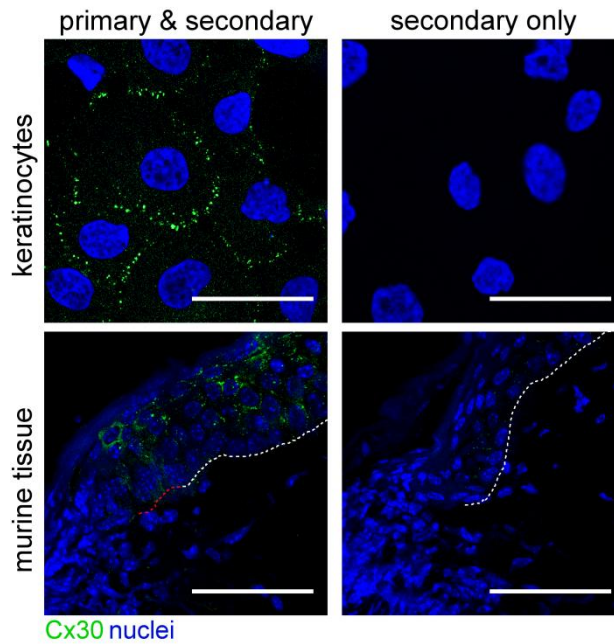
Supplementary 2 - Immunofluorescence staining of hemichannels

Panels are representative of staining and second antibody control staining of HC in NIH 3T3 fibroblast cells, and murine epidermal and upper dermal tissue. Tissue was immunolabeled HC (green) and nuclei (blue).



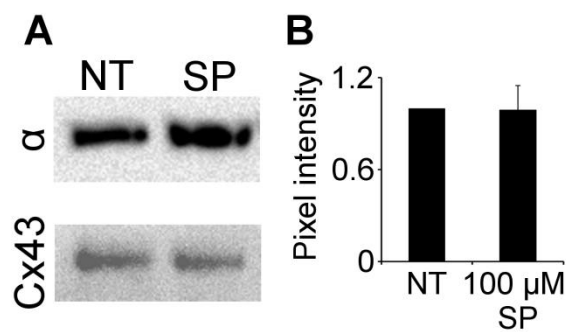
Supplementary 3 - Immunofluorescence staining of Cx26

Panels are representative of staining and second antibody control staining of Cx26 in HaCaT keratinocyte cells, and murine epidermal and upper dermal tissue. Tissue was immunolabeled Cx26 (green) and nuclei (blue).



Supplementary 4 - Immunofluorescence staining of Cx30

Panels are representative of staining and second antibody control staining of Cx30 in HaCaT keratinocyte cells, and murine epidermal and upper dermal tissue. Tissue was immunolabeled Cx30 (green) and nuclei (blue).



Supplementary 5 - Effect of scrambled peptide on Cx43 expression in fibroblast cells; Western blot analysis

(A) Cx43 protein expression in fibroblast cells during incubation with scrambled peptide with Gap27 was confirmed through Western blot analysis. The panels show representative blots. Alpha tubulin serves as a loading control protein. (B) The intensity of the protein was measured relative to the intensity of the housekeeping protein. The graph shows no difference in Cx43 protein expression between control and treated samples. The data are shown as the means \pm S.E.M. NT = No treatment, SP = Scrambled peptide.

Appendix III

Papers

Balasubramaniyan V, Dhar DK, Warner AE, Vivien Li WY, Amiri AF, **Bright B**, Mookerjee RP, Davies NA, Becker DL, Jalan R. 2013. Importance of Connexin-43 based gap junction in cirrhosis and acute-on-chronic liver failure. *J. Hepatal.* **58**: 1194-1200

For submission

Bright-Glass B, Cormie P, Becker D. 2013. Connexin 43 upregulation underlies cell death in fibroblasts following ischemia reperfusion injury.